

**Impact of rapid mixing and temperature on  
flocculation of clay suspensions in water**

by

Ravindra Mohan Srivastava

A Thesis Submitted to the  
Graduate Faculty in Partial Fulfillment of the  
Requirements for the Degree of  
**MASTER OF SCIENCE**

Department: Civil and Construction Engineering  
Mechanical Engineering

Signatures have been redacted for privacy

Iowa State University  
Ames, Iowa  
1988

Copyright © Ravindra Mohan Srivastava, 1988. All rights reserved.

**TABLE OF CONTENTS**

<b>ACKNOWLEDGEMENTS</b> . . . . .	vi
<b>1. INTRODUCTION</b> . . . . .	1
1.1. General . . . . .	1
1.2. Mixing . . . . .	2
<b>2. OBJECTIVE</b> . . . . .	5
<b>3. LITERATURE REVIEW</b> . . . . .	9
3.1. General . . . . .	9
3.2. Colloids . . . . .	16
3.2.1. Introduction . . . . .	16
3.2.2. Colloidal interactions . . . . .	20
3.2.3. Double layer . . . . .	25
3.2.4. Dynamics of a colloidal system . . . . .	30
3.2.5. Coagulation and flocculation . . . . .	36
3.2.6. Conclusion . . . . .	39
3.3. Coagulants . . . . .	40
3.3.1. Introduction . . . . .	40

3.3.2.	Hydrolysis and mononuclear hydrolysis products . . . . .	43
3.3.3.	Polynuclear species . . . . .	56
3.3.4.	Dilution, pH and nature of hydrolysis species . . . . .	62
3.3.5.	Precipitation . . . . .	63
3.3.6.	Conclusion . . . . .	65
3.4.	Colloid Destabilization . . . . .	66
3.4.1.	Introduction . . . . .	66
3.4.2.	Adsorption-destabilization . . . . .	67
3.4.3.	Surface reactions . . . . .	82
3.4.4.	Water treatment applications . . . . .	88
3.4.5.	Conclusion . . . . .	89
3.5.	Mixing . . . . .	89
3.5.1.	Introduction . . . . .	89
3.5.2.	Entropy and mixing . . . . .	90
3.5.3.	Molecular diffusion . . . . .	93
3.5.4.	Dispersion, diffusion and micromixing . . . . .	99
3.6.	Turbulence . . . . .	106
3.6.1.	Introduction . . . . .	106
3.6.2.	Defining turbulence . . . . .	108
3.6.3.	Other characteristics of turbulent flow . . . . .	110
3.6.4.	Transfer and dissipation of energy in turbulent flow . . . . .	117
3.7.	Turbulent Mixing . . . . .	132
3.7.1.	Introduction . . . . .	132

3.7.2.	Mechanisms of turbulent mixing . . . . .	134
3.7.3.	Mixing in a reactor . . . . .	139
3.8.	Turbulent Mixing and Fast Chemical Reactions . . . . .	144
3.8.1.	Introduction . . . . .	144
3.8.2.	Chemical reactions . . . . .	146
3.8.3.	Turbulence and fast chemical reactions . . . . .	153
3.9.	Flocculation . . . . .	161
3.9.1.	Introduction . . . . .	161
3.9.2.	Aggregation kinetics . . . . .	162
3.9.3.	Turbulent flow and flocculation . . . . .	177
3.9.4.	Conclusion . . . . .	180
<b>4.</b>	<b>EXPERIMENTS . . . . .</b>	<b>182</b>
4.1.	Introduction . . . . .	182
4.2.	Objective . . . . .	190
4.3.	Experimental plan and equipment . . . . .	193
4.4.	Experimental procedure . . . . .	207
4.5.	Conclusion . . . . .	214
<b>5.</b>	<b>RESULTS AND INFERENCES . . . . .</b>	<b>215</b>
5.1.	Results . . . . .	215
5.1.1.	Rapid mixing with alum . . . . .	217
5.1.2.	Rapid mixing with Magnifloc 573C polymer . . . . .	243
5.1.3.	Comparing rapid mixing of alum and Magnifloc 573C polymer . . . . .	253



5.1.4. Changes in particle size distribution with rapid mixing . . . .	263
5.2. Inferences . . . . .	278
5.3. Comparison With Results of Previous Studies . . . . .	280
5.4. Where Do We Go From Here? . . . . .	283
<b>6. BIBLIOGRAPHY . . . . .</b>	<b>286</b>
<b>7. APPENDIX . . . . .</b>	<b>297</b>

## **ACKNOWLEDGEMENTS**

Boy! Was this fun or what!

Ravi

## 1. INTRODUCTION

### 1.1. General

It is necessary to treat water obtained from natural sources in order to make it fit for human consumption, as well as satisfactory for industrial use.

This is so because natural water, drawn from surface water sources (like lakes and rivers) is usually contaminated. This may be because of chemical contaminants like clay and silt particles, humic acids, fulvic acids and other color causing compounds, or biological contaminants like bacteria, viruses, fungi and algae.

Even though it would be desirable to remove all contaminants completely from the water, such an approach is rarely taken because of the prohibitive expenses involved. Technologically and economically, it is much easier to merely reduce the amounts of contaminants to levels which have been deemed "acceptable". However, with every passing day, as our knowledge of the health risks associated with sundry contaminants increases, the levels to which contaminant concentration must be reduced, through treatment, is made even smaller; making the treatment of water a challenging feat.

In order to comply with these standards, while keeping the costs of treating water low, it is necessary to optimize the performance of the entire water treatment process.

Optimization, however, can take place only if one can mathematically analyze and predict each of the unit processes which comprise a given water treatment process stream. And, in order to arrive at a mathematical model of a system, it is absolutely necessary to have a conceptual model of the physical phenomena which govern the behavior of each of the unit processes.

Thus, it is imperative that a thorough understanding of these processes be acquired before any successes can be had in the achievement of complete control on their outcome.

## 1.2. Mixing

Extensive work has been done in the field of sanitary/environmental engineering in trying to develop an understanding of most of the critical unit processes involved in a water treatment process stream. For example, conventional water treatment operations for removal of turbidity from water consist of four unit processes: mixing, flocculation, sedimentation, and filtration. The basic purpose of each of these processes is as follows:

- **Mixing:** for dispersal of coagulant and destabilization of the colloids which are to be removed.
- **Flocculation:** for the growth of the destabilized particles for easy removal by settling and filtration.
- **Sedimentation:** for easy removal of large flocs by gravity.
- **Filtration:** for the removal of fine particles.

Of these four unit processes, the latter three have been studied in considerable detail by sanitary/environmental engineers; which is why their behavior is much better understood than that of the first process. The process of mixing, however, has not been investigated as thoroughly as the rest. The reasons for this are many. Some of them are as follows:

- Unlike flocculation, sedimentation, and filtration; rapid mixing does not have a pronounced visual impact on the water being treated, leading to a false conclusion that the process is a 'non-critical' one.
- Design guidelines for rapid mixing include very large safety factors (more appropriately called the factors of ignorance), leading to gross over-design, which rarely ever results in a water treatment plant operation problem being blamed on the mixing step.
- The processes of flocculation, sedimentation, and filtration, because of their 'physical' nature, have been studied (and explained) predominantly from a hydrodynamic/fluid mechanics standpoint, which is based on relatively well established principles. Mixing (rapid mixing or flash mixing), however, is a 'physico-chemical' phenomenon and needs to be studied from a joint chemical and hydrodynamics standpoint. In the absence of a well established theory coupling these diverse topics, not much progress could have been made in this direction.

Monumental work has been done in establishing the chemical aspects of coagulation, thanks to the efforts of colloid scientists. Given the colossal importance

of coagulant chemistry in water treatment, it is not hard to understand why researchers, in sanitary/environmental engineering, have concentrated their energies (and still continue to do so) trying to unravel the mystery of chemistry in coagulation. However, an excessive emphasis on the chemical aspects of the coagulation problem, accompanied by a veritable neglect of the hydrodynamic aspects, has resulted in a rather lop-sided understanding of the mechanisms underlying the effects caused by the process of rapid mixing.

In fact, until recently, a joint chemical and hydrodynamic approach has not been possible; partly due to a general lack of understanding of the phenomenon of turbulent fluid flow among sanitary and environmental engineers, and partly because of the extremely high speed with which the process of colloid destabilization takes place.

Fortunately, recent advances in the theory of fluid mixing, turbulent flows in continuous stirred-tank reactors (CSTRs) and mixing with fast chemical reactions in turbulent flows have provided some material which can be used in an attempt to make a conceptual model which combines the chemical and hydrodynamic aspects of such problems.

With these thoughts in mind, the prospects of achieving a better understanding of the physical phenomena which underlie the processes of mixing, colloid destabilization, and flocculation seem to have increased tremendously. This understanding can serve as the foundation on which a mathematical model of this process can be made, providing engineers with a tool to optimize mixing/colloid destabilization/flocculation as well as the overall water treatment process.

## 2. OBJECTIVE

The overall objective of this study is to make an attempt to understand better

- the mechanisms which underlie the process of fluid mixing, as applied to the unit process of rapid mixing and as practiced in the field of water treatment and
- how rapid coagulant mixing fits into the general scheme of things vis-a-vis water treatment.

Based on this understanding of the rapid mixing process, an attempt will also be made to explain the effects of

1. intensity of turbulence and
2. temperature

on the outcome of this process, as seen in experiments involving these variables.

This attempt will be slightly different from preceding attempts made by other investigators of this process. It is felt that so far, most of the experimental studies on the process of coagulant mixing tend to be based on concepts (like  $G$ ) which are still unproven (and often misused and abused) but, in the absence of any better substitutes, continue to be supported by the sanitary/environmental engineering

community. There have been few attempts at providing theoretical models for conceptual explanations of the effects of the process of rapid mixing because of reasons mentioned in Chapter 1.

This is decidedly *not* an attempt to formulate a mathematical model for the process of rapid mixing. It is merely an effort to look at the physical phenomena which constitute the entire process of mixing and coagulation. Having clarified these points, we now take a closer look at the problem.

The rapid mixing process in water treatment can be reduced to the effects of three interacting components:

1. Coagulants
2. Colloids
3. Turbulent Flow

and any attempt to understand mixing must be done in terms of these components.

As mentioned earlier, considerable information already exists, in the field of sanitary/environmental engineering, about the chemical nature of coagulants, colloids, water and any chemical interactions which exist between them and no specific experimental efforts will be directed in that direction. Thus, the objectives of this study can be more specifically stated as follows:

- To understand the general behavior of colloids.
- To understand the general behavior of metal coagulants in water.
- To study the chemical aspects of the manner in which the colloids and the metal coagulants interact.



- To define the problem of mixing in general and fluid mixing in particular, and the processes by which mixing occurs.
- To study the phenomenon of turbulent flow.
- To look at the effects of turbulent flow on the phenomenon of mixing.
- To understand the influence of turbulent flow on the behavior of fast chemical reactions and, in this light, the behavior of alum as a coagulant.
- To comprehend the effect of turbulent flow on colloids, and thus the process by which their interactions affect colloid destabilization and flocculation.
- To conduct experiments to detect the influence of intensity of mixing as well as temperature on rapid mixing and to explain these results on the basis of the phenomena underlying this process.

Based on the objectives specified above, it is obvious that in this study, the first part would involve a considerable fraction of the entire effort and would be rather theoretical in nature. The reason for this is that in order to arrive at a proper understanding of the crucial phenomena which govern the outcome of the rapid mixing process, a strong background in the fundamental behavior of the interacting components is a necessity. Since this involves drawing, from existing literature, the information necessary to arrive at the desired objectives; it is not incorrect to think that the first part of this study will, in essence, be a collection of the views of the experts in the various fields, including those which are normally not considered to be the prime domain of sanitary/environmental engineers, e.g., turbulent flow phenomenon, fast chemical reactions, etc.

The second part of this work would emphasize the experimental details involved in this study and the results obtained from it.

### 3. LITERATURE REVIEW

#### 3.1. General

Conventional water treatment for removal of turbidity causing substances can, as mentioned earlier, easily be divided into a three-step process:

1. Aggregation of colloids.
2. Sedimentation of larger agglomerated particles.
3. Filtration of the smaller particles, which escape the sedimentation step.

It is thought that the aggregation of colloids is actually a two-step process of which *colloid destabilization* is the first step and *flocculation*, the second. The overall process is traditionally called *coagulation* although some use the term coagulation only for the colloid destabilization step. In the first step of the aggregation process, which is thought to be predominantly chemical in nature, the coagulant species (preformed or nascent) interact with the colloids and, in the process, alter the surface chemistry of the colloids. This causes the colloids to be destabilized, rendering easy their aggregation into bigger particles. The flocculation step, which is the second part of this process, is the transport step. It helps in providing inter-particle collisions which, when successful, produce larger aggregates.

Traditionally, it has been thought that the sole purpose of rapid mixing units in water treatment is to disperse coagulants quickly and uniformly throughout the influent water stream [4,62], while the flocculating units provide the particle transport necessary for collisions to occur.

Recently, however, it has been recognized that rapid mixing does more than just that. According to Amirtharajah, "The initial mixing unit in a water treatment plant is a reactor designed to provide close encounters between the colloids in the raw water and the products of the coagulation reactions" [2]. O'Melia states, "... the primary purpose of rapid mix units is to accomplish destabilization of the particles in the raw water" [86]. This is much in line with the current thinking that even though particle aggregation is a two-step process, these two steps are not independent, as had been thought earlier. In fact, the chemical and transport steps of the problem are very much interdependent since coagulants cannot cause destabilization unless they are properly distributed and contacted with the colloids while destabilized colloids will not aggregate unless sufficient contact opportunities are provided [18].

Given the importance of rapid mixing in colloid destabilization, and the role of colloid destabilization in particle aggregation, it is not difficult to understand why Moffett said, "... coagulation takes place in the rapid mixer; and, from the viewpoint of the operator, this is the most important single step in a water treatment plant. Improper coagulation cannot be corrected at a later stage of the process, and the results of improper coagulation will be to reduce the quality of the effluent and the efficiency of the plant as a whole" [77].

Vrale and Jorden warn of the potential damage this process can do, if not handled properly and say, "... inefficient rapid mixing may have two harmful effects:

(1) wastage of chemical and (2) slower particle aggregation rates for a given chemical dosage” [113]. O’Melia thinks that “When alum and ferric salts are used, it is important that vigorous mixing be provided because many hydrolysis reactions are almost instantaneous and the products that are formed are very dependent on pH and coagulant concentration. Poor mixing permits local regions of high dose and uncertain pH, so that coagulant is wasted” [86].

At this point, one question which comes naturally to our minds is: Are these claims/observations really true?

In the absence of extensive research on this specific unit process, in the field of sanitary/environmental engineering, it is difficult to state authoritatively whether these claims are exaggerations or not. Given our present state of ignorance of this process, it becomes even more necessary that this problem be analyzed so that some of these persistent questions can be put to rest in a satisfactory manner.

So what, exactly, does rapid mixing do? In order to define the problem of rapid mixing, it is necessary to enumerate the parameters which have an impact on the outcome of this unit process.

Since we want to achieve coagulation, it is obvious that the coagulant is the most important parameter of all. Also, since a uniform mixture of the coagulant is desired in the influent stream, the process of mixing is yet another parameter to be considered. A third parameter—time—is involved, since the time of mixing is sought to be small so that economy can be achieved in the design of mixing units. Perhaps this is why the process is called *rapid mixing*, because the mixing needs to be done without spending too much time. Also, since the coagulant is used for the destabilization of the colloids present in water, it is but natural that the colloids be

considered as yet another parameter in our study of the process of rapid mixing. Last, but not the least, we must consider the suspending medium in which our entire process takes place: water. In other words, we have defined five parameters which have decidedly important roles to play in the outcome of rapid mixing. They are:

1. Coagulants
2. Mixing
3. Time
4. Colloids
5. Water

and any outcome of the rapid mixing process must depend primarily on these five parameters.

Even though five parameters have been listed above, not all of them are control parameters for an existing water treatment plant—parameters which can be varied by the operator at will in order to move the process in the desired direction. From the above list, we can see that the control parameters are:

- Coagulants
- Mixing

and they must be modified in order to match the “uncontrolled” varying parameters:

- Colloids

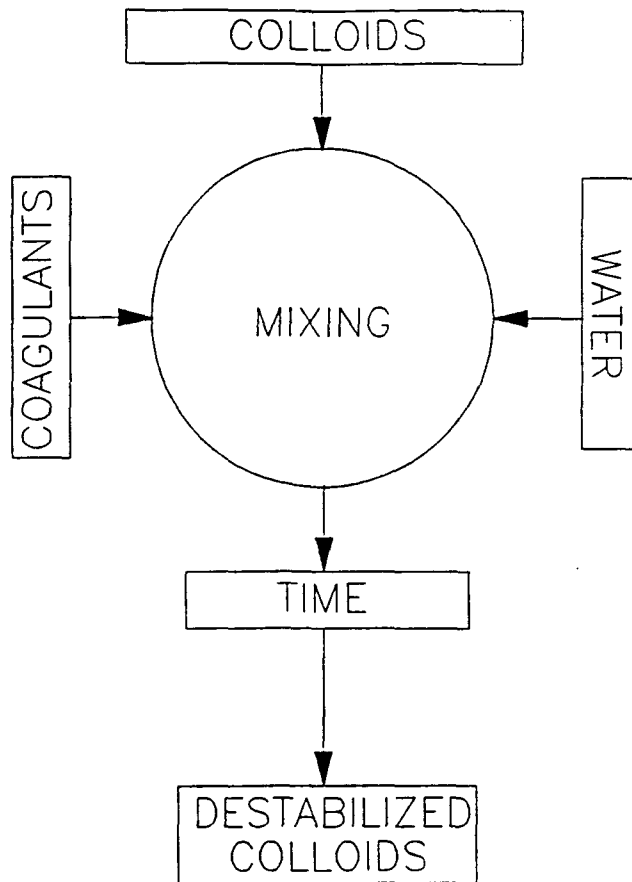


Figure 3.1: Parameters influencing the outcome of the rapid-mixing process

- Water

for a fixed

- Time

so as to keep the process in its desired, preferably optimal, state. The design engineer, however, is interested in only the first three variables:

- Coagulants
- Mixing
- Time

while a researcher should be interested in each of the parameters so that the behavior of this process can be understood well.

Even though the parameters which govern the outcome of this process have been itemized individually, it does not imply that their roles are independent of each other. In fact, they interactively affect the results of rapid mixing and their interaction can be visualized with the help of Figure 3.1. It is well known that the behavior of the coagulant and colloids is severely affected by the nature of the suspending medium—in our case water; mixing affects the manner in which coagulants are dispersed and thus their reactions (if any) with water and the colloids; time influences the extent to which such interactions are allowed to take place and brings to light the matter of their respective speed: the “kinetics” of rapid mixing.

In order to predict the consequences of rapid mixing, it is necessary to analyze each of the parameters which play a role in this unit process.



**Coagulants:** As mentioned earlier, considerable work has already been in trying to understand the manner in which various coagulants interact with water and, under different conditions of the reaction (e.g., solution chemistry, temperature) produce different effects. This complex picture gets even more complicated when one introduces colloids into the system and attempts to understand how each element influences every other element as a part of this process. Fortunately, sanitary/environmental engineering has a rich tradition in this aspect of water chemistry and most of the coagulant chemistry information in this study will be drawn from there.

**Mixing:** In water treatment processes, mixing of coagulants is usually done using turbulent flow of water because it is much more efficient at dispersing the coagulant uniformly than molecular diffusion alone or molecular diffusion coupled with laminar flow. Turbulent flow enhances the transport of coagulant and colloids, hastens the coagulant's reaction with water, influences the reaction products and, possibly, alters the destabilization of colloids. In this study, effort has been spent in trying to understand the phenomenon of turbulence per se, as well as the manner in which it influences the outcome of the unit process of rapid mixing.

**Time:** Virtually all the research in sanitary/environmental engineering on rapid mixing has focussed on the time over which forced turbulent mixing should be carried out, so that the optimal detention time of a mixing unit can be chosen. This prompts, in this study, a kinetic approach to the problem so that we know how long the various steps in this process take to complete, and

hopefully, possibly help us arrive at a reasonable time period over which rapid mixing should take place in water treatment plants.

**Colloids:** Obviously, the nature of the colloids, their physico-chemical characteristics and particle size distributions—among other properties—will influence the manner in which they are transported by the fluid flow as well as their physico-chemical interactions with the coagulant species and other colloids.

**Water:** The influence of some of the influent water characteristics is very well documented in sanitary/environmental engineering literature. Both, physical characteristics (e.g., temperature, viscosity) and chemical characteristics (e.g., ionic strength, presence of interfering ions, other substances in solution) of the water must affect the coagulant chemistry and the transport processes.

The following sections consider these aspects in greater detail.

## 3.2. Colloids

### 3.2.1. Introduction

Sedimentation and filtration are the commonest of the conventional solids-liquids separation processes used in water treatment industry. They are used for the removal of turbidity causing contaminants like bacteria, viruses, algae, clay, silt, other inorganic and organic particulate matter, color causing compounds as well as dissolved organic contaminants. Most of these contaminants exist as colloidal particles.

What is a colloid? Hunter [60] provides an excellent description/definition of colloids:

When one substance dissolves in another to form a true solution, the ultimate particles of the solute are of molecular dimensions: at most a few molecules may be joined together to form an associated species . . . . The radius of the solute molecule in these cases is seldom more than a nanometer in size and usually rather less. Solute and solvent molecules are of comparable size and we normally assume that the solute molecules are, on average, dispersed uniformly through the (continuous) solvent.

Colloids, on the other hand, constitute "... the class of materials in which the kinetic units that are dispersed through the solvent are very much larger in size than the molecules of the solvent" [60].

Colloidal dispersions can arise in a number of ways [60]:

1. If a substance, A, is insoluble in substance B, one can break A down into very small particles (colloids) which can be dispersed more or less uniformly throughout the substance B. Substance A is then called the disperse phase and substance B, the dispersion medium. The lower limit for dispersions of this kind is around 1 nm. If the size were to be reduced further, the particles would ultimately become indistinguishable from true solutions. The upper limit is normally set at a radius of 1  $\mu\text{m}$  but there is no clear distinction between the behavior of particles of 1  $\mu\text{m}$  and somewhat larger particles.
2. Molecules that are individually larger than 1 nm in size are another kind of colloid. These 'macromolecules' can often be uniformly dispersed throughout a fluid medium and they then form a colloidal solution or dispersion. Proteins, polysaccharides (like starch), humic acids, and many synthetic polymers fall into this category.

3. A colloidal dispersion can also arise when a number of molecules of normal size associate together to form an aggregate, e.g., soap micelles in water.

IUPAC (International Union of Pure and Applied Chemistry) defines a colloid as any material for which one or more of its three dimensions lie within the range of 1–1000 nm [57]. It is frequently quite difficult to distinguish between colloids and solutions at the lower end of the scale and colloids and suspensions at the upper end [18]. Figure 3.2, from *Aquatic Chemistry* [106], shows the size spectrum of particles found in water.

The most fundamental distinguishing feature of all colloidal systems is that the area of contact between the disperse particles and the dispersion medium is relatively large and the energy associated with creating and maintaining that interface is significant. Yet another distinguishing characteristic displayed by colloids is their ability to scatter light: the Tyndall effect [42,60]. True solutions, on the other hand, scatter very little light. The scattering pattern of colloidal dispersions (i.e., the intensity of the scattered light as a function of  $\theta$ , the angle between the incident beam and the scattered beam), depends very strongly on the particle size and on the wavelength of the light [60].

What about colloids in water? Quoting Kavanaugh and Leckie [65], “The size spectrum of particulates in water extends from colloidal humic substances 1 nm in size, to large aggregates such as fecal pellets or marine snow with sizes up to  $10^{-2}$ m (10 mm), covering about 6–7 orders of magnitude.” The distribution of shapes, densities, surface chemical properties, and chemical composition may vary widely with size, making the complete characterization of a given water sample fairly cumbersome [62,65].

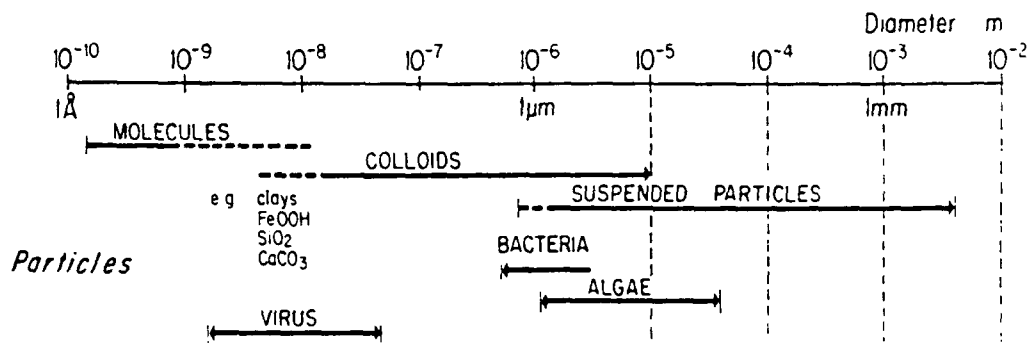


Figure 3.2: Size spectrum of colloids in water [106]

Despite the difficulties of characterizing a given colloidal dispersion in terms of the parameters mentioned above, we, in sanitary/environmental engineering, still use a fairly simple measure of the presence of colloids in water. We measure turbidity, which is an easily determined and practically useful parameter by which a gross measure of the colloidal content of a water can be made. It involves measuring the light scattering properties of a water sample. Small particles (e.g., those with a maximum dimension less than about  $0.1 \mu\text{m}$ ) do not scatter much visible light. Therefore a water containing asbestos fibers, viruses, or humic substances may have a larger particle number concentration, but have a low turbidity. Larger particles such as clay or plankton, which have particle diameters approximating the wavelength of visible light, scatter light more effectively and thus would yield higher turbidities [42]. Based on these facts, it is not incorrect to think of turbidity as being synonymous with colloidal contaminants of a super-micron size; and the removal of 'turbidity' being akin to the removal of such particulate contaminants from water. However, very low turbidities do not necessarily imply low total particulate concentrations. It simply means that the water does not have many particulates of a size range of the order of  $1 \mu\text{m}$  and above. It may still have large counts of sub-micron particles!

### 3.2.2. Colloidal interactions

Having discussed some preliminaries regarding colloids, we now consider the bulk behavior of colloids, i.e., how colloids—generally speaking—interact with each other and the solvent fluid.

Colloidal interactions are highly complex and depend on many physical and

chemical (and, in some cases, biological) factors. The properties which are of primary significance in determining the nature of these interactions and their outcome include particle size, particle shape, the flexibility (or lack thereof) of the particle, the chemical and electrical properties of the particle surface (such as charge and distribution of charge), the interactions of the particle with other particles, and the interactions of the particle with the solvent. Particle size distribution, among others, is one of the secondary factors in this matter [57].

Colloids display a wide range of behavior with regard to their interactions with the solvent. Hunter [60], quoting Freundlich [45] on this matter, says that on the basis of their interactions with the solvent, colloidal dispersions can be classified as being lyophobic (solvent hating) and lyophilic (solvent loving)—depending on the ease with which the system could be re-dispersed if once it was allowed to dry out. Lyophobic and lyophilic systems are also referred to as irreversible and reversible systems respectively. Shown in Table 3.1 (from Hunter [60]) are some of the properties of both kinds of colloids.

As mentioned earlier, the most crucial feature of colloids is the very great surface area of the dispersed phase for a given mass of matter, in comparison with the same amount of matter condensed into a single lump. Atkins [14] gives an example to prove this point. He shows that "...1 cm cube of a material has a surface area of  $6 \text{ cm}^2$ ; but when it is dispersed as little cubes of side 10 nm, the total surface area of the resulting  $10^{18}$  smaller cubes is  $6 \times 10^6 \text{ cm}^2$ . This steep increase in surface area dramatically enhances the importance of the role of surface effects in colloid chemistry."

The importance of surface area in colloid chemistry is very evident in the

Table 3.1: Lyophilic and Lyophobic Colloids [60]

Lyophilic	Lyophobic
<ul style="list-style-type: none"> <li>○ High concentrations of disperse phase frequently stable.</li> <li>○ Unaffected by small amounts of electrolytes. 'Salted out by large amounts.</li> <li>○ Stable to prolonged dialysis<sup>b</sup>.</li> <li>○ Residue after desiccation will take up dispersion medium spontaneously.</li> <li>○ Coagulation gives a gel or jelly.</li> <li>○ Usually give a weak Tyndall beam.</li> <li>○ Surface tension generally lower than dispersion medium.</li> <li>○ Viscosity frequently much higher than that of medium.</li> </ul>	<ul style="list-style-type: none"> <li>○ Only low concentrations of disperse phase stable<sup>a</sup>.</li> <li>○ Very easily precipitated by electrolytes.</li> <li>○ Unstable on prolonged dialysis<sup>c</sup> (due to removal of the small amount of electrolyte necessary for stabilization).</li> <li>○ Irreversibly coagulated on desiccation.</li> <li>○ Coagulation gives definite granules<sup>d</sup>.</li> <li>○ Very marked light scattering and Tyndall beam.</li> <li>○ Surface tension not affected.</li> <li>○ Viscosity only slightly increased<sup>e</sup>.</li> </ul>

<sup>a</sup>This is no longer true, especially if one allows the possibility of an adsorbed stabilizing layer of lyophilic material

<sup>b</sup>Dialysis refers to a membrane filtration technique for separating colloidal particles from small molecules or ions.

<sup>c</sup>Note that this is not true of lyophobic sols with dissociable ionic surface groups attached.

<sup>d</sup>Except for concentrated systems.

<sup>e</sup>This is true only for dilute, *stable* sols with more or less spherical particles.



differences in behavior between lyophilic and lyophobic colloids. One contributing factor to these differences is the extent to which the dispersion medium is able to interact with the atoms of the suspended particle [60]. If the solvent can come in contact with all or most of the atoms of the dispersed phase, then solvation energy will be important and the colloid should be lyophilic in some suitable solvent. If, however, the solvent is prevented, by the structure of the suspended particle (i.e., the disperse phase), from coming into contact with any but a small fraction of the atoms of those particles then the colloid will almost certainly be lyophobic in its behavior, even if the surface atoms interact strongly with the solvent.

Techniques for conventional treatment of water involve altering the surface chemistry of the contaminants so as to bring about the ‘destabilization’ of the colloids—to promote easy removal. What governs the stability of a colloidal dispersion?

Stability can arise from two counts [57]:

1. Thermodynamic stability
2. Kinetic stability.

Hunter [60] argues that

... a lyophilic colloid suspension is thermodynamically stable since there is a *reduction* in the Gibbs free energy when the ‘solute’ is dispersed. The *strong interaction* between ‘solute’ and solvent usually supplies sufficient energy to break up the disperse phase and there is often an increase in entropy as well; any reduction in solvent entropy due to the interaction with ‘solute’ is usually more than compensated by the entropy increase of the ‘solute’. For lyophobic colloid, the Gibbs free energy *increases* when the disperse phase is distributed throughout the dispersion medium so that it is a minimum when the disperse phase

remains in the form of a single lump. A lyophobic (i.e., solvent hating) colloid can, therefore, only be dispersed if its surface is treated in some way that causes a strong repulsion to exist between its particles. In this way, the particles can be prevented from aggregating (or coagulating) for long periods, although it must be emphasized that they are still *thermodynamically unstable* and the barrier to coagulation is merely a *kinetic* one.

In other words, even though thermodynamics favor the formation of larger colloid groups, the *rate* of coagulation is extremely slow. Such situations can arise in the presence of a stabilizer—either an electric charge or an adsorbed layer of charged particles—which sets up a Coulombic repulsion barrier between approaching particles. This decreases the efficiency of collisions so that only a small fraction of all collisions actually result in a permanent particle-particle contact. However, given enough time, they will ultimately form an aggregate [60].

The particulates normally found in water display the entire gamut of behavior: from hydrophobic to hydrophilic. Hydrophobic particulates are primarily of an inorganic origin and include some clay particulates and non-hydrated metal oxides. In contrast, hydrophilic particulates are primarily of organic origin and include a wide diversity of bio-colloids (humic and fulvic acids, viruses) and suspended living or dead microorganisms (bacteria, algae) [62].

There exist well developed theories describing the interaction between particles of lyophobic colloids but the behavior of lyophilic systems is much more difficult to describe. This is so because not only are all the forces of a lyophobic system important in a lyophilic system, there are very strong specific solvent effects that are difficult to predict [60].

### 3.2.3. Double layer

Of all the interactions which colloidal particles display, the electrical interactions are the most important. In fact, electrostatic (or Coulombic) interactions constitute one of the most important components of any theory describing colloidal phenomena. If a colloidal dispersion is placed in an electric field, particulates will move toward the electrodes, implying that they are electrically charged. It seems that at any interface between two phases, there is a tendency for charges (electrons or ions) to accumulate. Since the relative affinities of cations and anions for the two phases are generally different, one phase tends to acquire a positive and the other a negative charge—while still maintaining electro-neutrality of the system [60]. Most colloids carry charges which vary in sign and magnitude, depending on the environment [18]. In natural waters, it is the presence of such charges which provides a “kinetic” stability to these colloids, preventing their quick aggregation.

Such charges can arise in a variety of ways, which include [18,57,62]:

- Crystal imperfections, e.g., silica atoms in crystalline material can be replaced (i.e., isomorphic substitution of ions) by atoms with lower valence, such as aluminum, giving excess negative charge to crystal material. The clay particles responsible for turbidity in surface waters acquire their negative charges in this manner.
- Preferential adsorption of specific ions onto particle surface, e.g., adsorption of soluble positive or negative ions from bulk solution.
- Ionization of surface sites in the case of particulate surfaces containing functional groups (like hydroxyl, amino) which dissociate in water, producing a

surface electrical charge that depends on the solution pH.

- Ion dissolution, e.g., in the case of particulates whose constituent ionic groups do not dissolve equally in the solvent.
- Accumulation or depletion of electrons at interface.
- Adsorption of polyelectrolytes, e.g., adsorption of charged organic macromolecules, of the kind used in water treatment, onto particulate surfaces.

The presence of a charge concentration on the surface of the particle influences the distribution of ions in the medium. Counterions (ions of opposite charge) are attracted toward the particle by the Coulombic forces between the charges. However, they (the counterions) are also subject to entropic forces (like thermal motion) which tends to distribute them uniformly throughout the surrounding medium. The final result is usually a compromise in which a few counterions are bound strongly to the particle surface and the concentration of the remainder gradually decays away from the particle, ultimately reaching bulk concentration a few particle diameters away. This model is called the electrical diffuse double layer model [57,60].

Other forces may also be involved in the formation of this diffuse electrical double layer at a charged surface. Lyklema [76] terms all forces which are neither Coulombic nor entropic in nature as 'specific'. Such specific forces may be either chemical or physical in nature [57].

The diffuse electrical double layer and its properties play a primary role in many colloidal phenomena and are essential in interpreting colloidal stability and the electrokinetic properties of charged colloidal dispersions. The structure of the electrical double layer is generally regarded as consisting of two regions: an outer,

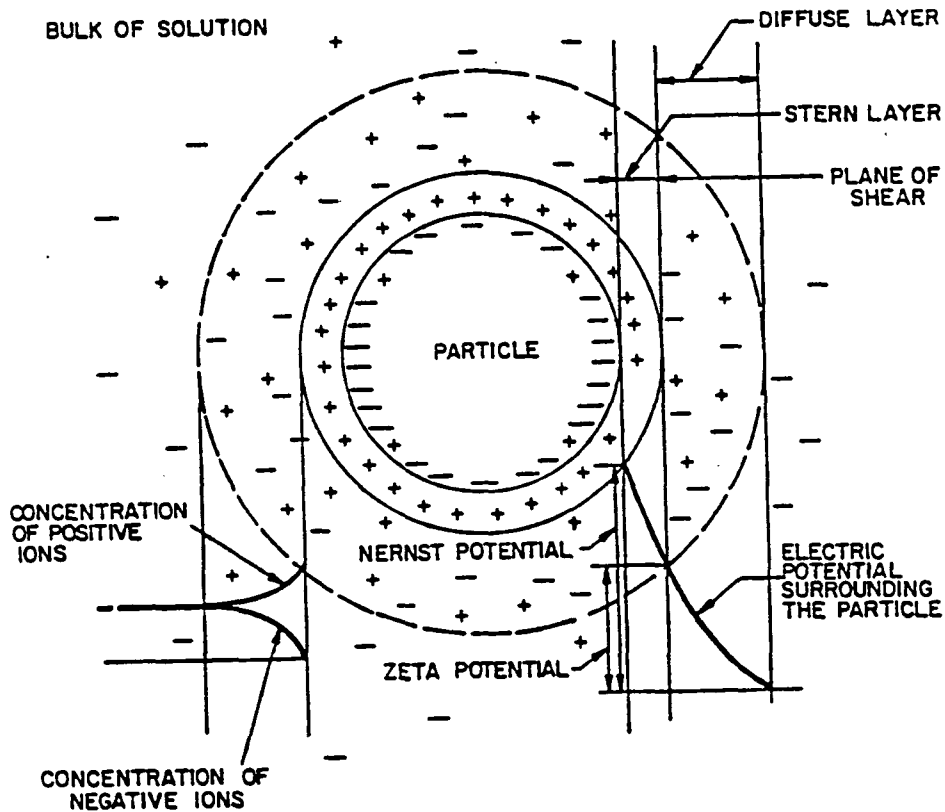


Figure 3.3: Schematic representation of a colloidal particle [57]

diffuse layer known as the Gouy (or Gouy-Chapman) layer, and an inner, compact layer known as the Stern layer. A schematic representation of a colloidal particle and its double layer is shown in Figure 3.3. The figure shows that the Stern layer is at the same distance away from the particle surface as the shear plane. Earlier, it had been thought that the shear plane was farther away from the surface than the Stern layer. Now, however, it is accepted that they are extremely close to each other, if not the same [60].

The distributions of ions in these two sections of the double layers are governed by complex physical and chemical variables and their interactions [57]. Usually, however, it is assumed that since the chemical forces are relatively short-ranged

in nature, they are significant only in the layer next to the surface (i.e., the Stern layer). On the other hand, the distribution of ions in the outer, diffuse layer is usually treated according to an ideal model. A simplistic description would show that the Stern layer is where adsorbed molecules are found and the outer layer is where most of the counterions exist, in order to maintain electro-neutrality around a colloid [62].

The original model of Stern was refined by Grahame. It distinguishes within the double layer, an 'inner Helmholtz plane' and an 'outer Helmholtz plane.' The former is representative of the plane through the centers of specifically adsorbed ions which are usually dehydrated upon adsorption, the 'outer Helmholtz plane' is the plane parallel to the surface and corresponds to the distance of closest approach of hydrated ions [57]. Figure 3.4 shows the location of the inner and outer Helmholtz planes. The outer Helmholtz plane is formed because because ions have a finite size and therefore, they can not get closer than a certain distance from the particle surface.

The outer diffuse layer is usually treated according to an ideal model in which the electric potential from the charged surface shows an exponential decay [57]. The opposing forces of electrostatic attraction and diffusion result in a negative concentration gradient of counterions with increasing distance from the particle surface. In this part of the double layer, the ions are thought to be influenced only by the local electrostatic potential. The only work done is the electrical work done on or by the ion as it moves in response to the field. This ignores the energies involved in moving aside other ions or creating a hole in the solvent, or any effect which the ion might have on the local structure of the solvent or the distribution of

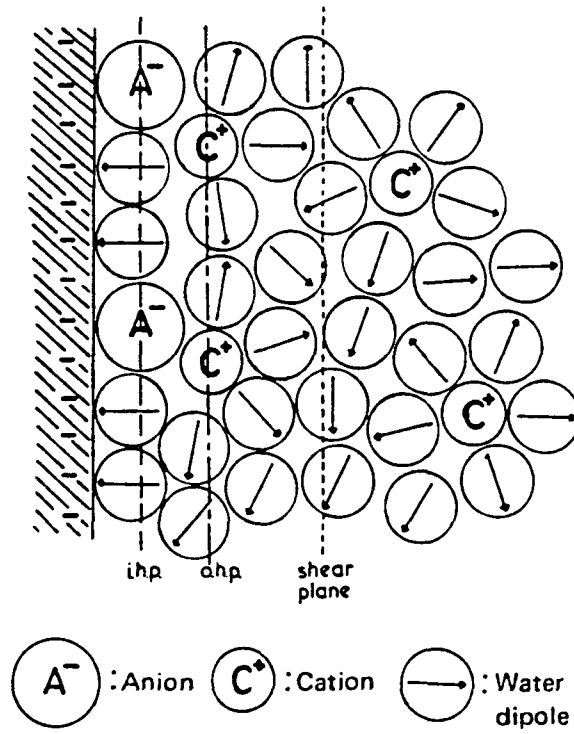


Figure 3.4: Inner and outer Helmholtz planes in the electrical double layer of a colloidal particle [39]

other ions [60].

The impact of the inner and outer parts of the double layer on the behavior of particulate surface is significant—e.g., a difference may exist between the bulk and the surface pH value at the solid-liquid interface; ions may accumulate in the inner layer—leading to adsorption, ion exchange, or precipitation reactions not normally predicted on the basis of equilibrium models [62].

#### 3.2.4. Dynamics of a colloidal system

Having looked at a simplified description of a colloidal particle, we now proceed to study its dynamical behavior—i.e., the various forces which act on a colloidal particle. “When two colloidal particles are brought close together, a variety of forces come into play—the outcome of which is determined not only by the interplay of these forces with each other, but also the time-rate at which their approach occurs, as the double layers may take a significant time to adjust to the new situation” [60]. In order to understand the behavior of a colloidal system, it is necessary to observe the fundamental forces which govern the actions of colloidal particles. The forces acting on colloids are many, some of which are described below.

**Repulsive forces:** When two like colloidal particles approach one another, ions associated with these particles move closely together with it. Due to interactions of the surface charges of the particles and the similarly charged diffuse portions of the electrical double layer, a repulsive force results—opposing further approach. While it may seem that the Stern layer has little to do vis-à-vis the interactions between surfaces, that is not true. Despite its miniscule dimensions—thickness of the order of a few molecules—it plays an indirect,



yet crucial, role in these interactions by influencing the potential of the diffuse portion of the double layer [57,60].

For flat plates, this effect can be understood in terms of the osmotic pressure created by the difference in ion concentration in the region between the two approaching surfaces compared to the bulk concentration [60]. The diffuse layers have a larger concentration of ions than the bulk solution. Thus, their approach to each other is opposed by the osmotic pressure exerted by the bulk solution on the interacting layers.

Several possible situations can arise when two surfaces approach one another. The approach may be slow enough for equilibrium to be established between the ions on the surface and in the bulk. Under these conditions, one would expect the surface potential to remain constant during approach. However, if the particle charge is caused by built-in crystal defects, (e.g., clay minerals) it may be more appropriate to assume that the surface charge is constant during approach. For other surfaces, the interaction may itself influence the degree of dissociation of surface. It is the constant potential case that has been studied extensively by the early workers in the field of colloid chemistry and is the basis of the DLVO (Derjaguin-Landau-Verwey-Overbeek) theory of colloid stability. The other possibilities are best understood as generalizations of the constant potential case [60].

**Attractive forces:** London-van der Waals forces are attractive forces which exist between atoms, molecules, ions and other surfaces and these give rise to attractive (usually) forces between particles and/or surfaces in proximity. The

London-van der Waals forces are a result in the fluctuations in the charge density of the electron cloud surrounding the nucleus. These fluctuations, in turn, produce an instantaneous dipole moment which produces an electric field, which can exert force on the interacting particles.

In London's expression for the interaction energy of two identical, single atoms, the attractive energy varies inversely with the sixth power of the intermolecular distance. However, London's analysis had two limitations: (i) when molecules or atoms are separated by a large distance and (ii) when the separation between atoms or molecules is very small—of the same order of magnitude as the diameter of the atoms or molecules themselves. Two different quantitative theories for London-van der Waals between macroscopic bodies were proposed: first by Hamaker and later by Lifshitz. The Hamaker theory, is not adequate to completely describe the van der Waals phenomenon quantitatively, but serves the purpose most successfully in a qualitative manner [57,94].

While the van der Waals interactions are relatively well understood for separations greater than 1 nm or so, at small separations or in situations of atomic contact, neither the Lifshitz nor the Hamaker theories are accurate [57]. Since colloidal particles are often very rough and rarely approach one another to such small distances, except possibly at a single point, such a force would seem inadequate to produce any significant attraction between like particles [60]. However, because van der Waals forces between the atoms in two approaching colloidal particles are somewhat additive, the overall effect is an attractive force of quite long range—of the order of tens of nanometers, quite

comparable with the range of the Coulombic forces [60].

**Structural forces:** Structural forces are strong repulsive forces which are important over very short ranges. They result from changes in the solvent structure (i.e., changes in the local ordering of molecules) in the vicinity of a surface or interface. Such changes arise as a result of packing constraints in interfacial regions. These forces may exert a relatively large effect for small separation distances between the particles or surface, but it is thought that they do not contribute significantly to the long range “tail” of forces. Thus, they may be of significance in determining colloidal stability [57]. Figure 3.5 provides a pictorial description of the nature of structural forces.

**Steric force:** Steric repulsion, which is in addition to electrostatic repulsion, arises when long-chain molecules adsorbed onto particle surface repel each other, resulting in large inter-particle repulsive forces. The physical basis of the steric repulsion between particles arises from (i) a volume restriction effect arising from the decrease in possible configurations in the region between the two surfaces, and (ii) an osmotic effect due to the relatively high concentration of adsorbed molecules or chains in the region between the particles as they approach [57].

**Other forces:** Other forces which, depending upon the situation, can play a role in the behavior of a colloid include the following [57]:

1. External forces such as those due to electric, magnetic or gravitational fields.

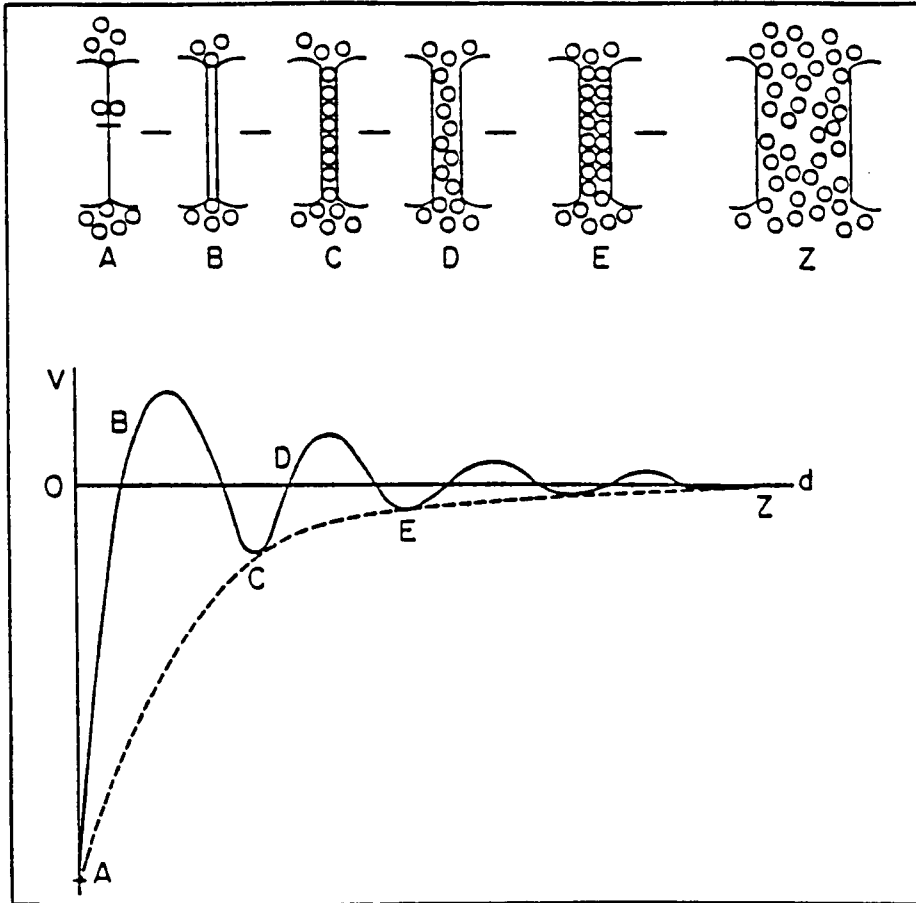


Figure 3.5: Structural forces [57]

Table 3.2: Characteristic forces on a colloidal particle ( $N/m^2$ ) [94]

Force	Sphere radius	
	$10^{-2} \mu\text{m}$	$1 \mu\text{m}$
Brownian	$10^{-13}$	$10^{-15}$
Viscous	$10^{-20}$	$10^{-14}$
Dispersion	$10^{-12}$	$10^{-14}$
Electrostatic	$10^{-12}$	$10^{-12}$

2. Chemical and colloidal forces which result from interactions of the molecules of the media (e.g., van der Waals, Coulombic forces and others).
3. Forces which arise from the motion of the particle in the fluid, e.g., hydrodynamic and diffusion forces.

We have, thus far, identified a variety of forces which could possibly act on a colloidal particle. “These different forces act simultaneously on various particles in a fluid dispersion and compete to determine the dynamics of colloid particles. The outcome of this is a delicate balance among a number of strong inter-particle forces. Since slight changes in chemical or mechanical environment can alter the magnitudes of these forces, such a change translates into large changes in the dominant forces, the structure and thus, the behavior of the colloidal system, it is not incorrect to think that the properties of the particles and the chemistry of the fluid are closely interrelated” [94]. Table 3.2, extracted from Russel [94], shows the importance of some of the forces for particles of different sizes.

The relevance of different forces to different particles is very strongly a function of the particle size. Russel [94] estimates the characteristic times and characteristic

strengths for Brownian, Viscous, Dispersion and Electrostatic forces and concludes that within the  $10^{\pm 1}$  uncertainty in the magnitudes, each of the forces can be important within the 0.1–1.0 $\mu$ m range, with the dominant ones depending on the specific conditions.

As an example, if a pair of interacting particles is considered in a hydrodynamic field, the outcome of the interaction depends on the relative position of the streamlines being followed by the particles, strength of the shear field, the size of the particles and the magnitude of the other attraction/repulsion/dispersion forces. Surprisingly enough, sanitary/environmental engineering literature seems to have been preoccupied with using merely the electrostatic and van der Waals forces to explain the behavior of colloidal suspensions in water treatment operations [18,62,84,85].

### 3.2.5. Coagulation and flocculation

At certain conditions of the suspension, the interplay of these forces results in the attractive forces being dominant. Under these circumstances, individual particles which happen to come close to each other tend to form doublets, triplets and so forth. This process of reduction of the number of basic or primary particles and the simultaneous formation of larger particle aggregates is often referred to as “coagulation” by chemists. If this process is allowed to continue for a long period of time, the particles eventually become macroscopically visible and are called “flocs” [60].

The terms “coagulation” and “flocculation” are used with slightly different connotations by the sanitary/environmental engineers. O’Melia [86] talks about the “coagulation” step consisting of two steps: (i) destabilization of particles and

(ii) transport of particulates for inter-particle contact while Amirtharajah [5] refers to “flocculation” as being the step in which particles being brought close to one another, resulting in their aggregation. Others refer to the step in which the surface chemistry of the colloids is altered as “coagulation” and the subsequent particulate collisions—brought about by transport phenomena—which result in aggregation as “flocculation” [62].

Since there are differing views as to whether the process of particle destabilization, transport and aggregation are “coagulation” or “flocculation” (not that it really matters), it is appropriate to specify what one is actually referring to when using these terms. In this work, the student prefers to use the definition as accepted by Benefield et al. [18]. They chose the definition by O’Melia [85] in which *coagulation* refers to the overall process of aggregation—including both destabilization, transport and aggregation—while *flocculation* refers solely to the particle transport step.

As mentioned earlier, like particles of a lyophobic colloid are thermodynamically unstable and have a tendency to lump together—but are prevented from doing so because of the kinetic stability imparted to them, thanks to their surface charges. In order to make the colloids coagulate, they have to be destabilized in a “kinetic” sense. This can be done using a variety of manners.

#### **Coagulation by potential control—Adsorption and charge neutralization:**

In this case, the surface potential of the particles is altered by the adsorption of the coagulant ions or precipitates, reducing the net charge on the particle surface. If this process is continued to a limit where the electric charge on the particles is actually zero, the state is referred to as the point of zero

charge (p.z.c.) for that colloid. Metal coagulants like alum and ferric sulfate display such coagulation properties at specific pH levels and are used in the destabilization of colloids in water treatment operations [18,60,85].

**Coagulation by electrolyte addition—Double layer compression:** Since the size of the repulsion barrier is determined by the nature of the material adsorbed on the particle surface, these ions are called potential-determining ions (p.d.i.). For colloids rendered stable due to their electrical surface charges, this barrier depends not only on the magnitude of these charges, but also on the physical extent of the double layer. If one adds to the suspension an electrolyte whose ions enjoy no special relationship with the surface, (called indifferent ions), the presence of these counterions in significant concentrations results in a smaller diffuse layer surrounding the colloidal particles. Larger and larger concentrations of such an electrolyte continue to reduce the volume, and thus the thickness of the diffuse layer to maintain electroneutrality. The range of the repulsive interactions between like colloidal particles decreases, and the energy barrier disappears. At this stage, the phenomenon of “rapid coagulation” occurs—i.e., there is no electrical barrier which needs to be overcome and every collision results in contact. The rate of coagulation, thus, is merely a function of the rate of particle transport. The concentration when such a phenomenon occurs is referred to as the critical coagulant concentration (c.c.c.). The behavior of colloids in such a manner is explained by the DLVO theory referred to earlier [60,85].

**Enmeshment in a precipitate:** While books in colloid sciences do not mention



any other manner in which colloids can be destabilized and coagulated (without the use of polymers), sanitary/environmental engineering literature is replete with yet another mechanism by which colloids can be removed. This is what is called the *enmeshment in a precipitate* mechanism. This mechanism should not be thought of as a “colloid destabilization” method, but merely as a “physical means of colloid removal”. Here, substantial amounts of inorganic coagulants (like alum) are added, at the appropriate pH, to the water. The coagulants, which are in amounts greatly in excess of their solubility in water, cause the water to be oversaturated with those compounds, resulting in their being precipitated out. The colloidal particles serve as nuclei around which precipitation occurs, causing the enmeshment of the particulates, which eventually settle out. Such a mode of action is referred to as “sweep-floc” coagulation.

The difference between adsorption/charge neutralization and double layer compression models is that the latter method of colloid destabilization does not reverse the charges on the colloid surface while the former mechanism can allow destabilization as well as restabilization (because of charge reversal) of the colloid. This restabilization occurs when an excess of the adsorbing, destabilizing species get attached to the particle surface, causing a reversal in the net surface charge. Such a behavior cannot be explained by the DLVO theory [85].

### 3.2.6. Conclusion

In this section, we have taken a brief overview of colloids and their behavior. Very little has been said about the manner in which the colloid destabilization step

of coagulation occurs because that is discussed later in this work in Section 3.4. The flocculation of colloids and the kinetics of the process will also be discussed later—in Section 3.9.

### 3.3. Coagulants

#### 3.3.1. Introduction

What are coagulants?

Coagulants are chemicals used for the destabilization of particulates so as to facilitate their aggregation into larger flocs as well as for the strengthening of flocs to reduce breakup [62].

A good coagulant is, among other things,

1. inexpensive
2. easily handled
3. reasonably stable with time and temperature
4. able to precipitate out/adsorb so as to result in small amounts of soluble residuals leaving in the effluent.

Alum is one such compound, as are Ferric Chloride, other  $Fe(III)$  and  $Al(III)$  salts, and synthetic organic polymers. Although we shall, in this section, only discuss the behavior of alum, the explanation can be very easily extended to understand the behavior of  $Fe(III)$  salts used as coagulants.

Now that a coagulant has been chosen, the question, naturally, arises: How much do we add? As mentioned by Kawamura [66], the coagulant dosage is one of

the most important factors in the coagulation/flocculation of colloids, as carried out in water treatment. This innocuous looking question opens a veritable Pandora's box for us. Let us look at some of the possible "what, how, when, where and why" type of questions regarding coagulants and their use. Some of these interesting questions have been posed by Edzwald in [42].

- What chemical reactions occur when the coagulant is added to water?
- How and where (in a water treatment plant) should the coagulant be added (and why)?
- What should be the final dosage in water?
- What should be the strength of the "feed solution"?
- Do feed solution characteristics have any impact on the final result?
- How should the coagulant be mixed?
- What happens to the coagulant when it interacts with particulates in the water?
- How do the characteristics of the water (like pH, alkalinity, hardness) affect the solubility, speciation and other aspects of the coagulant behavior?
- How fast/slow is the reaction of the coagulant with water/particulate matter?
- How do other entities (organic substances, e.g., those of humic origin, or ionic impurities like sulphates, phosphates) interfere with the behavior of a coagulant?

- Is there a specified set of conditions, e.g., pH, ionic strength, buffering capacity, etc. (as far as the coagulant is concerned) which must be fulfilled in order to obtain optimal results from the coagulation/flocculation/filtration process?

These are but a few of the questions which need to be answered.

Given the infinite variety of situations which can exist, vis-a-vis the nature of raw water brought into water treatment plants, as well as sundry other parameters under the control of the treatment plant operator, it is impossible to create one universal set of guidelines as far as the coagulant use is concerned. It is not unreasonable to think that some parameters might be much more important than others in terms of their influence on the behavior of a coagulant. As Kawamura [66] points out, "...alum coagulation and flocculation can be affected by factors such as salt concentration, pH, temperature, size of turbidity particles, mixing and alum concentration". Edzwald [42] points out that one also needs to consider chemical speciation of stock solutions, hydrolysis and complexation reactions with (water and) inorganic ions; pH-solubility relationships, speciation of products, reaction with organic substances (like those of humic origin), among other things, in order to describe coagulant behavior to any degree of thoroughness.

Stumm and Morgan [104] in their classic paper on coagulation say, "In order to achieve a greater degree of control over the coagulative treatment process, and in order to realize its potentialities for the removal of a number of dissolved as well as colloidal impurities from water, a more comprehensive chemical theory of coagulation phenomena is required. Such a theory should explain coagulation effectiveness in terms of pH, buffer capacity, hydrolysis equilibria of the coagulant metal ions, complex formation equilibria and the chemical equilibria of the colloidal or dissolved

substances to be removed.”

As we have seen, the variables which come into play during coagulation are numerous and, obviously, some play more important roles than others in the outcome of the coagulation/flocculation process. In order to visualize the interplay of these factors, it becomes necessary to describe the physical phenomena underlying the process in question. In order to do this, we shall break up the coagulation process into subprocesses which can be studied individually and can then be viewed simultaneously in order to get a ‘comprehensive’ overview of the phenomenon in question.

### 3.3.2. Hydrolysis and mononuclear hydrolysis products

Alum, as a solid, exists in many forms some of which are:

- as  $Al_2(SO_4)_3$ , a white powder with a formula weight of 342.14,
- as  $Al_2(SO_4)_3 \cdot 14(H_2O)$  or as  $Al_2(SO_4)_3 \cdot 18(H_2O)$  (hydrated forms of the above), a colorless, ionic compound with a monoclinic crystal structure and formula weights of 546.1 and 664.41 respectively [34,36].

In water treatment, most of the alum is usually used in the form of a solution.

What happens to alum when it is dissolved in water?

Ionic crystals like alum dissolve in solvents that can form an electrostatic association with the ions (of the crystal) [14]. Water molecules, formed by covalent bonding (which involves sharing of electrons), are polar in nature (in the sense that there is incomplete transfer of electrons from the hydrogen atoms to the oxygen and so the oxygen atoms acquire a slightly negative charge and the hydrogen atoms, a

positive charge). When alum crystals are introduced into water, the polar water molecules are able to associate with the positive  $Al^{3+}$  ions and the negative  $SO_4^{2-}$  ions, as shown in Figure 3.6. This results in a gradual breakup of the crystal, as ions leave the crystal and go into the solution as “solvated ions” [74]. This process is called solvation and the end result is that “. . . each ion in solution is surrounded by a sheath of a few solvent (water) molecules bound to the ion by electrostatic forces and travelling through the solution with the ion” [74]. Thus, although we talk of “free” Aluminum ions in solution, it is truly a misnomer since the ion is actually associated with the surrounding water molecules. We must visualize each solution as being constituted by many species of complex ions, i.e., both anions and cations. In fact, the “free” metal ions are actually “aquo complexes” with water being the ligand that binds to the metals [79].

Morel [79] describes the state of “free” ions in more detail. There are four solvent regions around a metal ion, as shown in Figure 3.7. (The descriptions below are based on his presentation [79].)

- A primary solvation shell where the water molecules are considered chemically bound to the ion. In the case of Aluminum, there are six such water molecules, leading to the often used, more accurate symbolism  $Al(H_2O)_6^{3+}$  instead of  $Al^{3+}$  for the hydrated Aluminum ion.
- A secondary solvation shell where the water molecules are ordered by the electrostatic influence of the ion. The volume of this shell increases with the charge of the ion and is inversely related to its size.

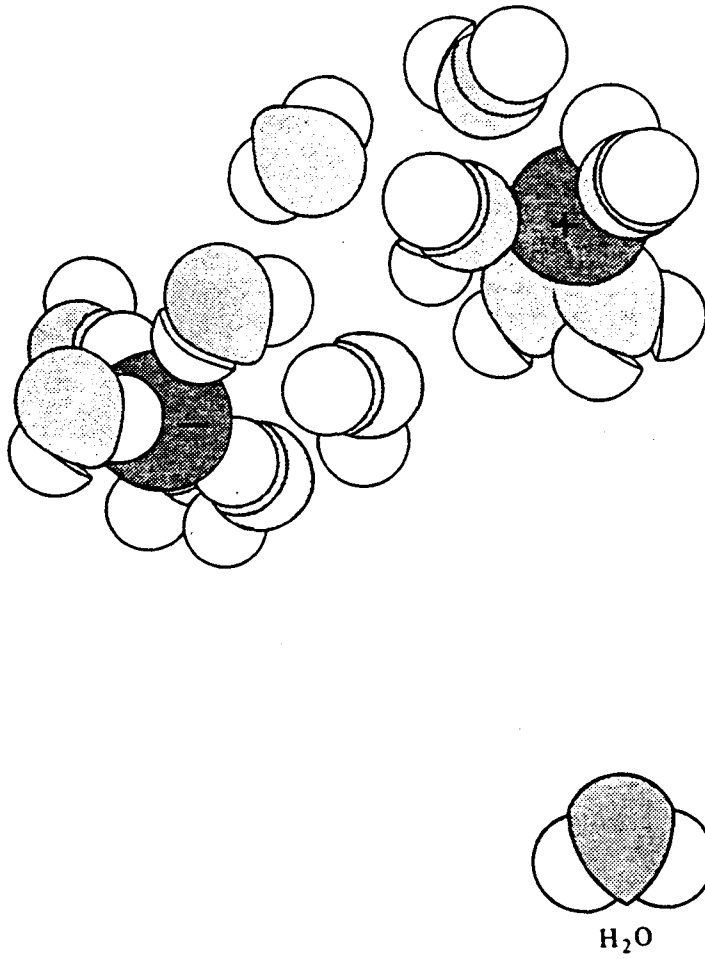


Figure 3.6: Solvation of ions in water [14]

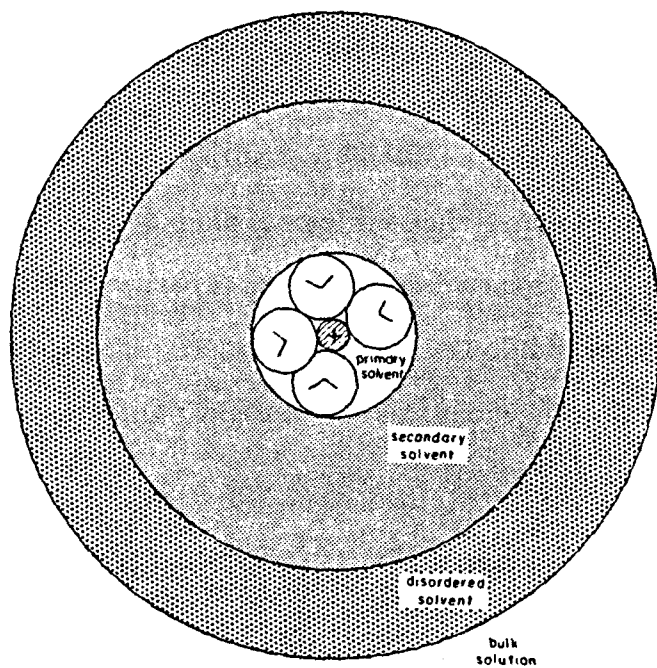


Figure 3.7: The various solvent regions around a metal ion [79]



- A transition region separating the hydrated metal ion from the bulk solution. In this region the water molecules are considered less ordered than in either the solvation shell or the bulk solution.
- The bulk solution, where the presence of the metal ion is not felt.

Six water molecules form the primary solvation shell around an Aluminum ( $Al^{3+}$ ) ion. Thus for  $Al(III)$ , the coordination number, which is "... the number of nearest neighbors—surrounding atoms/molecules—of a particular ion" is six [106]. Most metal cations show even coordination numbers of 2, 4, 6 or 8. The coordination number also describes the structural arrangement of the metal ion, called the *central atom*, and the surrounding molecules, atoms or ions, *ligands*. The ligand atoms are [106]:

- linearly arranged around the central ion for complexes of coordination number 2,
- arranged in a square planar or in a tetrahedral, configuration around a central ion for coordination number 4,
- occupying the corners of an octahedron with the central atom being in the center of the octahedron for complexes of coordination number 6.

According to Snoeyink and Jenkins [100], the coordination number for a metal ion is not a fixed quantity. It "... may vary from one ion to another .... Iron(III) has coordination number 6 for water  $Fe(H_2O)_6^{3+}$ , and cyanide  $Fe(CN)_6^{3-}$ , but 4 for chloride,  $FeCl_4^-$ ." The surrounding atoms or ligands may be any chemical species with a free pair of electrons to share with the metal and thus occupy the

site of the water molecules around the central atom. Anions like halides,  $NO_3^-$ ,  $CO_3^{2-}$ ,  $SO_4^{2-}$ ,  $PO_4^{3-}$  as well as  $OH^-$  are some such ligands [79].

The maximum ligand number associated with a given cation can be thought of as being equal to its maximum coordination number. One must add to this the fact that a more specific description would involve the cation, the ligand and the ligand number associated with the two entities. For example, Stumm and Morgan [106] in an example of Fe(III) hydration refer to "...the average number of hydroxide ions bound per iron(III) atom" as being "the ligand number."

Based on the description by Morel [79], we know that whenever a cation moves, it is not merely the "coordinated (or ligand) ions/atoms" (i.e., entities in the primary solvation shell) which move with it but many more, as shown in Figure 3.7. According to Levine [74] the average number of water molecules that move with the ion is called the *hydration number* ( $n_h$ ) of the ion. This number depends on the size (diameter) of the ion. Levine [74] also shows that smaller size cations of a given valence produce a more intense electric field around them than larger cations and, therefore, hold onto more water molecules than latter [74].

Having covered a few of the basic definitions, let us take a closer look at the process of hydrolysis. Hydrolysis, according to Baes and Mesmer [15] is a "... word applied to chemical reactions in which a substance is split or decomposed by water" such as "...the solution of salts and the reactions by which they are converted to new ionic species or to precipitates—oxides, hydroxides, or basic salts." Our primary interests lie in the hydrolysis of cations to form soluble hydroxide or oxide complexes as well as the formation of hydroxide and oxide precipitates.

Before going any further, it is prudent to clarify the term ionic species. This term refers to "...the actual form in which a molecule or ion is present in solution" [106]. Figure 3.8 shows the various forms in which metal species exist in an aqueous system. As mentioned in Section 3.2., it is virtually impossible to draw a line between fully dissolved and colloiddally dispersed substances. For example [106], "...colloidal metal-ion precipitates such as  $Fe(OH)_3(s)$  or  $FeOOH(s)$  may occasionally have particle sizes smaller than  $100 \text{ \AA}$ —sufficiently small to pass through a membrane filter. Organic substances can assist markedly in the formation of stable colloidal dispersions" which may be one of the reasons why the usual techniques of colloid destabilization and removal in conventional water treatment operations do not work as effectively in the presence of organic contaminants.

Having clarified this matter, we return to our discussion of metal ions. Most metal ions hydrolyze easily because of [15]:

1. their ability to form strong bonds with oxygen and
2. the presence of the  $OH^-$  ligand, in water, over an immense concentration range ( $> 1$  to  $< 10^{-14}$  Molar), as a result of the small self-dissociation constant of water ( $Q_w = [H^+][OH^-] \approx 10^{-14}$  at  $24^\circ C$  [36]).

The Brønsted theory of acids and bases tells us that [106], "...an acid is a substance which can donate a proton to any other substance, and a base as any substance that accepts a proton from another substance; that is, an acid is a proton donor and a base is a proton acceptor." So, we modify our conventional image of acids and bases to think of a proton donor as an acid and a proton acceptor as a base. Since a free proton (a hydrogen ion) cannot exist in water solution; in order

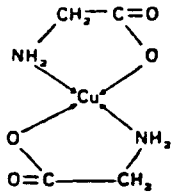
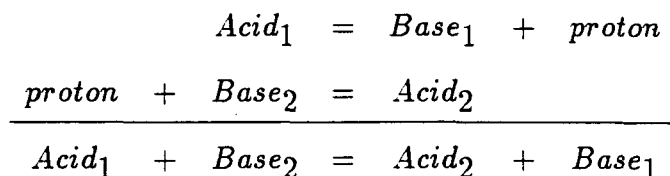
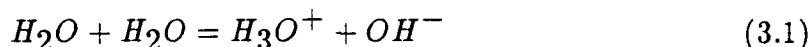
filterable membrane filterable dialysable in true solution						
Free metal ions	Inorganic ion pairs, inorganic complexes	Organic complexes, chelates	Metal species bound to high molecular wt. org. material	Metal species in the form of highly dispersed colloids	Metal species sorbed on colloids	Precipitates organic particles, remains of living organisms
Diameter range. $\leftarrow 10 \text{ \AA} \quad 100 \text{ \AA} \quad 1000 \text{ \AA} \rightarrow$						
<b>Examples:</b> $\text{Cu}^{2+}$ aq. $\text{Fe}^{3+}$ aq. $\text{Pb}^{2+}$ aq.	$\text{Cu}_2(\text{OH})_2^{2+}$ $\text{Pb}(\text{CO}_3)^0$ $\text{CuCO}_3$ $\text{AgSH}$ $\text{CdCl}^+$ $\text{CoOH}^+$ $\text{Zn}(\text{OH})_2$ $\text{Ag}_2\text{S}_3\text{H}_2^{2-}$	Me-SR Me-OOCR 	Me-lipids Me-humic-acid polymers "lakes" "Gelbstoffe" Me-polysaccharides	$\text{FeOOH}$ $\text{Fe}(\text{OH})_3$ Mn(IV) oxides $\text{Mn}_2\text{O}_3 \cdot \text{SH}_2\text{O}$ $\text{Na}_2\text{Mn}_{14}\text{O}_{29}$ $\text{Ag}_2\text{S}$	$\text{Me}_x(\text{OH})_y$ $\text{MeCO}_z$ , MeS etc. on clays. $\text{FeOOH}$ or Mn(IV) on oxides	

Figure 3.8: Forms of occurrence of metal species [106]

for a proton transfer to occur in an aqueous solution, an acid and a base must coexist [106]. Thus:



Water can be an acid as well as a base, as evident in the self-ionization reaction of solvent water:



However, water molecules which are coordinated with metal ions in a solution act as weak acids (remember: acids are proton donors). Stumm and Morgan [106]: "... the acidity of the  $H_2O$  molecules in the hydration shell of a metal ion is much larger than that of water. This enhancement of the acidity of the coordinated water may, in a primitive model, be visualized as the result of the repulsion of the protons of  $H_2O$  molecules by the positive charge of the metal ion .... Thus hydrated metal ions are acids." Or, in simple terms, the positively charged metal ion repels the positively charged hydrogen atoms which constitute the water molecules, making the water 'acidic'.

Given their ability to lose protons (or  $H^+$  ions), water molecules may exist with both their hydrogen atoms intact (i.e., as  $H_2O$ ), or with just one hydrogen atom (i.e., as  $OH^-$ ); or, perhaps, without any of the hydrogen atoms (i.e., as  $O^{2-}$ ). Thus, a metal ion in water has opportunity to coordinate with the ligands  $O^{2-}$  (to form oxo complexes),  $OH^-$  (to produce hydroxo complexes) and  $H_2O$  (to form aquo metal ion complexes). Since the pH of a solution describes the relative

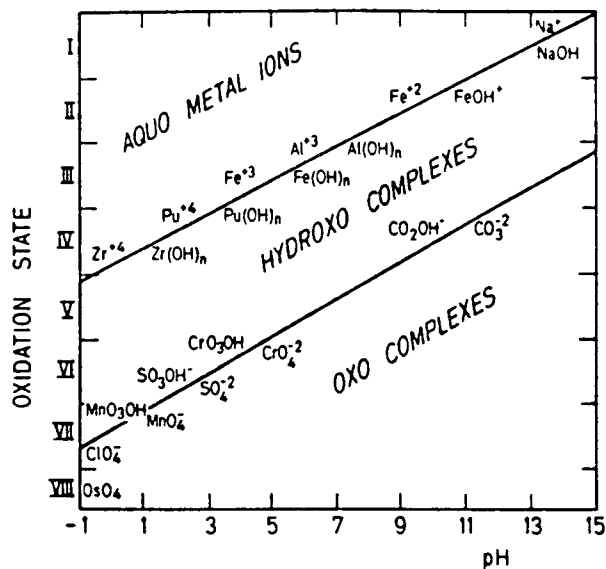
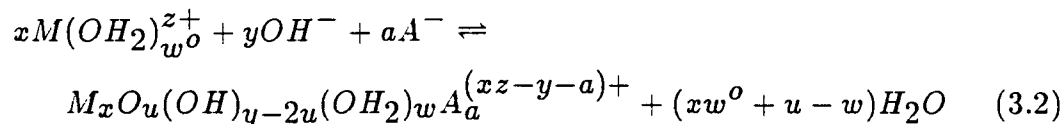


Figure 3.9: Hydrolysis of metal ions: Predominant pH range for the occurrence of aquo, hydroxo, and oxo complexes for various oxidation states of metal ions [106]

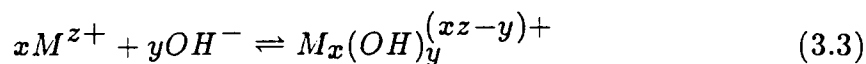
concentrations of the products of the self-ionization of water, the ligands which are coordinated with the central atom change with pH. Figure 3.9, from Stumm and Morgan [106] describes how the pH of the solution, coupled with the oxidation states of the ions, determines the nature of the predominant complex forming species. From this figure, one can see that most monovalent ions are generally coordinated with  $\text{H}_2\text{O}$  molecules while most bivalent metal ions are coordinated with water as well as the hydroxyl groups.

Since we now know that metal ions generally exist in hydrolyzed forms, let us look at the process of hydrolysis in some detail. A general formation reaction for

soluble hydrolysis products [15] is:



where one distinguishes the ligands  $O^{2-}$ ,  $OH^-$ ,  $H_2O$ , and another anion  $A^-$ . However, they add [15], "...most methods of investigation cannot distinguish one  $O^{2-}$  from two  $OH^-$  ligands, nor can they detect the  $H_2O$  ligand .... Thus, without wishing to lose sight of the possible complexity of the reactions which occur and the products formed, we will usually simplify the reaction and formulas by considering hydroxide to be the only ligand; for example, the last reaction can be rewritten as:



In most cases this will be an adequate representation for our purposes" [15].

Baes and Mesmer provide an excellent discussion of the hydrolysis of cations and the *soluble* species formed as a consequence of hydrolysis:

Most cations form one or more hydrolysis products .... Because of the number and diversity of the hydroxide complexes which can be formed in solution, the resulting chemical behavior of a given metal can be a complicated function of pH and concentration and—if the identity and stability of the hydrolysis products are not known—quite unpredictable.

The determination of the identity of dissolved hydrolysis products has proven to be a difficult and challenging task primarily for two reasons:

1. The hydrolysis complexes formed are often polynuclear, that is, they contain more than one metal ion. It can be readily perceived that this can result in the formation of a far greater variety of species than would be the case if only mononuclear species were

formed during the hydrolysis of a cation. Less obvious, perhaps, is that this can also allow more hydrolysis products to be present simultaneously in appreciable amounts. The diversity of possible species and the number which can appear more or less simultaneously greatly complicate the problem of identifying them and determining their stability.

2. The range of pH over which the formation of soluble hydrolysis products can be studied is often limited by the precipitation of the hydroxide or the oxide of the metal cation. While the range of conditions studied usually can be extended to quite supersaturated solutions, the limitations imposed by hydrolytic precipitation are often severe, rendering the problem of characterizing the hydrolysis products formed in solution even more difficult than would otherwise be the case.

They go on to describe the importance of soluble metal hydrolysis products [15]:

Soluble hydrolysis products are especially important in systems where the cation concentrations are relatively low . . . . The formulas and charges of the hydrolysis products formed in such systems can control such important aspects of chemical behavior as

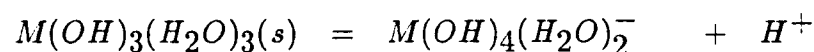
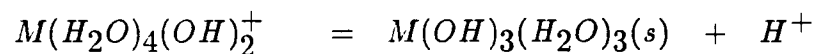
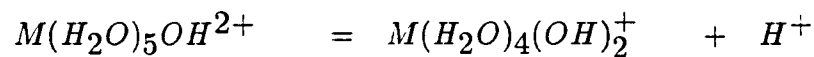
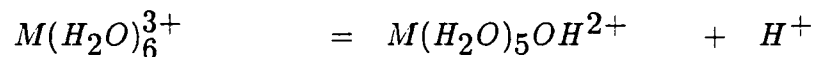
1. adsorption of the dissolved metal on the surface of mineral and soil particles,
2. the tendency of the metal species to coagulate colloidal particles,
3. the solubility of the hydroxide or oxide of the metal,
4. the oxidizability or reducibility of the metal to another valence state . . . .

We are already beginning to see the connection between metal ion hydrolysis and coagulation in water treatment.

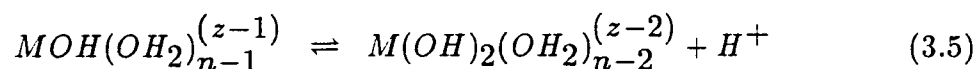
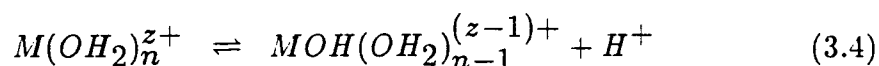
Now that we are somewhat aware of the hydrolysis behavior of metal cations, the question, logically, arises: "How does the hydrolysis occur?" Brønsted was the person who first proposed the mechanism of hydrolysis of multivalent metal ions



as being a series of consecutive proton transfer [106]. For example, for a metal  $M(III)$ ,



or, in general,

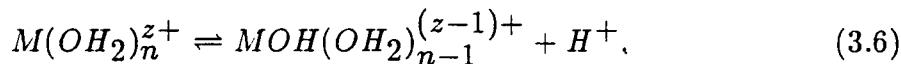


and so on.

As seen in Equations 3.4 and 3.5, "...all hydrated ions can, in principle, donate a larger number of protons than that corresponding to their charge and can form anionic hydroxo metal complexes" [106]. This explains the formation of the  $M(OH)_4(H_2O)_2^-$  species. This multistep hydrolysis mechanism is the reason why large varieties of species are formed. Moreover, in this way, species can be produced that contain  $O^{2-}$  as well as  $OH^-$  and  $H_2O$  ligands. Such hydrolysis reactions are usually rapid. Note that in all cases, only mononuclear hydrolysis species (i.e., species containing only one metal ion) are formed. For such processes, involving the formation of mononuclear hydrolysis species, this relatively simplistic picture is pretty accurate [15].

The mononuclear hydroxide complexes, known to be generated in reactions of the type shown in Equations 3.4 and 3.5, are stable. This suggests that the  $OH^-$  ions are bound directly to the cation, hence the formation of the first mononuclear

species can occur simply and rapidly by the loss of a proton from the hydrated cation as

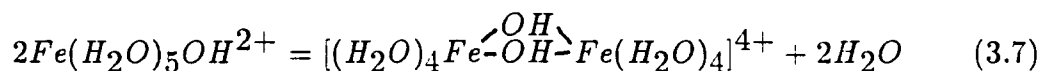


As additional protons are lost to produce the successive mononuclear species, at some point a decrease in coordination number may occur. For example, the  $Al(OH_2)_6^{3+}$  ion can be hydrolyzed ultimately to  $Al(OH)_4^-$ . Also, as mentioned earlier, this is a pH dependent phenomenon. Shown, in Figure 3.10 is the pH range over which the soluble mononuclear complexes of  $OH^-$  and/or  $O^{2-}$  ligand predominate provided the metal concentration is low enough to prevent the formation of polynuclear species. The formulas have been written excluding the  $H_2O$  ligands. Thus,  $Al(OH)_4(OH_2)_2^-$  is written as  $Al(OH)_4^-$ .

### 3.3.3. Polynuclear species

Most of our discussion, so far, has revolved around mononuclear species. While investigators initially assumed the existence of only mononuclear species, they soon became aware of polynuclear species in solution of metal cations. What are polynuclear species? As the name itself suggests, polynuclear species are just like mononuclear hydration complexes—except that they contain many metal ions and not just one metal ion. We can see some examples of such species in Figure 3.11.

According to Stumm and Morgan [106], "...the existence of multinuclear hydrolysis products is a rather general phenomenon. For example, the hydrolysis species like  $Fe(H_2O)_5OH^{2+}$  can be considered to dimerize by a



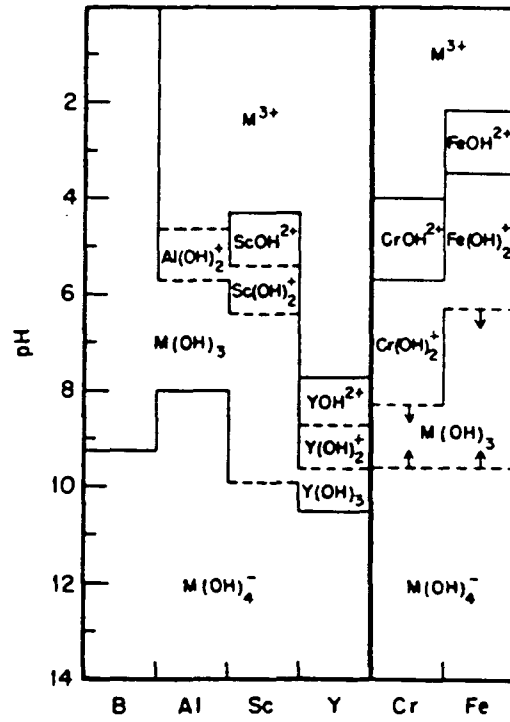

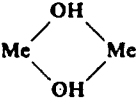
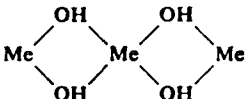
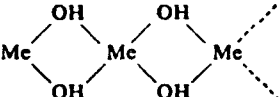
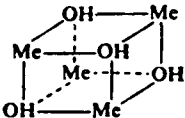


Figure 3.10: Predominance diagram for the mononuclear species of trivalent metals [15]

Type	Metals Believed to Form Such Complexes
	Be(II), Mn <sup>2+</sup> , Zn(II), Cd(II)
	Cu(II), Fe(III), Hg(II), Sc(II), UO <sub>2</sub> <sup>2+</sup>
	Hg(II), Sn(II), Pb(II), Sc(III)
 (Me(OH) <sub>2</sub> ) <sub>n</sub>	Sc(III), In(III)
 (Me <sub>4</sub> (OH) <sub>4</sub> ) <sub>n</sub> Varied	Pb(II)  Be <sub>3</sub> (OH) <sub>3</sub> <sup>3+</sup> , Bi <sub>6</sub> (OH) <sub>12</sub> <sup>6+</sup> , Pb <sub>6</sub> (OH) <sub>8</sub> <sup>4+</sup> Al <sub>7</sub> (OH) <sub>7</sub> <sup>7+</sup> , Al <sub>13</sub> (OH) <sub>13</sub> <sup>13+</sup> , Mo-O <sub>28</sub> <sup>6-</sup> V <sub>10</sub> O <sub>28</sub> <sup>6-</sup>

(b)

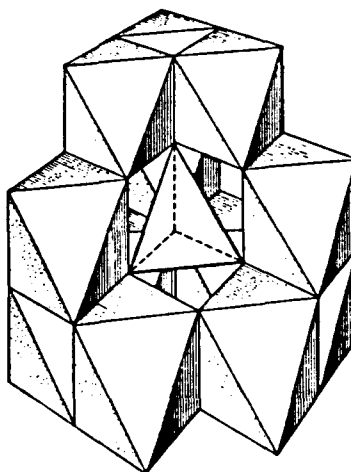


Figure 3.11: Multinuclear complexes. (a): Examples of multinuclear complexes and metals known to form such complexes [106]; (b): The  $[Al_{13}O_4(OH)_{24}(H_2O)_{12}]^{7+}$  ion. The drawing shows how the 12  $AlO_6$  octahedra are joined together by common edges. The tetrahedron of oxygen atoms in the center of the structure contains one four-coordinate aluminum atom. (Figure and caption copied from Baes & Mesmer [15])

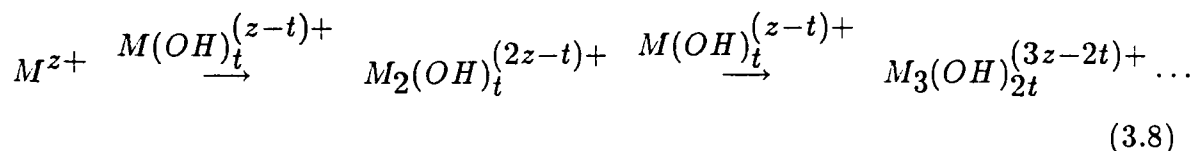
condensation process . . . . The dimer may undergo additional hydrolytic reactions which could provide additional hydroxo groups which then could form more bridges. The terms 'ol' and 'oxo' are often used in referring to the  $-OH-$  and the  $-O-$  bridges. A sequence of such hydrolytic and condensation reactions, sometimes called olation and oxolation, leads under conditions of oversaturation with respect to the (usually very insoluble) metal hydroxide, to the formation of colloidal hydroxo polymers and ultimately to the formation of precipitates."

In other words, the formation of most polynuclear species results from the almost unique tendency of  $OH^-$  among the simple ligands to form bridging linkages between two (or more) cations. Hydroxide bridges seem to be responsible for the formation of nearly all the polynuclear species of the  $M^{2+}$ ,  $M^{3+}$  and  $M^{4+}$  cations, the  $OH^-$  being shared by either two or three adjacent cations. Such reactions (i.e., the formation of polynuclear species), as well as the simple loss of a bound water molecule, involve the rupture of an  $M-OH_2$  bond, and this can be a much slower process as compared to the formation of mononuclear hydrolysis products. While the hydroxide complexes formed at very low concentrations are usually mononuclear, these simpler hydrolysis products often have not been characterized because, at the higher concentrations where hydrolysis is normally studied, the polynuclear complexes usually are dominant. The strong tendency of  $OH^-$  to coordinate more than one cation in solution to form bridges is almost unique among the simple ligands. It is probably caused by the relatively large negative charge that can reside on the oxygen atom in the electric field of two or more neighboring cations. In the pH range lower than the zero point of charge of the metal hydroxide precipitate, positively charged metal hydroxo polymers prevail. In solutions more alkaline than

the zero point of charge, anionic hydroxo complexes (isopolyanions) and negatively charged colloids exist.

While a variety of polynuclear species are formed, the number is by no means as large as investigators once thought. (For more details see Baes and Mesmer [15]). The most favored configurations for polynuclear species appears to be symmetrical ones [15], as shown in Table 3.3.

Some of the first proposals of a general mechanism of hydrolysis and formation of polynuclear species were by Sillén. He suggested that  $M(OH)_t^{(z-t)+}$  groups are added stepwise to the cation, as shown in Equation 3.8:



Quoting Baes and Mesmer [15], "This hypothesis of continuing polymerization (the "core-plus-links" hypothesis) was an appealing simple concept, but ... it soon became clear that this stepwise polymerization process rarely, if ever, occurred."

Now, after more extensive work on this phenomenon, it is thought that while [15] "... cations generally appear to hydrolyze to give mononuclear species at sufficiently low concentrations, they often produce a small number, usually one to three, of polymer species which predominate at ordinary concentrations. All but a few such species are to be found among the following dimers, trimers and tetramers such as shown below:

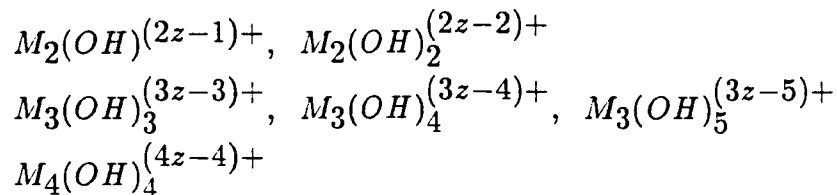

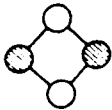
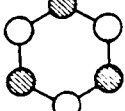
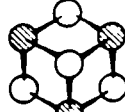
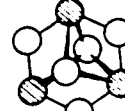

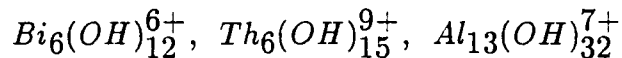


Table 3.3: Occurrence and structure of polynuclear hydrolysis products [15]

Species	Cation	Probable Structure ● = $M^{z+}$ , ○ = $OH^-$
$M_2OH^{3+}$	$Be^{2+}, Mn^{2+}, Co^{2+}, Ni^{2+}, Zn^{2+}, Cd^{2+}, Hg^{2+}, Pb^{2+}$	
$M_2(OH)_2^{(2z-2)+}$	$Cu^{2+}, Sn^{2+}, UO_2^{2+}, NpO_2^{2+}, PuO_2^{2+}, VO^{2+}, Al^{3+}, Sc^{3+}, Ln^{3+}, Ti^{3+}, Cr^{3+}, Th^{4+}$	
$M_3(OH)_3^{3+}$	$Be^{2+}, Hg^{2+}$	
$M_3(OH)_4^{(3z-4)+}$	$Sn^{2+}, Pb^{2+}, Al^{3+}, Cr^{3+}, Fe^{3+}, In^{3+}$	
$M_3(OH)_5^{(3z-5)+}$	$UO_2^{2+}, NpO_2^{2+}, PuO_2^{2+}, Sc^{3+}, Y^{3+}, Ln^{3+}$	
$M_4(OH)_4^{4+}$	$Mg^{2+}, Co^{2+}, Ni^{2+}, Cd^{2+}, Pb^{2+}$	
$M_4(OH)_8^{8+}$	$Zr^{4+}, Th^{4+}$	$M_4$ square with eight $OH^-$ ions, one centered over and under each edge.
$M_6(OH)_8^{4+}$	$Be^{2+}, Pb^{2+}$	$M_6$ octahedron with eight $OH^-$ ions centered on faces.
$M_6(OH)_{12}^{6+}$	$Bi^{3+}$	$M_6$ octahedron with 12 $OH^-$ ions centered along edges.

Occasionally, higher polymers such as



occur.”

It must be emphasized that the polynuclear species need not necessarily be linear species. They can be linear, planar or three dimensional complexes, as shown in Figure 3.11 and Table 3.3. As mentioned earlier, the formation of such polynuclear species is an intermediate step in the formation of insoluble precipitates.

#### 3.3.4. Dilution, pH and nature of hydrolysis species

We have, thus far, studied mononuclear and polynuclear species individually. Obviously, in a real solution, these will exist simultaneously. We now look at the relative amounts of each of the species, as they coexist in a real solution.

In the hydrolysis of metal cations, the following rules can be established [106]:

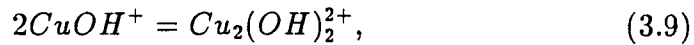
1. The tendency of metal ions solutions to protolyze (hydrolyze) increases with dilution and with decreasing  $[H^+]$ .
2. The fraction of polynuclear complexes in a solution decreases on dilution.

Therefore, there must exist concentration regimes where either the mononuclear species predominate or the polynuclear species, or both. For a given metal cation, one can calculate the conditions corresponding to a “mononuclear wall.” A “mononuclear wall” can be thought of as the concentration of the metal ion where the polynuclear species concentration is much, much less than the concentration of the mononuclear species. For example, we might want to find the concentration of a



salt in water when the concentration of the polynuclear species,  $M_{polynuclear}$ , is 1/100 of the concentration of the mononuclear species,  $M_{mononuclear}$ . Stumm and Morgan [106] illustrate this with an example:

In the dimerization of  $CuOH^+$ ,



... the dimerization is concentration dependent. Thus for a  $Cu(II)$  system where  $Cu_T = [Cu^{2+}] + [Cu(OH)^+] + 2[Cu_2(OH)_2^{2+}]$ , the equilibrium can be formulated as:

$$\frac{[Cu_2(OH)_2^{2+}]}{[CuOH^+]^2} = \frac{[Cu_2(OH)_2^{2+}]}{(Cu_T - [Cu^{2+}] - 2[Cu_2(OH)_2^{2+}])^2} =^* K_{22} \quad (3.10)$$

and it becomes obvious that  $[Cu_2(OH)_2^{2+}]$  is dependent upon  $Cu_T$ . With the help of Equation 3.10 and



for each pH, the mononuclear wall (e.g.,  $Cu_T$  for  $[Cu_{dimer}] = 1/100[Cu_{monomer}]$ ) can be calculated ....

In other words, given the ionic strength of the metal ion and the pH of the solution, it is possible to calculate the relative concentrations of the mononuclear and polynuclear species. Or, for a given pH, one can calculate the total metal ion concentration at which the concentration of one species will predominate over the other.

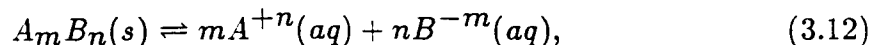
### 3.3.5. Precipitation

We have, so far, been concerned solely with soluble species formed when a salt is dissolved in water. What happens when the solution is "oversaturated"? Precipitation occurs. Since, in water treatment, most of the chemical dosage of

metal coagulants takes place at levels exceeding the solubility limits of the chemical (i.e., in the precipitation zone), we must study how this phenomenon occurs.

The formation of a precipitate can be thought of as the culmination of the process of hydrolysis and the formation of polynuclear complexes. These polynuclear species can be thought of as "... aggregates of ions that form the building stones in the lattice" which "... combine with other ions to form neutral compounds" [106]. How do these dissolved polymeric species end up forming insoluble precipitates? In order to form a precipitate, these species need a nucleation site around which they can precipitate out of solution. Quoting Morel [79], the "... initial formation of solid nuclei by precipitates in a saturated solution is a very complicated process, usually involving the formation of polymeric species. Owing to their large surface to volume ratios, and hence their large surface energies, small solids are inherently less stable than large solids .... In natural waters, there are usually plenty of suspended particles to serve as nuclei for precipitation substances." The precipitates form around these suspended particles, enveloping them in the process of precipitating out of solution.

The precipitation of ionic salts from their solutions in water brings us to the topic of solubility. Solubility equilibria can be described, mathematically, in terms of the conditions under which precipitation occurs. The dissolution of an ionic compound in water follows the equation [106]



the solubility expression being

$$K_{so} = \{A^{+m}(aq)\}^m \{B^{-m}(aq)\}^n \quad (3.13)$$

However, only in a few cases can one calculate the solubility of a salt from its solubility product alone. Since salts, cations, and anions interact with water and with each other to form complexes, we must consider this along with other factors, like the equilibrium of acid-base type reactions of salt with water. Stumm and Morgan [106] provide an excellent discussion of this topic.

While helpful in predicting regimes of “solubility” and “precipitate formation”, we must remember that for most substances, particularly those involved in complexation reaction with water and the hydroxide ion, these “solubility limits” are no magic lines which, if transgressed, result in spontaneous precipitation. In fact, most of such numbers which define the solubility products often have large errors associated with them and, therefore, need to be used with caution. In fact, “. . . an appreciation of the various types of precipitates that may be formed and an understanding of the changes the precipitates undergo in aging are prerequisites for understanding and interpreting solubility equilibrium constants” [106].

### **3.3.6. Conclusion**

Let us recapitulate our journey through the topic of metal salt coagulants. We started out with ionic, crystalline solids; we studied the state of “free” metal ions in water and their hydrolysis; the formation of mononuclear hydration species and polynuclear hydration species; and, finally, precipitate formation. In the next section, we shall combine our knowledge of colloids and metal coagulants and see how they interact in the process of coagulation.

### 3.4. Colloid Destabilization

#### 3.4.1. Introduction

As mentioned in Section 3.2., coagulation is the process by which the coagulant species interact with colloids (and, in the process, alter the surface chemistry of the colloidal particles) and these destabilized particles collide with each other and join to form larger particles. Colloid destabilization is undoubtedly the step which plays the most important role in conventional water treatment processes.

The question, naturally, arises: how does this tie in with coagulant hydrolysis and colloids? Particle destabilization in aqueous systems is a composite function of colloid-water, coagulant-water, and colloid-coagulant interactions [84]. We have already studied the behavior of colloids and coagulants separately and this section will bring forth the interaction between the two.

If we look back into Section 3.2. of this thesis, we notice that the methods of colloid destabilization include

1. double layer compression,
2. adsorption,
3. enmeshment in precipitates.

As far as water treatment is concerned, rarely does the “double layer compression” mechanism operate because the ionic strength in the waters is much, much lower than the levels where such a phenomenon would be deemed significant. So, it is one or both of the other two mechanisms that bring about the destabilization of colloids which are kinetically stable. As O’Melia [85] describes it, “. . . the destabilization

of colloids ... is probably accomplished either by adsorption of coagulant species or by enmeshment within hydroxide ... precipitates." Surprisingly, of these two mechanisms, most books on colloid chemistry discuss only the adsorption mode of colloid destabilization without ever mentioning the "sweep floc" type of process. Why?

Perhaps we can answer the question by the end of this section. So, let us examine these processes in detail.

### 3.4.2. Adsorption-destabilization

What is adsorption?

"Adsorption is normally thought of as a process by which a molecule or atom in a fluid is attached to a solid surface, and it is implied that the molecule (or atom) is in the same location as the site" [98].

The process of adsorption of a species from solution to the surface of a colloid involves two steps [57;98]:

- the transport step: process by which adsorbing chemical species are transported from the bulk solution to the adsorbing surface and is a "space process",
- the adsorption step: process by which the chemical species make contact with the adsorbing surface by overcoming any repulsive surface forces that may be important at short distances of separation. The interaction between the site and the species is thus a "point process".

The forces governing these two steps can be classified into three categories

Table 3.4: Intermolecular interactions of significance during adsorption [114]

---

A. Chemical Reactions with Surfaces
Surface hydrolysis
Surface complexation
Surface ligand exchange
Hydrogen bond formation
B. Electrical Interactions at Surfaces
Electrostatic interactions
Polarization interaction
C. Interactions with Solvent
Hydrophobic expulsion

---

[57,114]:

1. Forces and torques related to the motion of the fluid, motion of the particles relative to the fluid, and forces causing the Brownian motion of the particles (the hydrodynamic drag forces and torques and the 'diffusion forces' fall under this category.).
2. External forces such as those due to electric, magnetic and gravitational fields.
3. Chemical and colloidal forces which result from the interactions of particles and coagulant/solvent molecules (and/or ions) in the suspending medium. Intermolecular interactions which have some significance in these interactions include those shown in Table 3.4.

The process of transporting the chemical species from the bulk solution to the substrate is controlled by forces in the first two categories while the process of attachment to the substrate is governed by close range forces of the kind described

in the third category. Given the molecular dimensions of the chemical species in question, and knowing that conventional water treatment does not use external magnetic and electric fields, we can very easily discount the second set of factors from our problem, leaving us with hydrodynamic/diffusional forces which operate on large length scales and chemical forces operating at the smaller length scales.

How does adsorption occur? The adsorption of a molecule onto the surface of a solid involves the following steps [106]:

1. removal of solute molecule from solution
2. removal of solvent molecule from the solid surface
3. attachment of the solute molecule to the surface of the solid.

In an aqueous medium, adsorption can occur through a variety of mechanisms, which can be understood by studying the relationships between solvent, solute and surface. Among the latter, "...the chemical interactions of some importance are those of the solute with the surface and those of the solute with the solvent. The interaction of the solvent with the surface is of less importance in understanding the aquatic surface chemistry under normal circumstances, when water is the only solvent" [114].

Having discussed some generalities of adsorption, let us look at the process in the context of water treatment. As mentioned earlier, water treatment rarely involves waters of ionic strengths large enough to bring about flocculation of colloidal particles because of double layer compression. To explain the mechanism by which the presence of small amounts of metal coagulants ( $< 100$  mg/l or so) at the appropriate solution conditions (pH, temperature) brought about flocculation of colloids,

researchers [53,54,56,85,103,104,105] came to the conclusion that the adsorption of the metal species must have a hand in the process. More investigations led to the thought that it was not just any metal species that were adsorbed onto the colloid surface; only specific species behaved so.

If metal species are adsorbed from solution, what characteristic of the solution has greatest influence on adsorption? Intuition would tell us that the total concentration of the metal ions in bulk solution would be one of the factors. Actually, "Adsorption of metal ions is controlled only in part by the concentration of the free (aquo) metal ion; of considerable importance is the ability of hydroxo and other complex ions and molecules to adsorb" [56]. The same sentiments have been echoed by other workers in this field. For example, Stryker and Matijević [103] think that "...it was established without exception that the pH was the most important parameter affecting the adsorption .... As a rule, the adsorption of polyvalent metal ions increases dramatically above a certain pH. In some cases, the adsorbed amount rises continuously with an increase in pH. In other cases, pronounced adsorption maxima were observed at some intermediate pH values." Based on these arguments, the pH of the solution seems to be the most important control variable for metal ion adsorption. Quoting Schindler and Stumm [95], "The assumption that metal ion adsorption is based on competitive complex formation justifies the use of the pH value as the master variable that governs the extent of adsorption, as shown in Figure 3.12. For a given system consisting of metal ions,  $M^{z+}$  and an adsorbing (hydr) oxide, there is a range of 1-2 pH units where the extent of adsorption rises from 0% to almost 100%."

Although these general features are confirmed by numerous studies, unified



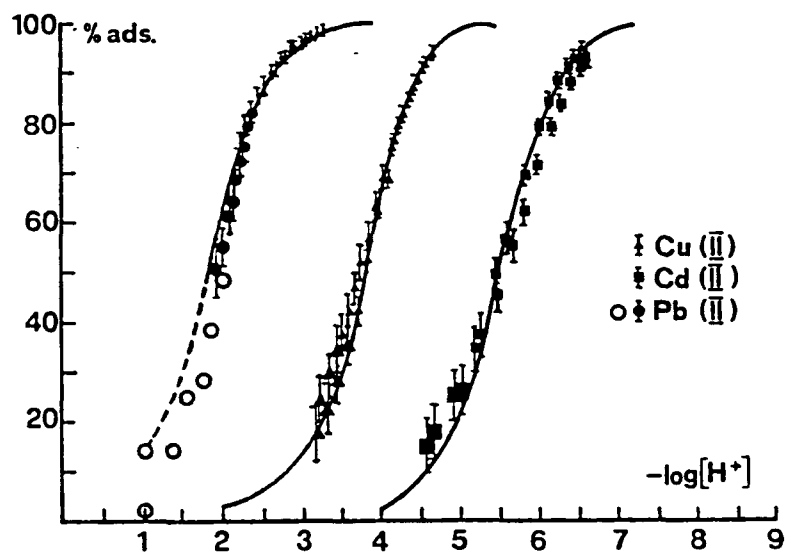


Figure 3.12: Adsorption of some divalent metal ions on  $TiO_2$ . For each metal ion there is an interval of 1-2 pH units where the extent of the adsorption rises from zero to almost 100 % [95]

interpretation has not yet been accepted. We shall now look at possible explanations for such behavior by a metal salt solution-colloids system. The increase in adsorption as a function of pH has been interpreted in a variety of ways of which two are most prominent. Both of these theories for the enhanced adsorption believe that the hydrolysis of metal ions is the cause of this improvement [56,103], though Stryker and Matijević [103] add that "...the use and the meaning of the term 'hydrolysis' is not always consistent. In some instances, this refers to the formation of soluble, while in other cases to insoluble products." It appears, though, that this observation was made prior to the point when the hydrolysis of metal ions to form soluble hydrolyzed monomeric, polymeric and finally insoluble polymeric species, as demonstrated in Section 3.3., became well established.

Questions were raised as to whether "...an enhanced adsorption at higher pH is caused by *soluble* hydrolyzed species or by the formation of *colloidal hydroxides*" [103]. Of the two competing theories the one espoused by Matijević uses *specific* hydrolysis products while some other workers rely on *general* hydrolysis products to explain this increased adsorption at higher pH. According to Healy et al. [56]:

Matijević proposed that specific hydrolysis products—e.g.,  $Al_8(OH)_{20}^{4+}$  in the  $Al(III)-H_2O$  system—are responsible for the extensive coagulation and charge reversal of hydrophobic colloids. It has also been demonstrated by Matijević that the free (aquo) species of ... metal ions is frequently unable to reverse the charge of a sol whereas the hydrolysis products, often of lower charge per ion, can reverse the electrophoretic mobilities of ... sols.

As an alternative to this explanation for the ability of *specific* hydrolyzed metal species to destabilize colloids, many workers have argued that as opposed to the free (aquo) ion, [56]

...not only is the soluble, zero charged hydrolysis product considerably more surface active than the free (aquo) ion, but also a polymeric charged or uncharged hydrolysis product may be formed at the solid-liquid interface at conditions well below saturation or precipitation in solution.

While some workers (working with the coagulation of kaolinite by aluminum(III)) "...concluded that *surface precipitates* related to hydrated aluminum hydroxide control the adsorption-coagulation behavior," others "...have postulated that the polymeric soluble uncharged  $Zn(OH)_2$  polymer can be nucleated catalytically at  $ZnO - H_2O$  interfaces and will flocculate the colloidal  $ZnO$  via a *bridging mechanism*" [56].

There are still others who believe that these two theories, the one emphasizing the "adsorption of specific often polynuclear hydrolysis products," while the other emphasizing the "role of polymeric species," are not mutually exclusive: a study on thorium (IV) adsorption has suggested a combined mechanism [56]. Thus, while the two groups of investigators do not see eye to eye on the specific hydrolyzed metal ionic species which adsorb onto solid surfaces, they all agree that the adsorption is not because of free aquo metal ions but due to hydrolyzed metal ions.

To emphasize this point, shown in Figure 3.13 is the remarkable change in the coagulation characteristics of metal ions as a function of pH. These figures, from Hahn and Stumm [53] show "...the correlation between the degree of hydrolysis of  $Al(III)$  and the effects of those aluminum species on the coagulation efficiency factor <sup>1</sup>."

---

<sup>1</sup>The collision efficiency factor is  $\alpha_p$  in the relationship  $k_p = \alpha_p 4K_B T / 3\eta$  which describes the perikinetic flocculation.  $k_p$  is a rate constant used in the equation

“A comparison of these figures leads to the assumption that  $Al(III)$  becomes an efficient destabilizing agent when it is present in hydrolyzed and multi-meric forms. The diagram shows that pH and aluminum concentrations were such that the solutions were oversaturated with respect to the solubility product of solid  $Al(OH)_3$ ” [53].

A similar behavior is displayed in the adsorption of cobalt(II) as reported by Healy et al. [56]. The adsorption of cobalt(II) at  $1.3 \times 10^{-4}$  Molar  $Co(ClO_4)_2$  is shown in the Figure 3.14. As is evident in this figure, and in all such situations, “...the most general feature of the adsorption behavior of metal ions at solid-aqueous solution interfaces is the abrupt rise in adsorption over a narrow pH range .... If we compare the pH range at which increased adsorption occurs with the properties of the solution in the same pH range, there is often a striking parallel observed” [56]. Healy et al. quote Matijević over an experiment in which “...the increase in adsorption of thorium occurs over the same pH range where the ratio  $[Th(OH)^{3+}]/[Th(NO_3)_4]$  also increases abruptly” [56]. If we look at this comment closely, we notice that it is the abrupt rise in adsorption corresponds to an increase in the amount of the hydrolyzed species.

Now look at Figure 3.15. We see that as a function of pH, adsorption of charged hydrolyzed metal species from the solution can alter the nature of the electrical charges on the surface (of the colloid) and thus, the electrophoretic mobility of the colloid. We see that the electrophoretic mobility of  $SiO_2$  in the cobalt solution

---

$-dN/dt = k_p N^2$ . In these relations,  $N$  is number of monodispersed particles/ml,  $t$  is time,  $K_B$  is Boltzmann's constant,  $T$  is the absolute temperature and  $\eta$  is the absolute viscosity [53].

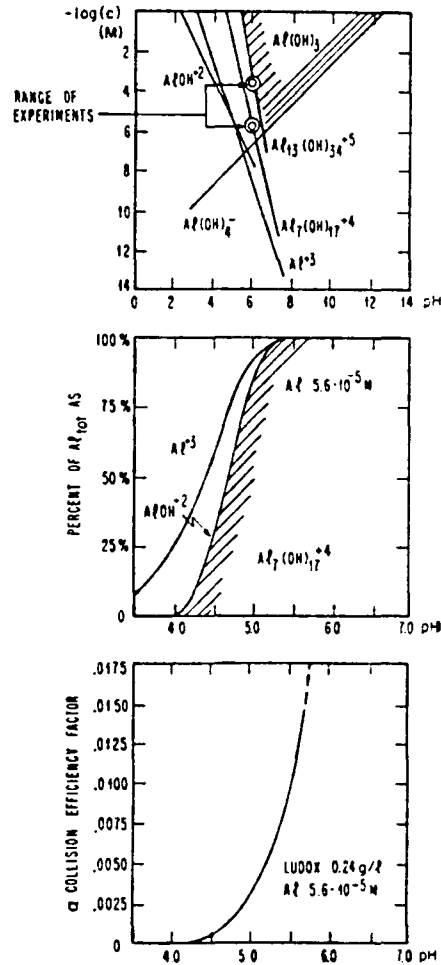


Figure 3.13: Hydrolysis of  $Al(III)$  and the effect of hydrolytic  $Al(III)$  species upon the coagulation rate. (a): Logarithmic diagram of  $Al(III)$  solubility as a function of  $Al$  concentration and pH; (b): Extent of  $Al$ -hydrolysis as a function of pH; (c): Variation of the coagulation rate, expressed as collision efficiency factor, with pH at constant  $Al$  dosage. (Figures and captions copied from [53])

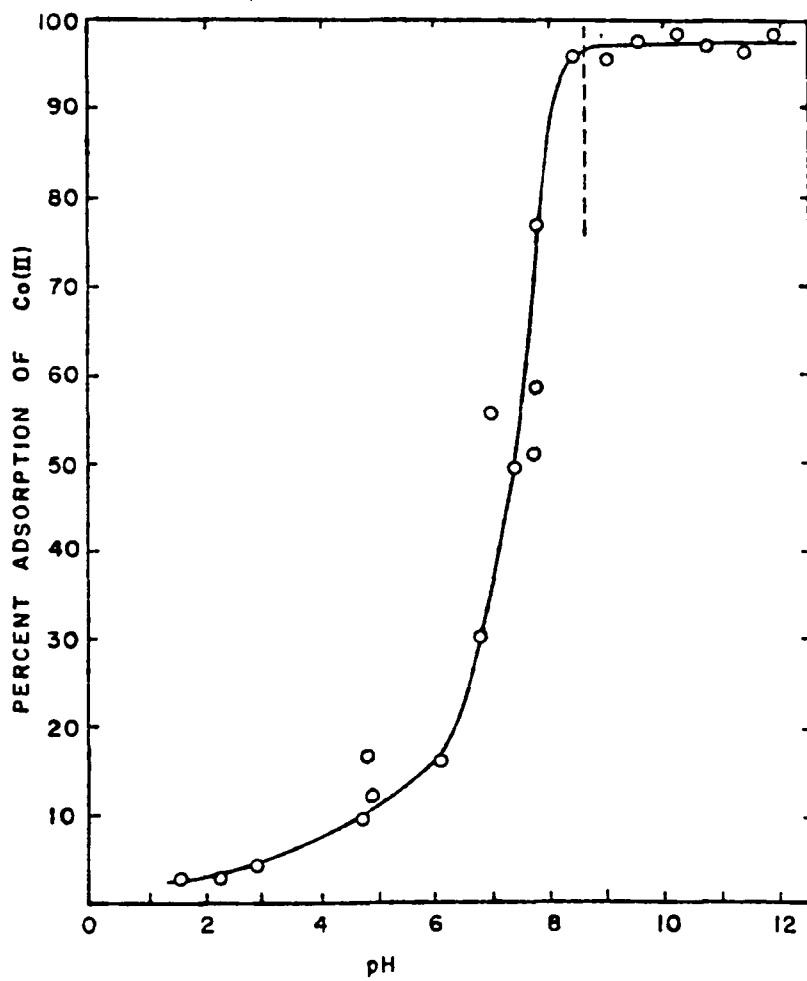


Figure 3.14: Percent adsorption on quartz of cobalt(II) as a function of pH for  $1.3 \times 10^{-4}$  Molar total  $Co(ClO_4)$  [56]

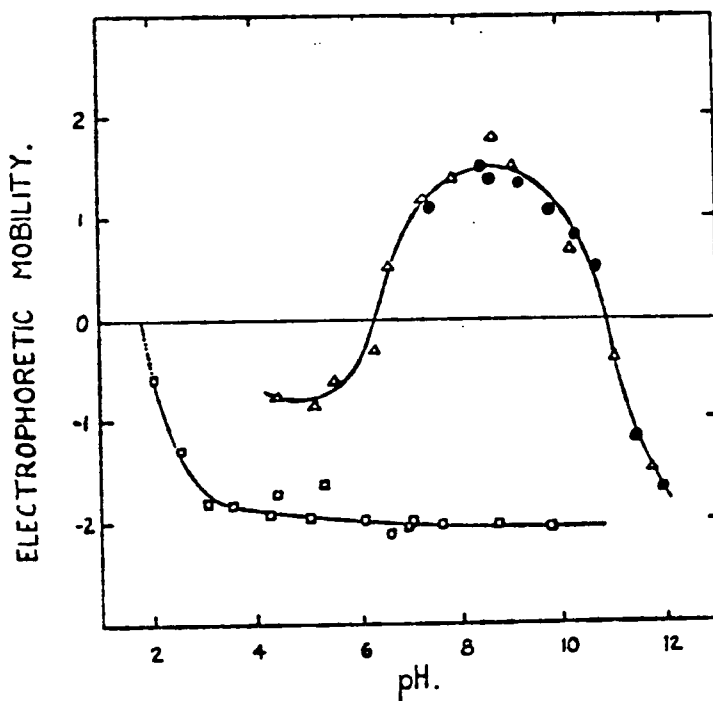
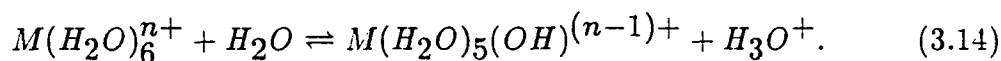


Figure 3.15: Electrophoretic mobility ( $\mu\text{m s}^{-1}/\text{volt cm}^{-1}$ ) of  $\text{SiO}_2$  in different electrolyte solutions together with the electrophoretic mobility of cobalt(II) hydroxide as a function of pH.  $\triangle$  represent  $\text{SiO}_2$  in a  $10^{-4}$  Molar solution of  $\text{Co(II)}$  in water;  $\bullet$  represent  $\text{Co(OH)}_2$  precipitates in a  $10^{-4}$  Molar  $\text{KCl}$  solution in water;  $\square$  represents  $\text{SiO}_2$  in water [56]

( $\triangle$ ) follows very much the same pattern as that of  $\text{Co(OH)}_2$  ( $\bullet$ ), as a function of pH. We can also see that in the pH region where the presence of  $\text{Co(II)}$  causes remarkable changes in the electrophoretic mobilities of  $\text{SiO}_2$ , the absence of  $\text{Co(II)}$  results in the  $\text{SiO}_2$  having an electrophoretic mobility that is almost constant with pH. This means that it is not just any hydrolysis species that is being adsorbed; it is the charged, polynuclear and colloidal hydrolysis products that adsorb onto the surface of the particles and assist in their coagulation.

Healy, James and Cooper generalize this behavior to apply to other metal ions by specifying that an increased adsorption occurs at the pH corresponding to the  $p^*K_1$  of the aquo complex; i.e.,  $*K_1$  for



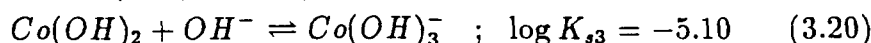
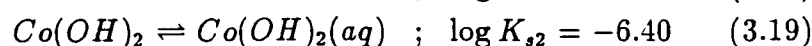
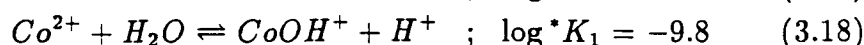
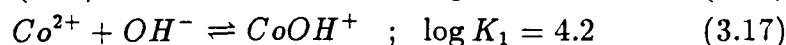
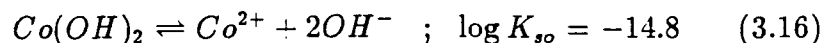
Perhaps it should be mentioned here that the hydrolysis reactions of the type mentioned in Section 3.3., i.e., of the type shown in Equation 3.15,



have their equilibrium constant preceded by a \* and they also have a subscript as shown above. This is the general relation for the addition of a protonated ligand to the complex, accompanied with the release of a proton.  $H_2O$  fits this description because  $OH^-$  is a ligand; and  $H^+$  coupled with  $OH^-$  makes water ( $H_2O$ ) a protonated ligand [97]. We now return to our discussion.

The portion below, quoted from Healy et al. [56] offers a very convincing explanation of the adsorption behavior of hydrolyzed metal species on particle surfaces:

Comparison of Figures 3.14 and 3.15 shows that at the pH range 6.5–7.5 where increased adsorption occurs, simultaneous reversal of charge and equivalent coagulation are both observed. This suggests that strong adsorption of cationic cobalt(II) species is occurring. The principal cobalt (II) solution species reported in the literature are represented in Figure 3.16 ... for the following self-consistent set of stability constants:





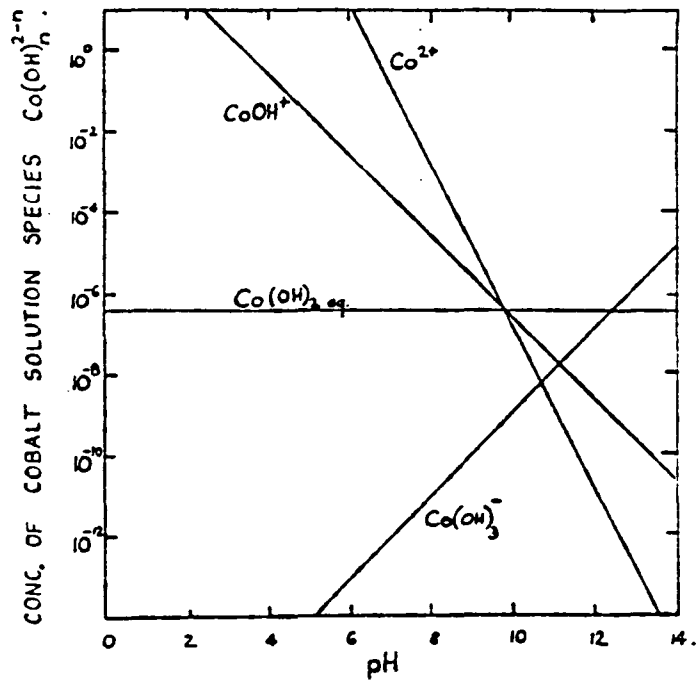


Figure 3.16: Variation with pH of the concentration of known solution species of cobalt(II) in aqueous solution in equilibrium with solid  $\text{Co(II)}$  hydroxide at  $25^\circ\text{C}$  [56]

Here,  $Co(OH)_2$  represents the solid hydroxide <sup>2</sup>. The solution data show that at pH values of 7.5 and 6.5 the dominant cobalt(II) species is the free (aquo) ion by factors of 100 and 1000 respectively. It is therefore highly unlikely that the coagulation at pH 6.5–7.5 and  $10^{-4}$  Molar  $Co(II)$  and the reversal of charge can be caused by the free  $CoOH^+$  species. If it is caused by polynuclear charged species then the log-linear relationship between the critical coagulation concentration and the valence of the coagulating ion would require a polynuclear species to have a charge of +5 or +6. Such a species has not been identified . . . . If we therefore reject polynuclear polyvalent  $Co(II)$  species, the pH 6.5–7.5 coagulation/charge reversal must be caused by the free (aquo) ion. However, since the silica surface charge is not increasing to any significant extent from pH 4.0 onwards, it is difficult to explain the drastic increase in adsorption shown in Figure 3.14 if the free  $Co^{2+}$  ion alone were the active species. However, if there is some cooperative adsorption of  $Co^{2+}$  with either bound or free hydroxide ions then an abrupt increase in adsorption is possible; remembering that the hydroxide ion concentration in the interface is greater than in solution, then specific  $Co^{2+}$  interaction with surface hydroxide ions occurs as observed at a lower pH than in bulk.

Or, in simple words, the question to be answered is that if, by the process of elimination, the ‘free’  $Co^{2+}$  species is suspected to be the culprit in the increased adsorption shown in Figure 3.14, how does this adsorption occur in a specific pH region and not others regions? The authors propose that the particle-surface and water interface has a higher  $OH^-$  concentration than the bulk solution. Thus, the pH in the interface will be larger than in the bulk solution. At this high pH (in the interface), the  $Co^{2+}$  is adsorbed onto the surface because of the presence of the hydroxide ions in the region. Why should the adsorption enhance when the bulk solution pH is not even close to being  $p^*K_1$ ? This is because the pH in the interface is greater than the pH in the bulk, according to the hypothesis of Healy et al. [56].

---

<sup>2</sup> $K_{s,i}$  represents the equilibrium constant for a solid in equilibrium with a complex  $ML_i$  and ligand  $L$  in solution [97].

Thus, the interface pH may be closer to  $p^*K_1$  even when the bulk solution pH is not. That would explain why such adsorption behavior is observed!

Summarizing the phenomenon, Healy et al. [56] conclude "... the adsorption of  $Co(II)$  at silica-water interface can be separated into 3 parts:

1. at low pH ( $< 6.0$ ) and low concentration ( $< 10^{-5}$  Molar) the active species is the  $Co^{2+}$  ion adsorbing as a nonspecifically adsorbing ion in the diffuse layer.
2. at the pH-concentration conditions above 6.5 but well below precipitation,  $Co^{2+}$  is specifically adsorbed into the Stern layer, with coagulation and charge reversal accompanying this process.
3. at pH-concentration conditions just below saturation the adsorbed species is probably a polymeric form of cobalt(II) hydroxide. At higher pH values the nucleation of cobalt(II) hydroxide is completed and the silica with adsorbed cobalt(II) behaves as cobalt(II) hydroxide. Some mutual coagulation between  $SiO_2$  and precipitated  $Co(OH)_2$  may occur for higher  $Co(II)$  concentrations."

Stumm and O'Melia [105] in their classic paper on coagulation reaffirm the conclusion that

... under favorable solution conditions (pH, temperature, applied metal ion concentration, time of aging) the hydrolysis products of iron(III) and alum(III) have a different charge than the metal ions themselves, and are adsorbed more readily at particle-water interfaces than non hydrolyzed metal ions. This tendency to be adsorbed is especially pronounced for polynuclear polyhydroxo species. No adequate theory for this enhanced adsorption by hydrolysis is available but a few qualitative reasons can be given.

- First, hydrolyzed species are larger and less hydrated than non-hydrolyzed species.
- Second, the enhancement of adsorption is due apparently to the presence of a coordinated hydroxide group. Simple hydroxide ions are bound strongly at many solid surfaces and are frequently potential determining ions; hydroxo-metal complexes may similarly or to an even larger extent be adsorbed to the solid surface. Alternatively, the replacement of an aquo group by a hydroxo group in the coordination sheath of a metal atom may render the complex more hydrophobic by reducing the interaction between the central metal atom and the remaining aquo groups. This reduction in solvent-coagulant interaction might, in turn, enhance the formation of covalent bonds between the metal atoms and specific sites on the surface of the colloidal particle by reducing the energy necessary to displace water molecules from the coordination sheath.
- Finally, adsorption becomes especially pronounced for poly hydroxo or poly metal species because more than one hydroxide group per “molecule” can become attached at the interface. Most species containing hydroxide groups in the ionic structure ... have been observed to adsorb at solid-liquid interfaces.

### 3.4.3. Surface reactions

So far, we have looked only at the coagulant behavior vis-a-vis adsorption of metal ion species on the particle. Since adsorption is a surface phenomenon, it is obvious that the particle, too, must have a role to play in this process.

A study of the surface chemistry of oxides, hydroxides and oxide minerals helps in explaining the behavior of inorganic colloidal contaminants found in natural waters.

In terms of the molecular dynamics, “The net energy of interaction of the surface with the adsorbate may result from short-range chemical forces (covalent bonding, hydrophobic bonding, hydrogen bonds, steric or orientation effects) and

long-range forces (electrostatic and van der Waals attraction forces). For some solutes, solid affinity for the solute can play a subordinate role in comparison to the affinity of the aqueous solvent" [106].

Stumm and Morgan [106] think that metal oxides surfaces, in the presence of water, are generally covered with hydroxyl groups, as shown in Figure 3.17. Quoting Schindler and Stumm [95]:

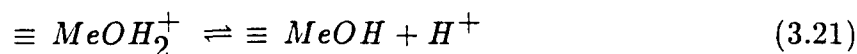
Surface chemistry of oxides, hydroxides, and oxide minerals in aquatic environments includes the reactions of hydrous oxide surfaces with electrolyte solutions. (Hydrous oxides include oxides, hydroxides, and oxide hydroxides). It thus specifically includes interactions of hydrous oxide surfaces with  $H^+$  (resp.  $OH^-$ ) ions, with dissolved metal ions, ligands, and metal-ligand complexes . . . .

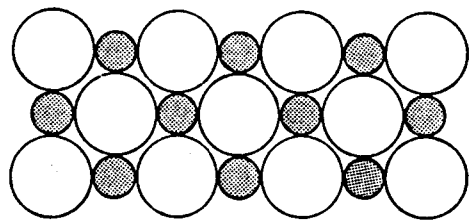
In a first step these interactions consist of adsorption of dissolved species from the bulk of the solution to the (hydrated) oxide-water interface. This step is fast and essentially reversible. It is followed by a series of slow and at least partially irreversible processes. The nature of these consecutive steps is dependent on the prevailing surface concentrations of adsorbed species.

They depict this issue very well in Figure 3.18.

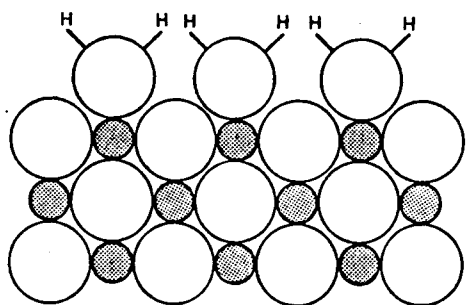
"A hydroxylated oxide particle can up to a certain degree be understood as a polymeric oxoacid or -base . . . . The specific adsorption of  $H^+$  and  $OH^-$  and of cations, anions, and weak acids (are treated) in terms of surface coordination reactions at the oxide-water interface, as shown in Figure 3.19" [106].

The pH dependent charge of metal or metalloid hydrous oxides results from proton transfers at the amphoteric surface:

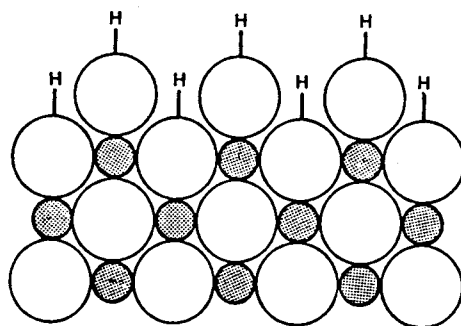




(a)



(b)



(c)

**Figure 3.17:** Schematic representation of the cross section of the surface layer of a metal oxide. ●, Metal ions; ○, oxide ions. (a): The metal ions in the surface layer have a reduced coordination number. They thus behave as Lewis acids. (b): In the presence of water the surface metal ions may first tend to coordinate  $H_2O$  molecules. (c): For most of the oxides dissociative chemisorption of water molecules seems energetically favored. Oxide surfaces carry typically 4–10 hydroxyl groups per square nanometer. (Figure and caption copied from [106])

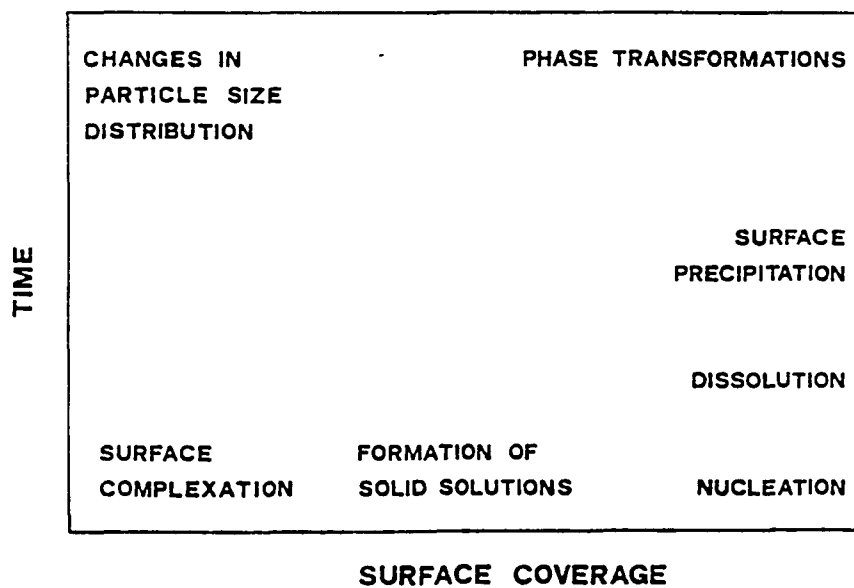


Figure 3.18: Surface chemistry of colloidal particles [95]

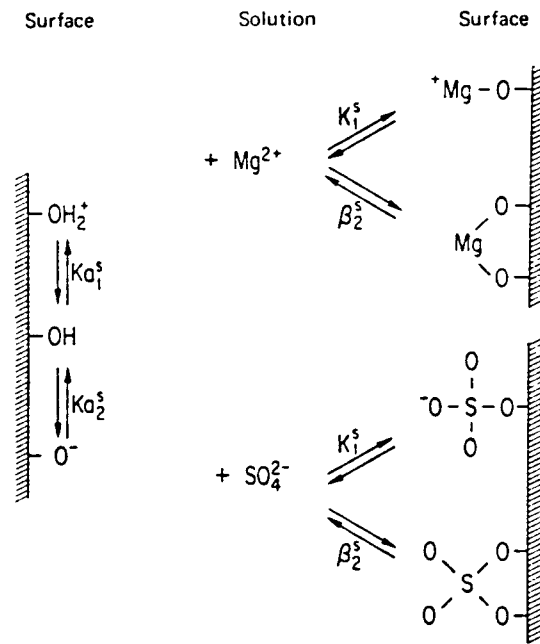


Figure 3.19: Interaction of hydrous oxides with acids and bases and with cations and anions [106]



where  $\equiv$  indicates the fact that the chemical entity exists on the surface of a particle.

“As Figure 3.19 illustrates qualitatively, the specific binding of  $H^+$  and cations increases and the specific binding of  $OH^-$  and anions decreases the net charge of the particle surface” [106].

According to Westall [114], “Adsorption driven by hydrophobic interactions is relatively easy to characterize since interactions are rather nonspecific. In contrast, adsorption at hydrous oxide surfaces is generally quite specific and correspondingly more difficult to characterize.” The immense diversity of colloids and coagulants as well as the specificity of these adsorption reactions may be one of the reasons why generalized models of adsorption of metal ions on inorganic colloids have not become very popular in environmental engineering.

Since adsorption sites on a colloidal particle are thought to be uniformly distributed all over the particle surface, it is natural to think that adsorption of species onto the surface, too, should occur uniformly and randomly over the entire surface. Actually, the adsorption pattern of these species on the surface of the solid need not be random. In fact, there is reason to suspect that it is *not* random and that there are distinct patterns in which the adsorbed species organize themselves on the surface of the solid [43]. However, “. . . adsorption of metal ions exceeding a critical surface concentration leads to formation of hydroxide clusters of the adsorbed metal on the adsorbing surface, a process that has been termed *surface precipitation*. Surface precipitation may result in complete coating of the initial surface and thus in a fundamental change in surface properties” [95].

What happens after adsorption of the species onto the surface? Once molecules are adsorbed, they undergo “. . . slow structural and chemical rearrangement . . . on

the colloid surface, directed towards the attainment of a more stable organization of the surface layer" [54]. That, perhaps, constitutes the last stage in the adsorption of hydrolyzed metal ions on a colloid and its (i.e., colloid) destabilization.

#### 3.4.4. Water treatment applications

Coming back to the water treatment context, we can now better visualize O'Melia's description of the adsorption destabilization mechanism vis-a-vis clay-like (inorganic) colloids in water. Quoting from his classic work [85]:

When a quantity of  $Fe(III)$  or  $Al(III)$  salt sufficient to exceed the solubility level of the metal hydroxide is added to water, a series of hydrolytic reactions occurs, proceeding from the production of simple hydroxo complexes through the formation of colloidal hydroxometal polymers to the formation of a metal hydroxide precipitate. These hydroxo metal complexes are readily adsorbed at the interface; simple aquometal ions are not adsorbed. It can be calculated and seen that simple soluble species do not contribute significantly to particle destabilization in water ... treatment ....

The dosages of  $Al(III)$  and  $Fe(III)$  salts required in practice for the destabilization of colloids are always sufficient to exceed the solubility of the metal hydroxide, thus it is plausible to consider that destabilization in these systems is brought about by  $Al(III)$  and  $Fe(III)$  polymers which are kinetic intermediates in the eventual precipitation of a metal hydroxide precipitate. These polymers are hydroxo metal complexes and are adsorbed on colloidal particles.

This ability of colloids to adsorb charged species from the solution results in their accumulation on the surface of these particles. This influences the net charge present on the colloid. Thus, if a negatively charged colloid adsorbs positively charged species from the solution, the net charge of the surface is decreases. As discussed in Section 3.2., this results in a lowering of the electrostatic potential which

must be overcome by another colliding particle so as to result in more 'efficient' collisions. However, since the adsorption of hydrolyzed metal species from the solution onto the colloid is not entirely governed by the electrical charges already present on the colloid, it is possible to adsorb more and more of the metal species onto the colloid so as to produce a charge reversal.

### 3.4.5. Conclusion

From the above discussion, the importance of the amount of coagulant added to a suspension as well as its pH come out as the master control variables which can make or break a coagulation process. It would be best to be able to predict, for a given amount of surface concentration (i.e., colloid surface area concentration) the dosage and pH of the suspension so as to obtain *optimal removal efficiency* in the subsequent water treatment processes—i.e., flocculation/sedimentation/filtration, direct filtration etc. However, the immense variety of raw water supplies and colloids with which water treatment plants have to grapple have made it somewhat difficult to get a generalized solution to this problem.

## 3.5. Mixing

### 3.5.1. Introduction

We have, thus far, examined the chemical aspects (colloids, coagulants) of our problem. We now go into its physical aspects.

In the process of rapid mixing, we seek to distribute coagulants in water so that we have a homogeneous mixture, at the molecular level, of coagulant species

in water. Since mechanical dispersion, by itself, cannot achieve a uniform coagulant distribution at the molecular level, molecular diffusion—in conjunction with dispersion—is needed to achieve this goal. In this section, we see the roles played by diffusion and dispersion in mixing.

### 3.5.2. Entropy and mixing

**First Law of Thermodynamics:** The energy of an isolated system is constant [14].

The first law says that in any thermodynamic process, the energy is conserved. However, we see changes all around us, some of which occur spontaneously while others do not. A hot body spontaneously loses heat to colder surroundings, gases expand irreversibly, chemical reactions run in one direction than the other. None of these phenomena are ever reversed spontaneously. The cold surroundings never pump heat into a body; gases do not spontaneously compress . . . .

In all of the cases mentioned above, even though the total internal energy of the system is conserved, there is an obvious selectivity in the processes which do take place. What is it that controls the direction of spontaneous changes?

“. . . when a change occurs the total energy remains constant, but it is parcelled out in different ways. Can the direction of the spontaneous change be related to some aspect of the *distribution* of energy? We shall see that this is so. Spontaneous changes are always accompanied by a reduction in the ‘quality’ of energy, in the sense that it is degraded into a more dispersed, chaotic form. Spontaneous, natural changes are simply manifestations of the natural tendency of the universe towards greater chaos” [14].

Let us examine the degradation of energy as illustrated by Haken [55]: “Consider a moving car whose engine has stopped. At first the car goes on moving. From a physicist’s point of view it has a single degree of freedom (motion in one direction) with a certain kinetic energy. This kinetic energy is eaten up by friction, converting that energy into heat (warming up the wheels, etc.). Since heat means thermal motion of many particles, the energy of a single degree of freedom (motion of the car) has been distributed over many degrees of freedom. On the other hand quite obviously, by merely heating up the wheels we cannot make a vehicle go.” That’s because for heat (motion of particles in all directions) to be converted to the motion of the car in one given direction is almost impossible. For such an event to occur, all the randomly moving chaotic molecules would have to become organized and move, simultaneously, in a given direction. This ‘event’ is so entirely unlikely that it can be thought of as being impossible.

Thus, the direction of spontaneous change is “...the direction of change that leads to chaotic dispersal of the total energy” or, more formally, “...the direction of spontaneous change is away from a state with a low intrinsic probability of occurring and towards one of greater intrinsic probability” [14].

“In the realm of thermodynamics, these phenomena have found a description. There exists a quantity called entropy which is a measure of the degree of disorder. The (phenomenologically derived) laws of thermodynamics state that in a closed system (i.e., a system with no contacts to the outer world) the entropy ever increases to its maximal value” [55]. Or, more formally stated,

**Second Law of Thermodynamics:** The entropy of an isolated system increases during any natural process [14].

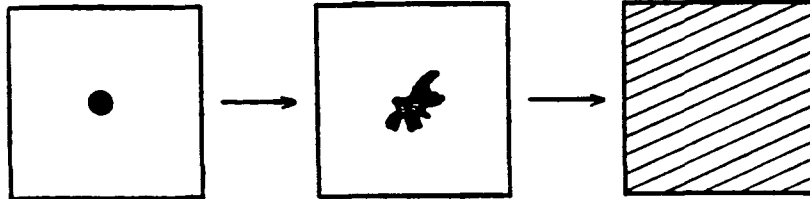


Figure 3.20: Drop of dye spreading in water [55]

How is entropy related to mixing? Increase of entropy is the principle which drives the phenomenon of mixing. It is one of the best examples of an irreversible process the result of which is an increase in entropy.

How does mixing occur? Consider a beaker full of water ( $\approx 1$  liter) into which a 1 ml drop of a concentrated dye (which has a dye content of 1 mg and the drop is of about the same density as the water) is introduced. If the beaker is left undisturbed for some time in a constant temperature environment, we will notice a gradual change in the system. The drop continues to diffuse outwards in all directions until, many hours later, the entire beaker is uniformly 'colored', as shown in Figure 3.20. The dye forms a homogeneous solution with a strength of 1 mg/liter. However, we also know that at the time of introduction, the entire dye was concentrated in just one spot.

### 3.5.3. Molecular diffusion

What caused the dye to spread? The spreading of the dye occurred through the phenomenon of diffusion. Diffusion is a “. . . macroscopic motion of components of a system that arises from concentration differences” [74] in space, at a given time. Or, being a little more specific, Adamson [1] says:

Diffusion is a process of spatial drift of molecules due to their kinetic motion; the physical picture is one of successive small, random movements. The process is often referred to as a random walk, the analogy being to a person taking successive steps but with each step unrelated in direction to the preceding one (the alternative scientific colloquialism is the “drunkard’s walk”). A given molecule will then drift away from its original position in the course of time, and purely as a statistical effect there will be a net average drift rate from a more concentrated to a more dilute region.

This is described by Fick’s law

$$J = -\mathcal{D} \frac{dn}{dx} \quad (3.23)$$

where  $J$  is the net drift expressed in molecules crossing a unit area per unit time, and  $dn/dx$  is the concentration gradient in the drift direction. The coefficient  $\mathcal{D}$  is known as the diffusion coefficient and at 1 atmosphere pressure and 25°C are typically  $10^{-1} \text{cm}^2 \text{s}^{-1}$  for gases,  $10^{-5} \text{cm}^2 \text{s}^{-1}$  for liquids, and extremely small for solids [74].

Another way of defining  $\mathcal{D}$ , as suggested by Einstein is as follows [1]:

As illustrated in Figure 3.21 a molecule will, as a result of its random walk, find itself some distance  $x$  from its starting point after an elapse of time  $t$  . . . . Consider a situation in which there is a concentration gradient in one direction only, as in the case of diffusion along the length of a long tube or cell. There will be some average distance  $x$  which a

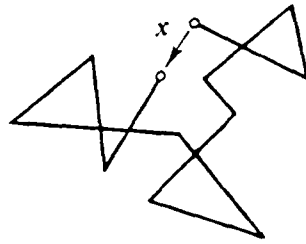


Figure 3.21: Random walk [1]

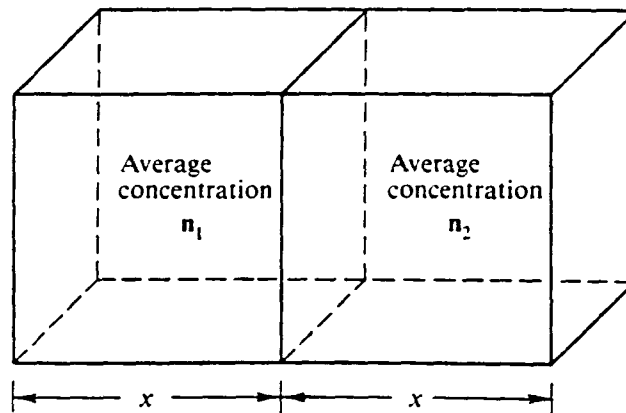


Figure 3.22: Unidirectional diffusion [1]



molecule will diffuse along the tube in time  $t$ . If we take a reference cross-section, then as illustrated in Figure 3.22, half of the molecules within a distance  $x$  on either side will cross the reference plane in time  $t$ . The diffusional flow from left to right is therefore  $\frac{1}{2}n_1x$  while from right to left is  $\frac{1}{2}n_2x$  . . . . Since  $n_2 = n_1 + x(dn/dx)$ , where  $dn/dx$  is the concentration gradient, the net flux across the reference plane is

$$J = \frac{1}{t} \left[ \frac{1}{2}n_1x - \frac{x}{2} \left( n_1 + x \frac{dn}{dx} \right) \right] = -\frac{x^2}{2t} \frac{dn}{dx}. \quad (3.24)$$

Comparison with the previous equation gives

$$\mathcal{D} = \frac{x^2}{2t}. \quad (3.25)$$

This process continues until the concentration gradient disappears ( $dn/dx = 0$ ) in the entire system. The concentration as a function of location in the above situation, can be visualized in Figure 3.23.

If we look back at the “dye-in-the-water” example, we can see that while the molecules of the dye are diffusing in all directions, moving away from the original ‘drop’ into the bulk of the solution; water molecules are diffusing from the regions surrounding the dye drop into regions of higher dye concentrations. Thus, the mixing of two substances depends on the ability of both the components to diffuse into each other, as characterized by the parameter  $\mathcal{D}$ .

Apart from  $\mathcal{D}$ , the (time) rate at which diffusion (per unit area) occurs is very strongly dependent on the concentration gradient  $dn/dx$ . The higher the concentration gradient, the faster the diffusion rate (with respect to time). In order to speed up the diffusion process, one could alter  $\mathcal{D}$  or  $dn/dx$ . However,  $\mathcal{D}$  is fixed for a given set of mixing substances and so, one cannot vary it in order to speed up mixing by diffusion.

One other variable left to play with is  $dn/dx$ —the concentration gradient. We see that in a spherical drop of dye in water, the concentration gradient between

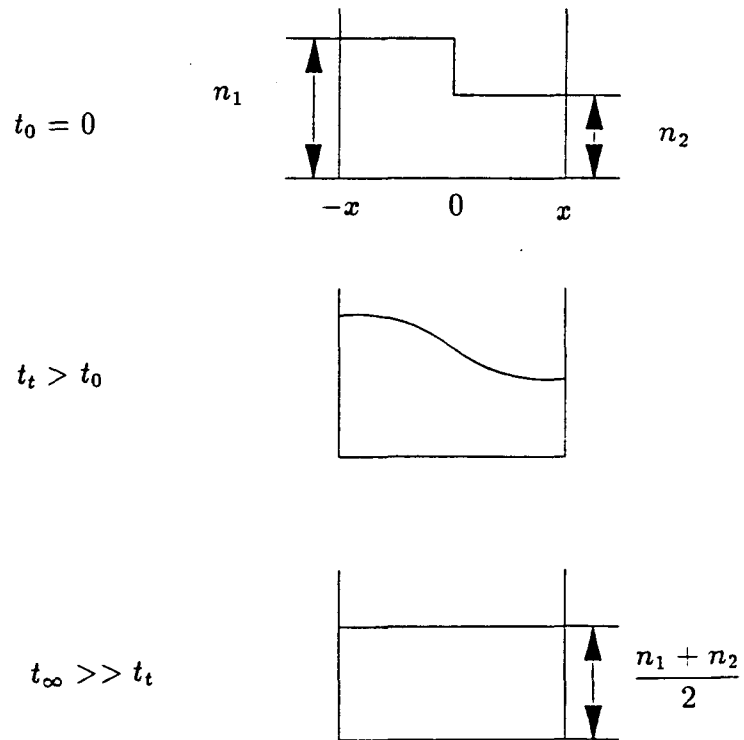


Figure 3.23: Concentration profiles during diffusion. Adapted from Levine [74]

the center of the drop and the water in the bulk of the container is  $\bar{n}/\frac{d}{2}$  where  $\bar{n}$  is the concentration of dye molecules in the drop and  $d$  is the diameter of the drop. The higher the concentration gradient, the faster the diffusion (time) rate. In order to increase the concentration gradient, one would either have to increase the concentration of dye  $\bar{n}$  in the drop, or reduce  $d$ , the diameter of the drop. Given the fact that solubility might be a limiting factor on the levels to which the concentration can be increased, the possibility of an increased diffusion because of a reduction in the drop size can be used to hasten diffusion. However, this decision would be case dependent and each mixing problem would need to be examined in order to make a proper decision.

Fick's Law (Equation 3.23) can be interpreted as saying that for a given substance, all other conditions being identical,  $J$ , the net drift expressed as molecules crossing a unit area per unit time, is directly proportional to the concentration gradient  $dn/dx$  and the drift is in the direction from a region of high concentration to a region of low concentration. Note the words "unit area". This means that for a given concentration gradient between two substances, the net diffusion will be greater for larger area of interaction.

In our case, we have a drop of volume  $1 \text{ ml} = 1 \text{ cm}^3$ . If we assume the drop is perfectly spherical to begin with, and has a diameter  $d$ , then  $\pi\frac{d^3}{6} = 1 \text{ cm}^3$ . The diameter  $d$  is 1.24 cm and the net surface area of the drop  $\pi d^2$  is  $4.84 \text{ cm}^2$ . At  $t = 0$ , we measure a concentration gradient across the drop,  $\frac{\bar{n}}{d/2} = 1.61\bar{n}$  is  $> 0$ . This means that the total instantaneous diffusion rate (at  $t = 0$ ) across the surface of the spherical drop is  $4.84 \text{ cm}^2 \times J$ .

Let us repeat this experiment by introducing into the water 100 smaller drops of the same dye solution whose combined volume is  $1 \text{ cm}^3$ , (instead of one large drop of  $1 \text{ cm}^3$  volume). The total surface area of the drops is now different, as is the concentration gradient between the center of the spherical drops and the water at the surface of these drops. The diameter of each drop is  $d_{100}$  and so  $100\pi\frac{d_{100}^3}{6} = 1 \text{ cm}^3$ ;  $d_{100} = 0.27 \text{ cm}$  and the total surface area of 100 drops is  $100\pi d_{100}^2 = 22.45 \text{ cm}^2$  which is almost 5 times the surface area of a single drop. The resulting concentration gradient at  $t = 0$  is  $\frac{\bar{n}}{d_{100}/2} = 7.41\bar{n}$ .

$J_{100}$ , the rate of diffusion per unit area per unit time when 100 droplets exist, is proportional to  $dn/dx$ .  $J_{100}/J = (-\mathcal{D}7.41\bar{n})/(-\mathcal{D}1.61\bar{n})$ . Since  $\mathcal{D}$  is the same in both cases,  $J_{100}/J = 7.41/1.61 = 4.60$ . Or,  $J_{100} = 4.60 \times J$ . If we calculate the total instantaneous diffusion rate (at  $t = 0$ ) through the entire surface area available, we get  $22.45 \text{ cm}^2 \times J_{100} = 103.27 \text{ cm}^2 \times J$  which is about 20 times the total diffusion rate as calculated for a single drop! In reducing the size of the spherical drops, we have also reduced the total distance which the molecules have to travel before they can start getting into the bulk solution. For example, for the smaller drops, the molecules originally at the center of the sphere must travel a distance  $\approx 0.14\text{cm}$  while the molecules at the center of the larger drop must travel  $\approx 0.62\text{cm}$  to reach the bulk solution. This will further reduce the time needed for uniform mixing of the molecules of the smaller droplet with the bulk fluid, as compared to the time taken by molecules of the larger drop.



Figure 3.24: The process of dispersion [28]

#### 3.5.4. Dispersion, diffusion and micromixing

It is obvious from the above example that for a given concentration of dye, the overall rate of diffusion can be increased by increasing the concentration gradient as well as increasing the “exposed” surface area of the mixing substances. We have already seen that this occurs when the drop size of the dye is reduced. If we follow these means of increasing the (time) rate of diffusion, we must find some mechanism by which larger drops can be dispersed into the other, i.e., a way by which dye can be rapidly broken into fine droplets and these droplets spread uniformly throughout the entire system so that diffusion proceeds at a faster rate than when just one big drop of dye is introduced into the system.

This point is well illustrated in the following set of figures taken from Brodkey [28]. Illustrated in Figure 3.24 is the process of dispersion—the process by which

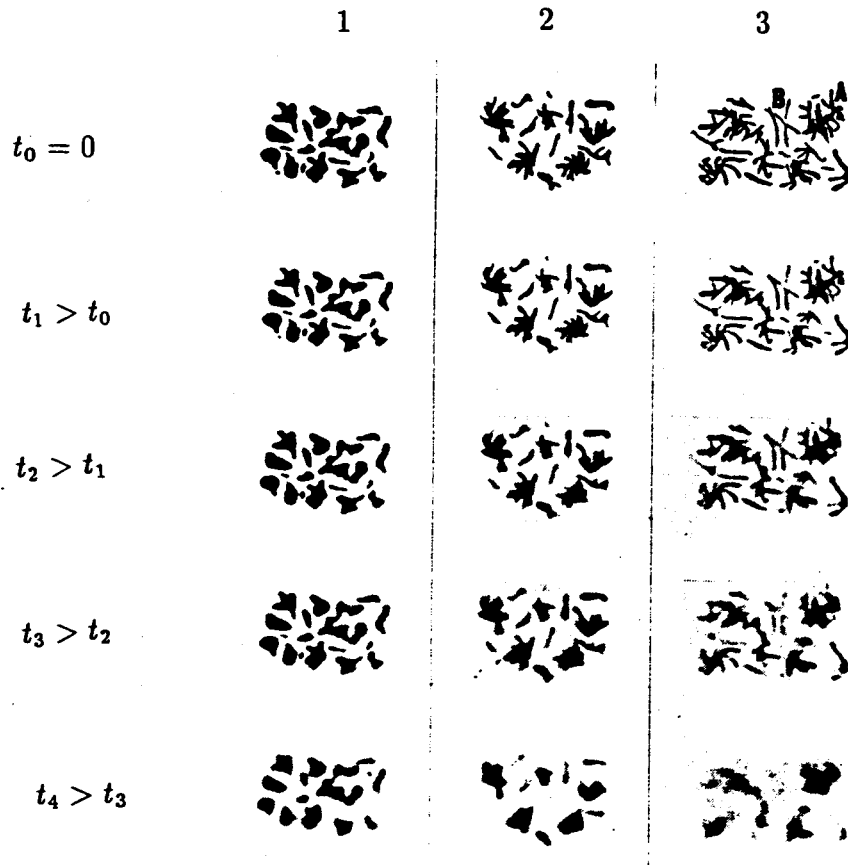


Figure 3.25: Influence of increased surface area and reduced dimensions on mixing. Adapted from Brodkey [28]

the solute fluid is broken down in a manner so as to substantially reduce the size of the ‘particles’ of solute fluid (e.g., dye solution), so as to increase the area “exposed” to the solvent (e.g., water) as well as to increase the concentration gradients.

Figure 3.25 displays the effects of size reduction on the overall rate of diffusion. We have 3 columns and 5 rows of pictures. The topmost row shows three different levels of dispersion of a dye, with increasing levels of dispersion from left to right. As we can see, the thin filamentous structure of the elements in the third column provides them with a surface area and a dye concentration gradient which is much greater than that of the elements in the first column. The elements in the middle column show an intermediate level of dispersion between the left and the right columns.

The topmost row of pictures can be regarded as  $t = 0 = t_0$  for diffusion. Pictures in the subsequent rows can be thought of as corresponding to times of diffusion  $t_1, t_2, t_3$  and  $t_4$  respectively, where  $t_4 > t_3 > t_2 > t_1 > t_0$ . These pictures show that the dye elements in the third column diffuse much faster than the elements in the first or second columns, causing the system to achieve a higher level of homogeneity than the elements in columns 1 or 2.

These figures (3.24,3.25) also illustrate the scaling nature of the mixing process. In other words, whenever we specify mixing, we must specify the scale at which we want mixing to occur. In fact, this leads to a most interesting definition of good mixing. On what basis is a mixture considered to be “homogeneously mixed” or “poorly mixed”? One way to detect homogeneity would be to take a sampler and sample the mixture at as many locations within the system as possible. If the concentration of the dye (or solute) is the same at all locations, (with due regard

to experimental errors), we can conclude that the mixture is indeed homogeneous.

This leads us to the next question: How big should the sample size be? In a beaker of water, should our sampler examine volumes of the order of  $\text{cm}^3$ ,  $\text{mm}^3$  or  $\mu\text{m}^3$ ? Aha! We have just hit upon the very heart of the scaling nature of mixing!

Once again, let us reconsider our dye experiment with which we now perform a ‘thought experiment’. This time, we have  $10^6$  spherical droplets with a total volume of  $1 \text{ cm}^3$  in 1 liter of the solution so that the dye concentration of a completely homogeneous solution is 1 mg/liter. Each droplet has a volume of  $0.000001 = 1 \times 10^{-6} \text{ cm}^3$  and these droplets are uniformly distributed throughout the entire volume.

At this instant, let us freeze the flow of time and look at the concentration of dye in the water. We know that concentration of a solute in a solvent is defined as being the mass of the solute per unit volume of the solvent. So, we take a volume of  $100 \text{ cm}^3$  and somehow separate the dye molecules from the water, weigh them and calculate the concentration. In this case, we will get a concentration of 1 mg/liter. We now repeat the same procedure by taking a volume of  $10 \text{ cm}^3$ . Again we calculate a dye concentration, which will be very close to 1 mg/liter. The same procedure is now repeated for yet smaller sample volume sizes like 1, 0.1, 0.01, 0.001...  $\text{cm}^3$  etc.

If we follow this line of action, we will notice that a plot of the calculated concentration vs. log of the size of sample volume (of the kind shown in Figure 3.26) will display a plateau for a range of sample volume sizes which lie on the right side of this figure. Given that  $10^6$  droplets of dye exist in  $1000 \text{ cm}^3$  of the solution, the smallest sample volume which will give a calculated concentration



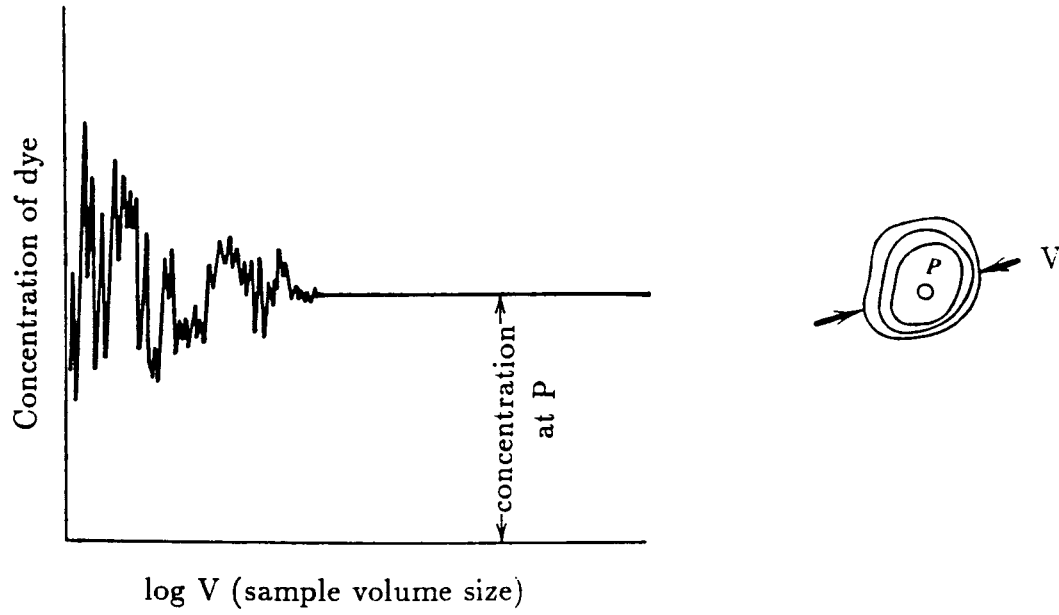


Figure 3.26: Variation of concentration with size of sample volume. Adapted from Panton [87]

similar to the “homogeneous solution concentration” is of the order of  $1000/10^6 \text{ cm}^3 = 1.0 \times 10^{-3} = 0.001 \text{ cm}^3$ . After this, as we reduce the sample volume sizes, the calculated concentrations will fluctuate wildly, giving values both above and below the “homogeneous concentration”—just as shown in Figure 3.26. If the spherical droplets had been bigger than  $1.0 \times 10^{-6} \text{ cm}^3$  in volume, this irregularity in the concentration would have been noticeable at larger sample volume sizes but if the droplets had been smaller, this irregularity in the concentration measured would have become noticeable only at smaller sample volume sizes.

Now, we “unfreeze” time and allow diffusion to spread the dye into the bulk solution. Let us call  $t_0, t_\infty$  and  $t_t$  as the times corresponding to situations where (i) diffusion has just started, (ii) diffusion has been allowed to continue for a long period of time, and (iii) an intermediate time period (i.e.,  $t_0 = 0 < t_t < t_\infty$ ) respectively. If, at  $t_t$  and  $t_\infty$  we “freeze” time and repeat our concentration calculation procedures, we will see that the sample volume size at which the calculated concentration starts behaving erratically is reduced. This means that diffusion has been reducing the inhomogeneity in dye concentrations in the “inter-droplet” region of the solution. And, at  $t_\infty$ , the solution will be as homogeneous as it can possibly be.

If we look at Figure 3.26, we see that despite homogeneity in concentration over a large range of sample volume sizes, there is still considerable variation in the region corresponding to very small sample volume sizes. These sample sizes correspond to volumes whose order of magnitude is just slightly greater than molecular volumes. Wild fluctuations in this zone occur because the dye and water molecules are in a dynamic equilibrium. Therefore, a momentary excess of either the dye or water

molecules will alter the instantaneous concentration calculations substantially.

The smallest sample volume size at which the calculated concentration is similar to the homogeneous concentration is the level at which a solution can actually be considered homogeneous. And this can only be achieved through diffusion. Dispersion, the mechanism by which the solute fluid is broken up into smaller “droplets” or “parts” can only go so far in reducing the sample volume size in an effort to make a solution “homogeneous”. After that, it is only diffusion which can bring about homogeneity at the molecular levels. Dispersion, on this basis, can be said to be able to make a solution homogeneous at larger scales of observation; while homogeneity at smaller scales of observation is the result of diffusion.

The concept of mixing at fine scales, more appropriately called *micromixing* [23,28,29] has attracted considerable attention in the field of Chemical Engineering. Bourne [23] quotes P. V. Danckwerts, the pioneer in the field of mixing:

Unless the reasons for making up a mixture are known, it is impossible to decide whether it is well or badly mixed. Any mixture, if scrutinized closely enough, will show regions of segregation—that is, the composition will vary from point to point. The size of the regions of segregations which can be tolerated will vary from one case to another. The term ‘scale of scrutiny’ will be applied here to the minimum size of the regions of segregation in the mixture which would cause it to be regarded as imperfectly mixed for a specified purpose. Defined in this imprecise way, the scale can only be expressed as an order of magnitude (length, volume or area), but the concept is a useful one.

In other words, whenever we specify mixing and homogeneity in a mixture, we must also specify the purpose of mixing as well as the scale at which we desire homogeneity—because each application may have a different requirement vis-a-vis mixing.

In a process like coagulation of colloidal particles with coagulants like alum and polymers, the coagulants must be mixed to scales far smaller than the size of the colloids onto which they are to be adsorbed so that the colloids see a uniform concentration of the coagulant around them and all the colloids are uniformly destabilized. If this is not done, some colloids may be overdosed with coagulants while the others may be underdosed, resulting in improper destabilization, poor flocculation and resulting inefficiency in their removal from water [113].

We can now appreciate why micromixing is required and how it occurs. In the next two sections, we shall look at turbulence and turbulent dispersion and its influence on micromixing.

## 3.6. Turbulence

### 3.6.1. Introduction

As we saw in Section 3.5., the need for micromixing of coagulants in water is a must. We have also seen that in order to make a solution homogeneous at the molecular scales, there must be diffusion of the coagulant solution into the water and vice-versa. However, the process of diffusion per se is too slow to uniformly distribute the coagulant within a reasonable amount of time so that subsequent treatment unit processes can be used. This requires that the homogenization process be expedited.

We have also seen earlier that a remarkable increase in the rate of diffusion occurs if the solute is finely dispersed in the solvent. One of the commonest ways by which this step is usually carried out is through the process of intense “turbulent

mixing". The result of turbulent mixing is that the entire solution can be homogenized in a time period which is almost infinitesimal as compared with the time period in which pure diffusion would bring about the same result.

Since turbulent mixing cannot be understood without a minimal acquaintance with the physical processes underlying turbulent flow, in this section, we will look at turbulent flow and its dissipative characteristics in order to better understand turbulent mixing.

Turbulence was a problem with pedigree. The great physicists all thought about it, formally or informally. A smooth flow breaks up into whorls and eddies. Wild patterns disrupt the boundary between fluid and solid. Energy drains rapidly from large-scale motions to small. Why? ...It seemed almost unknowable. There was a story about the quantum theorist Werner Heisenberg, on his deathbed, declaring that he will have two questions for God: why relativity, and why turbulence. Heisenberg says, "I really think He may have an answer to the first question." [49]

This quotation very aptly sums up the awe with which scientists and engineers have regarded the phenomenon of turbulent fluid flow and its complexities. Despite attempts by innumerable scientists, little is known about its origins and behavior. Lesieur in his book *Turbulence in Fluids* [71] even goes on to say "Turbulence is a dangerous topic which is often at the origin of serious fights in the scientific meetings devoted to it since it represents extremely different points of view, all of which have in common their complexity, as well as an inability to solve the problem. It is even difficult to agree on what exactly is the problem to be solved." Given this confusion among the ranks of researchers, there are bound to be conflicting theories/views on any aspect of turbulent flow. This caveat must be borne in mind while reading this section.

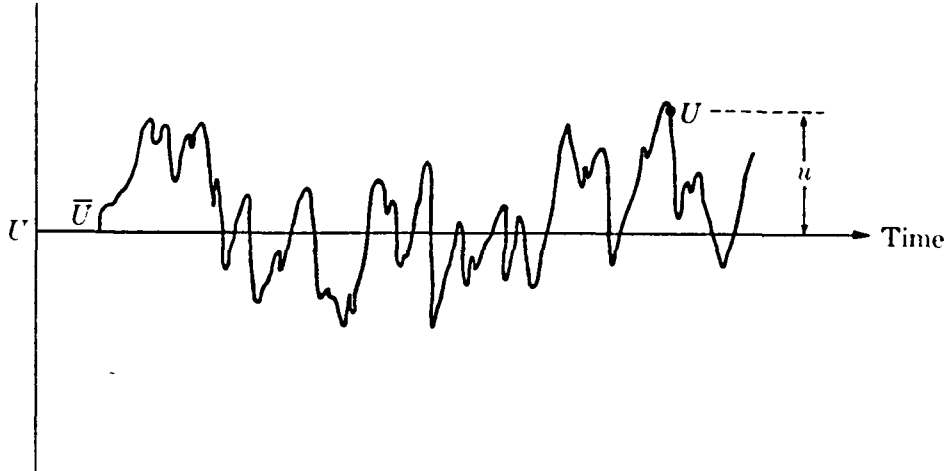


Figure 3.27: Velocity measurements at a fixed point in space in a turbulent fluid flow field.  $U$ : instantaneous velocity,  $\bar{U}$ : mean (time average) velocity,  $u$ : velocity fluctuations superimposed on the mean velocity, such that  $U = \bar{U} + u$  [27]

### 3.6.2. Defining turbulence

So, we ask ourselves: What does “turbulent” mean? Webster’s dictionary—*turbulent*: characterized by agitation or tumult.

When fluids flow at very low velocities, their motion is very orderly, easy to understand, explain and predict. However, as the rate of movement is increased, the flow becomes more and more complicated until a point is reached where (flow parameters like) the velocity, as measured in a fluid flow field, show chaotic variation (about a mean value) with time and space [2], as shown in Figure 3.27. This is turbulent flow.

It is very difficult to formally define turbulent flow. Some fluid dynamists think “It is probably not wise to make a rigid definition of a turbulent flow.” [87]. But the

question remains: What is turbulence? Shown below are two attempts to describe it:

- “It is a mess of disorder at all scales, small eddies within large ones. It is unstable. It is highly dissipative, meaning that turbulence drains energy and creates drag. It is motion turned random.” [49].
- “The turbulent flow of a viscous fluid is one of the most complex and beautiful macroscopic phenomena found in nature. It is essentially four-dimensional, involving the time-dependent interchange of energy and momentum between vortices of different sizes and lifetimes, oriented with respect to each other in three-dimensional space.” [112].

Descriptions of turbulent flow read like the story of the blind men and the elephant—with each person describing only a small part of the “whole”, without any universal descriptions involving its origins, existence and decay.

Despite this lack of a “grand unification theory” of turbulent flow, it is accepted that the flow **MUST** display some salient characteristics before it can be christened as being turbulent. These characteristics include [71,87,96,102]:

**disorder:** A turbulent flow must be unpredictable. This is synonymous with the criterion that turbulence must show disorder of such a nature that the flow is never reproducible in its entire detail even if all the experimental conditions are reproduced in greatest detail.

**mixing:** It must be able to mix transported quantities (like heat, momentum, dyes etc.) much more quickly than if only molecular diffusion were involved.

**vorticity:** Turbulence must have vorticity continuously and irregularly distributed in all spatial directions. This means that the flow must display rotation in all directions. [Later, we shall see this in greater detail].

### 3.6.3. Other characteristics of turbulent flow

Now that we know how to distinguish turbulent flow from “the rest”, we, naturally, want to know why some flows become turbulent and others not. That’s a million dollar question, which is yet to be answered to the satisfaction of any fluid dynamist worth her/his salt.

Before stepping into the treacherous grounds of turbulent flow, it needs to be re-emphasized that, as mentioned earlier (see quote by Lesieur [71] at the beginning of this section), this unsolved problem has attracted many explanations which are hotly contested by experts. There seems to be almost a vertical split among the fluid dynamists, based on the opposing approaches used to explain this phenomenon. And this tussle has become more pronounced in the last decade or so. One set of beliefs is advocated by followers of the *statistical* approach. They attempt to explain the dynamics of the flow in terms of the averaged flow characteristics. “This community, which has followed the glorious trail of Taylor and Kolmogorov, believes in the phenomenology of cascades and strongly disputes the possibility of any coherence or order associated to turbulence” [71]. The other set of beliefs are supported by an ever increasing number of scientists who identify themselves with the emerging theories, based upon the philosophy of *order within chaos*. These scientists consider “. . . turbulence from a purely deterministic point of view, by studying either the behavior of dynamical systems, or the stability of flows in



various situations. To this community are also associated the experimentalists who seek to identify coherent structures in shear flows” [71].

Though most fluid dynamists, today, follow either the deterministic or the stochastic approach to turbulence, these are not the only two kinds of theories which have been used to explain turbulent flow. These were preceded by phenomenological theories of turbulence. Some of the phenomenological theories included, among others, Boussinesque’s Eddy Viscosity theory, Prandtl’s Mixing-Length theory, Taylor’s Vorticity Transport theory, von Kármán’s Similarity hypothesis, etc. [27]. These theories, based on one mechanistic assumption or the other, were adequate for prediction of the mean velocity profile—necessary for solving many practical problems—but could not be of much help in trying to understand the true mechanism of turbulent flow. These will not be discussed here.

This student does not claim to be a fluid dynamist and, in the absence of an in-depth understanding of these rival theories, finds it hard to identify with either party or justify the use of these theories. So, the explanations used will be drawn from all “camps” of turbulence aficionados, with the realization that these theories have their respective strengths and weaknesses and, in the absence of a universal theory of turbulence, one must get by with whatever is available.

Let us now return to the reason why some flows become turbulent and some not. We are all familiar with the “dye-in-the-pipe” experiments of Osborne Reynolds and his identification of laminar and turbulent flows. We also know of Reynolds number, named after him, which is said to be a parameter most used in the description of turbulent flows. Reynolds number is an indicator of the relative strengths of the inertial and viscous forces in a fluid flow [36]. It is defined, rather arbitrarily [102]

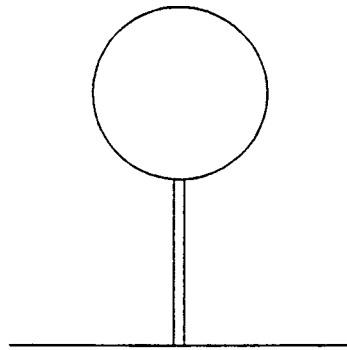
as

$$\Re = \frac{DV}{\nu} \quad (3.26)$$

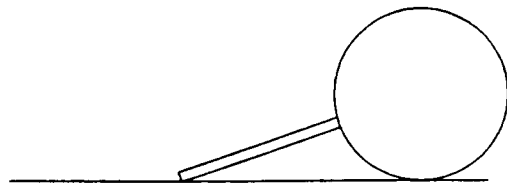
where  $\Re$  is the Reynolds number,  $D$  is a characteristic length, and  $V$  is a characteristic velocity associated with the flow;  $\nu$  is the kinematic viscosity of the fluid.

Laminar flows become turbulent at high Reynolds numbers. Perturbations in low Reynolds number flows are easily damped by viscosity. These perturbations may arise from a variety of factors including vibrations of the pipe, pipe roughness, etc. However, as the Reynolds number is made very large, these perturbations are able to grow because of much larger inertial forces—which tend to amplify the disturbances—while the damping capacity of the fluid stays almost the same. These perturbations cause the laminar flow to break down into turbulent flow [109,102]. It can be said that an “inherent instability” in high Reynolds number flows causes them to degenerate from a laminar to a turbulent nature. This inherent instability can be visualized as being similar to the instability of the structure shown in Figure 3.28. Small perturbations to this structure may not affect its status at all. Larger perturbations, however, will cause it to become unstable and topple over. In the words of James Gleick [49], when laminar flow turns turbulent, “. . . all the rules seem to break down. When flow is smooth or laminar, small disturbances die out. But past the onset of turbulence, disturbances grow catastrophically. This onset—this transition—became a critical mystery in science.” Even though the phenomenon is yet to be explained fully, we are closer to the grail today than ever before.

As noted in the last of the three criteria necessary for a fluid flow to be considered turbulent, the flow must have vorticity continuously and irregularly distributed in all spatial directions. Vorticity is a parameter used to describe the strength of a



small perturbations  
cause no change  
in status



large perturbations  
result in change  
in status

Figure 3.28: An example of instability. Small perturbations do not affect structure. Large perturbations cause the structure to topple over.

rotating fluid and “rotation” is sometimes used synonymously with “vorticity” but, as Shapiro [96] points out, “. . . this does not mean flow has to be curved for vorticity to be present.” Technically, it is “a measure of the moment of the momentum of a small fluid particle about its own center of mass” [96]. So, if a fluid particle rotates (like a solid body) about its own axis, it has a certain vorticity associated with it. See Figure 3.29.

We know that a streamline is a continuous line drawn through the fluid so that a tangent to it can give the direction of the velocity vector. Similar to streamlines, we have something called vorticity lines, which exist in rotational flows. A general flow field can be thought of as being pervaded by both, streamlines and vorticity lines. Vorticity lines are such that a tangent to these gives us the angular velocity of the fluid particles. Each vorticity line is the axis around which the fluid particles spin. Sometimes the vorticity is spread throughout the fluid while, at other times, it is concentrated in thin filaments of fluids while the remaining fluid is without vorticity. It is convenient to lump the vorticity into one filament called the “vortex core”. Fluid particles spin around these vortex cores, leaving the remaining fluid free of vorticity. In these vortex cores, vorticity is  $\infty$  because a finite amount of vorticity has been dumped into a region of zero cross-sectional area, as shown in Figure 3.30.

Obviously, each vorticity line (or vortex core) has its own velocity field. What happens when two vortex lines interact? Shown in Figure 3.31 are the results of a three-dimensional simulation of two “identical circular vortex tubes, each perpendicular to a different face” (of the orthogonal planes) [115]. As a function of (some dimensionless) time, we see how these two tubes get intertwined and entangled—

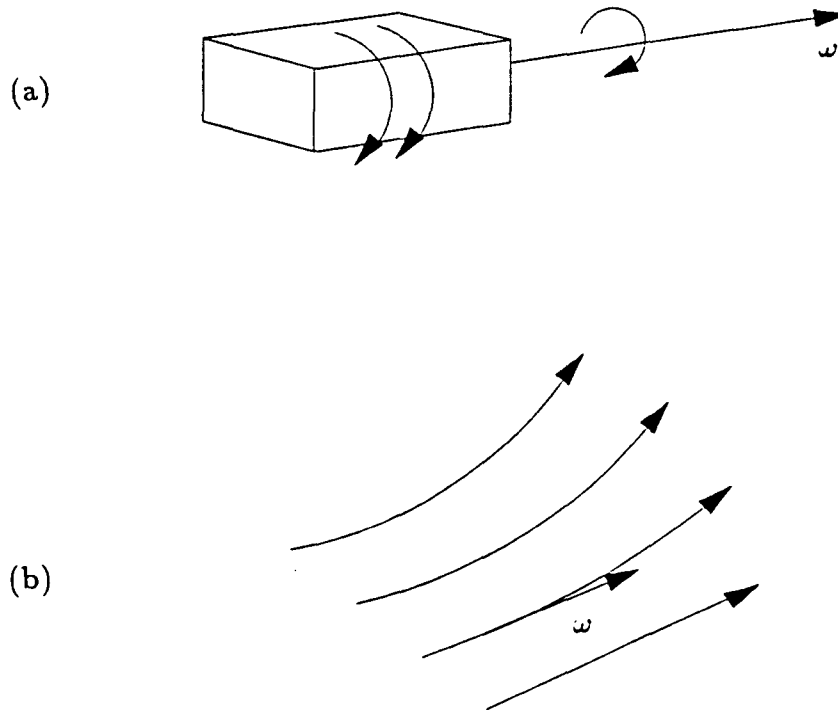


Figure 3.29: Vorticity. (a): Vorticity of a fluid particle. (b): Vorticity lines in a flow field. Both figures adapted from Shapiro [96]

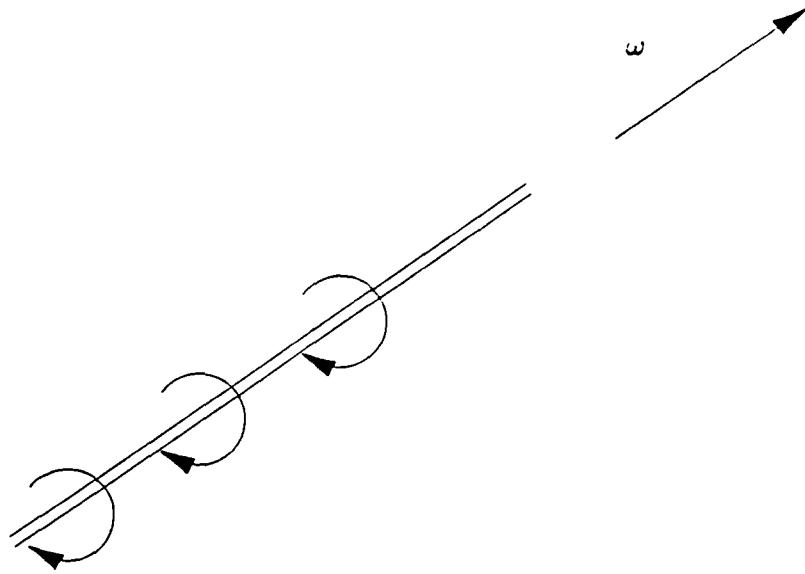


Figure 3.30: Vorticity line. Adapted from Shapiro [96]

much like two pythons coiling around each other.

It is plain to see that in a turbulent flow field, where “vorticity is continuously and irregularly distributed in all spatial directions,” (remember the third criterion for a flow to be turbulent?), the fluid space would be a veritable mess. Shapiro [96] describes it almost pictorially: “Turbulent flows are full of vorticity. The vortex lines are like tangled spaghetti,” in which the instantaneous movement/distortion of each vortex tube is governed by the configuration of all the vortices [48]. Shown in Figure 3.32 are the results of a computer simulation of how a set of 6 (six) symmetrically arranged vortex rings, subjected to a constant normal-fluid velocity in a channel with rough walls. These rings deform due to their interactions with each other. The liquid is superfluid helium<sup>3</sup> [48]. The last snapshot displays the chaotic array of the vortex tubes in the turbulent fluid. So, we now have at least some idea of why there is this constant fluctuation in the measured parameters (e.g., velocity (Figure 3.27)).

#### 3.6.4. Transfer and dissipation of energy in turbulent flow

Let us look a little more closely at the macroscopic behavior of turbulent flows. The following description is based on Stewart [102]. We know that under certain conditions, fluid motion may turn turbulent. A part of this energy of the large scale fluid motion is converted into turbulent energy. When the flow exhibits fully developed turbulence, one sees an immense range of length scales—bounded on the upper scale by the dimensions of the flow field. Being unstable, these large scale

---

<sup>3</sup>When liquid helium ( $He^4$ ) is cooled to  $2.17K$ , it changes from an ordinary fluid to a superfluid—i.e., a fluid which possesses zero viscosity [48]

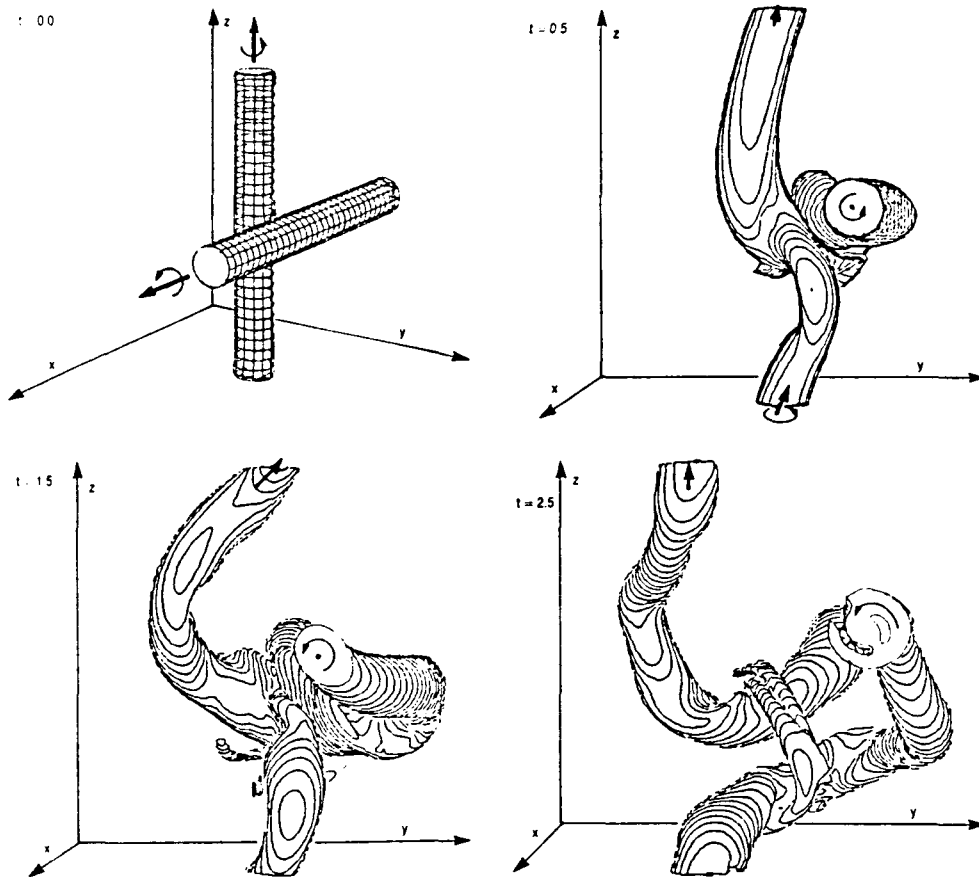


Figure 3.31: Evolution, with time, of two identical circular tubes of vorticity located in three dimensional space with offset, each perpendicular to a different face of the orthogonal planes of the coordinate system [115]



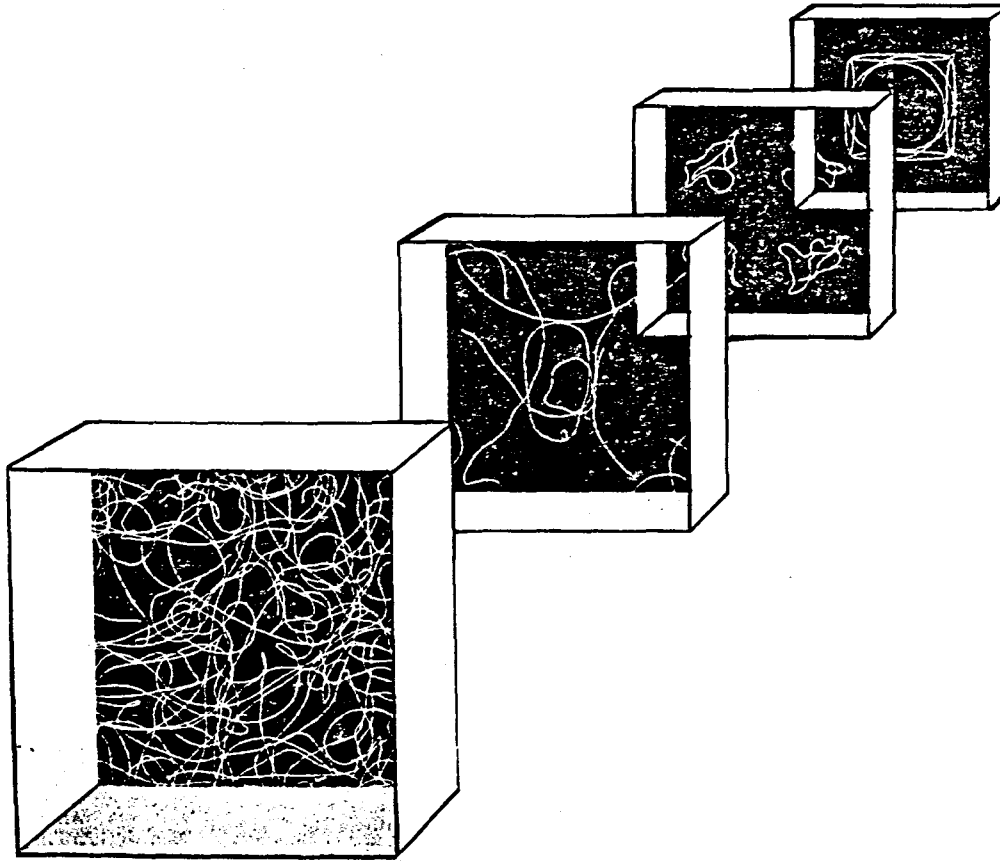


Figure 3.32: Evolution of a vortex tangle in superfluid helium [48]

motions break down into smaller and smaller scale motions, in the process removing energy from the larger scales. Eventually, the energy reaches length scales so small that the Reynolds number is too low for the flow to be unstable. At this juncture, the energy is dissipated by the action of viscosity.

Stewart provides a beautiful analogy of this cascade with a cascade of water.

Quoting him, [102]:

The analogy with a cascade of water is a useful one. Here, the only property at the top, which matters at the bottom, is the rate at which water passes down the cascade. Similarly, in the turbulent energy cascade at the smaller scale of motions, it is only the rate of energy dissipation which is of any consequence. This rate, together with the viscosity, determines the size of the smaller scales of motion. At high  $\mathfrak{R}$ , the smaller scale of motion loses all directional orientation. It becomes isotropic. Further, at small scales, the nature of the structure ceases to depend on the nature of the large scale flow. Macroscopically, the difference between a jet and an open channel is marked. But on a small enough scale (as seen in shadowgraphs), the dissimilarity disappears.

Thus, at the small scale of the energy cascade, there is a locally isotropic regime, which is similar for all kinds of turbulence . . . . What the  $\mathfrak{R}$  determines is the ratio of the larger scales to the smaller scales of the turbulent motion.

This idea of energy being transferred from larger length scales to smaller length scales was the brain-child of Lewis F. Richardson. Monin and Yaglom [78] describe Richardson's ideas as follows:

According to his assumption, developed turbulence consists of a hierarchy of "eddies" (i.e., disturbances or nonhomogeneities) of various orders. Here, the "eddies" of a given order arise as a result of the loss of stability of larger "eddies" of the preceding order, borrowing their energy, and, in their own turn, losing their stability and generating smaller "eddies" of the following order to which they transmit their energy. Thus there arises a peculiar "cascade process," of breaking-down of eddies in

which the energy of the overall flow is transmitted to motions of smaller and smaller scale, down to motion of the smallest possible scale, which is stable. To be stable, these extremely small-scale motions must be characterized by a sufficiently small Reynolds number. Thus it follows that viscosity will play an important role and, consequently, there will be considerable dissipation of kinetic energy into heat. The corresponding physical picture of developed turbulence is expressed in the following rhyme . . . often quoted (usually without the exact reference and the last line):

Big whorls have little whorls;  
Which feed on their velocity;  
And little whorls have lesser whorls,  
And so on to viscosity  
(in the molecular sense).

We have talked about “eddies” without really defining what an ‘eddy’ is. There are sundry descriptions of an eddy (some conflicting) available in the literature, some of which are shown below:

- Webster’s dictionary: An eddy is a current of water or air running contrary to the main current; *esp*: a small whirlpool.
- “Eddies are certain swirling motions of fluid, revealed by flow visualization” [93].
- “An ‘eddy’ is an assembly of strongly interacting vortex lines or sheets, interacting *comparatively* weakly with other eddies” [26].
- “Irregularities in a turbulent flow field have certain spatial structures known as eddies. This is a vague term that may be applied to any spatial flow pattern that persists for a short time. An eddy may be like a vortex, an imbedded jet, a mushroom shape, or any other recognizable form” [87].



Figure 3.33: “Typical eddy” in a turbulent boundary layer. Oil fog is illuminated by a sheet of laser light to show the lower two-thirds of a turbulent boundary layer in side view. The vortex-ring structure just below and to the right of center, which resembles a sliced mushroom leaning left, is an example of what Falco has called a “typical eddy.” *Photograph by R. E. Falco. Picture and caption copied from Van Dyke [111]*

Shown in Figure 3.33 is a flow pattern in which a “typical eddy” is illustrated [111].

As has been said earlier, turbulent fluid flow is a veritable soup of eddies—spanning many orders of magnitudes of length. “...at a Reynolds number of  $10^4$ , say, the range of eddy sizes involved covers some three orders of magnitude” [112]. The largest of the eddies are of the order of the dimensions of the width of turbulent flow, while the smallest ones are of dimensions over which molecular viscosity can effectively transport the fluid momentum, and thus shear out velocity gradients [80]. “The large eddies contain most of the energy, perform most of the turbulent transport, and interact most with the overall mean rate of strain of the flow. The small eddies are more isotropic, random, and dissipate most energy. Thus, many of the important practical properties of the flow are determined by the large eddies, while the small ones play a more passive role of removing kinetic energy from the large scales and dissipating it” [112].

We see that energy is transferred from the larger length scales to the smallest length scales and dissipated—thanks to viscosity. How does this come about? Voke and Collins [112] provide a beautiful, succinct description of this process:

The largest “eddy” of all is the gross mean flow whose energy arises from imposed shear, pressure gradients, buoyancy or other body forces, constrained by boundary conditions. The mean flow loses energy through vortex formation or other mechanisms to eddies of the next smaller size; these are the largest true turbulent eddies. They in turn lose energy to smaller structures through vortex stretching or tilting. The interactions become increasingly random and hence isotropic as the causal link with the original imposed force and the boundary constraints becomes more extended and tenuous.

The energy cascade may continue through many orders of magnitude in a high Reynolds number flow. The transfer is overwhelmingly in the

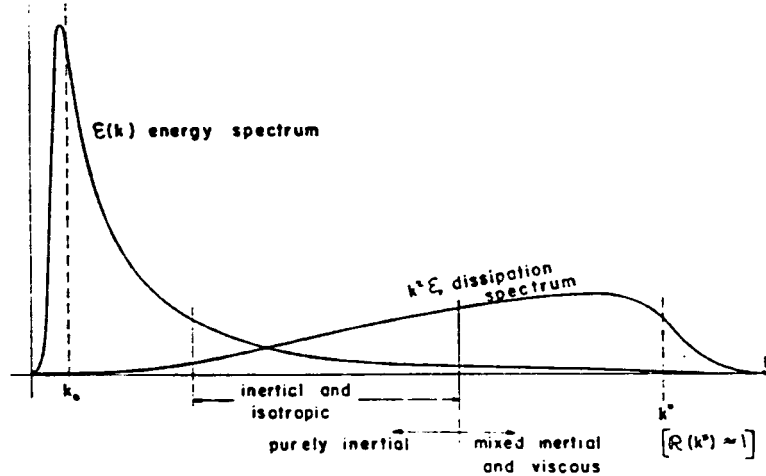


Figure 3.34: Three-dimensional turbulent energy spectrum and dissipation spectrum.  $k^*$  corresponds to the Kolmogorov microscale [35]

direction from lower wavenumbers to higher wavenumbers<sup>4</sup>. (This is not the case in two-dimensional turbulence—one key reason why true turbulence must be three-dimensional.)

The cascade peters out eventually because the smaller eddies, although they contain less energy and involve smaller vortical velocities, involve higher strain rates and vorticities than the larger eddies. The velocities are lower, but the velocity gradients larger. As a result, molecular viscosity comes to play an increasingly important role at higher wavenumbers, until eventually a scale is reached where nearly all the energy extracted from larger eddies is dissipated by friction, with none left to pass on down the cascade to smaller scales. At this point the energy spectrum starts to fall increasingly rapidly towards zero.

<sup>4</sup>The wavenumber is based on a concept from spectral theory and can be thought of as a “transform” such that small wave numbers correspond to large eddy sizes—which are fewer in number—and large wavenumbers correspond to small eddy sizes—much larger in number (or frequency) [2,26,35,47].

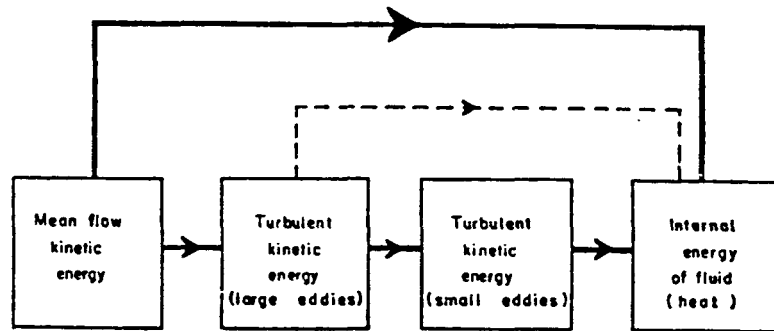


Figure 3.35: Crude representation of average energy degradation path [35]

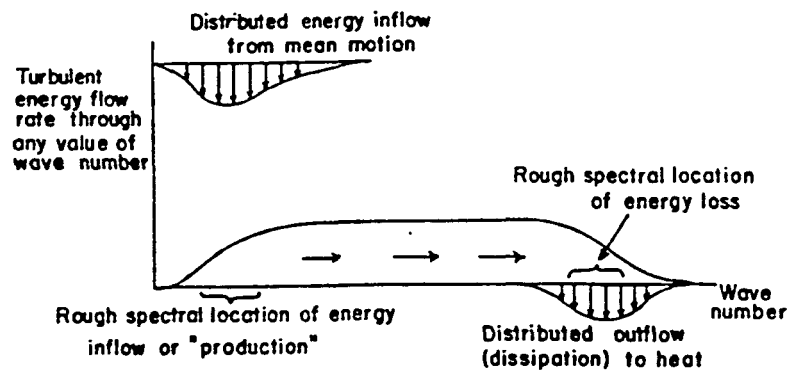


Figure 3.36: Schematic representation of average turbulent kinetic energy path in wave number space [35]

A glance at Figures 3.34, 3.35, and 3.36 sums up the entire energy picture of turbulent flow. Shown in Figure 3.34 is the three-dimensional turbulent energy spectrum and dissipation spectrum. We see that as far as the energy spectrum is concerned, the maximum energy is concentrated in the low wavenumbers (corresponding to larger eddy sizes) and this energy seems to decrease exponentially for larger wavenumbers. Also shown is the dissipation spectrum—corresponding to the energy dissipated by eddies of different sizes. We see that most of the dissipation occurs in the wavenumbers corresponding to the smaller eddy sizes.

Figure 3.35 shows, in an approximate manner, the route taken by energy of the mean flow, to be dissipated as heat. Mean flow loses a part of its kinetic energy directly to viscosity (converted to heat, just like in laminar flow). The remaining fraction goes into the production of large eddies which, in turn, lose some of their energy directly to viscosity. The remaining part of the energy of the large eddies goes into the energy of smaller eddies, which lost it to viscosity.

Figure 3.36 is a representation of Figure 3.35 in wavenumber space. It shows the location of the region where energy of the mean flow is acquired by the eddies and the region where the eddies lose their energy to viscosity (as heat).

How does energy get transferred from low wavenumbers to high wavenumbers? The process of vortex stretching is responsible for the transfer of energy from larger eddies to smaller ones. How does this come about? Tennekes and Lumley [109] and Frost and Bitte [46] provide excellent descriptions. Vortex stretching is the reason why such an immense range of eddy sizes is generated. Stretching causes larger eddies to become successively smaller. “It is generally accepted that eddies of significantly different size have no direct influence on one another and only eddies



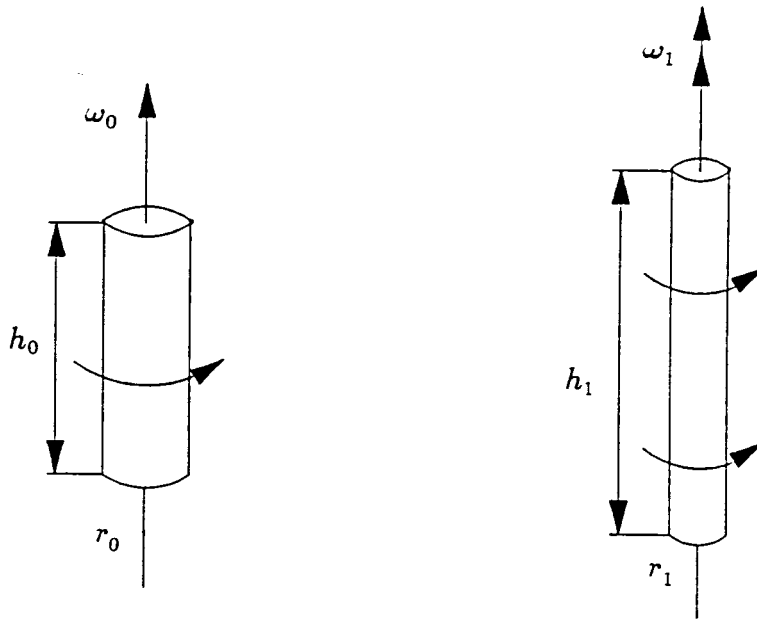


Figure 3.37: Principle behind energy transfer from large eddies to small eddies

of comparable size can exchange energy” [46].

Imagine a solid cylinder of radius  $r_0$ , height  $h_0$ , and density  $\rho$ , rotating about its longitudinal axis with an angular velocity  $\omega_0$  such as shown in Figure 3.37. If, while rotating, the cylinder is somehow stretched so that its new dimensions are  $r_1, h_1$  and its new angular velocity,  $\omega_1$ , such that  $r_1 < r_0$  so that  $h_1 = \frac{\pi r_0^2 h_0}{\pi r_1^2} = h_0 \left(\frac{r_0}{r_1}\right)^2 > h_0$ , because  $r_0 > r_1$ . The angular momentum (i.e., the moment of the momentum about the axis of rotation) of the cylinder (before stretching),  $L_0$ , is

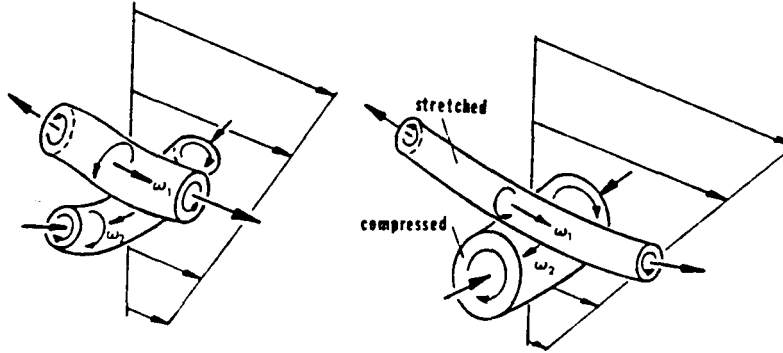


Figure 3.38: Vortex stretching [46]

given by

$$L_0 = \int_0^{r_0} (2\pi r h_0 dr \rho) (\omega_0 r) r = \frac{1}{2} \pi \rho h_0 \omega_0 r_0^4. \quad (3.27)$$

After stretching, the angular momentum of the cylinder is  $L_1$

$$L_1 = \frac{1}{2} \pi \rho h_1 \omega_1 r_1^4. \quad (3.28)$$

According to the principle of conservation of angular momentum,  $L_0 = L_1$ , i.e.,

$$\frac{1}{2} \pi \rho h_0 \omega_0 r_0^4 = \frac{1}{2} \pi \rho h_1 \omega_1 r_1^4. \quad (3.29)$$

Substituting the value of  $h_1$  in the above equation, we get

$$\frac{1}{2} \pi \rho h_0 \omega_0 r_0^4 = \frac{1}{2} \pi \rho h_0 \left(\frac{r_0}{r_1}\right)^2 \omega_1 r_1^4.$$

After cancelling like terms,

$$\omega_0 r_0^2 = \omega_1 r_1^2, \quad (3.30)$$

or

$$\omega_1 = \left(\frac{r_0}{r_1}\right)^2 \omega_0. \quad (3.31)$$

Since  $r_0 > r_1, \Rightarrow \omega_1 > \omega_0$ .

What happens to the kinetic energy of the cylinder? Before stretching, its kinetic energy  $K_0$  is given by

$$K_0 = \frac{1}{2}I_0\omega_0^2 \quad (3.32)$$

where  $I_0$  is the moment of inertia about the longitudinal axis of the cylinder<sup>5</sup>.

Since angular momentum  $L_0$  is given by

$$L_0 = I_0\omega_0, \quad (3.33)$$

the kinetic energy of rotation about the longitudinal axis will be

$$K_0 = \frac{1}{2}L_0\omega_0 \quad (3.34)$$

and

$$K_1 = \frac{1}{2}L_1\omega_1 \quad (3.35)$$

Since we already know (from the principle of conservation of angular momentum) that

$$L_0 = L_1 \quad (3.36)$$

and that

$$\omega_1 > \omega_0, \quad (3.37)$$

it implies that  $K_1 > K_0$  or, the process of stretching has resulted in an increased kinetic energy of the rotating cylinder.

The same phenomenon occurs when a ballerina, spinning with her arms spread outwards, pulls them closer to her body—resulting in a faster spin. Both, her

---

<sup>5</sup>The moment of inertia of a solid cylinder of radius  $r$ , height  $h$ , and density  $\rho$  about its longitudinal axis is given by  $\frac{1}{2}\pi\rho hr^4$  [36].

angular velocity and her kinetic energy have increased. The increase in her kinetic energy is supplied by the work done by her body muscles in bringing her arms closer to her body. In a similar manner, the increase in the kinetic energy of the rotating cylinder is caused by the work done by the process of stretching it.

Coming back to vortex stretching, if we look at Figure 3.38 we see essentially the same thing happening (ignoring viscous effects, for the time being). The bottom vortex segment is larger than the top vortex segment. The interaction of their flow field causes the upper vortex segment to stretch and the lower vortex segment to compress, causing a net energy transfer from the bottom vortex segment to the top segment. This top vortex segment, in turn, does the same thing to another vortex segment and so on. Thus, energy is transferred by vortex stretching.

As pointed out by Tennekes and Lumley [109] and others [46], this transfer occurs with greater rapidity from the bigger vortices to smaller ones than the other way round. Also, the magnitude of energy transfer from the smaller vortices to bigger ones is very small. The overall effect is a net transfer from larger eddies to the smaller ones until it is dissipated by viscosity.

Another question arises: How do large eddies get their energy? Quoting Voke and Collins [112]:

Production of turbulent energy from the mean flow takes place at low wavenumbers, so that the large eddies generated contain most of the energy. Dissipation takes place predominantly at high wavenumbers, where small eddies are destroyed. These two scales are characterized by two length parameters: the integral length scale of the velocity correlations,  $L$ , which is determined primarily by the geometry that encloses the flow or produces the turbulence, and which limits the size of possible

eddies<sup>6</sup>, and the Kolmogorov length  $\eta$ , which characterizes the size of the smallest, dissipating eddies. The latter simply adjusts itself in each flow so that the amount of energy passing down the cascade may be dissipated: where more energy has to be dissipated,  $\eta$  is smaller; where less, it is larger.

The relationship between  $\eta$ , the kinematic viscosity  $\nu$ , and the rate of dissipation of energy (per unit mass)  $\varepsilon$ , is [109]:

$$\eta^4 = \nu^3 / \varepsilon \quad (3.38)$$

At low Reynolds numbers,  $\eta$ , may be of the same order of magnitude as  $L$ , and the production and dissipation eddies are not distinct. but at a sufficiently large Reynolds number, a gap will open up between the range of wavenumbers in which production of turbulent energy is taking place and the dissipation range. The turbulent energy must then pass through the so-called inertial subrange, an intermediate zone of wavenumbers where neither production from the mean flow nor viscous dissipation have any great influence on the dynamics. Here the energy is extracted from larger eddies “upstream” and lost to smaller ones “downstream”. The energy dynamics is purely that of an energy-conserving cascade.

The inertial subrange is part of a larger range of wavenumbers which stretches down to include the dissipation subrange, also called the equilibrium range. Throughout this range, the time scales of eddies are so much smaller than the time scales of the mean flow or the large eddies that their properties adjust rapidly to changing local conditions. In this range the statistical properties of the turbulence are also expected to be isotropic.

Where do eddies exist? They, actually, pervade the entire turbulent flow field. Small eddies can be found within large eddies, and smaller eddies within small ones—much like the whorls described in the little verse by Richardson, quoted earlier. We must remember that an eddy of a given size is merely “fluid in swirling motion” and so, when the eddy loses its energy by viscous dissipation, no more do we have that “swirling motion” at the given length scale. The fluid, earlier swirling and spinning around, is not doing so any more. But, it may be picked up and moved

---

<sup>6</sup>It can be thought of as an upper bound to the possible eddy sizes.

about by other “eddies” and/or the mean flow and thus, become the part of yet another eddy. The energy which was making a small part of the fluid move and swirl around is now gone, dissipated as heat, and a fresh amount of energy is now moving the fluid around!

Another point to be remembered is that even though the eddies continue to be reduced in their length scale, even the smallest of the eddies has dimensions which are, generally, far greater than any “molecular length scale” [109] and so, for all practical purposes, the fluid can always be thought of as a continuum.

We have, so far, examined mainly the dissipative aspects of turbulent flow—enough to give us an intuitive, physical feel for such flow phenomena. Little or no mathematical descriptions have been used in order to avoid the complexities so characteristic of turbulent flow. By no means complete, this description is adequate for our purposes—that of examining and understanding the phenomena of turbulent mixing of coagulants in water, and its role in water treatment. The next section will explore the phenomenon of turbulent mixing or the “dispersive” aspects of turbulent flow.

## 3.7. Turbulent Mixing

### 3.7.1. Introduction

We have, so far, looked at the “dissipative” aspects of turbulent flow. Let us now examine its “diffusional” aspects. As we recollect, one of the criteria for a flow to be called “turbulent” was that *it must be able to mix transported quantities (like heat, momentum, dyes, etc.) much more quickly than if only molecular diffusion*

were involved.

We have earlier defined Reynolds number,  $\Re$ , as an index of the ratio of the inertial and viscous forces in a moving fluid. Tennekes and Lumley [109] show that this parameter, the Reynolds number, plays a multifaceted role in turbulent flows. They show that it (i.e., the Reynolds number) can be perceived as an indicator of the ratio of diffusion related quantities. Thus, the  $\Re$  of a turbulent flow can be interpreted as an index of the "...ratio of turbulence time scale to a molecular time scale that would prevail in the absence of turbulence in a problem with the same length scale" [109]. Or, in simple words, if molecular diffusion alone were to disperse a substance uniformly through space of length scale  $L$ , it would take a certain amount of time  $t_m$ . However, if turbulent mixing takes place in the same space, the time taken to transport it,  $t_t$  is much smaller than  $t_m$ . Tennekes and Lumley show that  $t_t/t_m$ , known as the inverse of the Péclet number, can—for gases—be almost of the same order of magnitude as the inverse of the Reynolds number! So, when  $\Re$  is high,  $t_t/t_m$  is low and vice versa; implying that at high Reynolds number, the time scale for turbulent "diffusion" of a substance over a given length scale is much smaller than the time scale for molecular diffusion. We must remember that this interpretation of  $\Re$  by Tennekes and Lumley [109] is merely a question of 'transport' and not 'mixing'. Later, however, we shall see that it does have a very important role to play in uniform mixing of substances at the molecular level, or 'micromixing.'

### 3.7.2. Mechanisms of turbulent mixing

In our discussion of the mixing process, we concluded that for the time rate of mixing to occur at a rate faster than that for pure diffusion, one could either increase the surface area of the interface between the unmixed components, or the concentration gradient driving the diffusion process, or both. It is usually easier (and more effective) to enhance the rate of mixing by increasing the area of the interface of the unmixed components.

What prompts a flow with high  $\mathcal{R}$  to achieve this? Some mechanisms which help turbulent flow in this aspect are discussed below.

- **Shear:** Let us first look at what pure fluid shear can do to help us in our endeavors of rapid mixing. Shown in part (a) of Figure 3.39 is the thinning out of a rectangular fluid element due to laminar flow. Shown in part (b) of the same figure is the fate of a spot of dye in a viscous fluid, subjected to a rectilinear shear flow, in the absence of molecular diffusion. We see that as a function of time, the circular spot is transformed first into an ellipse, and then into a thin, long “finger”, similar to the behavior of the thinning rectangular fluid element in part (a). The spot, in this form, possesses an interfacial area which is much larger than the circle (at  $t = 0$ ). In the process of distortion (stretching in one direction and contraction in the other), the fluid elements reach a stage where the molecules which would have had to travel long distances (e.g., from the center of the circular blob to the bulk fluid) in order to diffuse out of the blob into the bulk fluid now need to travel much shorter distances to diffuse out—making the overall process of diffusion



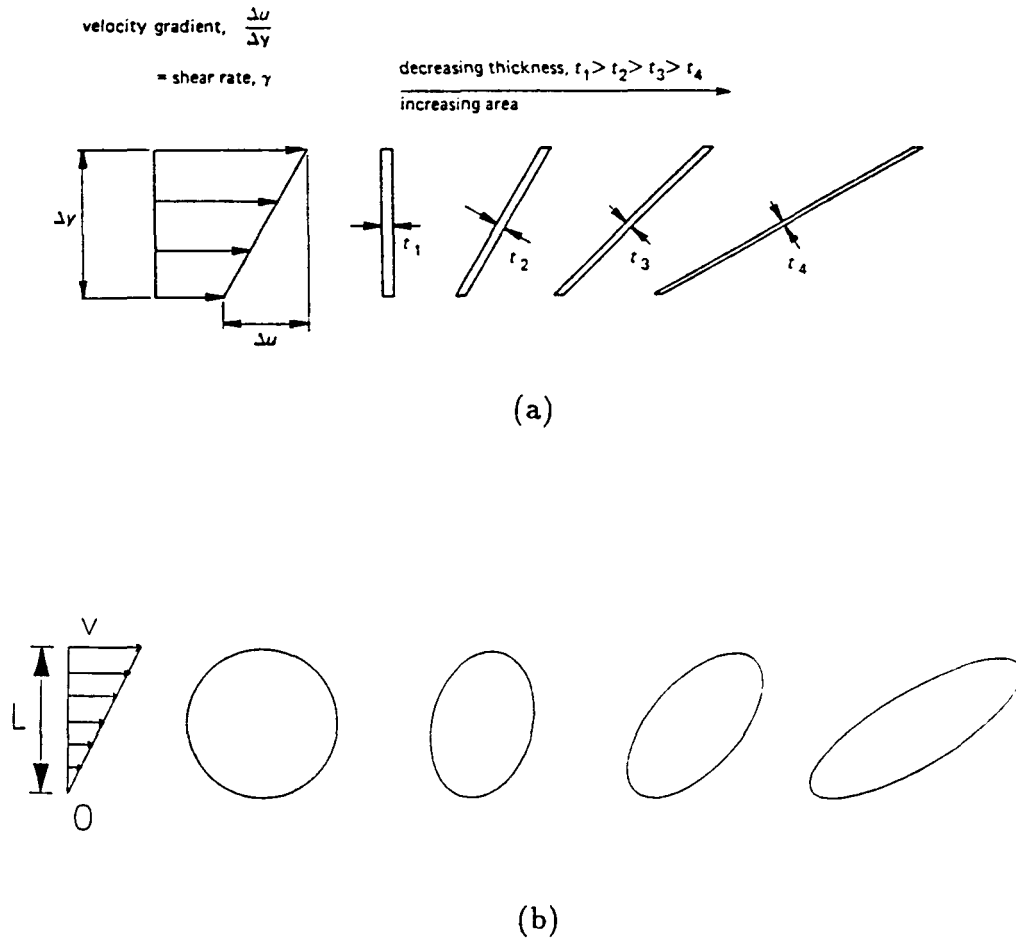


Figure 3.39: Role of shear in turbulent mixing. (a): Thinning of a rectangular fluid element in a rectilinear shear flow field [41]. (b): Distortion of a spot of dye (in the absence of molecular diffusion) in a viscous fluid subjected to a rectilinear shear flow field (figure based on Lumley [75])

much faster. So, based on what we saw in Section 3.5., we can conclude that the process of distorting a dye spot by shear can enhance the time rate of mixing.

- **Elongation and vortex stretching:** We know that turbulent flow is pervaded by eddies of various sizes; energy constantly being transferred from large eddies to small ones through the process of vortex stretching. This results in thinner and longer vortex tubes constantly being formed and dissipated. If we have a blob of dye in a turbulent flow field, some of it is likely to be trapped in a vortex tube which gets elongated and thinned, as shown in Figure 3.37. The deformation of the vortex tube containing this dye will result in an increase in the interfacial surface area as well as a reduction in the distances which the molecules must travel before mixing with the surrounding fluid, and consequently, an increase in the time rate of mixing of the dye with the bulk solution via molecular diffusion.

The process of elongation continues to distort the fluid elements to dimensions of the order of the Kolmogorov microscale and smaller. As the vortex tube is dissipated by the viscous forces, it has a much lower Reynolds number than before. This means that based on the interpretation of Tennekes and Lumley [109], the time scales for transport of the dye (over a given length scale) by molecular diffusion is smaller than transport by fluid motion. In the dissipating eddy exists a shear field which distorts the dye element as shown in Figure 3.39. Added to this is the fact that the flow has a very low Reynolds number, indicating that transport by diffusion continues to dominate.

In a turbulent flow field, both these mechanisms act simultaneously, resulting in an enhanced time rate of mixing of the dye with the bulk fluid. As mentioned earlier, once an eddy is dissipated, the fluid which has, till then, been under the influence of this eddy, doesn't come to rest; it continues to move under the influence of the bulk flow as well as other eddies. It becomes entrained in other eddies, going through the same process of mixing through elongation, shear and molecular diffusion over and over again.

One can think of this process of mixing via stretching in somewhat the same manner as the mixing of two lumps of dough—each colored differently. One needs to knead the dough, constantly pulling and stretching, folding back, kneading some more, re-stretching, refolding and again re-stretching—over and over again—with each cycle causing a reduction in the scale of non-uniformity until, after many, many cycles of such mixing, the dough acquires a uniform color. We must remember that in this case, given the high viscosity of the materials, mixing by molecular diffusion alone would never have been able to produce a uniform mixture in a short period of time. However, by the above process of stretching and folding we reduced the “scale of segregation”<sup>7</sup> in a time span much shorter than the time period taken by molecular diffusion to get similar results.

- **Bulk flow and velocity gradients in bulk flow:** Apart from pure shear and stretching mechanisms, there is yet a third mechanism associated with

---

<sup>7</sup>The scale of segregation can be thought of as the thickness of the (thinned out) layers of colored dough.

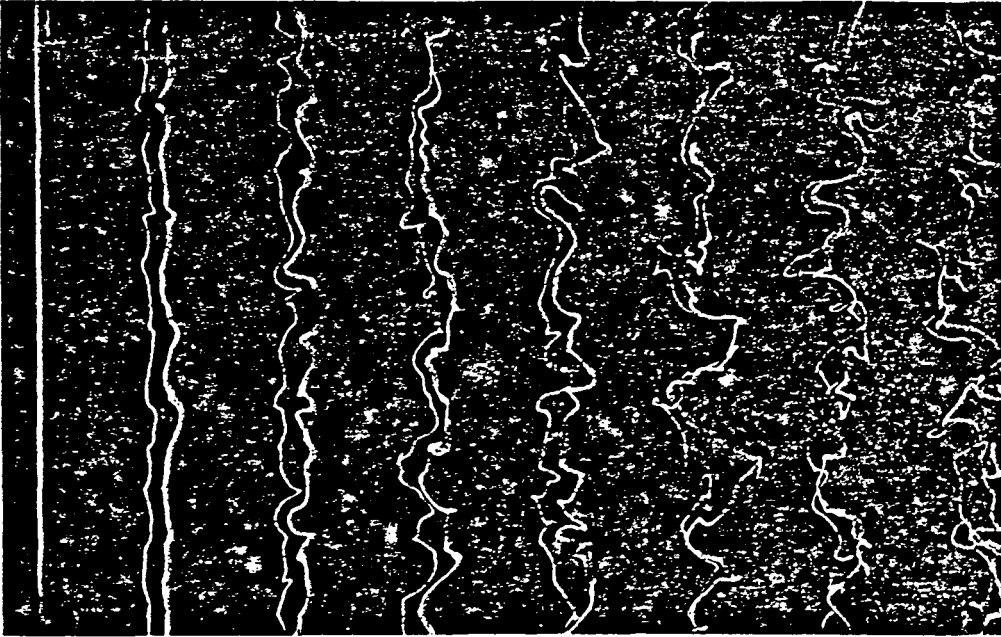


Figure 3.40: Influence of velocity gradients on mixing. A fine platinum wire at the left is stretched across a water tunnel behind a turbulence generating grid. Periodic electrical pulses generate double lines of hydrogen bubbles that are stretched and wrinkled as they are convected downstream. Note how bubbles which were initially close together get more and more separated as a function of time [111]

turbulent flow which helps in enhancing the time rate of mixing of two components. “In a turbulent flow field, fluid particles which initially are grouped together, become dispersed, moving relative to one another. This process of the separation of neighboring parts of the fluid is termed turbulent diffusion. Statistically considered, the mean distance between particles situated initially at any two points increases with time” [16]. The presence of spatial velocity gradients in a turbulent flow field causes particles close together to get separated. This is well illustrated in Figure 3.40. “A fine platinum wire at the left is stretched across a water tunnel 18 mesh lengths behind a turbulence generating grid . . . . Periodic electrical pulses generate double lines of hydrogen bubbles that are stretched and wrinkled as they are convected downstream” [111]. We see, here, that the presence of velocity gradients—which in this picture appear to be modest relative to the mean flow rate—has caused these hydrogen bubbles, initially close to each other, to get farther from each other and be a little more “spread out” in space—dispersed—which is precisely why we had wanted to use turbulence in the first place: to spread out coagulant/dye better all over the space of interest, so as to enhance the time rate of mixing in order to get a uniform solution throughout the container.

### 3.7.3. Mixing in a reactor

Now that we have identified the three distinct mechanisms of mixing prevalent in turbulent flow, it is only appropriate that we try and comprehend the role these play in real life situations involving turbulent mixing. In the context of our application, let us look at the manner in which dye (or coagulant) when introduced

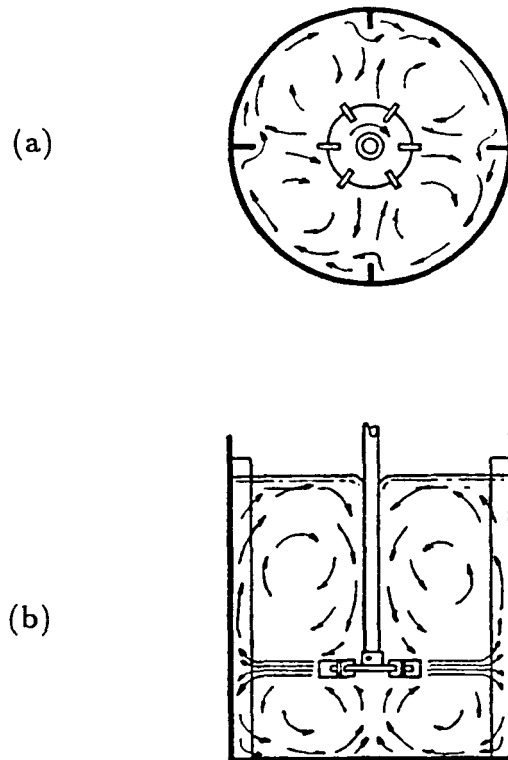


Figure 3.41: Bulk fluid flow patterns in a baffled cylindrical mixing vessel with a turbine impeller. (a): Plan view, (b): Elevation view [58]

at a given location in a mixing vessel gets dispersed so as to produce a (visually) uniform solution.

Consider the mixing vessel of the type shown in Figure 3.41. Let us introduce a spot of dye into the horizontal ‘jet’ of water emanating from the turbine impeller. Upon introduction, the spot of dye is transported throughout the mixing vessel by the bulk flow. During this stage, it appears as if a turbulent cloud of dye is moving around the container, leaving a trail of dye in its wake. The ‘cloud’ per se moves with the bulk flow. The trail of dye, on the other hand, is because of velocity gradients in the bulk flow. While the bulk flow transports the dye—which was introduced

as a spot in the mixing vessel—to various parts of the vessel, at the same time the turbulent eddies, many of which consist of fluid with dye, are stretched and distorted by other eddies. As mentioned earlier, these eddies eventually become very small in size and are dissipated by viscous shear, in the process greatly enhancing the interfacial area for diffusion of the dye molecules. As the eddies reach dimensions of the order of the Kolmogorov microscale and smaller, the shear resulting from the viscosity of the fluids (and the resulting velocity gradients) distort the dye elements even more, allowing for still faster diffusion of the dye molecules into the bulk fluid and vice-versa. Meanwhile, the bulk flow continues to cycle and recycle the ‘semi-well-mixed’ solution, causing these processes to occur over and over again. The final result of this process is a uniform mixture of the dye with the bulk fluid. Note that turbulent bulk flow transported the dye over large length scales during small time scales. The turbulent eddies help ‘cut’ the original spot of dye into smaller blobs which were stretched and distorted by the eddies as well as the bulk flow to still smaller length scales. Eventually, the blobs, which have been uniformly distributed throughout the space of the mixing vessel because of bulk flow, lose their dye content by diffusion. The final result of this entire process is a (visually) uniform dye solution.

What happens if the dye, instead of being introduced close to the impeller is introduced in a region which does not have such large velocities—e.g., in a spot of dye introduced very close to the baffles of the mixing vessel? The fate of this blob of dye is shown in the Figure 3.42. We see that as a function of time, turbulent eddies alter the shape of the dye spot, spreading it out. Shown in row (b) are plots of concentration of the dye, as shown in a cross section of the frames in row (a)—with

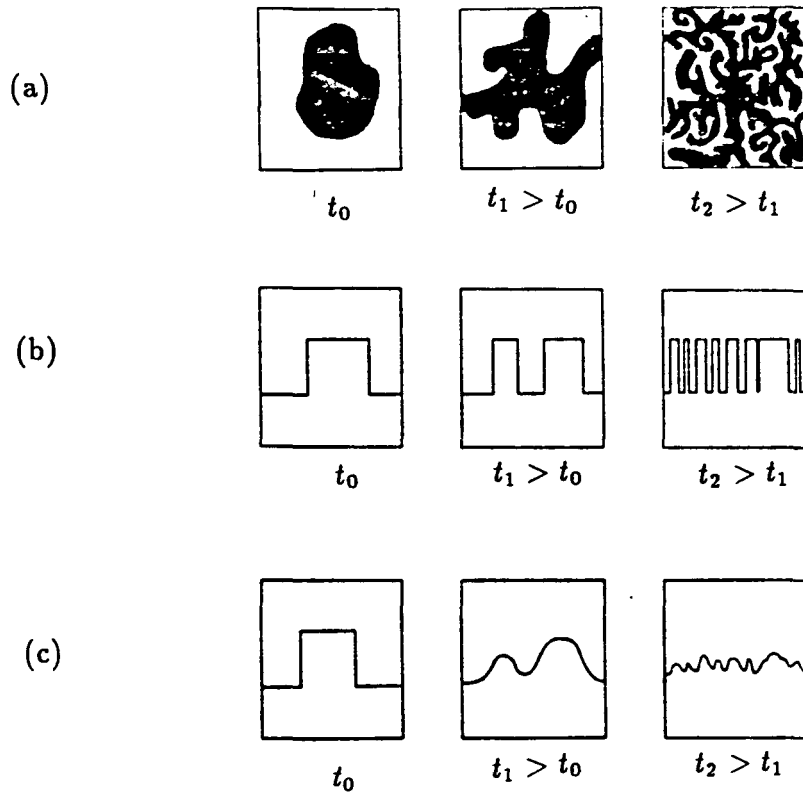


Figure 3.42: Turbulent mixing of a dye spot without predominant bulk flow. Also shown is the influence of diffusion in bringing about a uniform mixing of the dye in the solution. (a) Fate of a dye spot in a turbulent flow field, (b) Plot of concentration of the dye, as seen in a cross section of the frames in row (a)—in the absence of molecular diffusion, (c) Same as in (b) but with molecular diffusion [35]



the assumption that there is no molecular diffusion. Row (c) shows a cross-section of frames in row (a)—this time with the inclusion of molecular diffusion. We must note, however, that the absence of bulk flow to transport this dye all over the mixing vessel greatly hampers any attempts to get a uniform dye solution throughout the entire container with great rapidity.

What does it all mean? We see that while the turbulent diffusion is able to reduce the scale of segregation to a considerable degree, it is ultimately up to molecular diffusion to bring about fine scale mixing. The molecular level uniformity in the mixture is purely a consequence of the molecular diffusivity of the dye molecules. The turbulence assists in this process by dispersing the original dye spot, just like what we saw in Figure 3.24. It also transports these blobs throughout the mixing vessel, distributing them somewhat uniformly throughout the container. It is a combination of these steps that makes way for molecular diffusion to equalize the concentration differences on smaller length scales—length scales to which turbulence alone cannot be used to achieve uniformity in concentration. As shown in Figure 3.25 turbulence takes us from the first column to the third column. In this column, molecular diffusion takes us from the top row to the bottom row. All in all, the combination of turbulence with molecular diffusion provides us a uniform mixture of the dye and the bulk fluid in a much, much smaller time than would have been possible with just molecular diffusion.

This makes it apparent that answers to questions of the type, “how long and hard do we have to mix to get a uniform solution” are not trivial. If one were to increase the  $\mathcal{R}$  of (turbulent) flow in a given situation (say in the mixing vessel in Figure 3.41), its impact on the time rate at which vortex stretching, “fluid folding,

stretching, and refolding”, and thus, the time over which a (visually) uniform mixture is produced ends up being a rather difficult answer to seek, given the highly nonlinear nature of the processes involved.

We shall discuss this in greater detail at a later stage. But, for now, it is easy to see why turbulent flow, in combination with molecular diffusion, is able to *mix transported quantities (like heat momentum, dyes, etc.) much more quickly than if only molecular diffusion were involved.*

### 3.8. Turbulent Mixing and Fast Chemical Reactions

#### 3.8.1. Introduction

As we saw in the last section, it is necessary for us to use turbulence in order to uniformly distribute dye throughout a mixing vessel in a short span of time. The rapid mixing step in water treatment involves coagulants, but the basic purpose of mixing is the same for all processes: that of distributing some substance uniformly in space over a short period of time.

The feed stock of coagulants such as organic polyelectrolytes is normally a water based solution. When this solution is introduced into the raw water, the polymers undergo changes in terms of the response of their ionizable constituents to the pH, ionic strength and chemical composition of the water. Similarly, the feed stock of metal coagulants is also, generally speaking, a water based solution. When mixed with the raw water supply, the coagulants usually go through a series of hydrolysis steps of the kind mentioned in the Section 3.3. It is generally believed [2,3,4,8,54,85,113] that the hydrolysis of alum occurs through a series of very rapid

chemical reactions, all of which are thought to take a total time of about a few seconds at the maximum. O'Melia [84] was among the first few people to recognize the role of proper mixing in obtaining the appropriate hydrolysis species from the hydrolysis of metal coagulants so as to be able to destabilize the colloids in the desired fashion. Quoting him:

Coagulation by iron(III) and aluminum(III) salts can be brought about by polymeric species which are formed when quantities of these salts sufficient to exceed the solubility limit of the metal hydroxides ( $Fe(OH)_3$  and  $Al(OH)_3$ ) are added to a water or waste containing colloidal materials.

Polymers start to form very rapidly. Their properties (chemical composition, charge, size, etc.) are generally affected by the solution pH and the concentration of coagulant. If these salts are added to a poorly mixed system, local variations in pH and coagulant metal ion concentration will produce a more heterogeneous and less reproducible variety of polymeric species than well mixed systems will yield. In other words, the polymers which can bring about particle destabilization when iron(III) and aluminum(III) are used as coagulants are formed within the colloidal system (the raw water or wastewater) itself. Reproducible polymer formation can only be accomplished by intense mixing because of the rapid speed of these reactions.

Similar sentiments were echoed by Vrale and Jorden [113], who felt that inadequate mixing results in "...stimulation of  $Al(OH)_3$  formation and over- and under-reaction of some elements of fluid." They added that "...the rates and the species that develop are undoubtedly dependent upon, among other things, local concentrations of metal and hydroxide ion," and "...the existence of local, temporal excesses, and deficiencies of Al(III) from the average concentration."

Having seen the intricacies of turbulence, turbulent mixing, and hydrolysis of metal ions, it is apparent that the interplay of turbulent mixing with multi-step fast

chemical reactions is a phenomenon of great complexity and, in the context of our problem, needs to be understood to some degree.

While considerable work has been done by Chemical Engineers on this topic, environmental engineers have, by and large, stepped clear of this issue. Clark et al. [32], have been the first to make an assault on the “multi-step hydrolysis of aluminum” problem, as coupled with turbulent mixing. Amirtharajah and Mills [3], in their brilliant paper on the influence of mixing on the coagulant alum, proved beyond a shadow of doubt what Vrale and Jorden [113] and O’Melia [84] had conjectured—that rapid mixing *does* play a very vital role in the destabilization of colloids. This role cannot be understood without comprehending, to some degree, the interplay of turbulent mixing in fast chemical reactions and the effect on product selectivity in multi-step reactions—thus this section.

### 3.8.2. Chemical reactions

Let us begin with chemical reactions. What is a reaction? We go to a dictionary. Webster’s says a reaction is a “chemical transformation or change; the interaction of chemical entities.” Now let’s look in a chemistry text. According to Nebergall et al. [82], a reaction is a chemical change that “. . . produces one or more substances entirely different in composition and properties from that which existed before the change occurred.”

If we recollect from Section 3.5., we saw that the behavior of physical systems is described by, among others, the First Law of Thermodynamics—conservation of energy of an isolated system; and the Second Law of Thermodynamics—increase in the entropy of an isolated system during any natural process. We noted that

spontaneous changes, such as chemical reactions, are accompanied by a decrease in the Gibbs free energy and an increase in the entropy. In this section, we hope to understand the physical mechanisms underlying chemical reactions.

In terms of a molecular phenomenon, what happens during a chemical reaction?

Quoting Atkins [14], as he writes about molecular reaction dynamics:

Now we are at the very heart of chemistry. Here we examine the detailed behavior of molecules during the most crucial moments of reactions. Massive changes of form are occurring, energies of the size of dissociation energies are being redistributed among bonds, old bonds are being ripped apart and new bonds formed. The rate at which the molecules exchange atoms or groups of atoms, or a single molecule is switched into a different isomeric forms, depends on the forces that operate at the climax of the reaction, and these in turn depend on the detailed disposition of all the charged particles of all the molecules involved in the step.

One of the simpler theories attempting to explain the physical, molecular level mechanisms which underlie a “reaction” is called the collision theory [1,14,74]. This theory suggests that a chemical reaction is the consequence of the encounter of individual molecules of two species. As an example, consider a well mixed mixture of species  $A$  and  $B$  in a gaseous phase, which react in a reaction of the type



At low to moderate pressures, the molecules are much farther apart than their own (i.e., molecular) dimensions. This permits a molecule to move freely between collisions. Collisions, in this case, will be of the  $A$ - $A$ ,  $B$ - $B$  and  $A$ - $B$  kind and their relative frequencies will depend on their relative concentrations. The success of these collisions depends, among others, on the amounts of energies involved in the event [14].

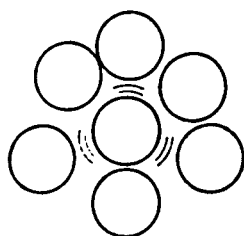
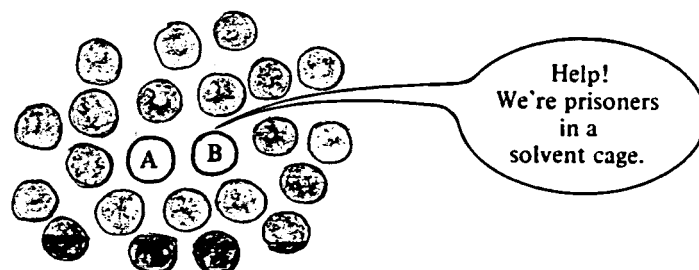


Figure 3.43: The solvent cage effect on a solute molecule in a liquid solvent [1,74]

Reactions in a liquid also occur through successful “encounters” between molecules of the appropriate species. But there is one major difference, which will be illustrated in the following example. Let’s imagine species *A* and *B* in a solvent. Quoting Adamson [1]:

The physical picture of molecular motions in a liquid is rather different from that in a gas. The molecules of a liquid are about as close together as in the crystalline solid ... there is usually about a 10% expansion on melting which allows some looseness and randomness in the liquid structure ... There is, nonetheless, a confinement which is usually referred to as the *solvent cage effect*. The physical picture is then one of a molecule vibrating a number of times against the walls of its cage, that is, against its immediate neighbors, with occasional escapes to some adjacent position.

In other words, a liquid has much less empty space separating its molecules compared to a gas, because of which molecules of the reacting species cannot move around as freely as they would in a gas. This is well illustrated in Figure 3.43, where a molecule each of *A* and *B* is in a “solvent cage”.

This cage effects makes molecular diffusion of any substance in a liquid much slower than in a gas. In fact, a molecule of *A* would collide many times with the molecules constituting the solvent cage before escaping to a new position, with new neighbors. The presence of solvent hampers solute molecules (like *A* and *B*) from approaching each other in the same manner as possible in a gas. But once they “find” each other, this confining nature of the solvent works to their advantage. The solvent cage forces the molecules to collide repeatedly with each other, as well as with the solvent molecules constituting the cage walls, as illustrated in Figure 3.44. Levine [74] says “A process in which *A* and *B* diffuse together to become neighbors

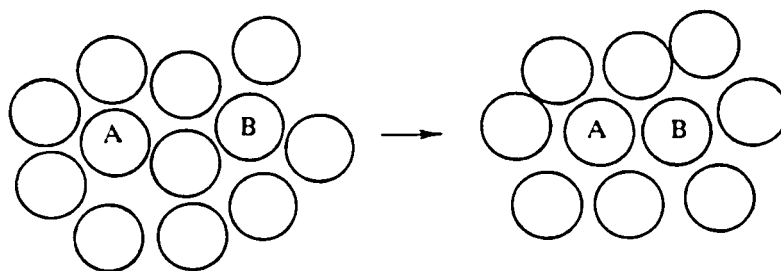


Figure 3.44: Diffusional encounter between reacting solutes *A* and *B* in a solvent [1]



is called an *encounter*. Each encounter in solution involves many *collisions* between *A* and *B* while they remain trapped in the solvent cage . . . .”

Thus, given the fact that a solvent results in many more collisions between the reactant molecules; and if the energy threshold necessary for a reaction is low, then the reaction would occur after a very few collisions. “Various theoretical estimates indicate that at room temperatures two molecules in a solvent cage will collide on the order of 20 to 200 times before they diffuse out of the cage . . . . The number of collisions will be greater the greater the viscosity of the solvent . . .” [74]. Therefore, one can safely say that in a system which meets the above criteria, *every* encounter should result in a reaction.

What does this mean? This implies that the rate at which the reaction proceeds depends on how rapidly “encounters” between *A* and *B* molecules occur. “Reactions which occur with every encounter are said to be diffusion controlled,” according to Adamson [1]. Levine [74] adds that most reactions in liquid solutions are not diffusion-controlled reactions, i.e., not all encounters lead to reaction. “Such reactions are called *chemically controlled*, since their rate depends on the probability that an encounter will lead to chemical reaction” [74].

As we have seen, the rate at which a reaction occurs is dependent upon the rates at which encounters occur and the energy availability. Atkins [14] explains the difference between a fast reaction and a slow one:

All reactions are fast. At least, the individual steps of a reaction . . . occur on an atomic time scale and are complete in less than about  $10^{-9}$  s. The slowness of the net reaction is due to the slowness with which molecules get activated, or come together; but even the net rate may become very fast when the activation energy can be provided very rapidly. This is the case, for example, when an explosion occurs: the sys-

tem is then beginning to demonstrate just how fast molecular processes can be.

Thus, if energy availability is not a problem, it is the rate of encounters which governs the net rate of a reaction. This is where the diffusion ability of the solute molecules in a given solvent comes into picture. Solute molecules having a larger coefficient of diffusion,  $\mathcal{D}$ , will be able to have more encounters in a given time period than molecules with smaller  $\mathcal{D}$ .

This ability of the molecules to move around in the solvent has a very important role to play in the case of competitive-consecutive reactions. What's a competitive-consecutive reaction? Reactions of the type shown below are usually classified in this category. Here,



$A$  and  $B$  react to produce  $C$  and  $D$ .  $C$ , however, competes with  $A$  in reacting with  $B$ , to form  $E$  and  $F$ . Also, since it is necessary for the first reaction to occur and form  $C$  before the second reaction can occur, the reactions are consecutive. Thus, overall, these two reactions are called competitive-consecutive reactions. In such a reaction, the amounts of  $C, D, E$  and  $F$  formed, which can be predicted by using the rate constants of these two reactions, depend fundamentally on the ability of the molecules of  $A, B$  and  $C$  to diffuse in the solvent.

In Section 3.7., we saw how turbulence affects the time rate of transport of dye at small scales. Here, we have studied how chemical reactions occur and why some reactions are fast while others are not. In the next subsection, we shall see how turbulence plays a role in the outcome of fast chemical reactions.

### 3.8.3. Turbulence and fast chemical reactions

Chemical Engineers have been grappling with this problem for quite some time, trying to understand and describe (mathematically) how such a system works so as to be able to accurately predict and/or control the outcome of chemical reactions which occur in a turbulent regime. The elements to be considered while formulating the problem, and their inter-relations, are shown in Figure 3.45. As Brodkey [28] describes it,

From a known geometry we would like to be able to predict or, if necessary, measure the parameters of turbulence. From this we want to obtain the mixing. Then, with incorporation of kinetics, we want to predict the full range of mixing with chemical reaction from the slow self-mixing (back-mixing) to the fast chemical reaction limit.

One of the ways of interpreting Figure 3.45 is that the geometry of the reactor defines the nature of turbulence in the system. Turbulence induces mixing which, in turn, affects the reactions. For a slow reaction, turbulent mixing may not be all that important while the reaction kinetics dictate the outcome of the process. In other words, even if the molecules of the reactants involved in a slow reaction are uniformly distributed throughout the system, the speed of the reaction would not change radically because the rate is controlled by the 'energy barrier' which prevents molecules of the reactants from reacting with each other. This implies that it will take a longer time for the reactants to react and form the products than the time needed to mix the reactants uniformly throughout the system and so, the major part of the reaction will occur in a system which has been uniformly mixed vis-a-vis reactant concentrations. Therefore, as we see in Figure 3.45, the kinetics element does not come into play for slow reactions. On the other hand, for fast

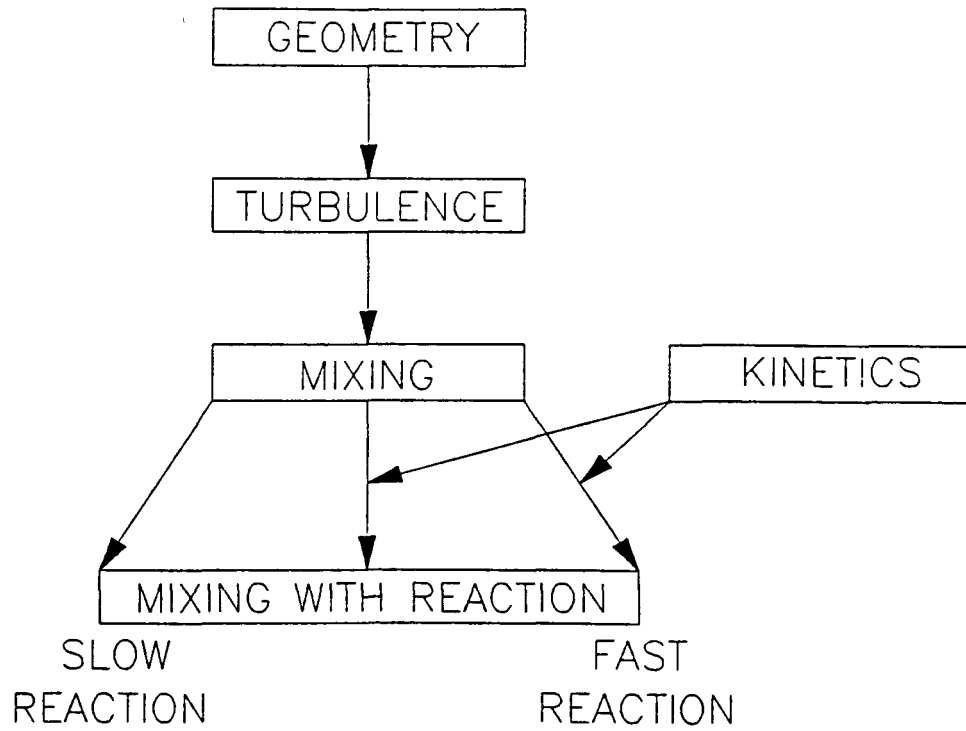


Figure 3.45: The turbulent flow, mixing and chemical reaction kinetics problem. Figure based on Brodkey [29]

chemical reactions, the turbulence and the resulting mixing play as important a role as the reaction kinetics. Here, the rate at which reactant molecules can come together is governing the overall speed and outcome of the reaction. For example, if there are regions of high and low concentrations of the reactants in the system, the outcome in these regions will be different for consecutive-competitive reactions shown in Equations 3.40 and 3.41.

To better understand how the role of turbulence changes with the inherent kinetics of a given chemical reaction, we quote O'Brien [83] (who quotes Toor [110]):

From a practical point of view, the most useful single parameter for describing the role of turbulence on chemical reactions is a ratio of time scales [a time scale  $\tau_k$  characteristic of the kinetic scheme to a time scale  $\tau_m$  characteristic of turbulent mixing]. In a single-step, irreversible reaction, the inverse of the reaction rate constant in conjunction with characteristic concentrations can represent the chemical reaction time; whereas, the time for the decay of fluctuations of a scalar field in the turbulence might represent the mixing time adequately. Three regimes suggest themselves:

1.  $\tau_k/\tau_m \gg 1$ , The slow reaction,
2.  $\tau_k/\tau_m \approx O(1)$ , Moderate reaction rate,
3.  $\tau_k/\tau_m \ll 1$ , The very rapid reaction.

In case one, it is abundantly clear, at least when approximate statistical homogeneity applies, that turbulence will induce chemical homogeneity before any significant reaction will occur and the fluctuations in concentration of any species at a *point* will generally be negligible compared to the mean concentration in determining the rate of reaction.

In the second case, complex coupling between the turbulence and the reaction is to be expected even under statistically homogeneous conditions.

In the third case, the behavior depends crucially on the nature of the reaction, as we shall see later. In particular, for multispecies reactions in which the species are not uniformly distributed in space, the progress of the reaction will be diffusion limited since molecules must first diffuse to

the same *point* before they can react. It is the rate of molecular diffusion, enhanced by the turbulence through stretching of isoconcentration lines, which must control the rate of progress of the reaction.

Before we go any further, let us define some parameters which describe the state of mixedness of a system. For a moment, reconsider the mixing process described in Section 3.5. We noted that we first needed to break-up large blobs of dye into smaller blobs and this was done by creating turbulence in the mixing vessel. This was shown in Figure 3.24. We also noted that molecular diffusion was necessary to bring about uniformity in mixing at the molecular level, as shown in Figure 3.25.

How does one describe the various states of mixedness exhibited in these figures? We define parameters like *scale of segregation*,  $L_s$  and *intensity of segregation*,  $I_s$ , for this purpose. The former is "... a measure of the size of unmixed clumps of pure components. This is a measure of some average size. As the clumps are pulled and contorted, the scale of segregation is reduced; this would be going from left to right along the top of Figure 3.25" [28]. The intensity of segregation "... describes the effect of molecular diffusion on the mixing process. It is a measure of the difference in concentration between neighboring clumps of fluid" [28]. Thus, as we move down the columns in Figure 3.25, the concentration difference between the "clumps" and the "inter-clump region" decreases as molecules of the dye diffuse out of the clump. This corresponds to a decreasing intensity of segregation. So, we can say that while a decrease in the intensity of segregation (i.e., a more uniform, 'non-clumpy' mixture) can only be created by molecular diffusion, turbulence is necessary to help speed up the process by very rapidly reducing the scale of segregation (i.e., smaller clumps).

In order for a reaction to occur, the molecules of the reactants must collide. And for the reaction to occur at a uniform rate throughout the reactor, the collision opportunities must be equal throughout the different regions of the vessel. Let's play with this idea a little bit. Suppose we have a solution of  $A$  which we want to react with a solution of  $B$  in a reaction



Reactant  $B$  is already in the reactor and we introduce solution  $A$  into this vessel and gently mix it using an impeller. As the impeller moves the fluid around, clumps of  $A$  are formed in the solution of  $B$ . These clumps of pure  $A$  are constantly losing molecules due to diffusion. Thus, the only place where  $A$  and  $B$  molecules can establish contact with each other is at the surfaces of these clumps of pure  $A$ . In this case, we see that the reason why the reaction proceeds slowly is because of the slowness with which molecules of  $A$  diffuse out of their clumps and meet  $B$  molecules (and vice-versa).

Now let us repeat this experiment, this time with high intensity turbulence to rapidly reduce the scale of segregation (i.e., make clumps smaller). The molecules, as we saw in the Section 3.5., have to diffuse over smaller distances in order to meet molecules of the other reactant, thus radically improving the overall rate of the chemical reaction! For complicated reactions, the influence of turbulence will show itself not merely in the rate at which the reactions occur but also in the products formed! Quoting Brodkey [28]

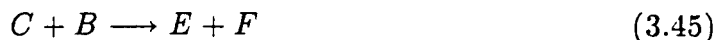
Dankwerts has discussed the importance of this degree of mixing of two reactants; the intensity of segregation must be reduced rapidly so as

to avoid local spots of concentrated reactant and the usually associated undesirable side reactions.

If, instead of a simple reaction of the kind



we have a set of competitive-consecutive reactions of the type



where  $A$  and  $B$  react to produce  $C$  and  $D$  while  $C$  and  $B$  react to form  $E$  and  $F$ , the results obtained are very much dependent on the mixing conditions.

How does such a situation arise? Let us do a thought experiment to visualize this. We have a reactor vessel full of  $A$ , into which we introduce a blob of  $B$ . In the first case, we will have no mechanical mixing taking place: we will let the molecules take their own time. In the second case, we subject the solution in the mixing vessel to very intense turbulence while we introduce a blob of  $B$ , making turbulence help us in rapid mixing. Let us also assume that all species ( $A, B, C, D, E, F$ ) have equal diffusivities. In the former case, the only regions where  $A$  and  $B$  molecules interact are the interfaces of the blob of  $B$ , because that's the only place from where molecules of  $B$  can diffuse into the bulk solution of  $A$ , meet them, and react. So, any  $C$  formed in the first step of this reaction sequence is very likely to diffuse equally in all directions (including in the direction of the blob of pure  $B$ ), resulting in a fraction of the total  $C$  reacting with  $B$  through the second step of the consecutive-competitive reaction set, to form  $E$  and  $F$ .



We now repeat the experiment with extremely intense mixing. The turbulence causes the blobs of pure  $B$  to become very small. As the blobs are rapidly reduced in size, diffusion is able to spread  $B$  molecules into  $A$  over a much smaller time period, resulting in a relatively better (more uniform, as compared to the previous case) spatial distribution of  $A$  and  $B$ . Thus, any  $C$  formed by the reaction of  $A$  and  $B$  has much lesser  $B$  to react with, than in the earlier, unmixed case. Therefore, as compared to the first case, more  $C$  and  $D$  will be formed and very little  $E$  and  $F$ . We must remember that we did not consider the speed of the individual reactions in our discussion above. For example, when the reaction shown in Equation 3.44 is much, much faster than the reaction shown in Equation 3.45 (or vice versa), the presence of turbulence and its diffusive action complicates the situation even more by tilting the balance in favor of the faster reaction—particularly if the time scale of the reaction is comparable to the time scale of turbulent diffusion.

As we have seen in the above example, for reactions of this sort, turbulent mixing plays a very significant role in the nature and amounts of the products formed! A good amount of this has been discussed in the following papers (and their discussions) [9,20,25,40,44,67,81,99]. For example, Nabholz et al. [81] model mixing-disguised chemical selectivities; Bourne et al. [20] describe the influence of fluid viscosity, stirrer speed, feed rate of reactants; Angst et al. [9] show the influence of different mixing impellers as well as the location of the feed pipe in the reactor on the differing amounts of products  $C$ ,  $D$ ,  $E$  and  $F$  obtained!

Many mathematical models have been proposed, e.g., by Jenson [63], by David et al. [38], etc. But the one that seems simplest and most easy to understand is that by Bourne and his colleagues, who document this model in a series of nine

articles entitled *Mixing and Fast Chemical Reactions* [21,17,22,10,11,19,24,16,12].

In this series, they showed [12] that:

The product distribution from fast, competitive consecutive reactions ... was found experimentally to depend upon the following variables:

- Stoichiometric ratio,  $N_{A0}/N_{B0}$ ,
- Volumetric ratio of reagent solution,  $\alpha = V_A/V_B$ ,
- Location of feed point,
- Backmixing into the feed pipe,
- Operating mode of reactor, e.g. CSTR and semi-batch,
- Viscosity of solutions,  $\nu$ ,
- Type, diameter  $d$  and rotation speed  $N$  of impeller,
- Concentrations of feed solution and concentrations in tank.

As we saw in the Section 3.3., the hydrolysis step of metal coagulants is also a multi-step reaction of the consecutive, competitive type. Clark and colleagues [31,32] have applied the “mixing and fast chemical reaction and its effect on product selectivity” concept to the problem involving aluminum coagulant  $AlCl_3$ . They show “... that aluminum precipitation itself is micromixing sensitive over the ranges of pH and aluminum concentration commonly found in water treatment ...” [32].

This angle of attack on the rapid-mix problem vis-a-vis metal coagulants is very likely to be the route which explains the behavior of the coagulant-colloid system, as seen by Amirtharajah and Mills [3] in their experiments involving extremely high intensity rapid mixing ( $G = 16000s^{-1}$ ) of alum coagulant on colloids. This will be discussed at a later stage in this thesis.

### 3.9. Flocculation

#### 3.9.1. Introduction

We have, so far, looked at the chemistry of colloids and coagulants and their interaction in the first step of ‘coagulation’. We have also examined mixing, turbulent flow, the role of turbulent flow in mixing, as well as the interaction of turbulent flow and mixing with fast chemical reactions. Thus far, the picture has been only sketchy. In this jigsaw puzzle, we now recognize the individual pieces well and we see how some of them interlock to form bigger composites—but there are still a few pieces missing. It is the aim of this section to tie together loose ends and unify them so as to complete the jigsaw puzzle we had started out to solve: that of understanding rapid-mixing of coagulants in water and its role in the flocculation process—leading onto subsequent water treatment unit processes.

Before we go any further, it is proper that we clarify, once again, what we mean by ‘flocculation’. As mentioned in the Section 3.2., this student adheres to the terms as specified by Benefield et al. [18] and O’Melia [85], i.e., *coagulation* refers to the overall process of aggregation—including both, destabilization of colloids and transport-aggregation—while *flocculation* refers solely to the particle transport-aggregation step.

Let’s put this step, flocculation, in a proper perspective. We start out with colloids in our raw water supply. In the rapid-mix step, we add to the raw water our coagulant, under conditions of high turbulence intensity and the appropriate chemistry (e.g., pH of water). This serves to form the proper species (if a metal salt coagulant is used) as well as to distribute them rapidly and uniformly throughout the

mixing vessel to provide all colloidal particles similar opportunities to interact with the coagulant and coagulant-hydrolysis products. This destabilizes the particles (see Section 3.2. for more details), which are now gently stirred, enabling them to aggregate. This is followed by other unit processes for treating the water—but we shall not get into that.

We notice that the term ‘aggregation’ is an intrinsic part of our definition of flocculation. What is aggregation? We quote Jullien and Botet [64]:

*Aggregation is an irreversible physical process in which initially dispersed basic units (particles or microaggregates) stick together, under the action of given attractive forces, to build characteristic structures, the aggregates, whose size increases with time.*

### 3.9.2. Aggregation kinetics

The dynamics of aggregation are, obviously, described by the forces acting on the particles—something we looked into in Section 3.2. which will not be repeated here.

The kinetics of aggregation are a different story altogether. It is thought that aggregation processes of the type involved in water treatment are generally ‘diffusion limited’ processes. In simple terms, the coagulant is able to transform the colloid chemistry to an extent such that the overall rate of particle aggregation is limited by collisions between particles. The situation is not different from what we have encountered in our discussions of diffusion limited chemical reactions in Section 3.8. We saw that some chemical reactions are energy limited while others are diffusion limited. Colloidal aggregation can also be thought of along the same lines. When particles are ‘kinetically stable’ (remember Section 3.2. ?), i.e., prior to

being destabilized, they are limited in their ability to collide and form aggregates by their lack of energy which is necessary to overcome the opposing forces. Once we use coagulants to 'kinetically destabilize' these particles, we have, in some way, considerably reduced the 'energy barrier' which had been responsible for a lack of aggregation.

Now, however, the rate of aggregation is governed by the rate at which particles can collide with each other. Analogous to what we saw in our study of fast chemical reactions under the influence of turbulent mixing, the faster we can get particles to collide with each other, the speedier the overall aggregation rate will be. This ability of particles to be transported can be thought of, to some extent, as their 'diffusivity' (similar to the diffusivity of molecules in a chemical reaction). This is why particle-particle aggregation, as generally encountered in natural processes, is often identified as *diffusion limited aggregation* or DLA [64].

Having agreed to the fact that in our case, transport of the particles limits the kinetics of particle aggregation, we now seek to understand the transport aspects of particles so as to identify the physical mechanisms which have the greatest role to play in our problem. Scientists have identified three major means by which transport of particles takes place in flocculation, as practiced in water treatment:

- The Brownian transport mechanism, in which the particles get moved around in the fluid because of the action of the fluid molecules which surround it and continue to bump into it, eventually resulting in particle-particle interaction.
- The fluid flow mechanism, in which the moving fluid generates velocity gradients which permit particles to move relative to each other and, if the situation permits, collisions and flocculation.

- Transport of particles by gravity, which may result in relative motion between particles and thus, inter-particle collisions, resulting in flocculation.

In all cases, the consequence is that particles are transported close to other particles, providing greater possible collision opportunities and, perhaps, aggregation. Of course, as a function of time, there is a net reduction in the total number of particles!

In working with such problems, researchers have found it convenient to work with ‘population balance models’. Why? Let’s visualize a situation which will help us see why this problem calls for such an approach. Suppose we have within a fluid, at time  $t = 0$ , a large number of uniformly sized particles which form aggregates upon collision. To simplify this even further, we give them a collision efficiency of 1 (i.e., every collision results in irreversible aggregation). We now allow time to pass. Individual particles may collide to form some ‘two-particle’ clusters. These, in turn, might interact with single particles or other ‘two-particle’ clusters to form 3- or 4-particle clusters. As more and more time passes, we see that the following things happen:

- The total number of single particles at any given time  $t$ ,  $n_{1,t}$ , should decrease as a function of time.
- The number of multi-particle clusters should change with time.

Let’s define  $n_{p,t}$  as the number of  $p^{th}$  order clusters (i.e., clusters consisting of  $p$  primary particles) at time  $t$ . We note that smaller clusters may join together to enter this ‘ $p^{th}$  order’ class while, on the other hand, the  $p^{th}$  order clusters already in this class may interact with other particles/clusters to form still larger clusters of size greater than  $p^{th}$  order clusters. Thus, each ‘order’ larger than the primary

particle order has particles simultaneously growing into its size range as well as out of it. To put it simply, growth of larger clusters is favored at the expense of smaller ones.

In order to keep track of the changes in the numbers of particle clusters of different size, a population balance is a necessary component of the description of the system. Von Smoluchowski was the first person to propose a mathematical description encompassing the above process. Quoting Jullien and Botet [64]:

To our knowledge, the first theoretical works dealing with aggregation appeared in 1916, when Von Smoluchowski introduced his famous equation, now well known as the *Smoluchowski equation*, able to describe the kinetics of aggregation. This equation can be considered as a classical equation of irreversible chemical reaction kinetics. The reactions in presence are:



where  $[i]$  refers to the chemical species: [ensemble of aggregates containing  $i$  particles],  $K_{ij}$  is the kinetic constant of the reaction. It is essential to understand that these are coupled chemical reactions: a given species  $[k]$  appears in the right-hand side of some reactions as well as in the left-hand side of other ones. More precisely, the  $[k]$  species may appear as a product of the reaction between the  $[i]$  and  $[j]$  species, so that  $[i + j = k]$ , but may also disappear to form  $[k + i]$  species, by reacting with any  $[i]$ . As usually in the classical theory of chemical kinetics, the equation giving the time evolution of the concentration  $c_k$ , where  $c_k$  is the number of aggregates of size  $k$  per unit volume, is given by:

$$\frac{dc_k}{dt} = \frac{1}{2} \sum_{i+j=k} K_{ij} c_i c_j - \sum_i K_{ik} c_i c_k \quad (3.47)$$

The  $1/2$  factor is due to the fact that one counts twice the same term in the sum:  $i, j$  and  $j, i \dots$

The quantity  $K_{ij} c_i c_j$  can be interpreted as the rate of events of the type  $[i] + [j] \rightarrow [i + j]$  per unit volume or, equivalently, as the probability, per unit time and per unit volume, that such event occurs. The

assumption that this probability is proportional to the concentrations  $c_i$  and  $c_j$  corresponds to neglect spatial fluctuations of concentrations . . . .

The main problem with Smoluchowski's formalism is that all physics is entirely contained within the  $K_{ij}$ , and thus, as long as we do not get any precise idea on their  $i$ - and  $j$ -dependence, we will be able to play with very interesting mathematical games, but without any obvious link with physical reality. To this is added another problem: even if the  $K_{ij}$  are known, the mathematical solution of the equation is often very hard to get.

Considerable literature has been generated in attempts to make Smoluchowski type rate expressions for flocculation processes in general and in water treatment in particular [61]. These models include the effects of Brownian motion, fluid flow (laminar and turbulent velocity gradients) and differential settling. Some models have also attempted to incorporate the breakup of flocs and are fairly complicated [61]. We shall examine some of the simpler models described by Letterman [73] without going into details of their complexities.

In a system which contains particles of different sizes, the equation

$$N(d_1, d_2) = k(d_1, d_2) \cdot n(d_1) \cdot n(d_2) \quad (3.48)$$

where  $N(d_1, d_2)$  is the number of collisions per unit volume per unit time between particles of diameters  $d_1, d_2$ ;  $n(d_1), n(d_2)$  are the numbers of particles of diameters  $d_1, d_2$  respectively in a unit volume, and  $k(d_1, d_2)$  is the 'rate constant' which "... is determined by the mechanism which causes the relative motion of particles 1 and 2" [73]. We see that Jullien and Botet [64] were very accurate when they said that for Smoluchowski's formulation, all the physics is contained within  $k_{ij}$ !

For flocculation ensuing as a consequence of Brownian transport of colloidal particles (called Brownian or perikinetic flocculation), the rate constant in the rate



equation (i.e., Equation 3.48),  $k(d_1, d_2)$  is thought to be

$$k_p = \frac{2 kT (d_1 + d_2)^2}{3 \mu d_1 \cdot d_2} \quad (3.49)$$

where  $k$  is the Boltzmann constant ( $1.38 \times 10^{-16}$  erg  $K^{-1}$ );  $T$  is the absolute temperature (Kelvin), and  $\mu$  is the absolute viscosity of the fluid.

A set of equations has been developed for flocculation resulting from transport by velocity gradients present in fluid flow. This kind of flocculation is called orthokinetic flocculation. A distinction is made between laminar fluid flow and turbulent flow. The equations are

$$k_{os} = \frac{(d_1 + d_2)^3}{6} \frac{dU}{dz} \quad (3.50)$$

for laminar shear type flocculation (where the subscript  $os$  in  $k_{os}$  presumably signifies 'orthokinetic shear'), and  $dU/dz$  is the velocity gradient. A similar equation for turbulent orthokinetic flocculation is

$$k_{ot} = \frac{(d_1 + d_2)^3}{6.18} G \quad (3.51)$$

where  $G$  is said to be a velocity gradient similar to  $dU/dz$ .  $G = \sqrt{(\varepsilon/\nu)}$  where  $\varepsilon$  is the rate of energy dissipation by turbulence per unit mass of fluid, and  $\nu$  is the kinematic viscosity of the fluid. Here, the subscript  $ot$  in  $k_{ot}$  signifies 'orthokinetic turbulent' flocculation.

Based upon these equations, one can evaluate the rate constants for various mechanisms. First, we consider Brownian flocculation. If we look at Figures 3.46 and 3.47 (note the log scales), we see that the rate constant is smallest for encounters between particles of the same diameter. Also, the collision rate is highest for collisions between a very large particle and a very small one. This is apparent

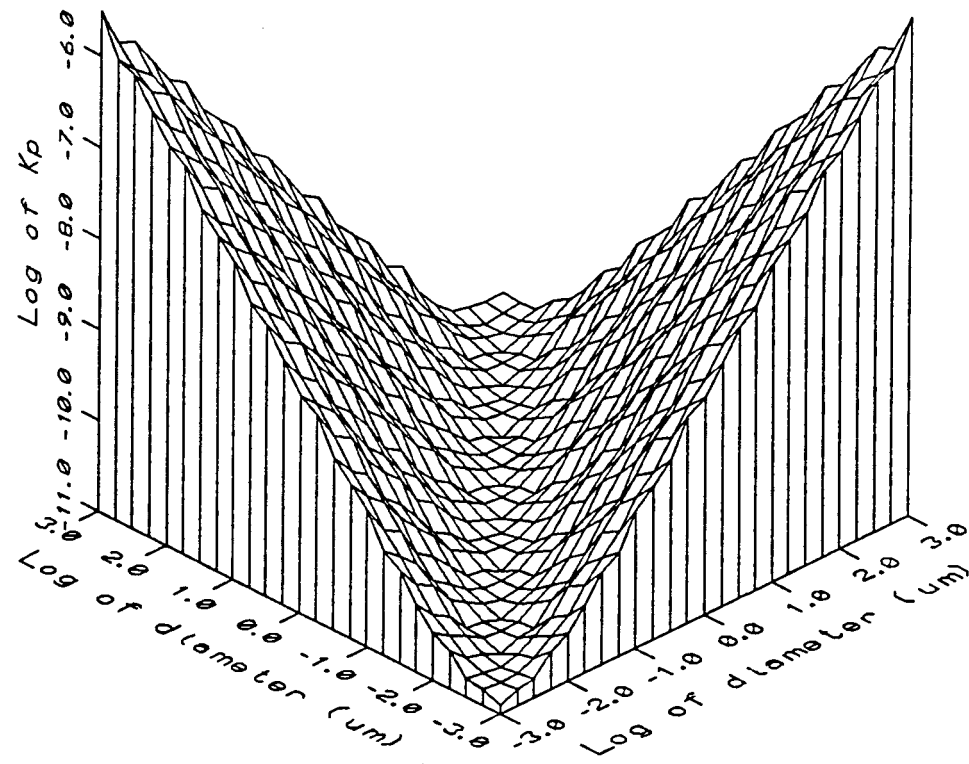


Figure 3.46: Perikinetic flocculation constant,  $k_{p(i,j)}$ , as a function of the diameters of the interacting particles ( $d_i, d_j$ ). The plot shows the surface generated for  $k_{p(i,j)}$  using water at 25°C. Note the log scales on all three axes

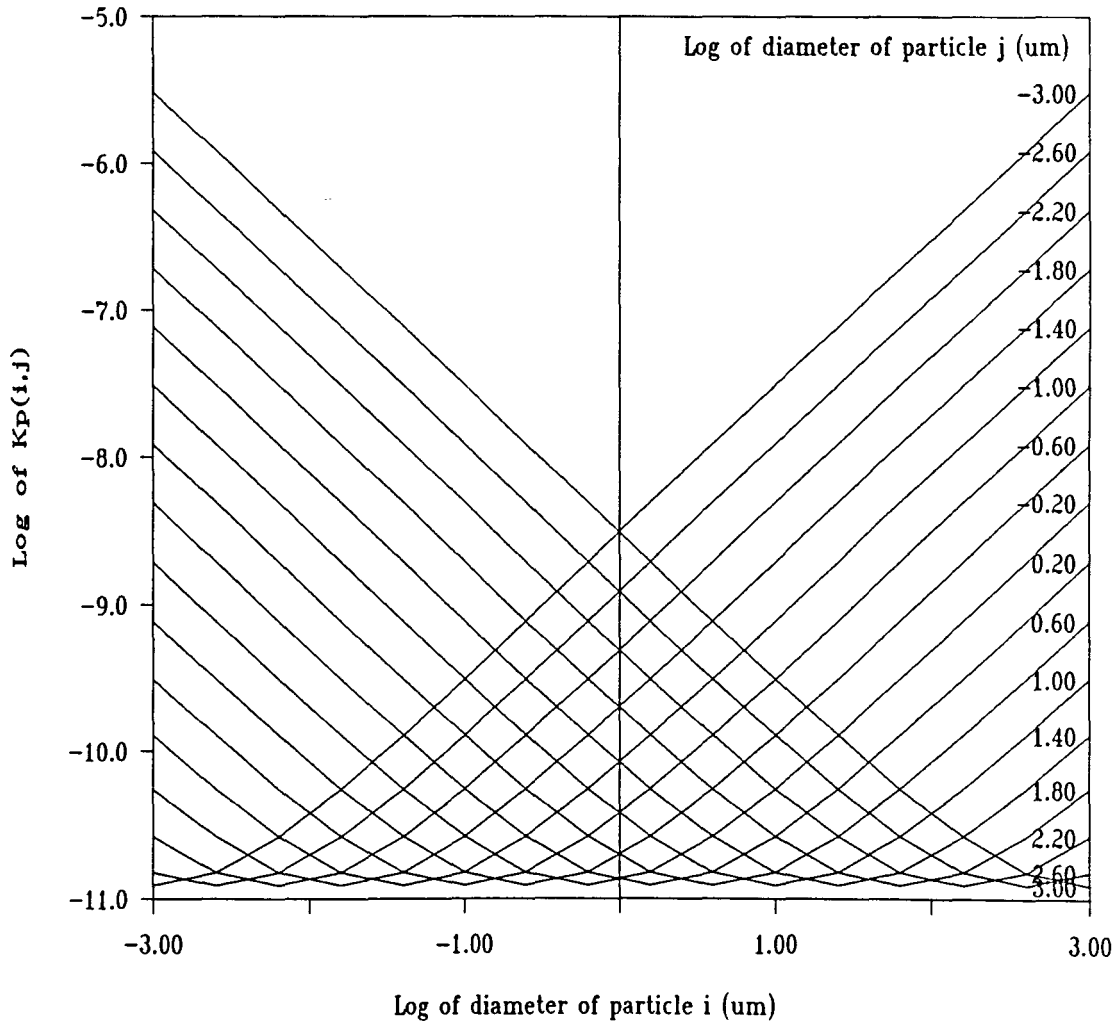


Figure 3.47: Perikinetic flocculation constant,  $k_{p(i,j)}$ , as a function of the diameters of the interacting particles ( $d_i, d_j$ ). The plot shows the cross section of the  $k_{p(i,j)}$  surface, corresponding to different diameters of particles. The conditions for calculations are water at  $25^\circ\text{C}$ . Note the log scales on both the axes

from the equation itself. If  $d_2 \gg d_1$ , then  $k_p \propto d_2/d_1$ , which shows that the relationship reduces to a mere ratio of the sizes of the two particles!

Now consider orthokinetic flocculation of the turbulent fluid flow kind. If we look at Figures 3.48, 3.49 and 3.50, we see that once again, the larger particle dominates the value of the flocculation constant. For example, we consider a particle of diameter  $0.1\mu\text{m}$  ( $\log(0.1) = -1.0$ ). In Figure 3.50, at  $25^\circ\text{C}$ , we locate the curve corresponding to  $-1.0$ . We see that for interaction with particles smaller than its own size, the orthokinetic flocculation 'constant' is virtually constant (because it is dominated by the diameter of the larger particles—which, in our case is  $0.1\mu\text{m}$ ). However, this constant increases rapidly as the diameter of its pairing particle increases and is soon dominated by the pairing particles which are bigger than it.

If we now compare the two constants evaluated, (i.e.,  $k_p$  and  $k_{ot}$ ), we see that for particles generally encountered in water systems ( $> 0.1\mu\text{m}$  in size), the orthokinetic flocculation constant  $k_{ot}$ , for  $G = 50\text{s}^{-1}$ , is much, much greater than the  $k_p$  at  $25^\circ\text{C}$ . This means that if the mathematical descriptions of the system are accurate then, as far as water treatment is concerned, we can ignore the effects of Brownian flocculation. That leaves us with the orthokinetic flocculation to play with. Perhaps it is proper to emphasize that since most water treatment flocculation occurs in turbulent fluid flow regime, we must use the mathematical expression corresponding to the turbulent orthokinetic flocculation (Equation 3.51) and not the laminar orthokinetic flocculation (Equation 3.50).

The collision frequency for this can be calculated from Equation 3.48. This has been calculated for a particle system (kaolinite clay  $25\text{ mg/l}$  in water) with an initial (i.e., at time  $t = 0$ ) particle size distribution as shown in Figure 3.51. Based

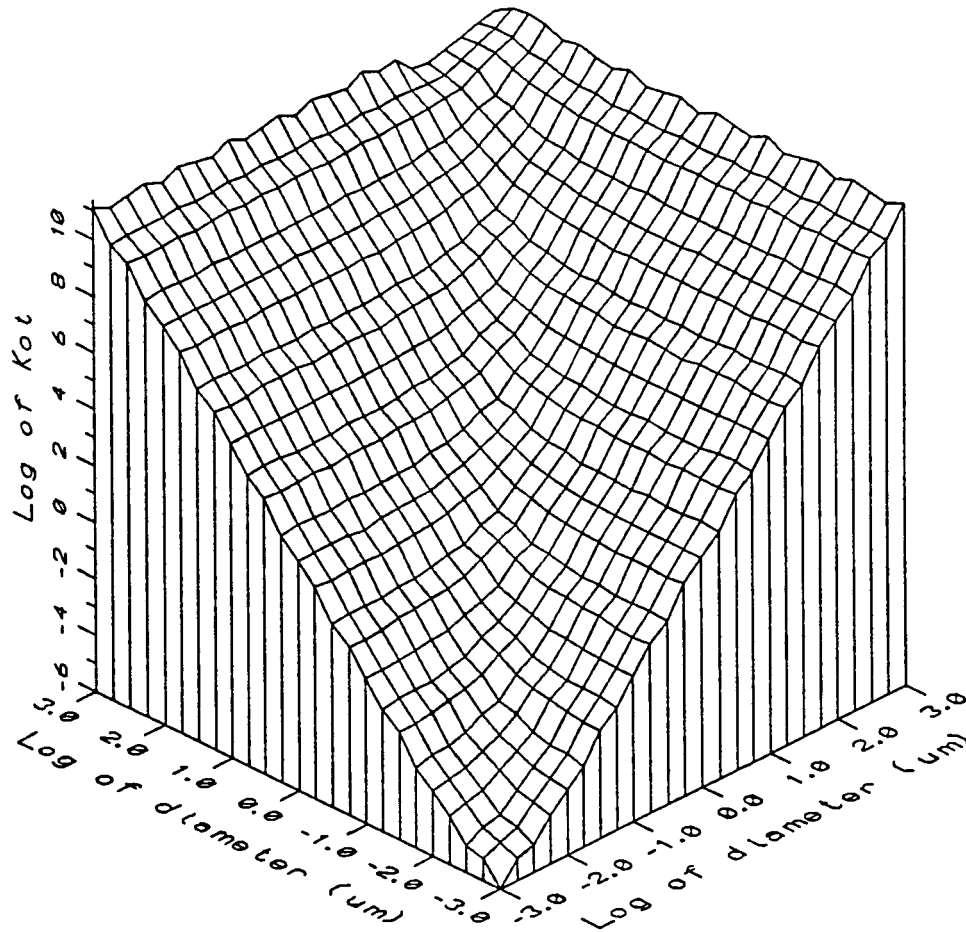


Figure 3.48: Orthokinetic flocculation constant,  $k_{ot(i,j)}$  as a function of the diameters of the interacting particles ( $d_i, d_j$ ). The plot shows the surface generated for  $k_{ot(i,j)}$  using water mixed at a  $G = 100s^{-1}$ . Note the log scales on all three axes

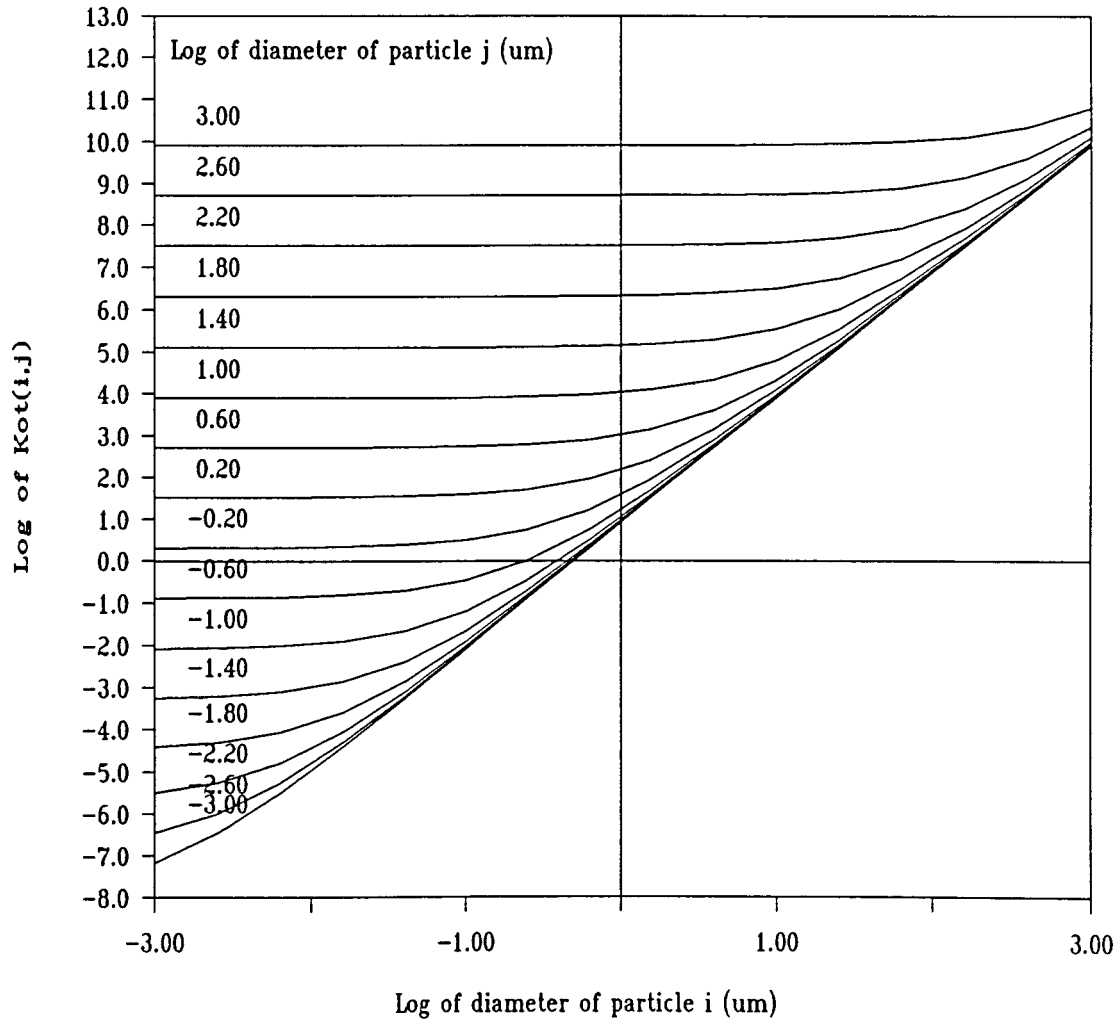


Figure 3.49: Orthokinetic flocculation constant  $k_{ot(i,j)}$  as a function of the diameters of the interacting particles ( $d_i, d_j$ ). The plot shows cross section of the surface generated for  $k_{ot(i,j)}$  using water mixed at a  $G = 50s^{-1}$ . Note the log scales on both the axes

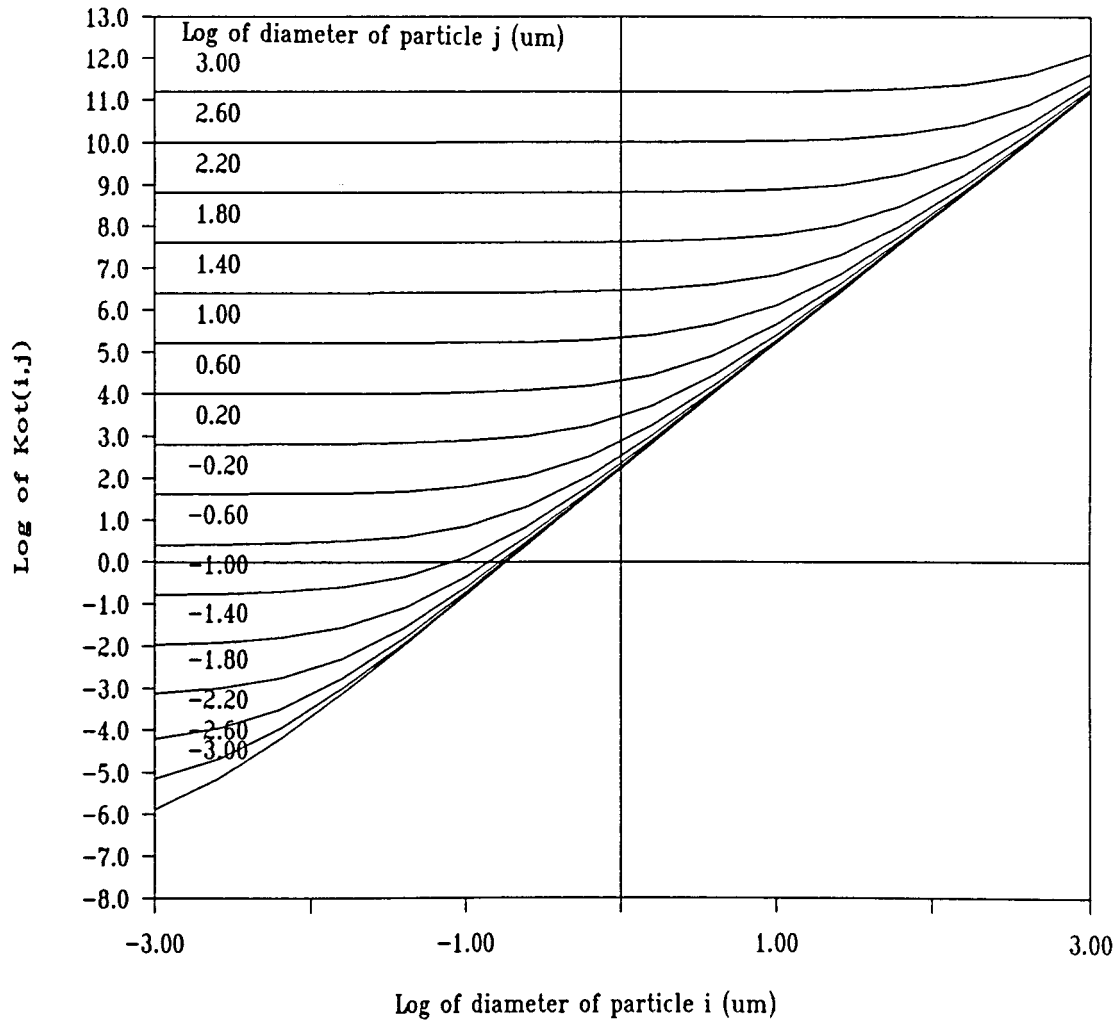


Figure 3.50: Orthokinetic flocculation constant  $k_{ot(i,j)}$  as a function of the diameters of the interacting particles ( $d_i, d_j$ ). The plot shows cross section of the surface generated for  $k_{ot(i,j)}$  using water mixed at a  $G = 1000s^{-1}$ . Note the log scales on both the axes

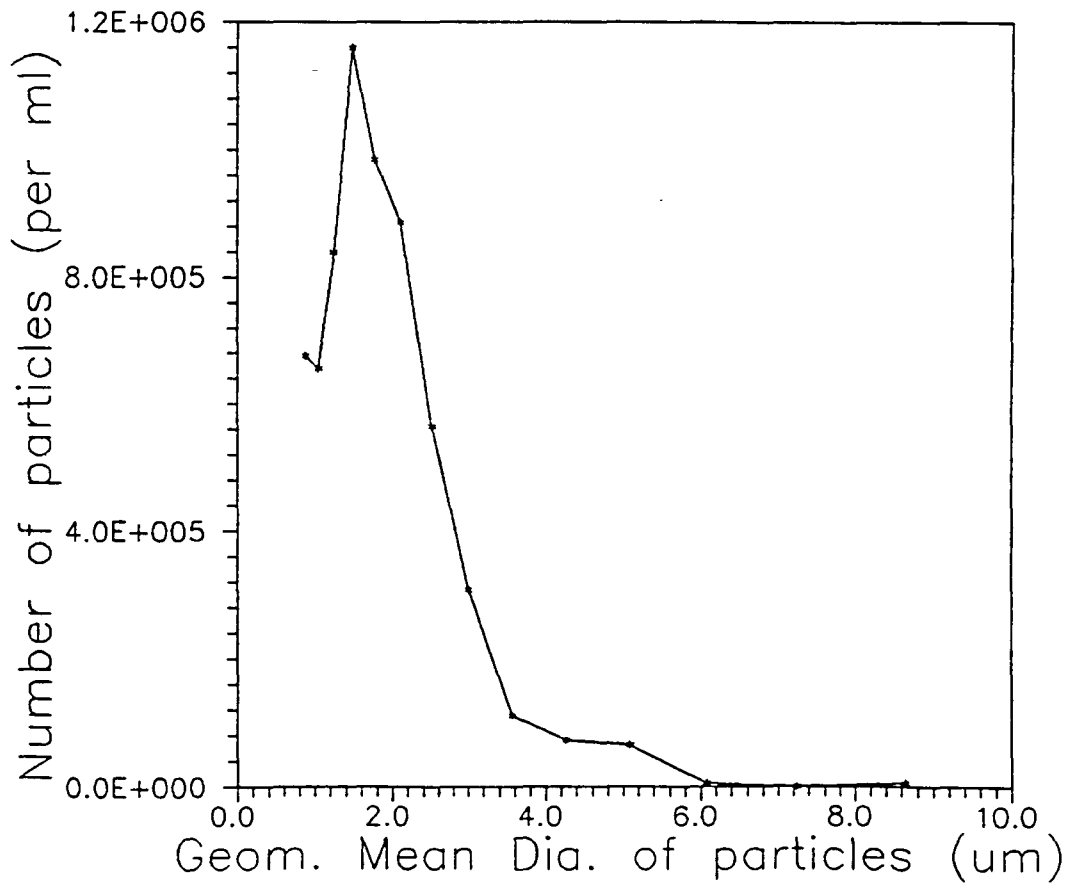


Figure 3.51: Particle size distribution of a 25 mg/l clay suspension



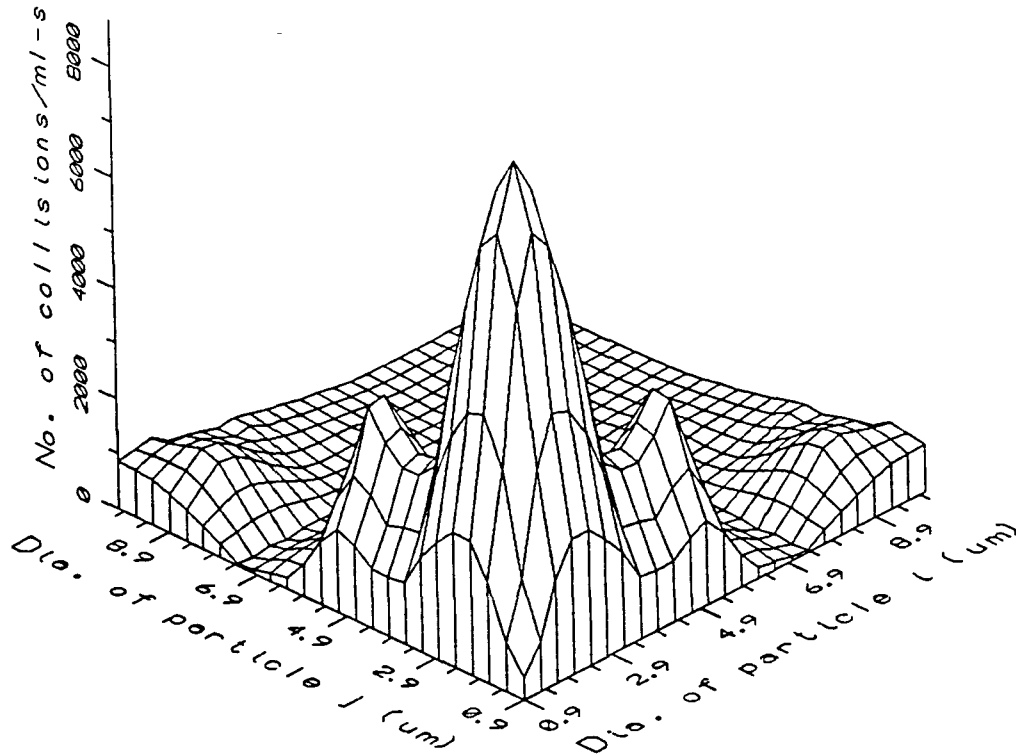


Figure 3.52: Variation in collision frequency,  $N(d_i, d_j)$ , per unit volume per unit time as a function of the diameters ( $d_i, d_j$ ) of particles for the clay suspension identified in Figure 3.51, mixed with a  $G = 50s^{-1}$

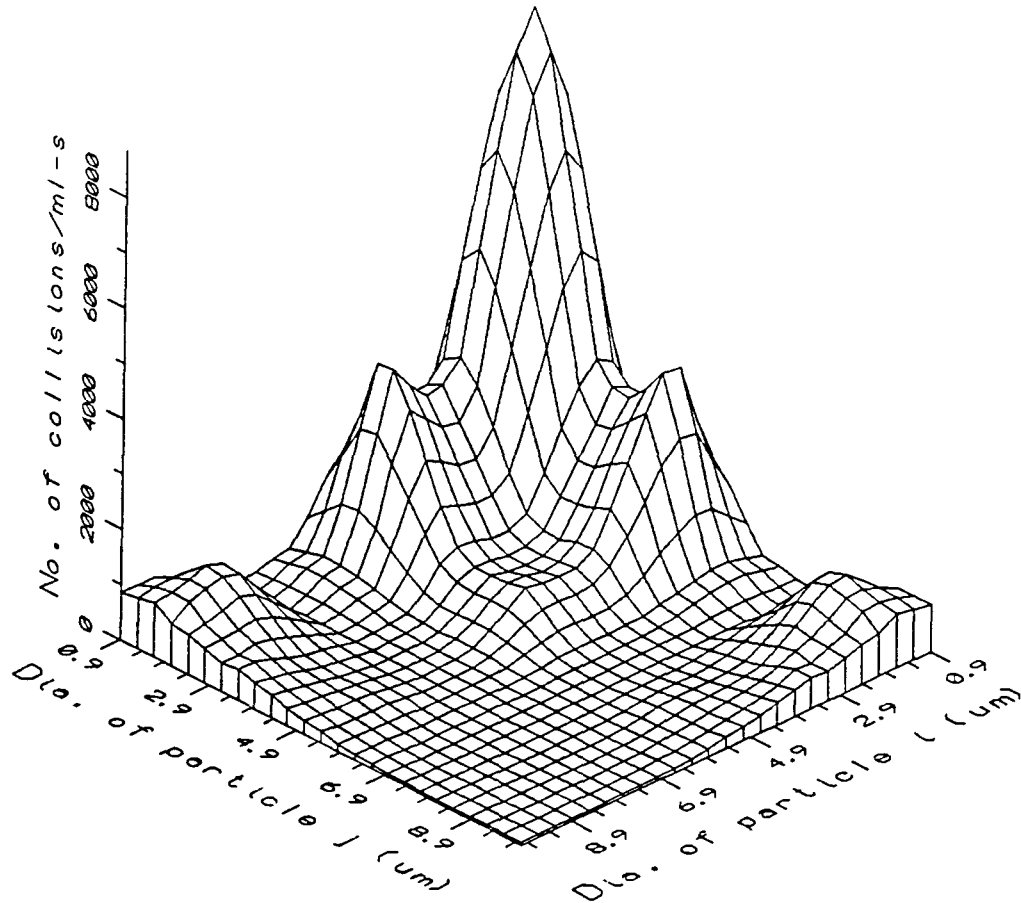


Figure 3.53: Variation in collision frequency,  $N(d_i, d_j)$ . Another view of the surface shown in Figure 3.52

on the calculations, we get results shown in Figures 3.52 and 3.53. As we see, the collision frequency is greatest for particles in the size range  $\approx 2\mu\text{m}$ . What does this mean? This means that orthokinetic flocculation is the dominating mechanism in particle growth in water and that for a system like clay (which has a particle size distribution similar to that of particles found naturally in surface waters), the frequency of collision of smaller particles is the highest—a reason why, as a function of time, there is a much more rapid reduction in the number of the smaller particles than in other size ranges! We also note that this high frequency of collisions is because of their high concentrations or  $n(d_1)$ . Thus, even though we know from Equation 3.51 that  $d_2$  dominates the collision frequency if  $d_2 > d_1$ , we see that size alone cannot have much influence. We must have a large number of particles (i.e., a large  $n(d_i)$ ) and must mix more intensely (i.e., greater  $G$ ) for more collisions and, therefore, better flocculation. Thus, a proper increase in number of large diameter particles can go a long way in assisting us in speeding up flocculation. This is the reason why Kawamura thinks "... there is clear evidence that recirculation of small amounts of preformed floc does improve both flocculation and sedimentation. This is particularly true for low turbidity waters ..." [66].

### 3.9.3. Turbulent flow and flocculation

Though we have played around with a very simple mathematical model of particle aggregation, we haven't really looked into the 'physics' behind it. Since we already know a little about colloids and coagulants, let us now look, very briefly, at the hydrodynamics of turbulent flocculation. We know that turbulent flow, by itself, is fairly complicated. The presence of a second phase compounds the problem

considerably because one now needs to consider fluid-particle interactions, too. For example, Pourhamadi and Humphrey [91] discuss the work of other researchers who have shown that "... an increase in dissipation rate of turbulent kinetic energy with increasing particulate concentrations," (i.e., the energy is dissipated at a faster rate in a fluid containing a large number of particles than in a fluid which does not contain particles) among other things! Amirtharajah and Kawamura [6] mention that "... the maximum size to which flocs will grow is controlled by the turbulence characteristics in the stirred vessel." They classify the turbulent regime into three categories:

- Flocs or aggregates with sizes ( $d$ ) much larger than the Kolmogorov microscale ( $\eta$ ) in regions where inertial effects dominate.
- Flocs of sizes ( $d$ ) which are much smaller than the Kolmogorov microscale ( $\eta$ ) where viscous effects predominate.
- Flocs of intermediate size.

Most of the particles found in waters to be treated are, in general, much smaller than the 'typical' Kolmogorov microscale size ( $\eta$ ) in turbulent flocculators. This implies that the particles essentially experience pure shear and extensional flows. This sentiment is also echoed by Koh et al. [68], who say:

For solid-liquid systems, the collision of particles between 1 and 20  $\mu\text{m}$  in size invariably occurs by a laminar mechanism even though the general flow field may be fully turbulent as in a baffled stirred tank. This may be interpreted as a complete containment of colliding particles within a turbulent eddy where the particles follow the local fluid motion closely and where orthokinetic flocculation can be assumed.

However, assumptions notwithstanding, the fluid does *not* have uniform energy dissipation over the entire flocculator. There exist regions of high energy dissipation (and correspondingly high shear and extensional rates as well as small  $\eta$ s) near the impeller and lower energy dissipation (with lower shear and extensional rates as well as large  $\eta$ s) farther away from the mixing device. That is why, during the flocculation process, the flocs are subjected to varying shearing and erosion forces, resulting in "... disruption of some of the floc aggregates, or floc breakup" [62]. Thus, we have here a give-and-take situation, where we know that a greater turbulence intensity will give a faster aggregation rate but we also have to realize that a breakup will have a much bigger role to play as the turbulence intensities are increased.

What if we use purely laminar flow instead of turbulent flow for flocculation? That would reduce the rate of flocculation considerably. How? We quote Koh [69]:

The type of flow, whether it be laminar or fully turbulent is not important, rather it is the degree of mixing. In a system with no mixing such as in laminar tube flow, the particles remain in the same shear zone and are subjected to the same shear rate during the entire flocculation process. Whilst in a perfectly mixed system such as in a baffled stirred tank, all the particles would eventually be exposed to the full range of shear rates present. For a system with distributed shear rate, the degree of mixing affects individual steps in the flocculation process, from doublet formation to floc growth and floc breakup. Due to the mixing of fluid between zones of high and low shear rate, flocs formed in a particular shear zone can be broken up elsewhere in the system.

As we have said earlier, a compromise must be made in terms of the intensity of agitation so as to not have excessive breakup of flocs but have adequate collision frequency so that the rate of flocculation is high.

### 3.9.4. Conclusion

So, how else can we increase the rate of primary particle number reduction? One of the ways would be to increase the 'efficiency of collision'! It is a fact that not all collisions result in irreversible aggregation. O'Melia [85,86] considers various aspects of this efficiency factor ( $\alpha$ ) and says "... the collision efficiency factor will depend upon the colloids in the water to be treated and the other chemical characteristics of the solution as well as the coagulant which is used." Tambo and Watanabe [107] go even deeper into this parameter:

...under the turbulent condition,  $\alpha$  is not constant because (an assumption of a) constant collision-agglomeration factor  $\alpha$  cannot change the floc size distribution but only the rate of floc growth.

Since the 'efficiency' of these collisions depends on a multitude of factors, and given the infinite range of conditions which could exist in a real situation—coupled with our ignorance of details of such a complex phenomenon—it is not surprising that there is, yet, no general model which properly describes such processes.

Where does this leave us? Let's step back from all this for a while and look at the process from afar, without getting bogged down in the details. We get colloids in the raw water and their chemistry is altered by our coagulants. These changes are all dependent on the coagulants, the colloids, the manner and extent of rapid mixing, the water chemistry, as well as their interactions. Once this is done, we gently stir these 'altered' colloids and flocculate them. Given the constraints on the intensity of flocculation vis-a-vis growth and breakup, we choose a reasonable intensity of flocculation. Once this is fixed, we have little control over it except for time (or duration) of flocculation. However, we want this rate of growth to

be as rapid as possible. The option of having overly extended periods of time for flocculating the suspension is out of question. That doesn't seem to leave us with many options.

One way to do this would be to make the collisions more efficient! And that's where the role of the proper coagulant dosages and rapid mixing comes into picture. Obviously, the process of rapid mixing deserves more attention than it has received thus far. Perhaps it was his understanding of this unit process that prompted Moffett [77] to say, "...coagulation takes place in the rapid mixer; and, from the viewpoint of the operator, this is the most important single step in a water treatment plant. Improper coagulation cannot be corrected at a later stage of the process, and the results of improper coagulation will be to reduce the quality of the effluent and the efficiency of the plant as a whole."

## 4. EXPERIMENTS

### 4.1. Introduction

In this study, experiments were conducted with the objectives of investigating the impact of

- rapid mixing conditions and
- temperature of water

on the flocculation of dilute clay suspensions in water. The experiments were a part of an ongoing NSF (National Science Foundation) project to study the effect of temperature and reactor geometry on flocculation kinetics.

Before we get into the details of the experiment, it is proper that we specify the reasons why such an endeavor was necessary.

One of the earlier references on the mixing criteria to be used for distributing coagulants uniformly throughout the water was “Design of Mixing and Flocculating Basins” by Hudson and Wolfner [59]. It dealt with mixing of metal coagulants in water. Quoting them,

Coagulation can be defined as the process of chemical reaction of the coagulant in water. The function of a rapid-mix chamber is to insure completely homogeneous coagulation. To accomplish this requires



intense mixing to distribute the coagulating agent uniformly throughout the water, so that it makes contact with suspended particles before the reaction is completed. In the absence of intense mixing, part of the water is over-treated with coagulant, while other parts are under-treated or not treated at all. Mixing needs may be gaged by two observations: coagulants hydrolyze and begin to polymerize a fraction of a second after being added to water, and, a milliliter of water contains more than 10,000,000 particles to be coagulated<sup>1</sup>. Practice in design has been to use not more than 30 sec in a rapid-mix, with relatively high-powered mixing devices. The in-line “blender” is coming into use for this purpose. A 24-in. unit can apply 10 hp to 20 mgd in a fraction of a second, during which time the coagulant is introduced.

Note the reference to a finite amount of power being applied to mix a given amount of water in a specific time interval. We shall come back to that sometime later.

Not much research was done on determining, experimentally, the design criteria for rapid-mixing units until Vrale and Jorden published their insightful paper “Rapid Mixing in Water Treatment” [113]. Their attempt was to “...show that the general design criteria (for rapid mixing units) are not compatible with the nature and rates of the chemical and physical reactions that occur when  $Al(III)$  or  $Fe(III)$  are used” [113]. First, they identified the factors influencing mixing:

To understand this problem, the following must be taken into consideration:

1. the type and rates of chemical reaction which  $Al(III)$  or  $Fe(III)$  undergo,
2. the chemical and physical factors which affect these rates,
3. how different mixing regimes affect these physical and chemical factors,
4. how the various reaction products of  $Al(III)$  and  $Fe(III)$  affect the collision efficiency of particles.

---

<sup>1</sup> This, presumably, refers to particulate matter present in the raw water.

These considerations are necessary because the physical-chemical reactions not only appear to be extremely rapid, they are essentially irreversible. Also, the rates and reaction products depend upon local concentrations, while the collision efficiency is highly dependent upon the type of reaction products adsorbed to the colloid surface and the concentration and distribution of them upon the colloid surface.

Does this sound familiar? It should. From what we saw in Chapter 3., we can easily visualize why their observations might be true.

They also went on to give reasons why they thought the design criteria for mixing units were inadequate. Quoting, [113]:

The design criteria suggest that the principal parameters of rapid mixing are intensity and duration<sup>2</sup>. However, because of the speed and nature of the reactions, additional detail must be considered. The speed of homogenization of the destabilant chemical and the raw stream are thought to be a function of:

1. the intensity and scale of turbulence at and downstream of the precise point of contact of the two streams<sup>3</sup>,
2. the number of points of addition of the destabilant,
3. the relative concentrations and flow rate of the two streams, and
4. the flow conditions, i.e., backmix versus plug-flow.

Again, we have seen in Chapter 3. why these criteria are important in the process of coagulant mixing.

Vrale and Jorden [113] did experiments which showed that for the adsorption-destabilization mode of colloid treatment,

---

<sup>2</sup> This is often referred to as the  $G$  and  $t$  specification because  $G$  is an indicator of the mixing intensity, and  $t$  is the time for which mixing at such an intensity is to be carried out.

<sup>3</sup> The two streams are the raw water stream and the coagulant stream.

1. A backmix reactor is very inefficient for rapid mixing.
2. A tubular reactor appears to be the most efficient type. Points of application and the details of the turbulent scale and intensity immediately at, and downstream of, the application point are very important design considerations.
3. Average mixing velocity gradient ( $G$ ) is inadequate for characterizing rapid-mix-unit efficiency in terms of achieving maximum aggregation rate for a given chemical dosage.
4. Proper rapid-mix design can lead to two operational improvements: a decrease in the required chemical dosage and an increase in flocculation unit capacity.

This student does not agree with *all* of their conclusions—specifically item 1, for reasons to be discussed later—but agrees wholeheartedly with the other three conclusions.

In fact, Vrale and Jorden's conclusion about the inadequacy of  $G$  alone in characterizing rapid-mix-unit efficiency—as well as the incorrectness of the generally accepted design criterion that  $Gt$  in rapid mixing/flocculation be kept within given specific limits—were proven in experiments conducted by TeKippe and Ham [108]. In their paper "Velocity-Gradient Paths in Coagulation" [108], they say that:

The  $Gt$  parameter, alone, obviously is inadequate for the selection of an optimum coagulation-basin design. The above data suggest that a more useful concept is to rapid-mix until visible floc formation has occurred and then to decrease the velocity gradient to permit floc growth.

Earlier chemical destabilization studies revealed that such variables as pH, alum concentration, and velocity gradient, affect the time required to form visible floc in the rapid-mix process. The results presented here indicate that the rapid-mix process is a very important portion of the total velocity-gradient path. If, for example, the rapid-mix period is too short, the floc formation will be slow, necessitating a longer detention time in the coagulation basin. Since the velocity gradients in the coagulation basin are generally much lower than those of a rapid

mixer, the required additional detention time in the coagulation basin may be considerable to achieve equal treatment results.

In the year following the publication of the paper by TeKippe and Ham [108], EPA published the report "Initial Mixing in Coagulation Processes" by Stenquist and Kaufman [101]. This report developed the theory of mixing, in general, and contained results of experiments conducted to "...demonstrate that rapid initial mixing is important in certain water and wastewater treatment processes, specifically alum coagulation-flocculation of a turbid water. Another purpose was to show that grid-type initial mixers ... can be used to effect the rapid mixing" [101].

Stenquist and Kaufman conducted experiments involving the mixing of alum coagulant, comparing a 'grid in the pipe' type of device with a 'flash mixer'<sup>4</sup> in a continuous flow system. Comparing a 24-orifice grid, a 4-orifice grid and the flash mixer, they concluded that "There was a pronounced tendency for the 24-orifice grid to provide the best results and for the flash mixer to provide the poorest results" [101]. They went on to say that

The present study produced no conclusive evidence as to whether backmixing is inherently inferior to plug-flow mixing for alum coagulation-flocculation. While the mixing provided by the flash mixer was quite rapid, it is believed that the time of mixing was probably lower than that provided by the grid mixers .... It was assumed that with a mean

---

<sup>4</sup>Based on the information provided in their report, it appears that the reactor which they call as 'flash mixer' was actually a backmix reactor. This clarification is necessary because the in-line "blenders" referred to by Hudson and Wolfner earlier in this section are often called 'flash mixers' while the reactors of the type used by Stenquist and Kaufman are generally referred to as backmix reactors.

residence time of 23 sec, the concentration fluctuations at the outlet were probably quite low. That the flash mixer gave the poorest results cannot be taken to mean that backmixing necessarily results in poorer performance. It may only mean that it is difficult to obtain very rapid mixing with such a device.

This comment is extremely confusing because, talking about the flash mixer, they first say that "...it is believed that the time of mixing was probably lower than that provided by the grid mixers." However, a few lines later, they say "That the flash mixer gave the poorest results cannot be taken to mean that backmixing necessarily results in poorer performance. It may only mean that it is difficult to obtain very rapid mixing with such a device." If the grid mixer displayed superior performance as compared to the flash mixer even though the time of mixing in the flash mixer was lower than that in the grid mixer, then their conclusion that "...it is difficult to obtain very rapid mixing with such a device" is incorrect! There must be some other reason why the flash mixer performed worse than the grid type mixer. Possible reasons for this will be demonstrated later in the thesis.

A year after Stenquist and Kaufman's work, Letterman, Quon and Gemmell published their paper "Influence of Rapid-Mix Parameters on Flocculation" [72] with the objective to

...evaluate the influence of

1. the length of the rapid-mix period,
2. the rapid-mix intensity,
3. the initial turbidity,
4. the concentration of alum coagulant, and
5. the type of impeller and vessel on the removal of turbidity by subsequent flocculation and sedimentation processes.

Their experiments indicated that for a given set of suspended solids concentration, alum dosage and mixing intensity, the residual turbidity following sedimentation showed a strong dependence on the time of rapid-mix! This led them to conclude "...that the early conditions of floc formation are important and the function of the rapid-mix operation is more than simply to disperse the coagulant" [72]. They also showed that two different types of impellers, when operated at the same  $G$ , gave different final residual settled turbidities: proving once again that  $G$  was an inadequate parameter to characterize coagulant mixing.

Following the paper by Letterman et al., there was a lull in experimental work involving rapid-mixing involving metal coagulants until, in 1982, Amirtharajah and Mills published their classic paper "Rapid-mix Design for Mechanisms of Alum Coagulation" [3]. In this marvelous work, they identified, based on theoretical considerations and experimental results, various zones of coagulation for alum coagulant on a log-concentration vs. pH diagram for aluminum. They also advanced the argument that for the adsorption-destabilization mode of alum coagulation, intense mixing would be preferable because the hydrolysis products are formed with great rapidity. Intense mixing would disperse the alum uniformly at the molecular level even before hydrolysis takes place so that the hydrolysis products formed are able to adsorb onto all the colloids. Also, they argued, since the sweep floc mode of coagulation is a slower process, occurring over 1-7 sec, mixing would not be all that important for this mode of colloid destabilization. They conducted experiments to verify this theory and concluded that:

1. When coagulation occurs under optimum-sweep conditions ... there is no difference in coagulation results for rapid mixing at  $G$  values

of 300, 1000, or 16000  $s^{-1}$  . . . .

2. In the adsorption-destabilization corona around the restabilization zone the high-intensity-blender rapid mixing is superior to the back-mix reactors with  $G$ s of 300 and 1000  $s^{-1}$  . . . .

They saw a similar improvement in the adsorption-destabilization region below the restabilization zone (in the pH-concentration diagram for alum), reaffirming their theory.

Following this paper, Amirtharjah and Trusler published "Destabilization of Particles by Turbulent Rapid Mixing" [7] in which experimental work involving direct filtration of colloids destabilized using alum coagulant, subjected to a variety of mixing conditions. A theoretical model was proposed for the destabilization of particles. "However," as the authors wrote, "the evidence was not incontrovertible" [7]. They added that

An important conclusion from the theory and experiments is that particle destabilization seems to be controlled by the maximum turbulence in the zone around the impeller of a backmix rapid mixing device. This is substantiated by the correspondence of the experiments with the microscale eddies in the zone around the impeller.

This student does not agree with this statement entirely. Reasons for this will be presented later in the thesis.

This, to the best of my knowledge, has been the latest of the experimental efforts involving the process of rapid mixing. While Clark et al. [32] did publish their study on micromixing, their approach was more of an attempt geared towards understanding the distribution of alum in water and its hydrolysis. Their experiments did not involve particulate colloids of the kind found in water treatment. Therefore, even though it is a brilliant paper, it belongs to a different genre and so

we cannot include it in the same category as the other studies discussed so far in this chapter.

Having discussed the earlier attempts, we now proceed to “define the problem”.

## 4.2. Objective

Based on what we saw in Section 4.1., it is obvious that despite many attempts, the phenomena that occur during the process of rapid-mixing are yet to be fully understood. Most of the experiments conducted thus far have relied on turbidity readings of samples which were rapid mixed, flocculated and settled. This means that the experiments did not measure the direct impact of rapid mixing on the colloidal systems.

We know that turbulent fluid flow is the transport mechanism underlying both, rapid mixing and flocculation. The difference is that while the former occurs at a much greater intensity of turbulence, the latter is carried out at much lower levels, as we saw in Chapter 3. Therefore, if a given set of colloids is destabilized, flocculation serves to “amplify” the destabilization effect. This point is well illustrated by an example. Let us take two identical colloidal suspensions and measure the particle size distribution of the suspensions. To one, we add the “optimal” coagulant dose while to the other, we add a dose which is different from the optimal coagulant dose. We subject both suspensions to similar conditions of rapid mixing, say 300 rpm of mixing for 1 minute. Obviously, the former suspension will contain colloids which are better destabilized than the colloids in the latter suspension. If we take a sample from the poorly destabilized colloidal suspension and compare its particle size distribution with that of the well destabilized colloidal suspension directly after



rapid mixing, we will not see much of a difference between the two. However, if we flocculate the two suspensions with a reasonable flocculation intensity for a period of, say, 30 minutes, we will see that the well destabilized colloidal suspension contains particles whose size distribution is radically different from the initial particle size distribution. At this point, if we measure the particle size distribution of the poorly destabilized colloidal suspension, we will see that it is substantially different from that of the well destabilized colloidal suspension. What does this mean? It simply means that in such conditions, as mentioned in the example, flocculation can be thought of as a process which amplifies the state of destabilization of the colloids.

If the process of flocculation of a colloidal suspension is followed by sedimentation, the larger particles will settle out preferentially over the smaller particles. Thus, one can see that the residual suspended turbidity in the supernatant can be thought of as an indicator of the amount of small particles in the suspension. The settling velocity of the particles is dependent not only on the size of the particle, but, among other things, on their density, and shape. Therefore, measurements of the particle size distribution of the supernatant collected from a settled suspension would not tell us as much about the effect of the rapid mixing conditions on the ability of particles to grow, whereas the information about the supernatant would be an indicator of their ability to grow and settle out of suspension! Based on this idea, it was decided to restrict the sampling of the suspension up to the end of the flocculation period. This was different from earlier studies, where most experiments involved measurements of turbidities of the supernatant from suspension which had been rapid mixed, flocculated and settled.

Therefore, one can see that measurements of particle size distribution directly after the end of the rapid mixing period would give us indications of the effect of rapid mixing per se on the particle size distribution of the colloids; whereas a measure of the particle size distribution of the suspension at the end of the flocculation period would give us an indication of the level of destabilization of the colloids and their ability to flocculate. Since the experiments were a part of a study involving flocculation kinetics, it was decided to restrict the sampling up to the end of the flocculation step.

It was also thought that if a colloidal suspension could be characterized (in terms of its particle size distribution) before rapid mixing, after rapid mixing as well as during and after flocculation, one could easily delineate the effects of both, the rapid mixing step as well as the flocculation step on the particle size distribution of the particles in suspension. And, if this information was available, it would be somewhat easier to predict how the suspension might behave if it were subjected to a treatment like direct filtration (i.e., rapid mixing followed by filtration) or conventional treatment (i.e., rapid mixing, flocculation, sedimentation and filtration), because considerable information is already available on the manner in which particle size distribution of the suspension affects its ability to filter or sediment.

Based on these premises, it was decided to study the influence of temperature of suspension, and the rapid mixing conditions (i.e., intensity and duration of mixing) on the particle size distribution of a suspension after rapid mixing as well as at different stages (i.e., different times) of flocculation; indicating its influence on flocculation kinetics.

Table 4.1: Parameters involved in the experimental plan

Control Parameters:	Energy input Time Temperature Coagulants Colloidal suspension				
Variable and Fixed Parameters:	<table border="0"> <tr> <td>Variable:</td> <td>Temperature Time Energy</td> </tr> <tr> <td>Fixed:</td> <td>Apparatus Colloidal suspension Coagulants</td> </tr> </table>	Variable:	Temperature Time Energy	Fixed:	Apparatus Colloidal suspension Coagulants
Variable:	Temperature Time Energy				
Fixed:	Apparatus Colloidal suspension Coagulants				

### 4.3. Experimental plan and equipment

The experimental plan can be easily visualized by looking at Table 4.1. The variable parameters in these experiments were the energy input into the system during initial mixing (i.e., intensity of mixing), the duration of the initial mixing step and the temperature at which the experiments were carried out. The fixed parameters in these experiments were the mixing and particle counting equipment, the colloid suspension to be chosen for these experiments as well as the destabilizing chemicals.

We first discuss the fixed parameters, which included clay as the colloid, alum and organic polymers as coagulants, water as the suspending medium, and the mixing and particle counting equipment. The apparatus consisted of (1) the reactor in which rapid mixing and flocculation were carried out as well as the equipment asso-

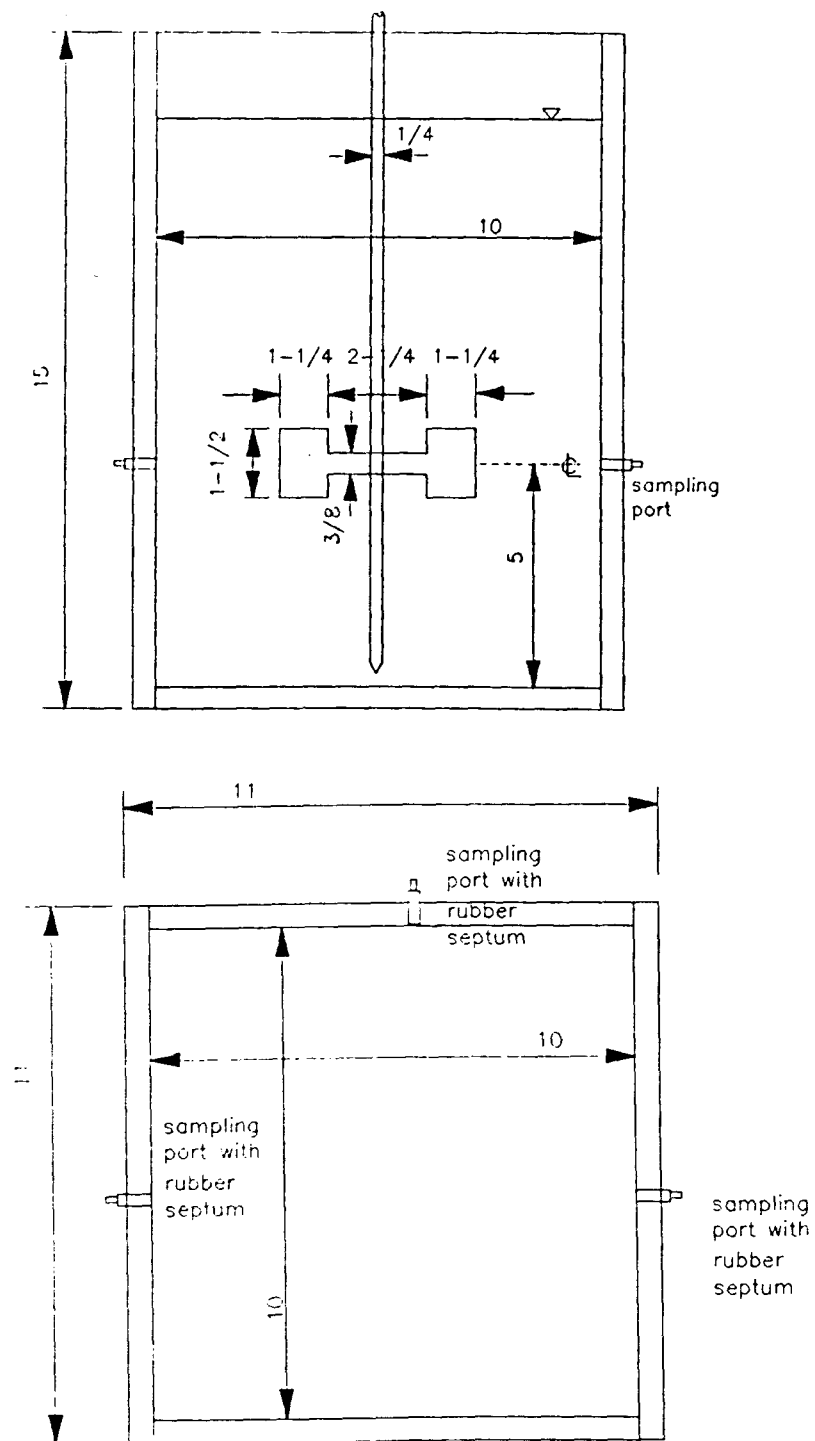


Figure 4.1: Elevation and plan views of the reactor. All dimensions are in inches

ciated with the reactor; (2) the primary measuring equipment used in characterizing the suspensions—namely, the particle sizing system and such things.

Let us first consider the reactor used in this study. Essential features of the plexiglass reactor used in the study are shown in Figure 4.1. This is the same reactor which was used by Argaman and Kaufman [13] in their studies on flocculation kinetics. The stirrer was a 1/4 inch diameter stainless steel shaft onto which a flat (1/16 inch thick) stainless steel piece of the dimensions shown in Figure 4.1 was mounted using a screw. This stirrer was attached, via a steel or plexiglass coupler, to an electric motor which formed a part of the Cole-Parmer Master Servodyne<sup>5</sup>. The electric motor was mounted on a wooden support which was rigidly attached to the top of the reactor. Attached to the electric motor was an Ametek Model 1736 tachometer, also obtained from Cole-Parmer. The Master Servodyne could be used to control the speed at which the motor was rotating as well as hold it constant at that level. The Servodyne also measured (in DC millivolt) the torque being exerted on the motor, which could be used to calculate the rate at which energy was being applied to the contents of the reactor. The wooden support for the motor also contained holes through which a pH probe as well as thermocouple type temperature sensor were introduced into the reactor to monitor its contents. The pH probe was connected to a Fisher Accumet pH Meter Model 610<sup>6</sup>. The reactor was placed in a Nor-Lake<sup>7</sup> constant temperature room, whose temperature could be controlled at the desired level.

<sup>5</sup>Cole-Parmer Instrument Company, Chicago, Illinois.

<sup>6</sup>Fisher Scientific Company, Pittsburgh, Pennsylvania.

<sup>7</sup>Nor-Lake, Hudson, Wisconsin.

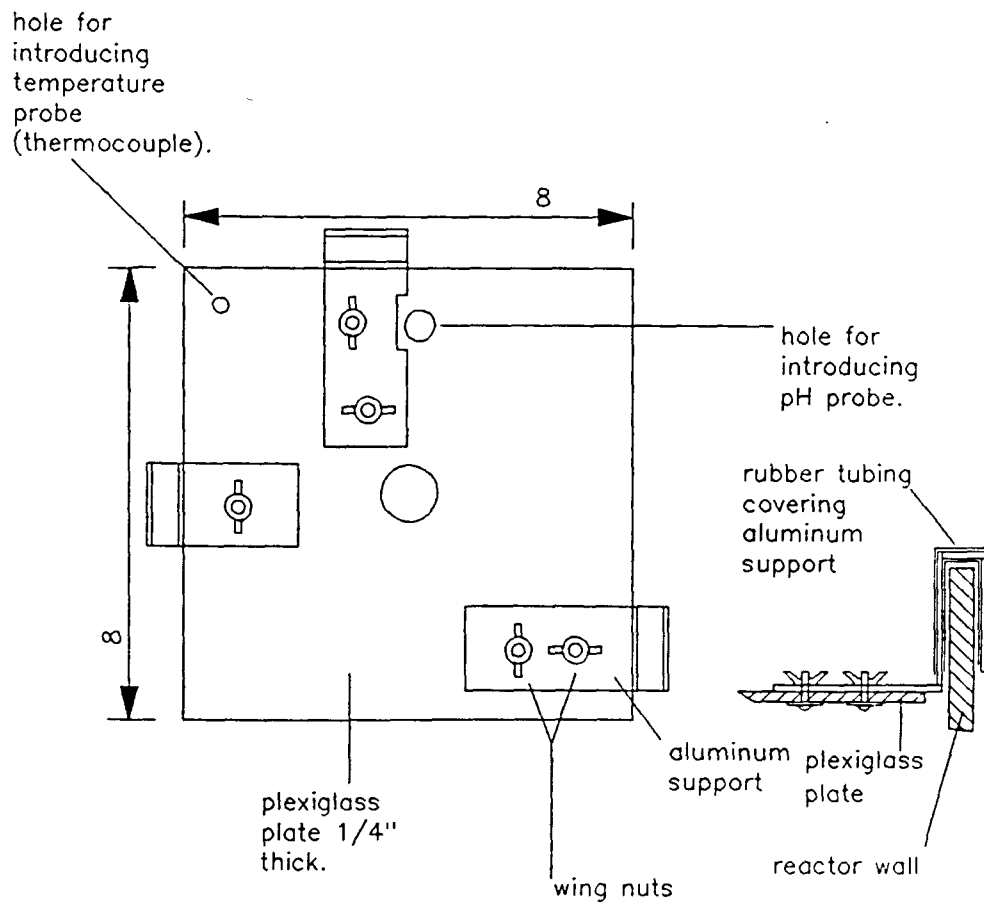


Figure 4.2: Plan view of the confining plate for high speed mixing. All dimensions in inches

For the experiments which involved high speed mixing, it was discovered that considerable vortexing occurred in the reactor contents which made it difficult to reach 500 rpm, the speed at which the high speed mixing experiments were to be conducted. A confining plate, shown in Figure 4.2 was used to confine the flow and reduce vortexing. It was placed in the reactor in the manner shown in the figure, with its plate being approximately 0.5 inch above the normal water surface.

As shown in Figure 4.3, leads from the tachometer, servodyne, pH meter and thermocouple were attached to a terminal panel which was connected to the analog card of the ACPC-16 Analog Connection PC<sup>8</sup> personal computer based data acquisition/control system. It was housed in a Z-159 Zenith Desktop Personal Computer System<sup>9</sup>. This data acquisition/control system controlled the temperature of the constant temperature room by appropriately switching on/off the compressor, based on the temperature sensed by the thermocouple. This arrangement provided a much finer control of the temperature than possible with an ordinary thermostat controlling the turning on/off of the compressor. The data acquisition system was set up to constantly monitor the temperature, pH, rpm and torque of the system, 24 hours a day. It was also capable of collecting data provided by the instruments it was monitoring, and writing the information to a printer, a 5-1/4 inch floppy disk or a hard drive.

The computer system, servodyne control box, pH meter, and tachometer display were placed outside the constant temperature room so as to shield them from

---

<sup>8</sup>Strawberry Tree Computers, Sunnyvale, California.

<sup>9</sup>Zenith Data Systems, St. Joseph, Michigan.

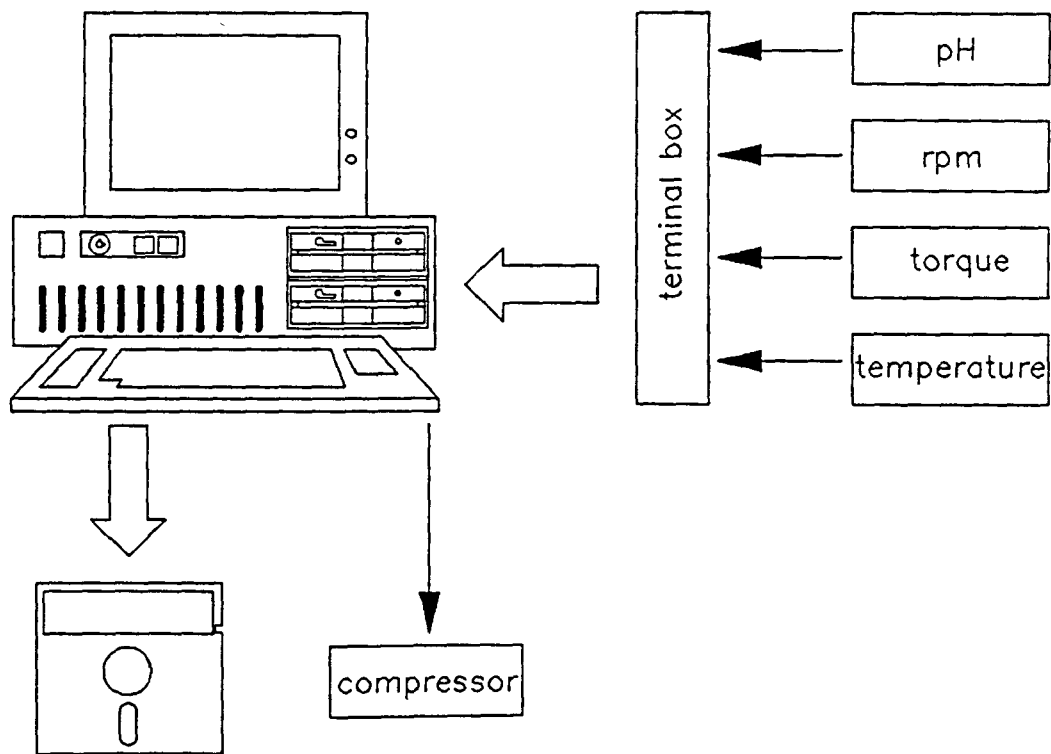


Figure 4.3: A schematic showing the Z-159 microcomputer based data acquisition system and related instruments



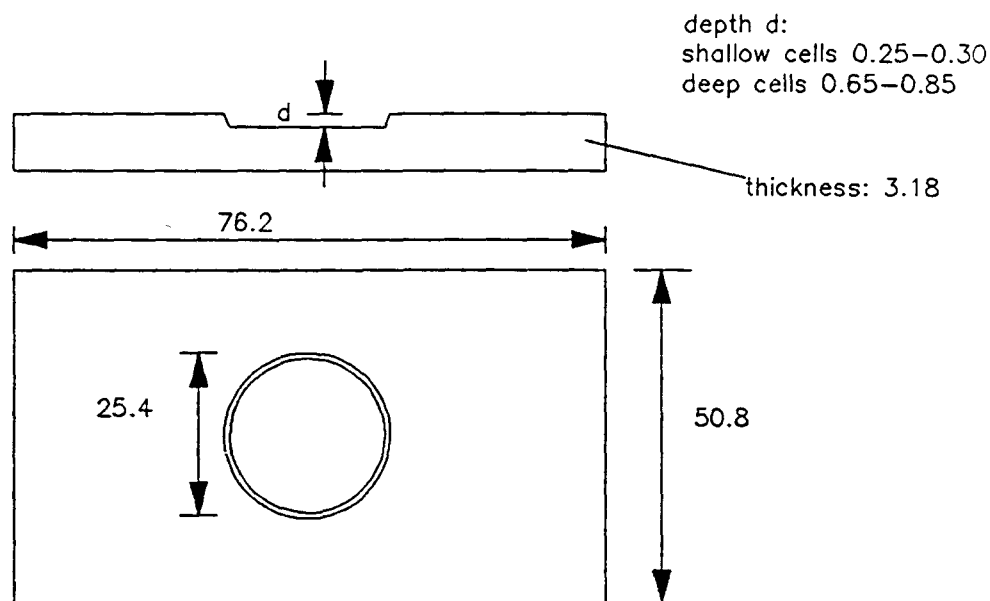


Figure 4.4: Cross section and plan view of a sampling cell. All dimensions in mm

possible interference in their performance because of the low temperatures at which some of the experiments were conducted.

The samples of the colloid suspension withdrawn from the reactor were placed in plexiglass cells of the kind shown in Figure 4.4. Each sample cell was covered with 45 × 50 mm Number 1-1/2 (0.16–0.19 mm thick) Fisherbrand Microscope Cover Glass<sup>10</sup>. There were two types of sample cells: one type of cells were 0.65–0.85 mm deep while the second type were 0.25–0.30 mm deep. The deeper cells were to be used for the homogenized, rapid-mixed, and samples taken after 1, 3, 5, 10, 15, 20,

<sup>10</sup>Allied Fisher Scientific, Pittsburgh, Pennsylvania.

25, 30 and 45 minutes of flocculation. The shallow cells were used solely for the homogenized and rapid-mixed samples. The shallow cells were necessary in order to be able to detect even the smallest changes which might occur in the clay suspension during the rapid-mixing period.

We now discuss the equipment used for analyzing the samples. The samples were analyzed using an Automatic Image Analysis (AIA) system. This consisted of an Olympus BH-2 optical microscope<sup>11</sup> on which the plexiglass cells containing the colloid suspension samples were viewed. The optical image visible in the microscope was picked up by a video camera which formed the input for the Lemont Image Analysis System<sup>12</sup>. The AIA system was capable of collecting images of the colloids, counting them, and classifying them in various size blocks. A schematic of the image analysis system can be seen in Figure 4.5.

Before we go any further, let us examine how the AIA system works. The AIA system works on the principle of identifying levels of gray in a visual field. If we take any black and white picture, we see that it actually consists of regions of different amounts of 'gray'. In fact, these gray levels are drawn from the continuous spectrum between pure white and pure black. The AIA system assigns a number '0' to the pure black level and '255' to pure white level and divides the continuum between pure black and pure white into 255 zones of gray. The AIA system has the ability to take an image and transform it into a  $512 \times 480$  pixel digitized image. In other words, any picture (whether it is color or black or white) is perceived by

---

<sup>11</sup>Olympus Corporation, Lake Success, New York.

<sup>12</sup>Lemont Scientific Inc., State College, Pennsylvania.

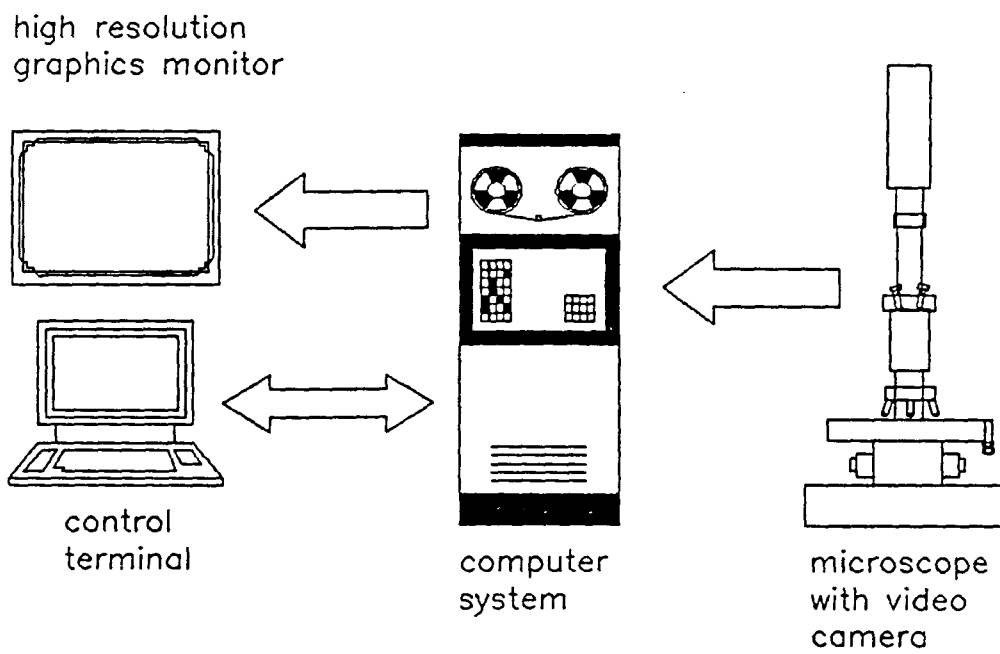


Figure 4.5: A schematic diagram of the Automatic Image Analysis (AIA) system

the AIA as being a black and white picture which consists of 245,760 ( $512 \times 480$ ) individual dots (pixels), each of which has a distinct gray level associated with it. The AIA stores this image by identifying, within the computer's memory, each pixel by the location of the pixel (its X and Y coordinates on the image) as well as the gray level associated with it. This is what is called the 'digitized' image.

How does this help us? Let us say we have a suspension of clay in water which we place in a sample cell of the type mentioned above. We set the microscope to operate in the dark-field mode. In this mode, the sample is illuminated in such a way that only the light rays that strike an object in the sample cell are visible to an observer. Thus, the effect is that objects on the cell are very brightly illuminated against a pitch dark background. Therefore, the image we see would be one in which the clay particles are all very bright while the background is completely dark. Such an image would be ideal for analysis using the AIA system. If we collect the image in the AIA, we know that all the pixels associated with each of the clay particles have a gray level above, say, 180. Therefore, we can instruct the AIA to regard all regions on the image which have a gray level above 180 as being particles and ask it to analyze the image and provide us with a particle size distribution. It will consider all *contiguous* pixels which have a gray level above 180 as one particle. Based on the calibration, it will provide a particle size distribution of the clay suspension analyzed in this manner. In using this technique, we must remember that the concentration of the clay particles (in our sample) should be such that there are no overlapping particles. This is essentially how the samples were analyzed using the AIA. The microscope-AIA combination was calibrated for

different magnifications using a Nikken 0.01mm Objective Micrometer<sup>13</sup>. It must be added that the resolution of the system, the way it was set up to analyze the samples, was  $0.73\mu\text{m}$ .

Having discussed most of the significant constituents of the experimental apparatus, we now turn to the other fixed parameters involved in the experimental plan, as outlined in Table 4.1. Kaolin (Kentucky Ball Clay) was chosen to be the colloidal system used in the study. Studies were carried out using a 25 mg/l suspension. The colloids showed an equivalent circular diameter of about  $1.8\mu\text{m}$ . A stock clay suspension of 800 mg/l was prepared from which appropriate samples were withdrawn for each experiment. The stock clay suspension was made in Ames tap water by suspending 36 g of the clay in 45 liters of the water. The mixing was done in a  $12 \times 24 \times 12$  inch Nalgene<sup>14</sup> plastic tank, the contents of which were pumped out of and into the tank in a closed circuit, using a pump with a stainless steel impeller and volute. Extended pumping with the pump ensured the homogenization of the clay suspension. Each batch of clay prepared in the tank lasted for many experimental runs.

Since the experiments were carried out with a clay concentration of 25 mg/l, it was necessary to dilute the stock clay suspension. The turbidity of the diluted suspension was checked on a Hach Model 18900 Ratio Turbidimeter<sup>15</sup> before the experiment and recorded. It did not show much variation over the course of the

---

<sup>13</sup>Nikken, Tokyo, Japan.

<sup>14</sup>Nalge Company, Rochester, New York.

<sup>15</sup>Hach Chemical Company, Ames, Iowa.

experiments.

The dilution water, i.e., the water in which the clay was suspended so as to conduct the mixing and flocculation experiments, was Ames tap water, buffered with 100 mg/l of sodium bicarbonate. The water was prepared by first creating a 1 Molar solution of  $NaHCO_3$ , i.e., a 84 mg/ml stock solution of sodium bicarbonate. 357 ml of this stock solution were then thoroughly mixed with 300 liters of Ames tap water in a large stainless steel tank and the mixture allowed to stand overnight. The next day, the water was transferred to 18 liter carboys which were then placed in the constant temperature room for storage. It was this water which was used for all the experiments. A sample of each such batch of water prepared was analyzed by the ERI Analytical Laboratory. All of the batches were found to be satisfactory in that no significant departures from the mean were observed.

Alum was one of the coagulants used in this study. The alum used was in the form of Certified A.C.S. Aluminum Sulfate Crystals  $Al(SO_4)_3 \cdot 18H_2O$ , 98.7% pure<sup>16</sup>. It was dissolved in distilled water to make a 0.25 Molar stock solution (i.e., 41.6575 g/250 ml). This stock solution was always stored at room temperature. The dosing of alum to the reactor was done using a dosing solution of 10 mg/ml, based on crystals as received. The dosing solution was prepared fresh 24 hours before the day of the experiment by diluting the appropriate amount of the stock alum solution to the desired volume. No precipitates were observed in the dosing solution. This dosing solution was also stored at room temperature. The dosage at which the experiments were carried out was 5 mg/l of the reactor volume. At the end of the experiment the dosing solution was discarded. Based on extensive jar

<sup>16</sup>Fisher Scientific, Fair Lawn, New Jersey.

tests with the clay suspension and alum coagulant, the pH for coagulation at 20°C was chosen to be 6.80. This, in combination with the dosage being used, would put the experimental conditions square in the adsorption-destabilization zone of the alum coagulation diagram published by Amirtharajah and Mills [3]. In order to carry out the experiment at these conditions, preliminary investigations were carried out so as to determine the amounts of 0.09698 Normal *HCl* to be added at the same time as the alum so that the final pH of the suspension was at the desired level. This was also done using jar tests conducted using a Model 7790-300 Phipps & Bird 6 Paddle Stirrer<sup>17</sup>. Eventually, a titration technique was used to deduce the amount of 0.09698 Normal *HCl* for this purpose. In experiments involving alum, conducted at low temperatures, the alum dosage was kept at a constant level. Initial experiments at low temperatures at a pH of 6.80 revealed poor flocculation. Therefore, it was decided to maintain the pOH at the same level as the pOH of the experiments done at 20°C. The reason for this was that since the hydroxyl ion is associated with the hydrolysis species formed, it would be more reasonable to keep the pOH constant in order to compare the performance of the coagulant at two temperatures. This improved flocculation considerably.

In this study, it was initially planned to investigate the influence of alum coagulant on the clay suspension. Later, however, the scope of the study was expanded slightly to include the influence of rapid mixing on the behavior of a polymeric coagulant, Magnifloc 573C<sup>18</sup>. This is a polyquarternary amine with high molecular weight, available in the form of a viscous liquid [52]. On the basis of jar tests, the

---

<sup>17</sup>Phipps & Bird Inc., Richmond, Virginia.

<sup>18</sup>American Cyanamid Company, Wayne, New Jersey.

optimum dosage for the polymeric flocculant was determined to be 0.1 mg/l of the reactor volume, at a pH of 7.0. The stock solution for the polymeric coagulant was a 1 g/l polymer solution. The dosing solution was a 0.1 g/l (i.e., 0.1 mg/ml) polymer solution. While the stock polymer solution was prepared (in distilled water) 24 hours before the experiment and kept at room temperature, the dosing solution was prepared 1 hour before the experiment. Both the solutions were discarded following the experimental run.

We have, so far, discussed fixed parameters of the experimental investigations. We now consider the variable parameters. In this study, the primary variable to be considered was temperature. Experiments were conducted at two temperatures: 5 and 20°C. The second variable to be considered was the duration of the initial mixing period. Experiments were conducted which involved either a 1.0 minute or a 5.0 minute period of rapid mixing. However, in some of the experiments—those involving mixing at 500 rpm—the equipment being used was unable to provide mixing at this intensity for the full duration of 5 minutes. This resulted in some experiments having either a 2.25 or a 3.0 minute mixing period. The third variable parameter was energy. Since the power input is dependent on the speed (rpm) at which initial mixing is carried out, it was decided to conduct the experiments at two levels of mixing: 250 and 500 rpm. In just one case, was the mixing speed changed to yet another level: 340 rpm. The flocculation was carried out at two levels: 30 rpm or 60 rpm—designated as the ‘low’ and ‘high’ energy levels.



#### 4.4. Experimental procedure

On the day prior to the experiment, the water from one of the carboys was introduced into the reactor and allowed to come to thermal equilibrium with the surroundings. The stock 0.25 Molar alum solution was diluted using distilled water to create a 10 g/l (or 10 mg/ml) dosing solution, which was stored at room temperature.

Then, on the morning of the experiment, the clay in the stock clay suspension tank was first stirred and homogenized by turning on the mixing pump. This mixing was carried on for at least 10 minutes. After this period, a fixed amount of this clay suspension was pumped out into a graduated cylinder so that when added to the reactor, the total volume of the reactor contents would be 18 liters. The contents of the graduated cylinder were promptly mixed with the reactor contents and stirred so as to have a homogeneous clay suspension of 25 mg/l in the reactor. A sample of this suspension was taken and its turbidity measured on the Hach ratio turbidimeter and recorded. Yet another sample of this suspension was taken for monitoring the zeta potential using a Model 102 Lazer Zee Meter<sup>19</sup>.

During this period, 9 ml of the alum dosing solution were loaded into a plastic, disposable syringe with a Perfectum PS 13 Hospi-Luer 4-1/2 inch stainless steel hypodermic needle<sup>20</sup>. This amount, when injected through a rubber septum into the reactor resulted in an alum dosage of 5 mg/l in the suspension in the reactor. In the case of experiments involving the polymeric coagulant, on the morning

---

<sup>19</sup>Pen-Kem Inc., Croton-on-Hudson, New York.

<sup>20</sup>Popper & Sons, Inc., New Hyde Park, New York.

of the experiment, the stock solution of 1 g/l was diluted to make a 0.1 g/l (or 0.1 mg/ml) dosing solution. Eighteen ml of this dosing solution was loaded into a syringe similar to that described for alum. The resulting polymer dosage in the reactor was 0.1 mg/l. For both, alum and polymeric coagulants, the dosing solution was discarded at the end of the experiment. Standardized *HCl*, which had been prepared earlier and stored at room temperature, was also loaded into a syringe. The pH meter was also standardized prior to each experiment.

In the experiments involving low temperatures ( $5^{\circ}\text{C}$ ), some time was allowed to permit the contents of the reactor, which had warmed up because of mixing of clay suspension, which had been stored at room temperature; with dilution water which had been at the control temperature. If the contents of the reactor were within  $0.2^{\circ}\text{C}$  of the desired temperature, the experiment was started. Prior to the start of the experiment, the data acquisition system was instructed to start recording data, at 5 second intervals, to a floppy disk. Also, the sample cells were loaded during the experiment, with samples taken from the sampling ports shown in Figure 4.1. These sampling ports were brass fittings on the ends of which rubber septa<sup>21</sup> were placed. The samples were extracted by inserting the stainless steel hypodermic needle, attached to a plastic syringe, through the rubber septum, into the reactor. The plunger of the syringe was slowly withdrawn so that the sample was gradually inducted into the body of the syringe. After an adequate amount of sample was present in the syringe, it was withdrawn from the septum. The syringe was then used to slowly fill the sample cell on which the microscope glass cover was placed.

---

<sup>21</sup> Aldrich Chemical Company, Inc., Milwaukee, Wisconsin.

The glass cover was then gently pressed using Kimwipes<sup>22</sup> and excess sample, which emerged from under the cover, was absorbed and wiped off. Once this was done, the sample cell was placed in a felt-lined container—to prevent scratching of the cells. The syringe was rid of the excess sample and rinsed with distilled water, making it ready for collecting the next sample.

The actual experiment involved two students. One student was needed outside the constant temperature room: to monitor and adjust the rpm, as well as monitor, visually, the pH; while the other student was needed to inject the coagulant/acid into the reactor and collect samples. Just before the experiment, two syringes—one containing the coagulant and the other the standardized acid—were loaded into two sampling ports. The first student readied himself for injecting the chemicals while the other student raised the speed of the motor to the desired level. At the appropriate time, the second student informed the first student to inject the chemicals and timed the duration over which mixing was carried out. During this mixing period, the second student relayed to the first student the pH as it changed with time. If necessary, additional adjustments to the pH were made during the rapid-mixing period. As the mixing period came to an end, the second student informed the first one to collect the 'rapid-mixed' sample and reduced the speed of the mixing motor to the level at which flocculation was to be carried out. Then, at the time intervals of 1, 3, 5, 10, 15, 20, 25, 30 and—in most cases—45 minutes of flocculation, samples from the reactor were collected in a manner described earlier. During this process, qualitative comments describing the visual observations made on the sample, were recorded. These included naked-eye observations as well as observations made by

---

<sup>22</sup>Kimberly-Clark Corporation, Roswell, Georgia.

using a hand-held Macroscope 25,  $8 \times 30$  monocular microscope<sup>23</sup>. A sample of the clay suspension was also collected for a measure of the zeta potential of the destabilized clay particles.

Following the desired duration of the flocculation, the motor was turned off. The pH meter was checked with the standards to see if there had been any drift in its measurements. The data acquisition system was also instructed to stop recording data to the floppy disk. The reactor was drained, rinsed with tap water, and allowed to dry out. While this was being done, the pH, temperature, rpm and torque data; which had been recorded in a file on the floppy disk, were imported into Lotus 1-2-3 spreadsheet program<sup>24</sup> and processed by a series of macro-commands. Graphs were generated to detect the manner in which the aforementioned parameters varied over the duration of the experiment and, if any anomalies were found, the experiment was abandoned.

The zeta-potential of the raw and coagulated clay suspensions was also measured during this period. While all this was being done, the sample cells were allowed to sit undisturbed and in this period of almost two hours, most of the suspension settled over the distance of depth of the cells, to the bottom of the sample cell. A test had earlier been conducted to see if the particles underwent any changes when left undisturbed in a sampling cell over a 24 hour period. No changes were detected and so, it was concluded that leaving the sample cells undisturbed did not alter the particle size distribution of the sample.

---

<sup>23</sup>RF Inter-Science Co., New York.

<sup>24</sup>Lotus Development Corporation, Cambridge, Massachusetts.

Following this period of settling, the samples were taken to the Lemont Automatic Image Analysis system and analyzed for their particle size distributions. The analysis was carried out by selecting fields at random from the sample cells and analyzing these fields. When counting particles in the shallow sampling cells, fields were analyzed until a total of about 1000 particles had been counted. This was decided on the basis of an experiment in which changes in the calculated particle size distribution were measured as a function of the number of particles counted. It was found that by the time 600 or so particles had been counted, there was little change in the calculated particle size distribution by any increments in the total number of particles counted. As a conservative measure, it was decided to count a total of 1000 particles in order to define the particle size distribution for a given sample. For the deep sampling cells, the counting was done up to about 1000 particles in the earlier samples (i.e., the homogenized and rapid mixed clay suspension, and for flocculated suspensions up to 10 minutes of flocculation). For samples corresponding to longer flocculation times, when the particle concentration was relatively reduced as compared to the homogenized and rapid-mixed samples; the count requirements were reduced to about 600 total particle count. For the samples corresponding to a flocculation period of 30 or 45 minutes, the total count requirement was reduced to about 400 or so. Again, this was because of the fact that the particle concentration in those later samples was much, much lower than that in the homogenized samples. In the case of all samples counted using the deep cells, the criterion to be satisfied was that there should be at least 100 counts in the mode of the particle size distribution, a minimum of 10 counts in any division which influences the shape of the particle size distribution, and a minimum of 250

total particle counts.

The fields to be analyzed by the AIA were selected at random. The X and Y verniers on the microscope stage were used as references against which the fields were located. A random number generator was used to arrive at an X and a Y coordinate of the field. This field was then viewed by the AIA and analyzed. Occasionally, however, the bottom of the cell would be scratched or the field being viewed would contain air bubbles or, perhaps, the field might be on the edge of the sampling cell. In such cases, that field was discarded and the next randomly chosen field was selected for analysis.

The basic principles of the AIA have already been described. In most cases, the image collected by the AIA had to be edited somewhat so as to enhance the digitized image to make it more amenable to analysis. The editing included, on some occasions, erasing scratches on the cell bottom from the image so that they were not counted as particles; small feature enhancement which was necessary to enhance the image of the smaller particles, etc. In all cases, it was ensured that the edited image was as close as possible to the true visual image of the field.

The AIA analyzed each visual field and recorded the relevant information of each particle in a magnetic file on an 8 inch floppy disk. Once all the samples had been analyzed, each file, corresponding to a given sample, was processed by yet another computer program of the AIA, which provided the particle size distribution for that sample as well as the area (in  $\text{cm}^2$ ) of the sample analyzed. Since the depth of the sample cell was known, the volume of the sample analyzed could be calculated. All such information generated by this program was collected by a personal computer and recorded in a magnetic file on a 5-1/4 inch floppy disk.

Meanwhile, after all the samples had been processed, the sample cells were, once again, placed on the microscope and a photographic record was made of about 2-3 fields of each sample. This helped in making a somewhat permanent visual record of the status of clay suspension, as it underwent flocculation. Following this photography, the sample cells and the glass covers were rinsed under tap water and then placed in a specially constructed plexiglass cell cleaning rack. This rack was a 1/2 inch plexiglass plate into which slots had been made so as to permit the sampling cells and the glass covers to stand vertically. The rack with the rinsed cells/glass covers was then transferred to a Branson 220 Ultrasonic Cleaner<sup>25</sup>. The rack and the cells were completely submerged in a detergent solution using a special detergent, Micro liquid laboratory cleaner<sup>26</sup>. The cells and glass covers were sonicated for a minimum period of 5 minutes. Following the sonication, they were rinsed: first with tap water and then with distilled water. Following the rinsing, the cells and the glass covers were placed between layers of lint free towels and allowed to dry under the weight of a moderately heavy book or a wooden box. This was necessary to prevent water spots from forming on any of the items. All this was necessary in order to ensure ultra-clean sample cells so that the particle counts were not adversely influenced by any residual dirt on the cells/glass covers.

The particle size distribution data, which were present as ASCII (American Standard Code for Information Interchange) files on 5-1/4 inch floppy disks were imported into Lotus 1-2-3 spreadsheets and processed further to provide particle concentrations and other information so that all the samples could be compared on

---

<sup>25</sup>Branson Ultrasonics Corporation, Danbury, Connecticut.

<sup>26</sup>International Products Corporation, Trenton, New Jersey.

the same basis.

#### 4.5. Conclusion

We have, in this chapter, looked at (1) a general discussion of the experiments which have been done on this topic, (2) the general setup involved in the experiments and (3) the experimental procedure used.

In the next chapter, we shall see the results of these investigations and the reasons for their being so.



## 5. RESULTS AND INFERENCES

### 5.1. Results

As was mentioned in Chapter 4., experiments were conducted with the objective of observing the influence of

- mixing intensity,
- duration of mixing, and
- temperature of water

on the outcome of the rapid mixing process. In order to make the impact appear more pronounced and easily discernible, most of the clay suspensions were flocculated for 45 minutes. Since this study was a subset of an NSF project on flocculation kinetics, most experiments involved flocculation at two levels: at 30 rpm (corresponding to 'low' flocculation energy) and at 60 rpm (corresponding to the 'high' flocculation energy).

While conducting experiments involving temperature effects, it was arbitrarily decided to keep the energy of mixing same at both temperatures (i.e., at 5°C as well as 20°C). This was done based on tests conducted with the servodyne, which showed that for a given speed of rotation, the amount of *measurable* torque exerted

on the motor was the same at both temperatures. The power input into the reactor is given by  $\tau \times \omega$ ; where  $\tau$  is the applied torque and  $\omega$ , the angular velocity at which the motor is running. Comparing the situation at 20 and 5°C;  $\tau_{20} = \tau_5$  and  $\omega_{20} = \omega_5$ . This means that the power input into the system at both temperatures would be the same at the same mixing speed. The power input was chosen instead of  $G$  or  $\eta$  (the Kolmogorov microscale) based on work by Cleasby [33] and Clark [30], in which convincing arguments have been advanced about the validity of  $G$  as a parameter for characterizing turbulent flow phenomena of the kind encountered in turbulent rapid mixing or turbulent flocculation. Since the Kolmogorov microscale varies from one point to another in space (and time) in a given reactor, the idea of keeping a fictitious “time and space averaged Kolmogorov microscale” constant was not very appealing. We must remember that it is more of a conceptual length scale than a real, physical entity and it merely provides an *approximate* description of the intensity of the turbulent fluid flow. Compared to the two parameters ( $G$  and  $\eta$ ), the power input into the system is unquestionably superior in terms of our requirements because it *dictates* the very dynamics of the turbulent fluid flow and is a true physical parameter which can be readily measured. Based on these reasons, it was decided to keep the speed of the mixer constant at both temperatures during rapid mixing and flocculation.

As mentioned in Chapter 4., the study involved work with two different coagulants: alum—a metal coagulant, and Magnifloc 573C—a polymeric coagulant. We shall first consider each coagulant separately. Later, the performance of the two coagulants will be compared.

### 5.1.1. Rapid mixing with alum

The general conditions under which experiments involving alum coagulant were carried out have been summarized in Figure 5.1. This is an important figure and its location in this thesis should be marked because we shall repeatedly refer to it in order to keep track of the comparisons being made. In this figure, we can also see that while the experiments involving rapid mixing at 250 rpm have mixing periods of 1 and 5 minutes, those involving rapid mixing at 500 rpm have mixing times of 1 and 3 minutes. This was due to the shortcomings of the mixing system. At this rapid mixing intensity (500 rpm), the servodyne control box quickly became excessively hot, causing the circuit breaker to 'trip' and break the circuit. In order to avoid damaging the reactor/mixing apparatus and thereby jeopardizing the project schedule, it was decided to restrict the maximum mixing period to 1 minute for experiments involving rapid mixing at 500 rpm, although one experiment was conducted with a mixing duration of 3 minutes. Later in this section, we shall see that the absence of experiments involving 5 minutes of mixing at 500 rpm did not really make much of a difference in terms of the inferences drawn from these experiments.

If we look back at Figure 5.1, we see that each set of experimental conditions is identified with a label. Thus 'AD' refers to the experiment conducted with the following characteristics:

- Temperature: 20°C,
- Intensity of rapid mixing: 250 rpm,
- Duration of rapid mixing: 5.0 min.,

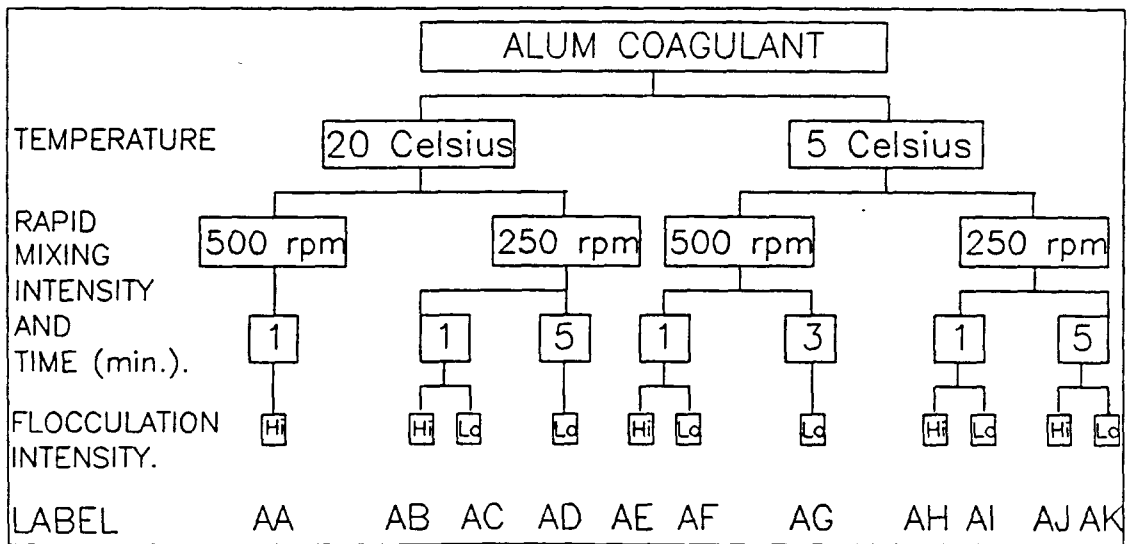


Figure 5.1: Experimental plan involving alum coagulant. 'Hi' and 'Lo' flocculation intensities correspond to 60 and 30 rpm respectively. Samples in all of these experiments were collected and analyzed in the deep sample cells

- Flocculation intensity: Low.

As mentioned earlier, flocculation was usually carried out for a 45 minute period.

In order to detect the influence of temperature, we would compare the results of this experiment with results obtained from experiment 'AK' which was carried out at exactly the same conditions as 'AD' except for its temperature: 'AK' was carried out at 5°C while 'AD' was conducted at 20°C.

If, however, we wanted to see the influence of the duration of rapid mixing on the outcome of the flocculation process, we could compare experiment 'AD' with experiment 'AC'. In 'AC', all the conditions were identical to those in 'AD', except for the duration of the rapid mixing period.

We can see that such a process of making comparisons could easily get fairly confusing. In order to keep things in order, we shall make a list of all comparisons which are likely to tell us something about the influence of temperature, rapid mixing intensity and duration of rapid mixing. This list is shown in Table 5.1.

We can also compare

- 'AE-AH-AJ' to see which set of rapid mixing conditions (i.e., both, the intensity and duration of mixing are varied) gave the best performance at 5°C and high flocculation intensity;
- 'AF-AG-AI-AK' to see which set of rapid mixing conditions (i.e., intensity and mixing time combination) gave the best performance at 5°C and low flocculation intensity.

Such comparisons (to see which combination of rapid mixing conditions produce best performance vis-a-vis particle growth) for experiments conducted at 20°C would

Table 5.1: List of experiments to be compared to detect the influence of various rapid mixing conditions on the clay suspension using alum as a coagulant

Variable	Comparison
Temperature	AA-AE
	AB-AH
	AC-AI
	AD-AK
Intensity	AA-AB
	AE-AH
	AF-AI
Time	AC-AD
	AF-AG
	AH-AJ
	AI-AK

amount to comparing 'AA-AB' and 'AC-AD'. In fact, these combinations have already been identified in Table 5.1 and conclusions will be drawn based on just that.

As we can see, we have identified a total of 13 possible combinations for comparison. We shall now discuss these comparisons in the context of detecting the influence of variables identified in Table 5.1.

**5.1.1.1. Alum: Temperature Effects** Shown in Figures 5.2, 5.3, 5.4, and 5.5 are comparisons of experiments to detect the influence of temperature on the rapid mixing/flocculation process. In these figures, the parameter with which the rapid mixing/flocculation process is being gauged is the total particle count/ml at any given time. All these totals have been normalized with respect to the total count/ml in the homogenized sample. The rationale behind this is that during water treatment, the processes of rapid mixing and flocculation alter the characteristics of the colloids present in the raw water. Therefore, it is logical to compare all changes in the colloid characteristics—due to the rapid mixing/flocculation processes—with the characteristics of the colloids, as identified in the raw water. This is the reason why, in all these experiments, the total counts have all been normalized with the counts measured in the homogenized sample. This 'Total count fraction' (i.e., (total count/ml at time  $t$ )/(total count/ml in the homogenized sample)) is plotted as a function of time. The time at which flocculation was started is taken as time zero. In other words,  $t = 0$  at the end of the rapid mixing process. This means that the rapid mixing period will be plotted as 'negative time' in these graphs. Another thing to note is that while some experiments were conducted with many replicates,

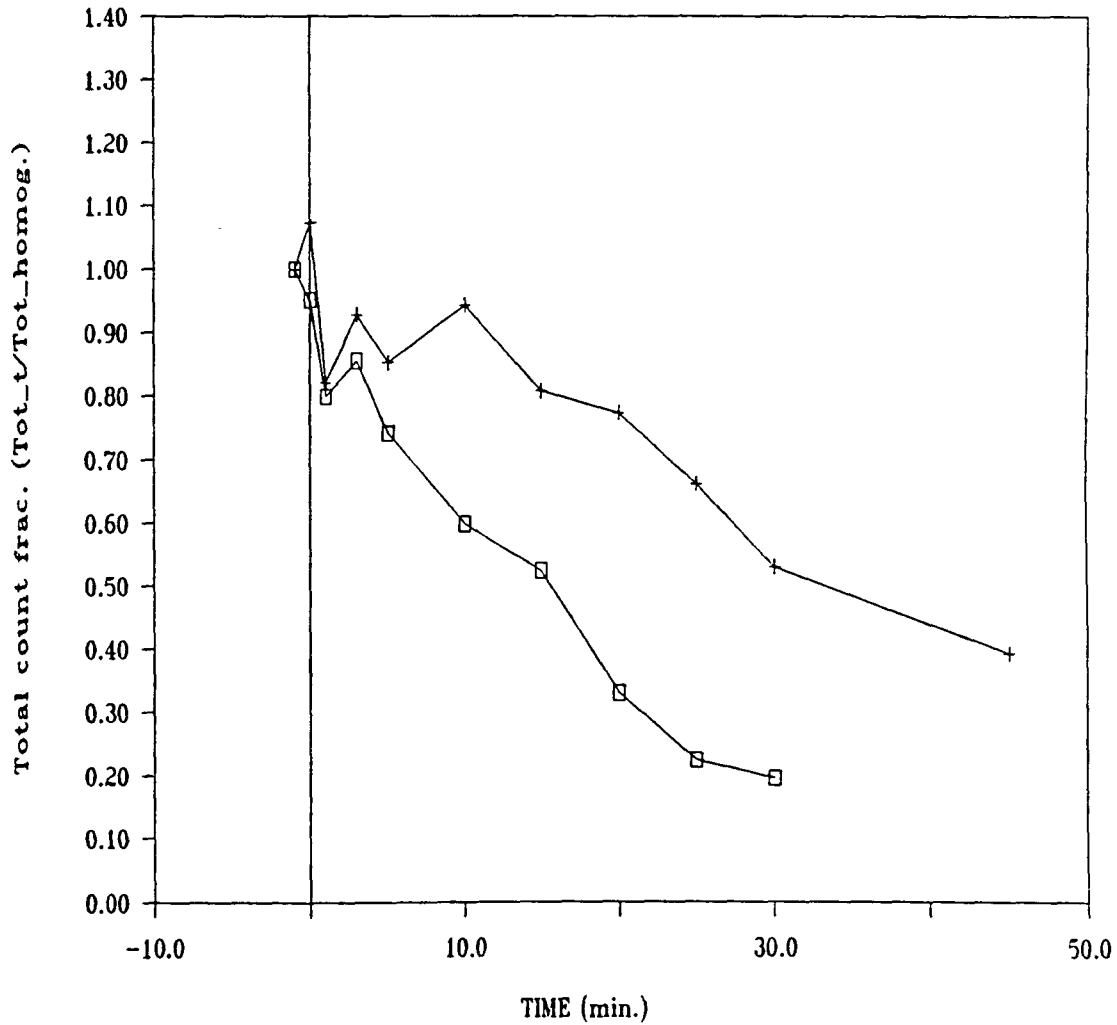


Figure 5.2: Comparison of experiments 'AC' and 'AI' to identify the influence of temperature on rapid mixing/flocculation. □ represents 20°C while + represents 5°C. Other conditions—mixing: 250 rpm for 1 min., flocculation at 30 rpm



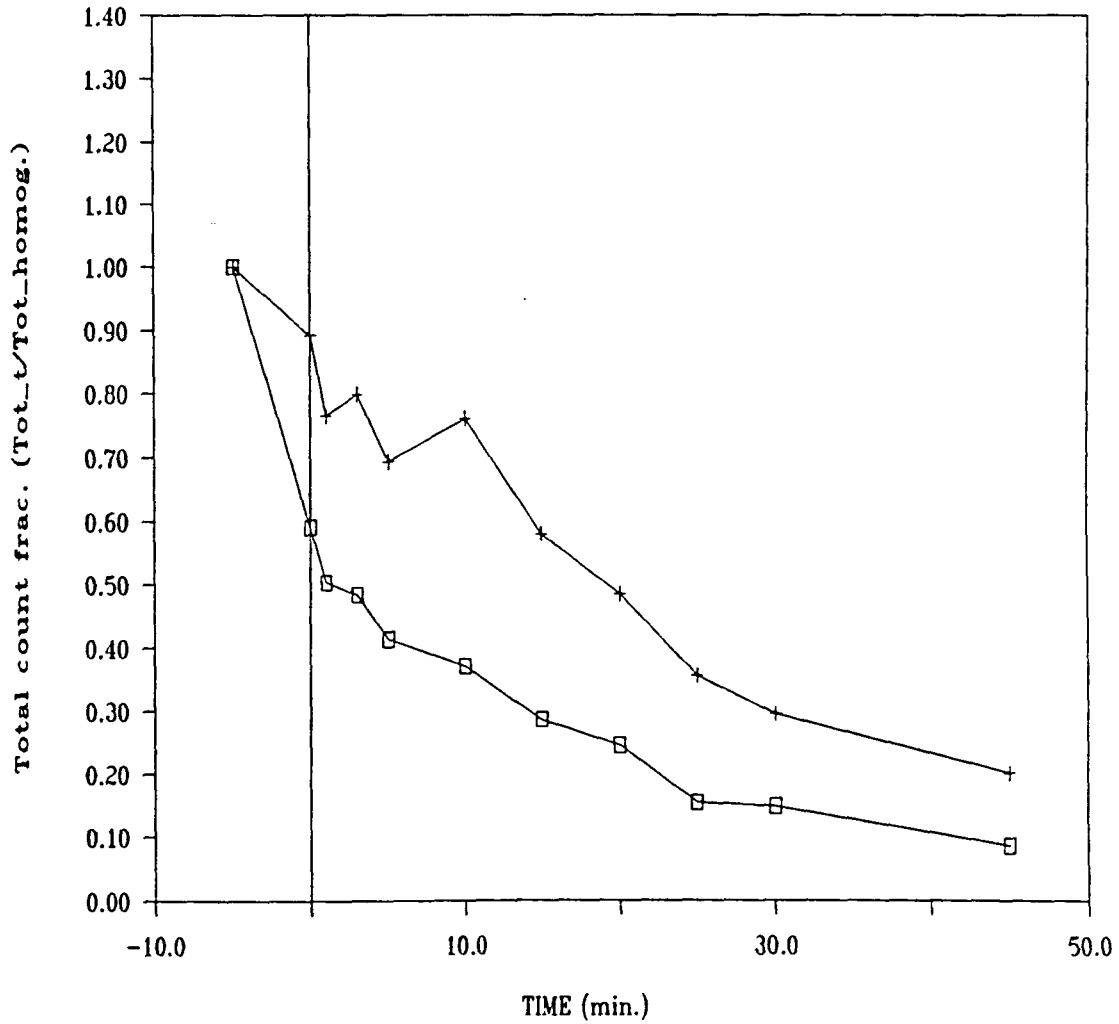


Figure 5.3: Comparison of experiments 'AD' and 'AK' to identify the influence of temperature on rapid mixing/flocculation. □ represents 20°C while + represents 5°C. Other conditions—mixing: 250 rpm for 5 min., flocculation at 30 rpm

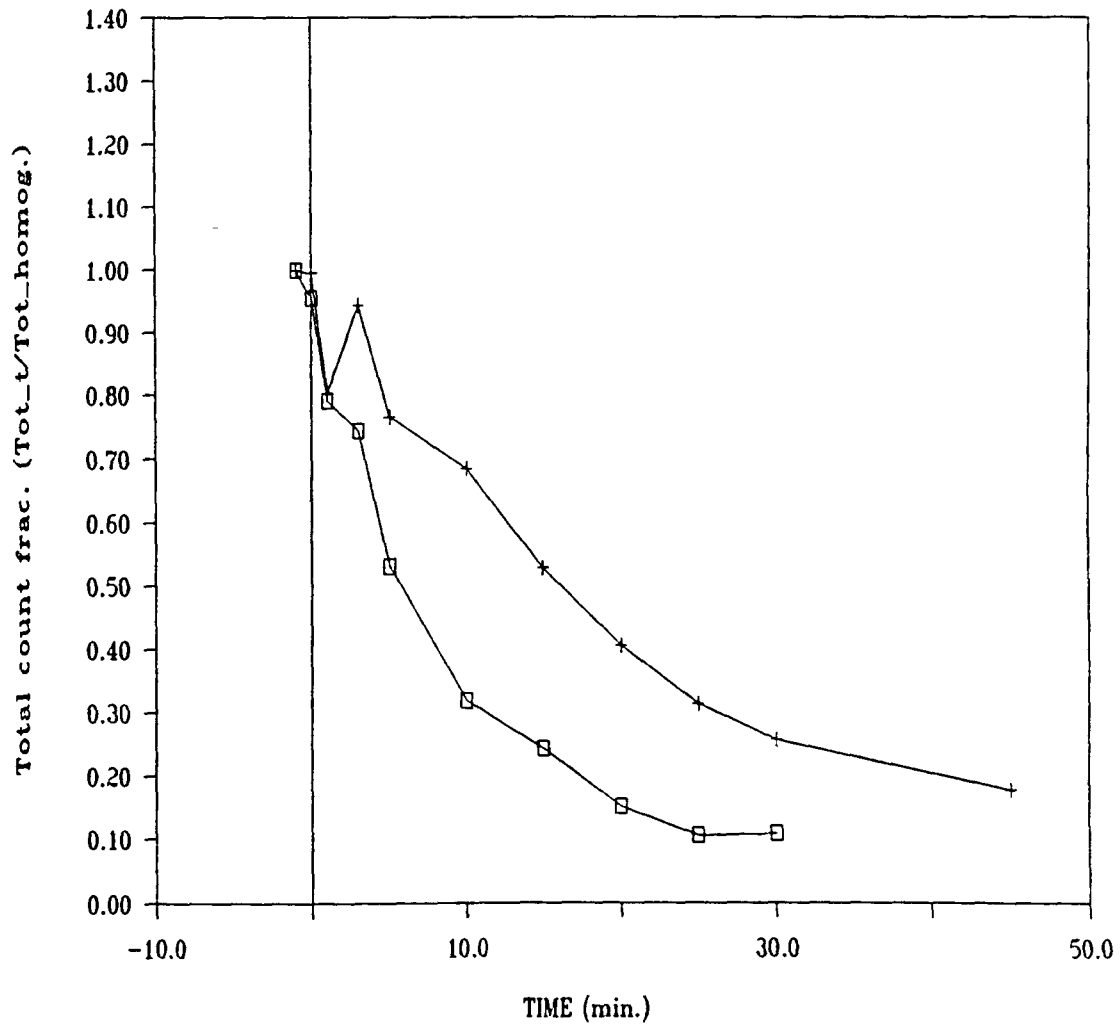


Figure 5.4: Comparison of experiments 'AB' and 'AH' to identify the influence of temperature on rapid mixing/flocculation.  $\square$  represents 20°C while  $+$  represents 5°C. Other conditions—mixing: 250 rpm for 1 min., flocculation at 60 rpm

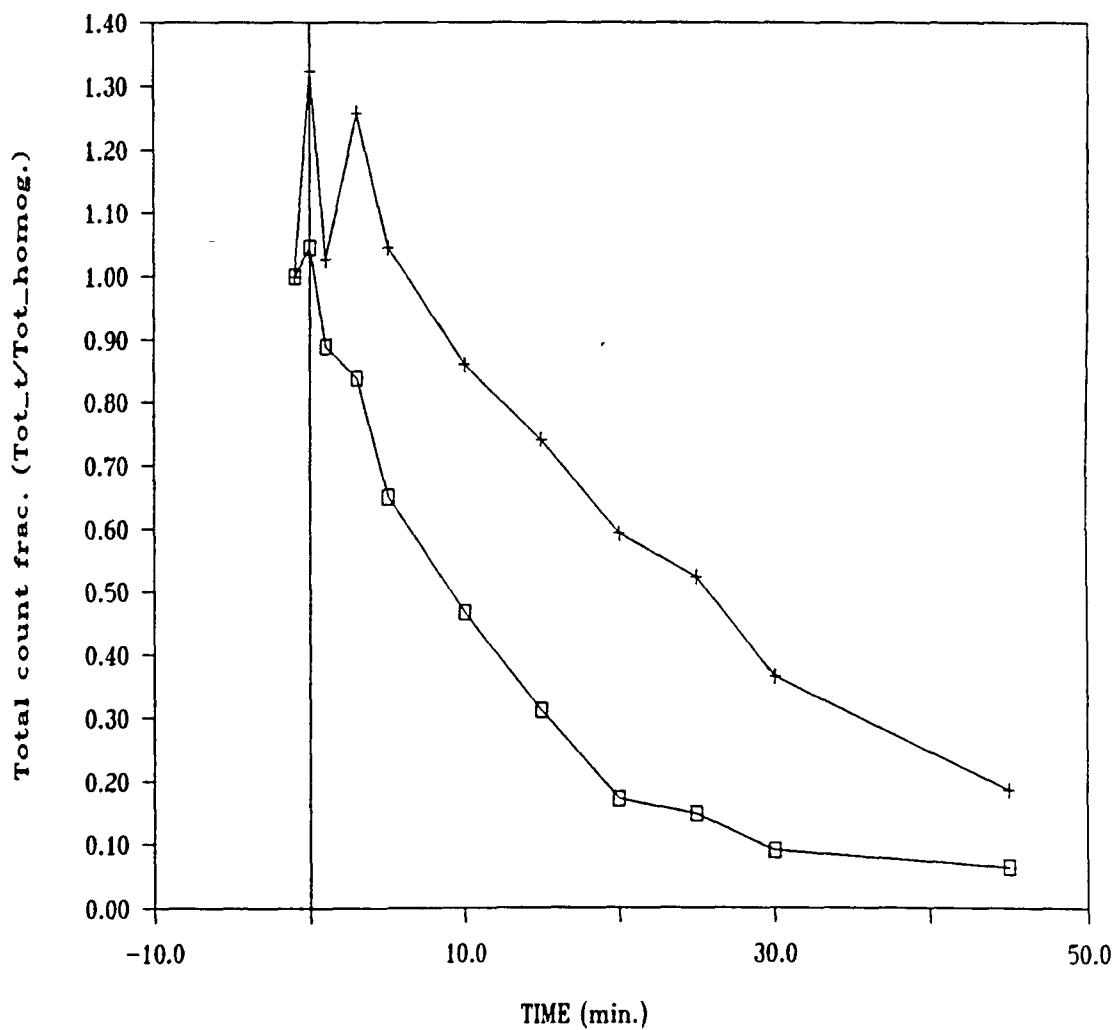


Figure 5.5: Comparison of experiments 'AA' and 'AE' to identify the influence of temperature on rapid mixing/flocculation.  $\square$  represents 20°C while  $+$  represents 5°C. Other conditions—mixing: 500 rpm for 1 min., flocculation at 60 rpm

others were conducted just once. In order to make comparisons easy, total count fractions for replicate experiments (if any) at a given set of experimental conditions are averaged for each of the sampling periods and then plotted in figures of the type being discussed here. The original data are presented in the appendix, where each set of experimental conditions and the associated results are identified.

Before we go any further, let us ponder over what's happening in the system. If we look back at the section relating to flocculation (Section 3.9.), we can recollect that flocculation is a diffusion-limited growth process in which destabilized particles come together to form bigger particles. Therefore, as a function of time, the total number of particles should decrease. Here, we must caution ourselves of the pitfalls of Smoluchowski's assumptions: he had assumed a *growth-only* type of behavior while real flocs in a turbulent fluid field undergo *growth and breakup*. Therefore, a reduction in the total number of particles at a given time, as compared to the homogenized clay suspension (i.e., the suspension, prior to being rapid-mixed and flocculated), would be an indicator of the net reduction in the numbers of particles due to growth and breakup.

Coming back to the figures at hand, a smaller total count fraction for a given duration of flocculation would mean that most particles have flocculated and that a net reduction in the total particle count, and therefore, a net growth of particle sizes has occurred. On the other hand, a larger total count fraction would indicate that not much net aggregation has taken place. Therefore, when watching these graphs, the thing to keep in mind is this: a high total count fraction means poor particle aggregation while a low total count fraction means good particle aggregation.

Now let us go back to Figures 5.2, 5.3, 5.4 and 5.5. In all these cases, we see

that at any given time during the flocculation period, the total count fraction is smaller for experiments conducted at 20°C than at 5°C. We can, therefore, say that a reduction in temperature has a markedly deleterious effect on the flocculation of dilute clay suspension. In almost all experiments, we see some unruly behavior in terms of the particle counts measured in samples corresponding to the first few minutes of flocculation. The source of this erratic behavior is not easily identified. However, if one looks at the general reduction in the total count fraction as a function of time, one can see that the slope of the plot gradually becomes less and less steep, indicating that the reduction in the number of particles in the system greatly slows down the rate of flocculation. Also, we see that at later points in time during the flocculation process, not only is the total count fraction much smaller in experiments at 20°C, the same is true of the rate of particle growth. In other words, the slope of the total count fraction versus time relation becomes flatter much earlier than in the experiments at 5°C.

In the context of rapid mixing, the thing to note is the total count fraction corresponding to  $t = 0$ , i.e., at the end of the rapid mixing period. Figures 5.2, and 5.4 show very slight changes in the total count fraction, as compared to the homogenized sample (for which the total count fraction = 1.0). Figure 5.5 shows that a large *increase* in the total count fraction at  $t = 0$  for the 5°C sample. This increase is an artifact of the particle counting instrument being used in this study. It was noticed that while the Automatic Image Analysis system (AIA) equipment was able to see the smallest of the particles in the clay suspension (in that it would display their image on the high resolution graphics monitor), they were much smaller than the resolution limit of the system. In other words, even

though they were big enough to be displayed on the graphics monitor, they were smaller than the 'detection limit' of the instrument. However, at the end of the rapid mixing period, these particles grew into a size range which was larger than the 'detection limit' of the instrument, permitting their detection and counting by the AIA system. Thus, this caused an increase in the total count fraction at  $t = 0$ . Disregarding this increase in total count fraction and looking at the general trend with time, it appears that the high speed rapid mixing (i.e., at 500 rpm) for a duration of 1 min. at low temperature is not beneficial to flocculation.

Now let us consider Figure 5.3. What do we see at  $t = 0$ ? We note that for both,  $5^{\circ}\text{C}$  as well as  $20^{\circ}\text{C}$ , there is a distinct reduction in the total count fraction. This reduction is of the order of 40 % at the higher temperature and 10 % at the lower temperature! This reduction would lead us to conclude that during the period of rapid mixing, too, the particles undergo flocculation. This *flocculation* (during the rapid mixing period) occurs at a much faster rate at higher temperatures than at lower temperatures.

To sum up, briefly, we can say that a reduction in temperature reduces the 'flocculation' rate during the rapid mixing period (for extended mixing periods) as well as the general rate of flocculation—carried out at 30 or 60 rpm.

**5.1.1.2. Alum: Rapid Mixing Intensity** Shown in Figures 5.6, 5.7 and 5.8 are comparisons of experiments to detect the influence of rapid mixing intensity on flocculation. Again, as we saw earlier, all plots involve plotting the total count fraction as a function of time.

First consider Figure 5.6. If we jump back to Figure 5.1, we see that this par-

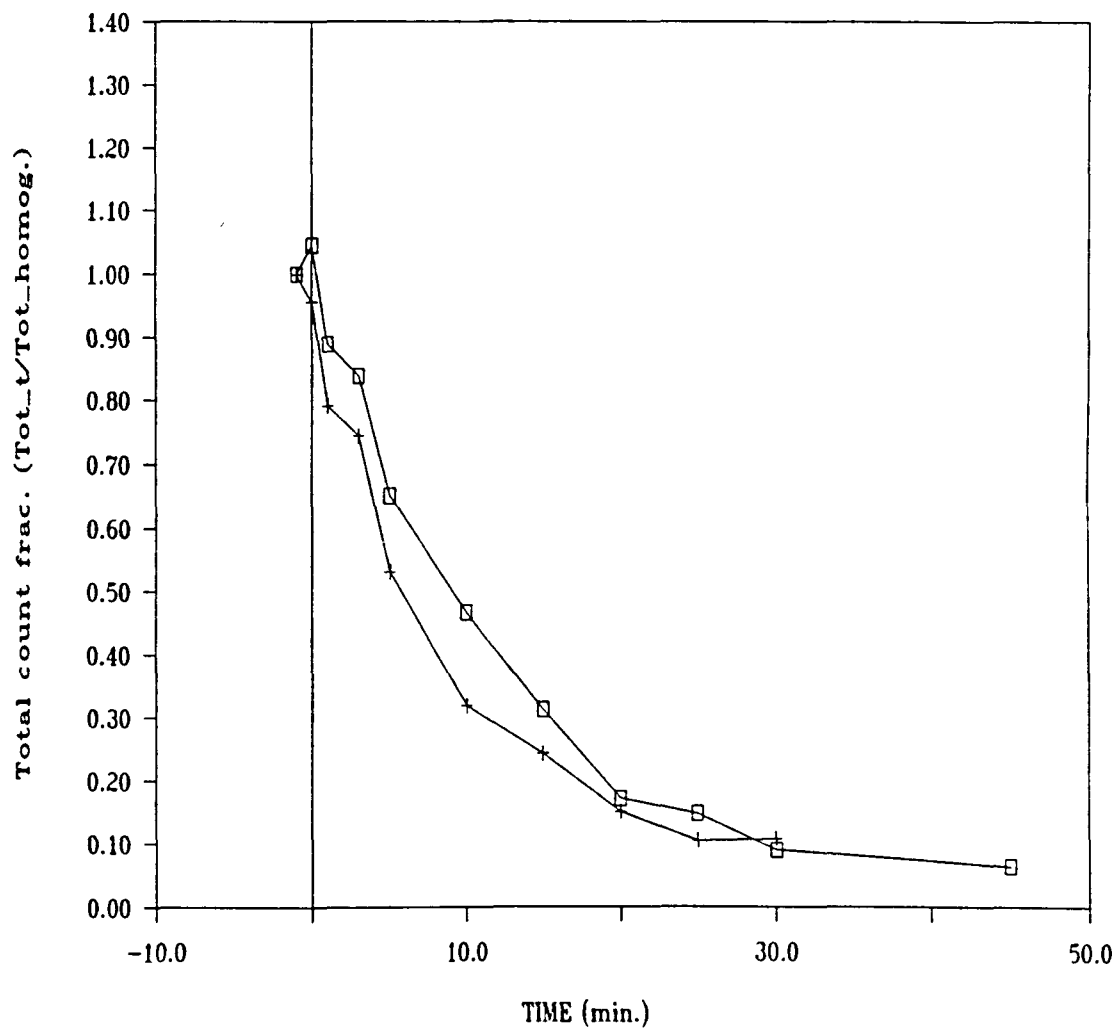


Figure 5.6: Comparison of experiments 'AA' and 'AB' to identify the influence of rapid mixing intensity on flocculation.  $\square$  represents mixing at 500 rpm while  $+$  represents mixing at 250 rpm. Other conditions—rapid mixing: 1 min., temperature: 20°C, flocculation at 60 rpm

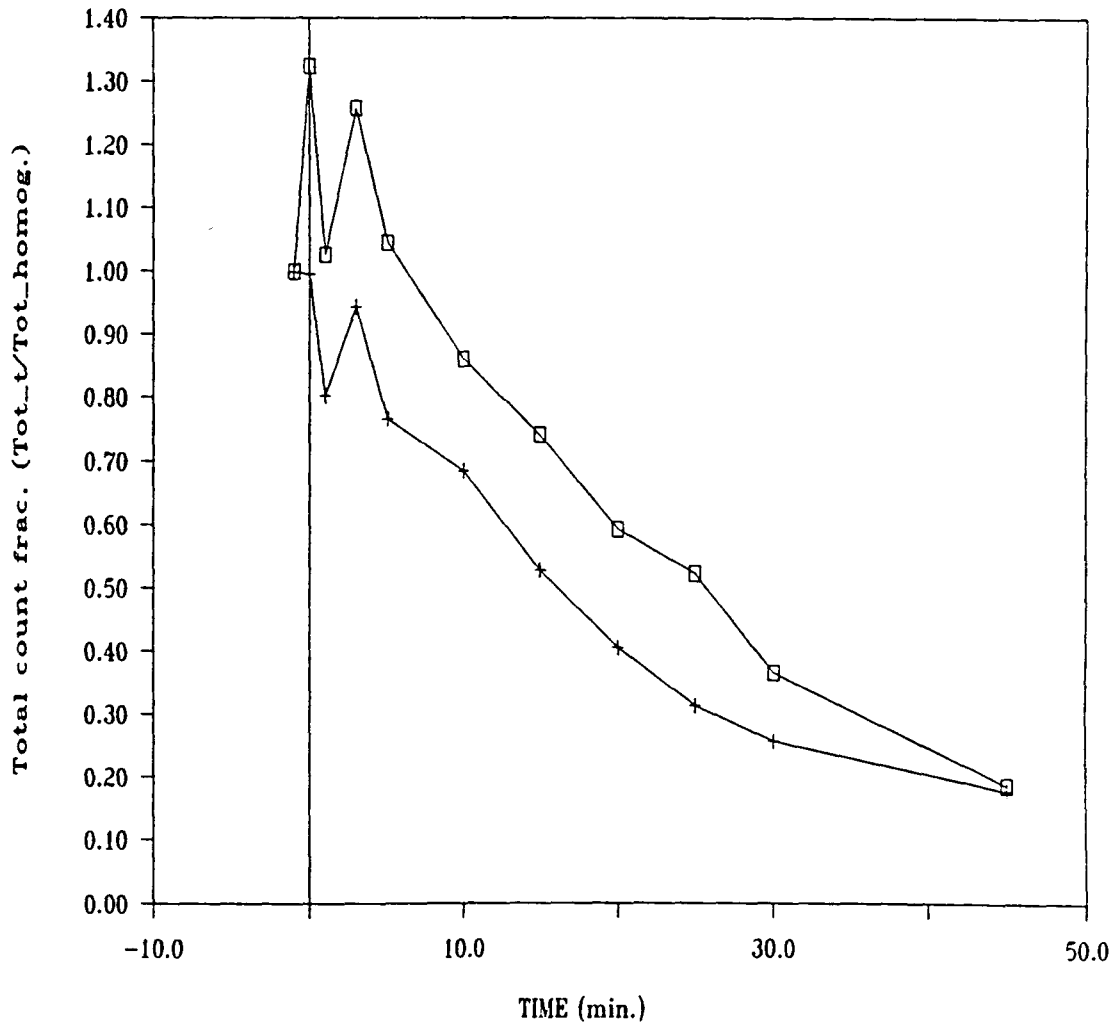


Figure 5.7: Comparison of experiments 'AE' and 'AH' to identify the influence of rapid mixing intensity on flocculation.  $\square$  represents mixing at 500 rpm while  $+$  represents mixing at 250 rpm. Other conditions—rapid mixing: 1 min., temperature: 5°C, flocculation at 60 rpm



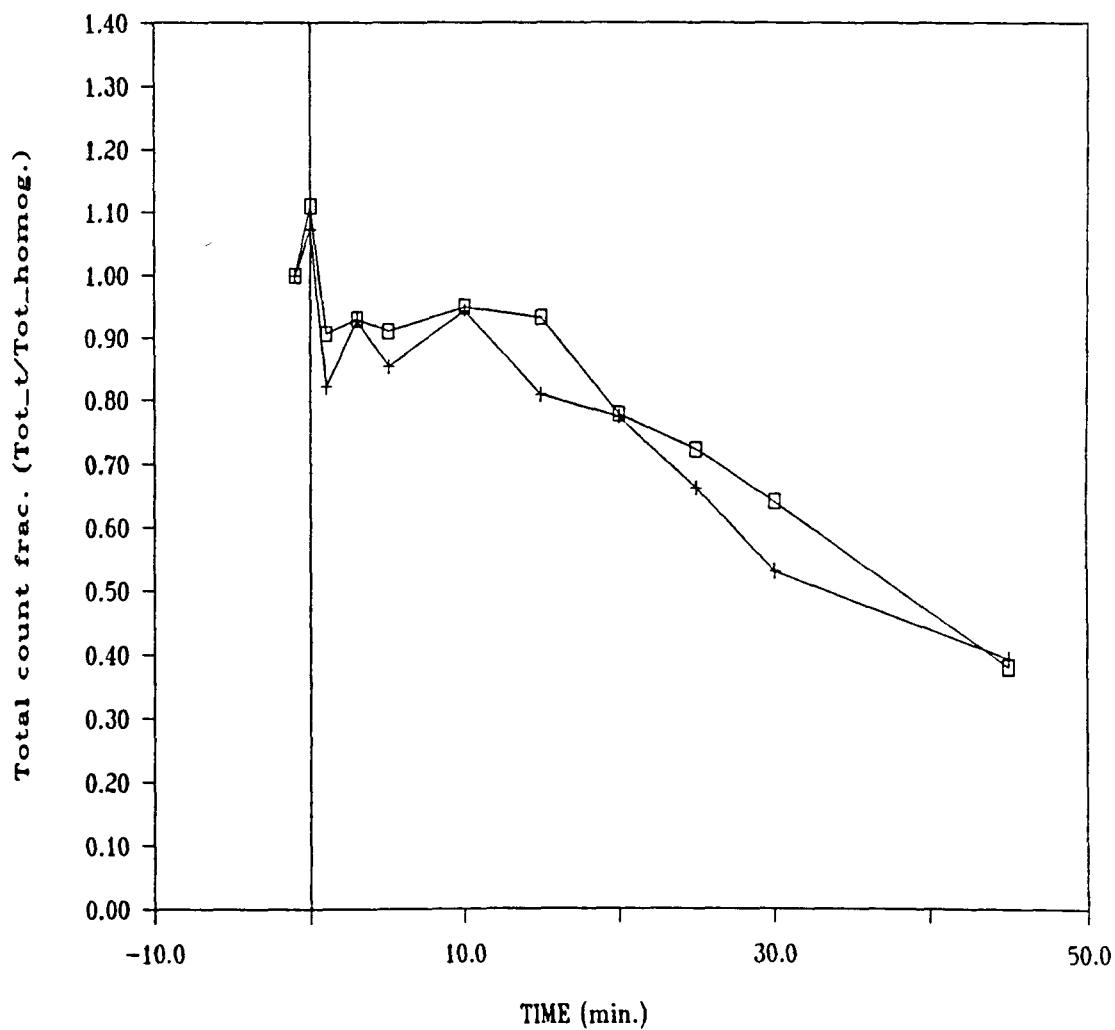


Figure 5.8: Comparison of experiments 'AF' and 'AI' to identify the influence of rapid mixing intensity on flocculation.  $\square$  represents mixing at 500 rpm while  $+$  represents mixing at 250 rpm. Other conditions—rapid mixing: 1 min., temperature: 5°C, flocculation at 30 rpm

ticular set of experiments was conducted at 20°C with high intensity flocculation. Coming back to Figure 5.6, we see that at different stages of flocculation, the suspension rapid mixed at 500 rpm seems to perform somewhat more poorly than that mixed at 250 rpm. Why? The reasons for this are discussed below.

Figure 5.7 involves experiments conducted at 5°C with high flocculation intensity (see Figure 5.1 for reference). We can see that for all time periods between  $t = 0$  and  $t = 30$ , the flocculation of the suspension rapid mixed at 500 rpm is *poorer* than that of the suspension rapid mixed at 250 rpm. Based on this, could one conclude that, (based on the concept that flocculation can be thought of as an ‘amplifier’ of the state of destabilization of the colloids, as mentioned in Chapter 4.), rapid mixing at 500 rpm produces inferior flocculation because of poorer destabilization? Not really. Based on our studies in Chapter 3., we agree that if the sole purpose of rapid mixing is to distribute coagulants quickly and uniformly throughout the reactor, then the results of more intense rapid mixing should be superior to those obtained from the less intense rapid mixing. The validity of this idea—in the adsorption destabilization zone of alum coagulation—was demonstrated by Amirtharajah and Mills [3]. However, we can see in Figure 5.3 that rapid mixing not only *mixed* the coagulant uniformly throughout the reactor, it also *flocculated* the destabilized colloids, causing a reduction in the total count fraction by the end of the rapid mixing period!

In this context, it appears that the reason why rapid mixing of the suspension at 500 rpm appears to be inferior to that at 250 rpm (Figure 5.7) is because the intense turbulence at the higher speed not only increases the rapidity with which the coagulants are distributed throughout the reactor; it also increases the colli-

sion opportunities between particles—and therefore the growth opportunities. This increased speed, though, has a rather severe side effect: an increase in turbulence intensity also increases the shearing stress in the fluid. This increased shearing stress causes the flocculated particles to break up. It is generally accepted that flocs which break up into smaller particles do not re-flocculate as well as particles which are not broken up—even though they may have similar sizes. This may be the reason why the suspension which had been rapid mixed at the higher mixing intensity flocculated poorly as compared to the suspension rapid mixed at a lower mixing intensity.

In the same figure (Figure 5.7), after 45 minutes of flocculation, the total count fraction is almost the same for both rapid mixing conditions! Why? This may be so because at those periods, the actual particle concentration in the suspension is low, with a much greater predominance of large particles than at time periods prior to that. These large particles act like large brooms, sweeping the suspension and in the process, catching any small particles which might be encountered. This process very quickly reduces the number of small, unattached particles in the system, leaving only larger particles to interact with each other. Given the low particle concentrations, the particle growth process becomes severely collision limited (see Section 3.9.). Moreover, the size of these large particles makes them prime targets for break-up due to localized spots of high shear (e.g., around the impeller zone). This combination of factors may be the reason why we have the overall effect of the type shown in the 45 min. samples in Figure 5.7. In fact, merely out of interest, if the flocculation period in these experiments were to be extended to, say, 2 hours, all the suspensions would most probably look alike.

Let us now consider Figure 5.8. If we check with Figure 5.1, we see that the experimental conditions are such that flocculation is conducted at low intensity (30 rpm) and the temperature of the experiments is 5°C. We have already seen the deleterious effects of temperature on flocculation. It seems, in this figure (Figure 5.8), that the influence of temperature on the flocculation kinetics may have the dominant effect, causing both suspensions—one rapid mixed at 500 rpm and the other at 250 rpm—to behave poorly. Whether the sample rapid mixed at 500 rpm is significantly different from that mixed at 250 rpm is arguable. But it does seem to indicate that the former is generally worse than the latter in terms of the total count fraction at various time intervals of flocculation.

One thing to note is that this is precisely the same set of experiments as identified in Figure 5.7 except that this set (Figure 5.8) was conducted at the lower flocculation intensity than the one in Figure 5.7. A glance at these two figures reminds us of the great importance of the flocculation intensity in accelerating flocculation kinetics.

In summing up, all three figures (5.6, 5.7 and 5.8) show that intense rapid mixing at 500 rpm produced poorer results than that at 250 rpm. However, while the differences in flocculation due to rapid mixing in Figures 5.6 and 5.8 were not as pronounced as in Figure 5.7, it would not be exaggeration to conclude that intense rapid mixing at 500 rpm for 1 minute is inferior to rapid mixing at 250 rpm for the same duration, when using alum as a coagulant.

**5.1.1.3. Alum: Time Effects** We now come to the most interesting part of the investigations. Consider Figures 5.9, 5.10, 5.11 and 5.12, where we desire to

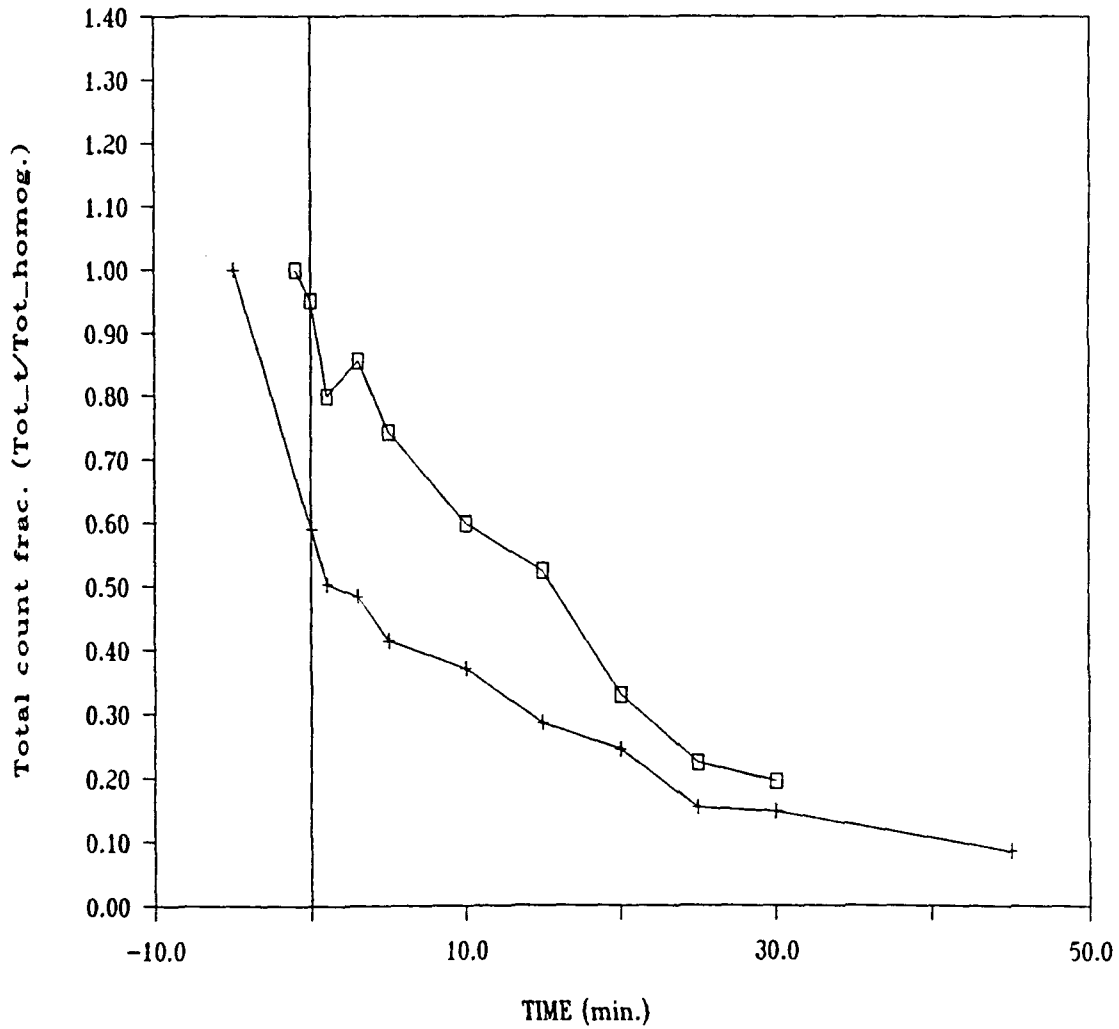


Figure 5.9: Comparison of experiments 'AC' and 'AD' to identify the influence of duration of rapid mixing on a suspension. □ represents a 1 min. mixing time while + represents a 5 min. mixing time. Other conditions—mixing: 250 rpm, temperature: 20°C, flocculation at 30 rpm

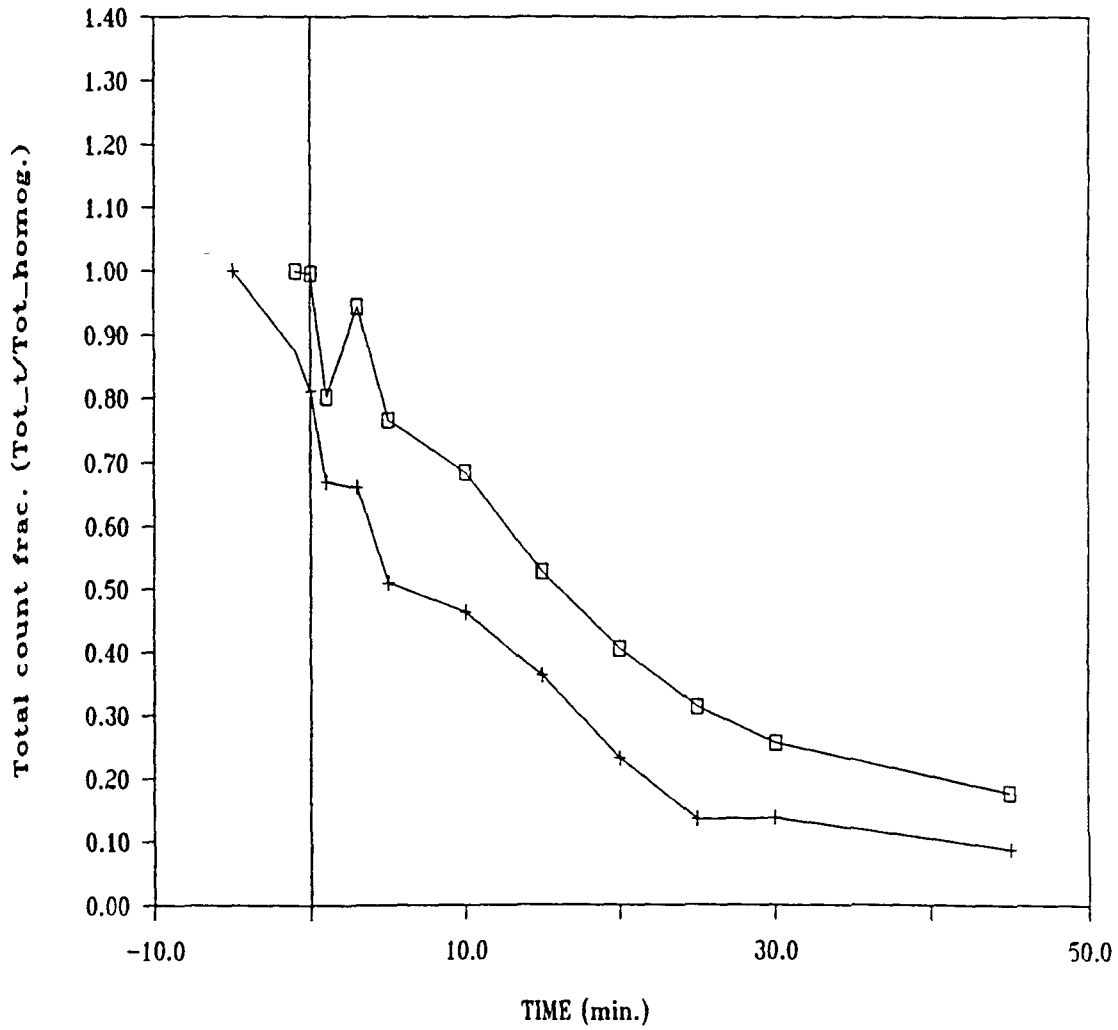


Figure 5.10: Comparison of experiments 'AH' and 'AJ' to identify the influence of duration of rapid mixing on a suspension. □ represents a 1 min. mixing time while + represents a 5 min. mixing time. Other conditions—mixing: 250 rpm, temperature: 5°C, flocculation at 60 rpm

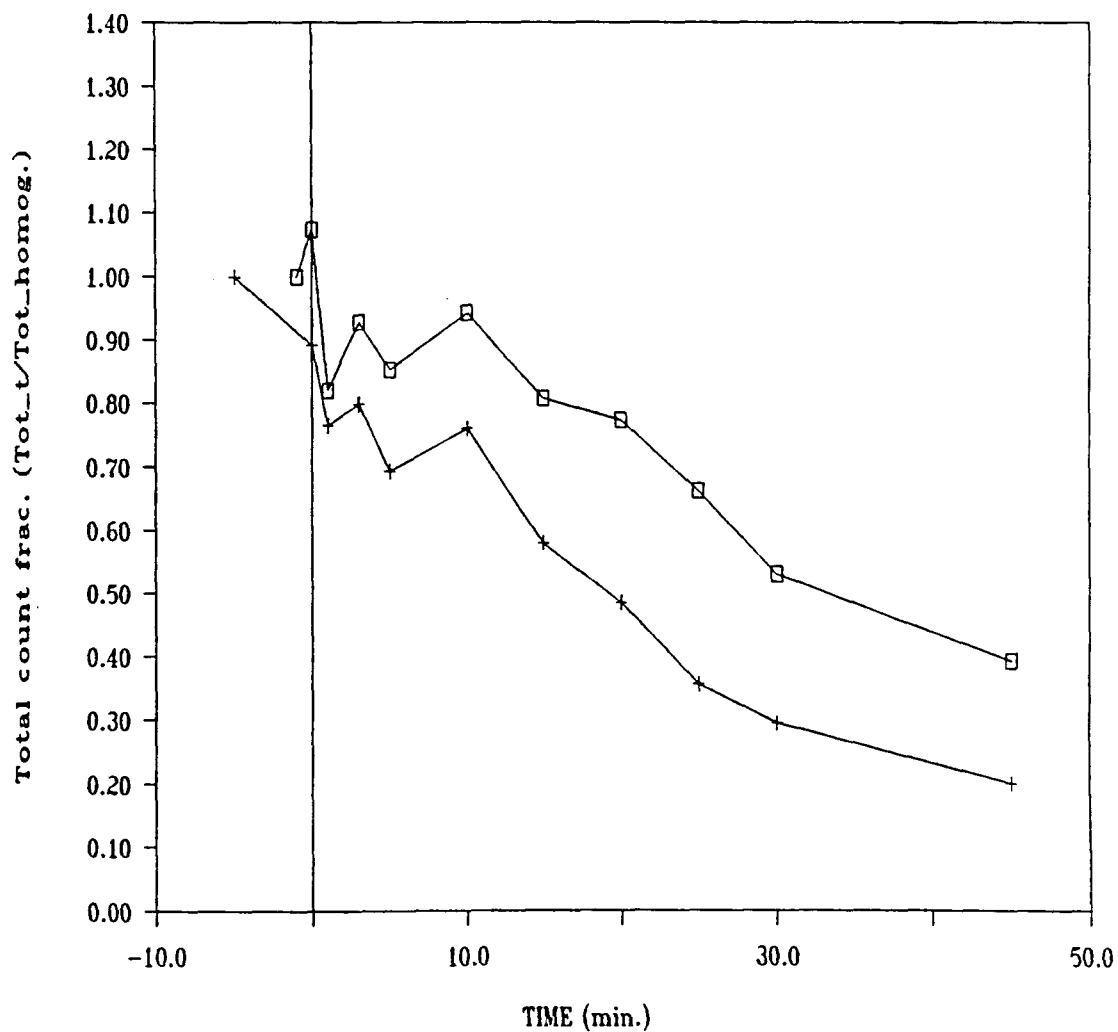


Figure 5.11: Comparison of experiments 'AI' and 'AK' to identify the influence of duration of rapid mixing on a suspension.  $\square$  represents a 1 min. mixing time while  $+$  represents a 5 min. mixing time. Other conditions—mixing: 250 rpm, temperature: 5°C, flocculation at 30 rpm

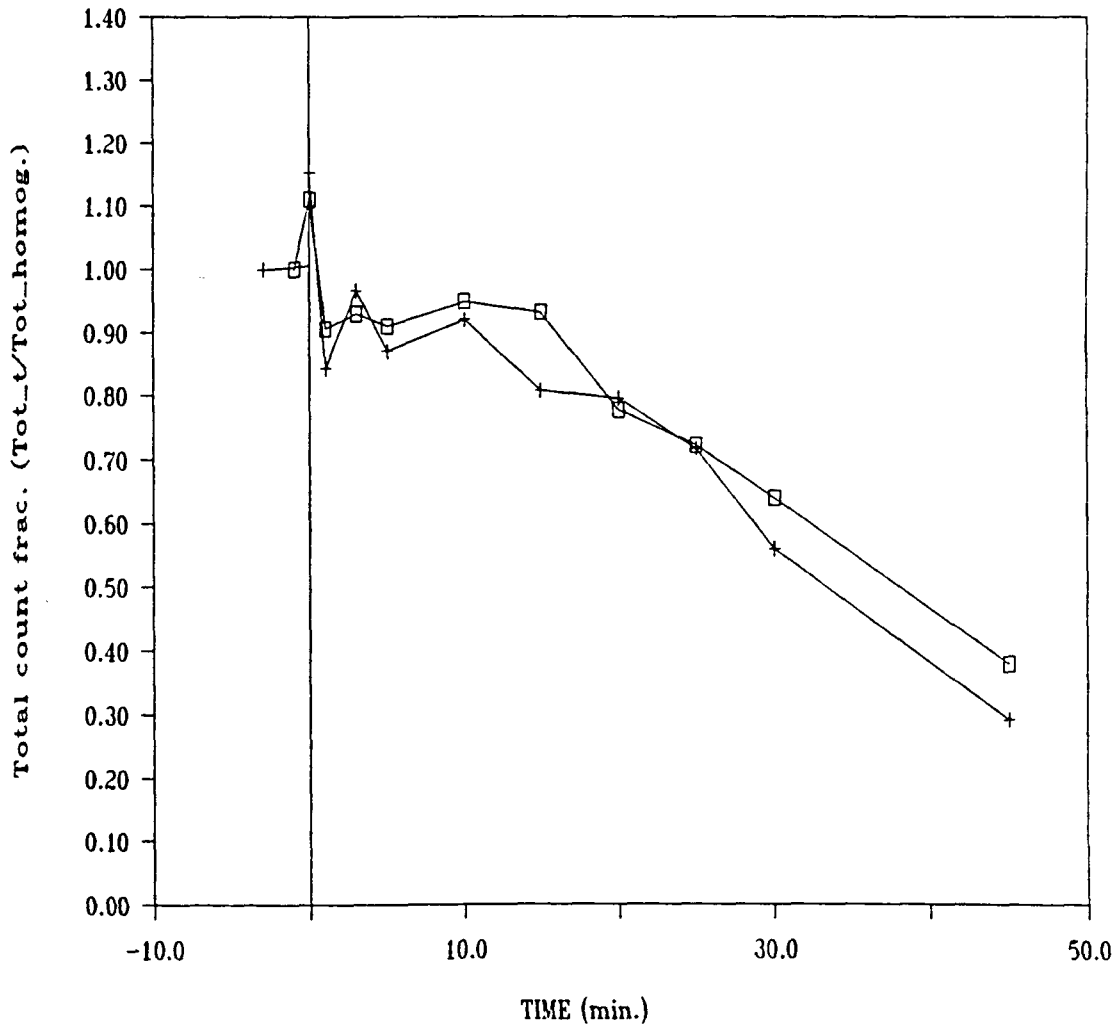


Figure 5.12: Comparison of experiments 'AF' and 'AG' to identify the influence of duration of rapid mixing on a suspension. □ represents a 1 min. mixing time while + represents a 3 min. mixing time. Other conditions—mixing: 500 rpm, temperature: 5°C, flocculation at 30 rpm



detect the influence of the duration of rapid mixing on a colloidal suspension. In all these figures, we plot the total count fraction versus time.

First we choose Figure 5.9. Comparing this with the reference Figure 5.1, we see that the conditions of these experiments involve suspensions at 20°C rapid mixed at 250 rpm and flocculated at 30 rpm. At time  $t = 0$ , we see an enormous—almost 40%—reduction in the number of particles (as compared with the homogenized sample) in the suspension rapid mixed for 5 min. while in the suspension rapid mixed for 1 min., this reduction is less than 5%!

This extended rapid mixing period results in an extremely high slope in the total count fraction versus time relation—implying that the turbulence intensity in the reactor, at 250 rpm of mixing, is high enough to mix the coagulant uniformly as well as permit the particles to have more collisions per unit time (see Section 3.9.) but it does not have such high shearing stresses that would cause any growing particles to break-up or disintegrate under the influence of this shear. At this mixing intensity, it appears that there is a net reduction in total particle counts, meaning that the growth processes must predominate over the break-up processes. The same trend is visible in Figures 5.10 and 5.11.

In these two cases (Figures 5.10 and 5.11), the erratic behavior in the samples corresponding to 1 and 3 minutes of flocculation is difficult to explain. Despite this characteristic, in the general context of experiments involving extended periods of rapid mixing, it can be said, without any doubts, that the extended rapid mixing period at 250 rpm not only disperses the coagulant well, permitting the destabilization of all colloids, it also *flocculates* the destabilized colloidal suspension in a much better fashion than results during “flocculation” at 30 or 60 rpm during the

first few minutes of the “flocculation period”. This is obvious by the much steeper slope of the total count fraction versus time plot, particularly evident in Figure 5.9.

What happens if the rapid mixing is carried out at 500 rpm? We turn to Figure 5.12. We see that at  $t = 0$ , there has been an *increase* in the total number of particles counted. This, as explained on page 227, is an artifact of the image analysis equipment being used to count the particles. While in the initial few minutes of the flocculation period, we do not see any distinct superiority of the extended rapid mixing period; we do notice an improvement in the reduction of the total count fraction for the suspension rapid mixed for an extended period, when we consider the later time periods of flocculation.

Based on these figures, we can conclude that rapid mixing not only serves to mix the coagulant uniformly throughout the reactor, at the appropriate intensity, it also flocculates these destabilized colloids, accelerating the overall flocculation process considerably.

**5.1.1.4. Alum: Best Mixing Conditions** We have, thus far, made paired comparisons listed in Table 5.1 to identify the effects of individual variables, like temperature, on a suspension undergoing rapid mixing. A treatment plant designer/operator has little control over the temperature of the influent water. However, she can definitely exercise some control over the other mixing variables—intensity of mixing and its duration. In order to choose the proper combination, we must compare all rapid mixing conditions. This is done in the following paragraphs.

Consider Figure 5.13. If we refer back to Figure 5.1, we see that all these experiments involved a temperature of  $5^{\circ}\text{C}$  and a low flocculation intensity. In this

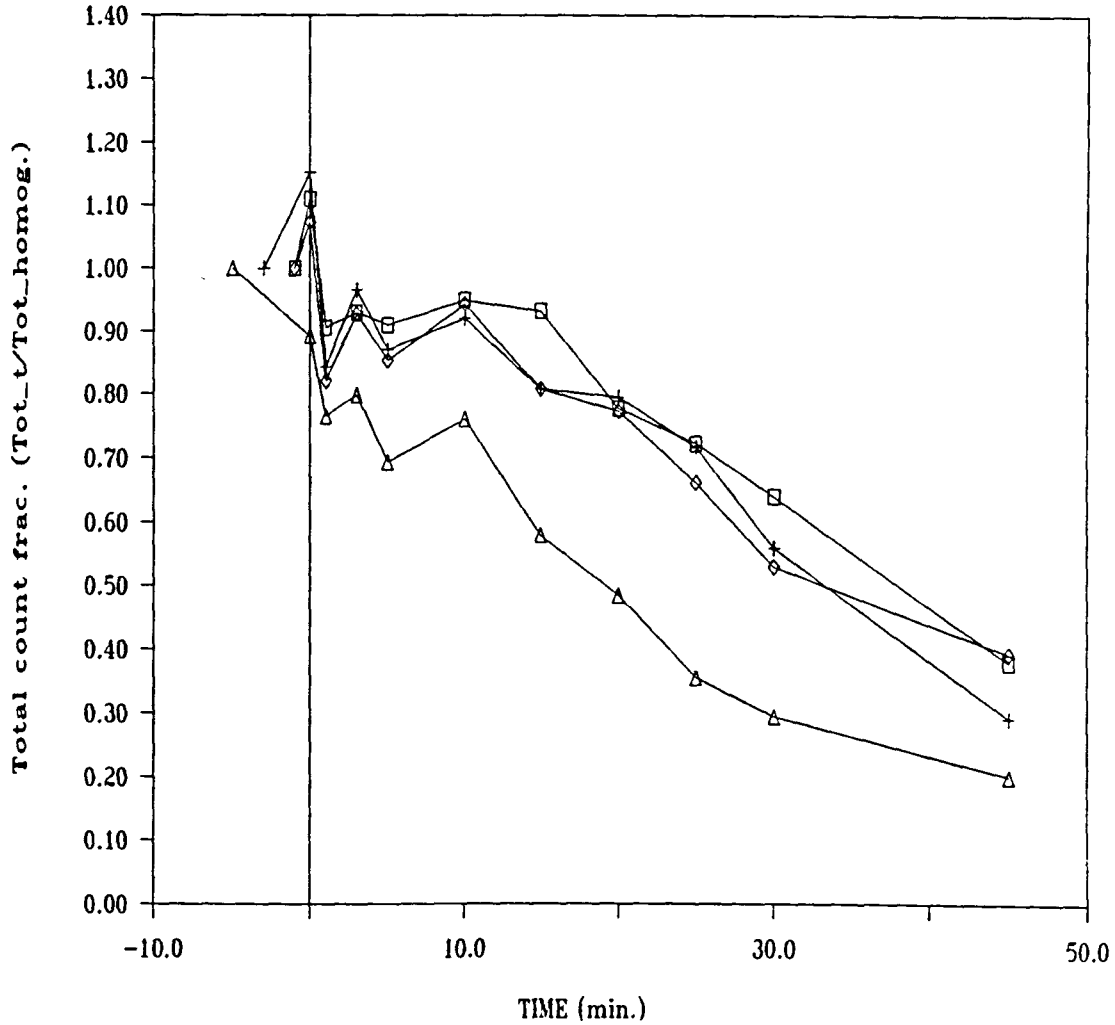


Figure 5.13: Comparison of experiments 'AF', 'AG', 'AI' and 'AK' to identify the best rapid mixing intensity-duration combination. □ represents mixing at 500 rpm for 1 minute, + 500 rpm for 3 minutes, ◇ 250 rpm for 1 minute, △ 250 rpm for 5 minutes. Other conditions—temperature: 5°C, flocculation at 30 rpm

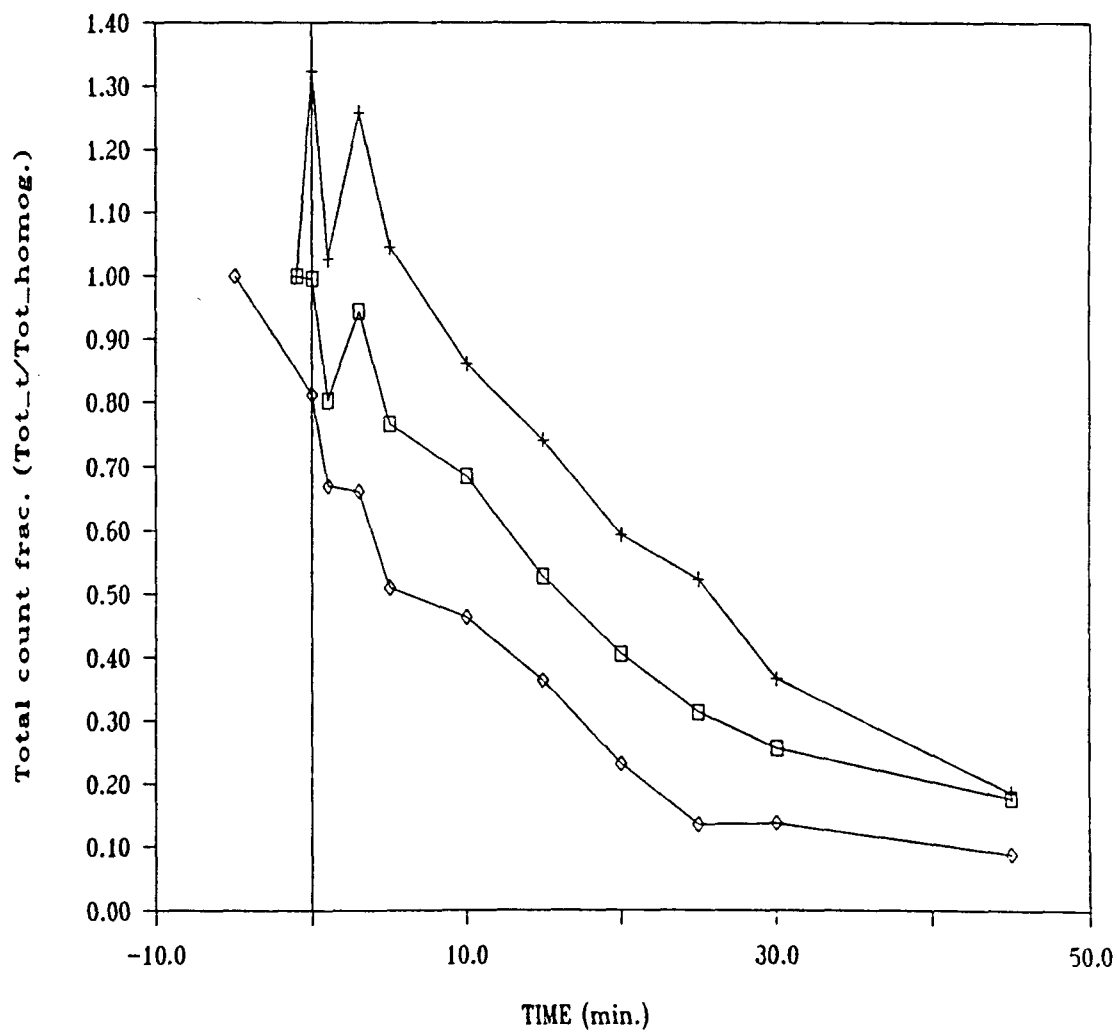


Figure 5.14: Comparison of experiments 'AE', 'AH' and 'AJ' to identify the best rapid mixing intensity-duration combination. + represents mixing at 500 rpm for 1 minute, □ mixing at 250 rpm for 1 minute and ◇ 250 rpm for 5 minutes. Other conditions—temperature: 5°C, flocculation at 60 rpm

comparison, we can see that the best performance is exhibited by the suspension which has been mixed for an extended period of 5 minutes at 250 rpm. The other combinations produce results which are decidedly inferior to those produced by experiments at this set of mixing conditions.

Similarly, Figure 5.14 compares experiments conducted at a temperature of 5°C and a high flocculation intensity (see Figure 5.1 for reference). We see, again, that rapid mixing at 250 rpm for 5 minutes produces the best overall result.

Reasons for the superiority of 250 rpm mixing over 500 rpm mixing, as well as the superiority of extended rapid mixing over mixing occurring over a shorter duration have already been discussed and will not be repeated here.

In conclusion, we can say that low intensity rapid mixing for an extended period of time produces better results than mixing at any other combination of rapid mixing conditions when using alum as a coagulant.

### **5.1.2. Rapid mixing with Magnifloc 573C polymer**

Experiments involving Magnifloc 573C polymeric coagulant have been summarized in Figure 5.15. Again, the location of this figure in this thesis should be marked because repeated references will be made to it later in this sub-section. We see that the experiments here are designed such that the low intensity rapid mixing (at 250 rpm) was carried out for 1 minute while the high intensity rapid mixing (500 rpm) was carried out for 2.25 minutes. This, obviously, is not a balanced experimental plan. In fact, originally, it was not planned to conduct experiments involving variation of the rapid mixing conditions using polymers as coagulants. However, an exploratory experimental run yielded some surprising results, prompt-

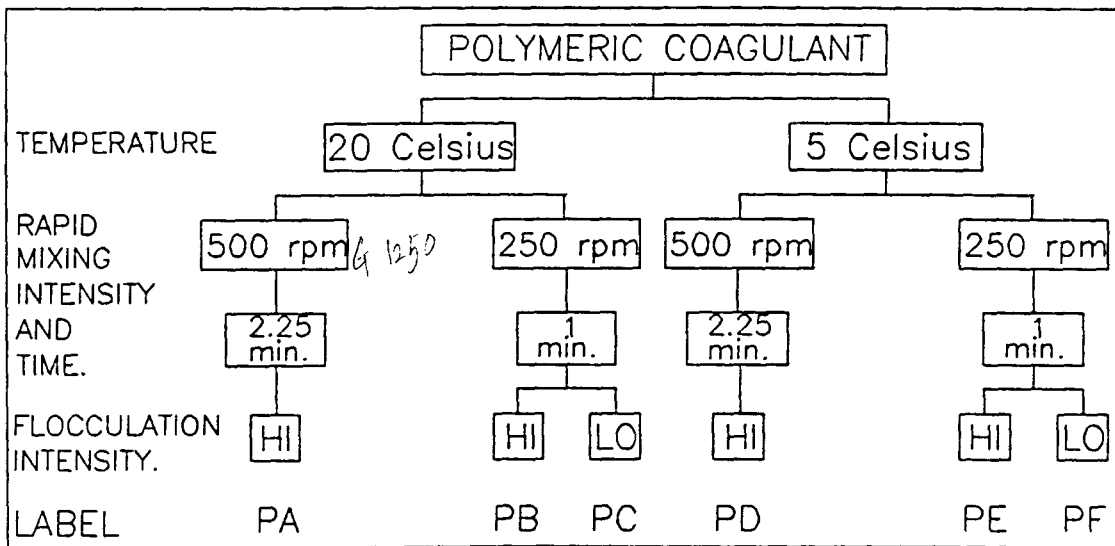


Figure 5.15: Experimental plan involving Magnifloc 573C polymer. 'Hi' and 'Lo' flocculation intensities correspond to 60 and 30 rpm respectively. Samples in all of these experiments were collected and analyzed in the deep sample cells

Table 5.2: List of experiments to be compared to detect the influence of various rapid mixing conditions on the clay suspension using Magnifloc 573C

Variable	Comparison
Temperature	PA-PD
	PB-PE
	PC-PF
Mixing Conditions	PA-PB
	PD-PE

ing the set of experiments shown in this figure.

Before we go any further, we should do exactly what we did in the case of polymers: identify the possible comparisons to be made among these experiments in order to detect the influence of various experimental conditions. This is done in Table 5.2.

This amounts to a total of 5 comparisons. We shall discuss each of the variables separately.

**5.1.2.1. Polymer: Temperature Effects** Figures 5.16, 5.17 and 5.18 identify the influence of temperature on rapid mixing/flocculation of the clay suspension using a polymer. The parameter being used to gauge the performance of the experiment is the total count fraction and its variation as a function of time.

In Figure 5.16 we see that the suspension at 20°C seems to show, as a function of time, a better reduction in the total count fraction than the suspension at 5°C. If we look back at Figure 5.15, we see that the experiments involved a rapid mixing

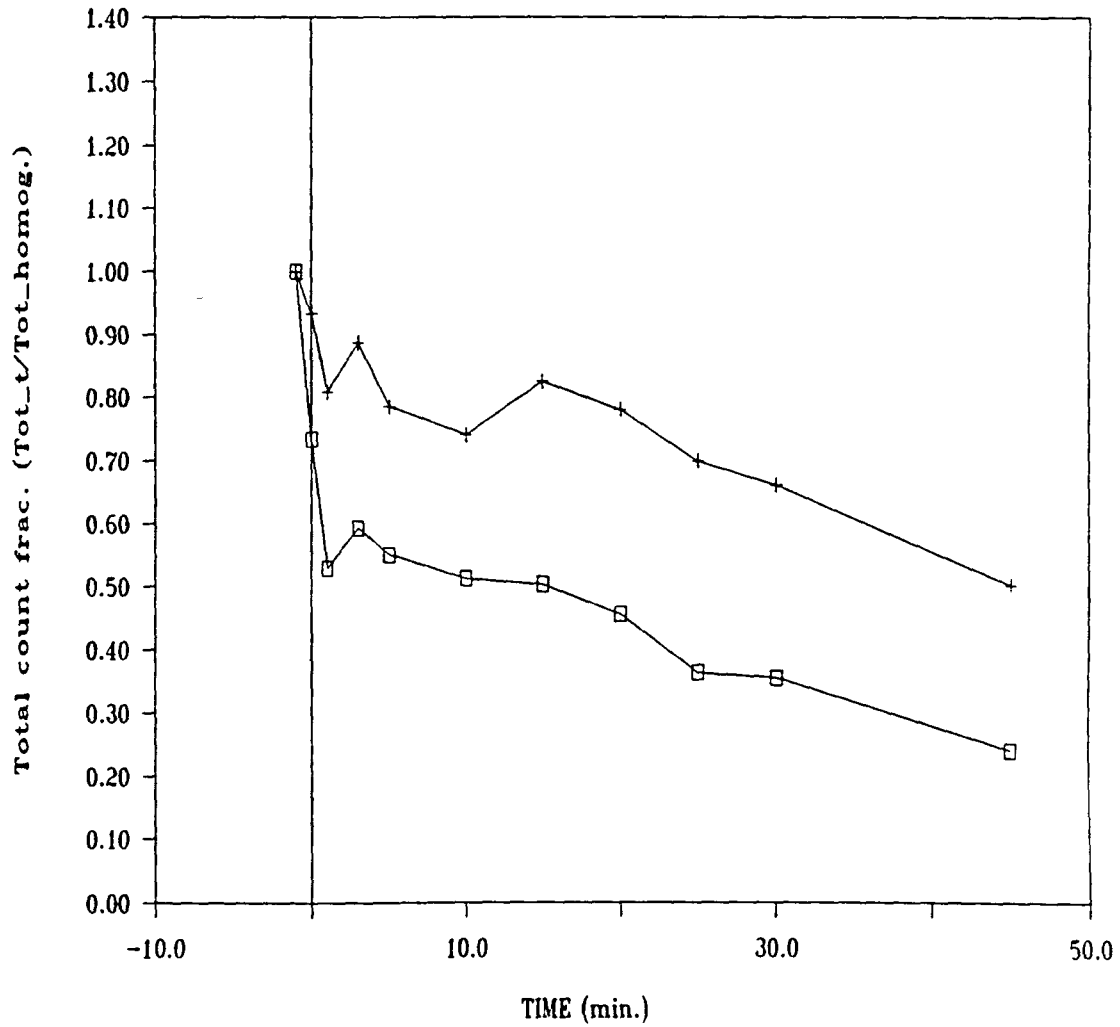


Figure 5.16: Comparison of experiments 'PC' and 'PF' to identify the influence of temperature on rapid mixing/flocculation.  $\square$  represents 20°C while + represents 5°C. Other conditions—mixing: 250 rpm for 1 min., flocculation at 30 rpm



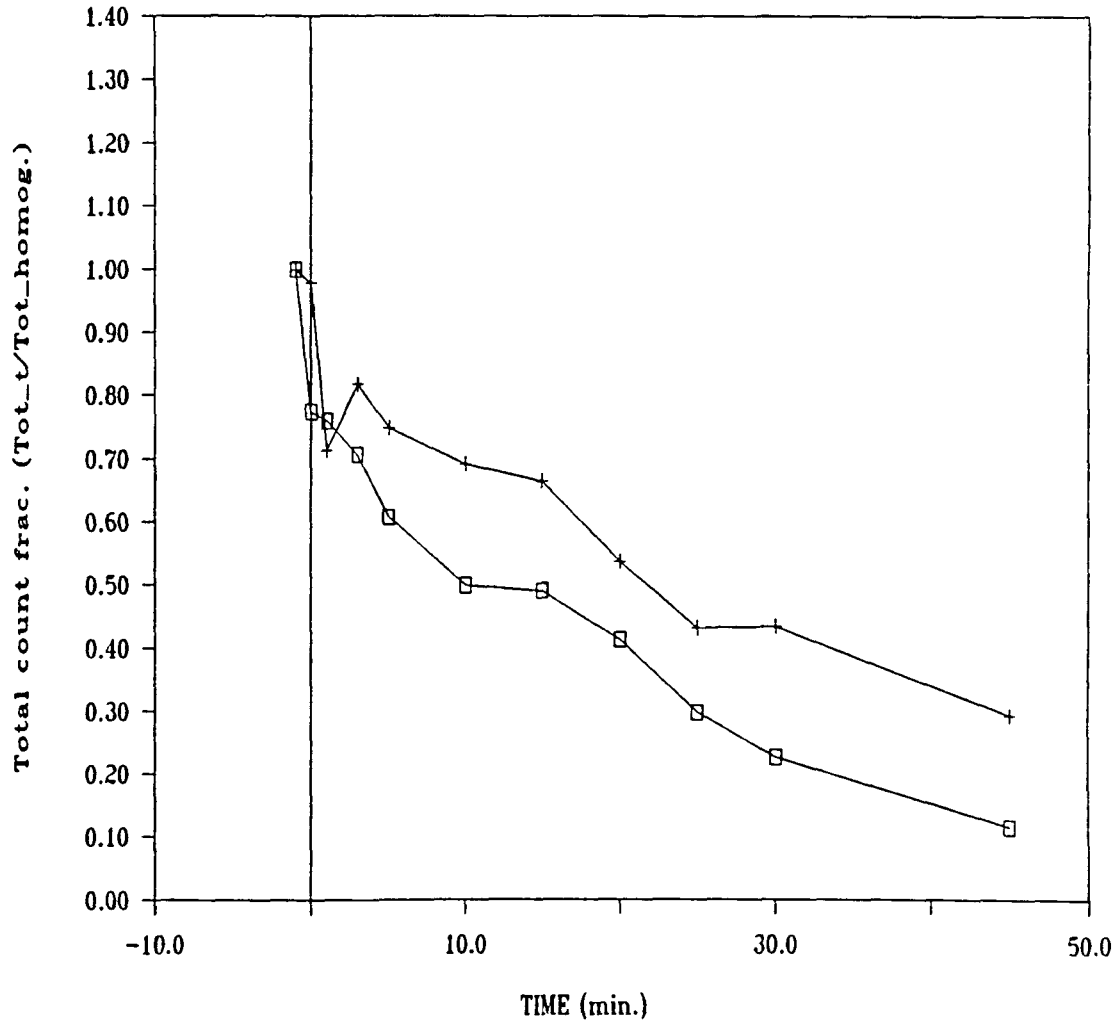


Figure 5.17: Comparison of experiments 'PB' and 'PE' to identify the influence of temperature on rapid mixing/flocculation.  $\square$  represents 20°C while + represents 5°C. Other conditions—mixing: 250 rpm for 1 min., flocculation at 60 rpm

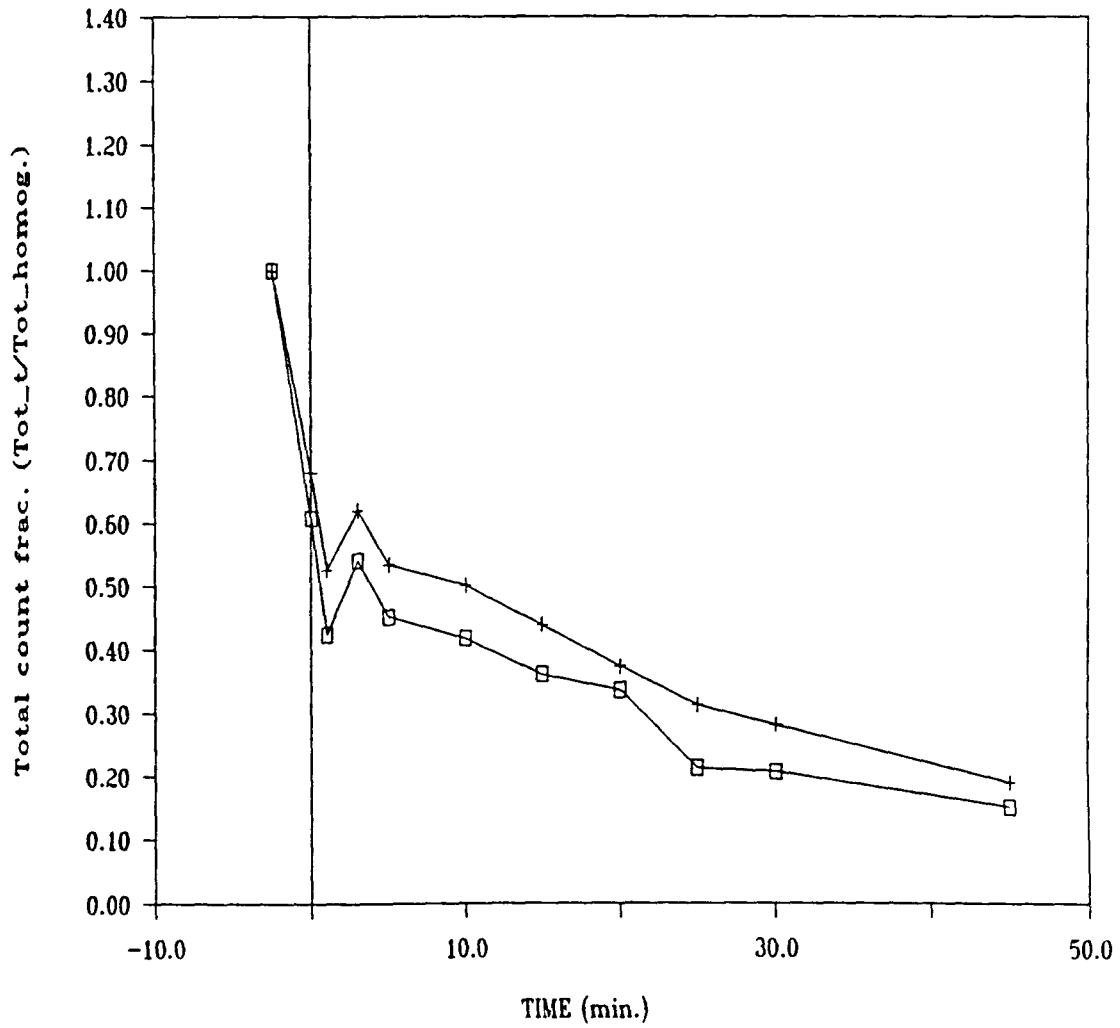


Figure 5.18: Comparison of experiments 'PA' and 'PD' to identify the influence of temperature on rapid mixing/flocculation. □ represents 20°C while + represents 5°C. Other conditions—mixing: 500 rpm for 2.25 min., flocculation at 60 rpm

intensity of 250 rpm for a duration of 1 minute, with flocculation occurring at 30 rpm.

Comparing Figure 5.16 with Figure 5.17 (same conditions of rapid mixing in both sets—different flocculation intensities, as seen in Figure 5.15), we see that even though the use of a higher flocculation intensity improves the process performance at both temperatures—in terms of reduction in the total count fraction—the overall performance at 20°C is superior to that at 5°C.

If we look at the total count fraction corresponding to  $t = 0$  in both the figures (5.16 and 5.17), we see that at 5°C, there is a miniscule reduction in the total count fraction while at 20°C, the reduction is nearly 25%! This is very similar to what we saw in experiments involving alum—proving, once again, that we do see *flocculation* occurring during the period of rapid mixing.

In Figure 5.18, we see the results of experiments conducted at the high rapid mixing intensity (500 rpm) for an extended period of 2.25 minutes (see Figure 5.15). Note that at 20°C as well as 5°C, we have a substantial reduction in the total count fraction at  $t = 0$ . At 20°C, this reduction is almost 40% while at 5°C, it is about 25%, reinforcing the idea that rapid mixing serves a dual purpose—that of mixing the coagulant to destabilize the colloids, as well as flocculating the destabilized colloids.

Note that at these rapid mixing and flocculation conditions, the difference in performance between 20°C and 5°C is not as much as in other conditions. We could, therefore, conclude that we can considerably reduce the deleterious effects of temperature on colloid flocculation—an influence obvious in Figures 5.16 and 5.17—by using a polymeric coagulant rapid mixed at higher mixing intensities for

an extended period of mixing.

In conclusion, one can say that temperature has a deleterious effect on the rapid mixing/flocculation of colloids using a polymeric coagulant. But, this detrimental effect can be somewhat lessened by rapid mixing at a higher intensity for an extended period.

**5.1.2.2. Polymer: Rapid Mixing Condition Effects** Figures 5.19 and 5.20 are for identifying the influence of rapid mixing conditions on flocculation of the clay suspensions (check Figure 5.15). In both of these figures, we can see that rapid mixing at 500 rpm for 2.25 min. results in a decidedly superior performance than rapid mixing at 250 rpm for 1 minute.

In the absence of experiments involving rapid mixing at (1) 250 rpm for 3–5 minutes and (2) 500 rpm for 1 minute, it is difficult to say with confidence—based solely on these figures—whether the improvement in flocculation is because of the higher intensity of rapid mixing, or the added time for which this mixing was done, or both! I think it was primarily due to the higher intensity of turbulence associated with 500 rpm of mixing, with some added assistance from the longer duration of mixing. The reason for this is based partly on visual observations made on the contents of the reactor when they were being flocculated using polymers. During the flocculation experiments involving rapid mixing at the lower mixing intensity, one could see many tight little lumps of clay in the suspension. These ‘lumps’ persisted throughout the flocculation period. However, at higher rapid mixing intensities, these ‘lumps’ never appeared! It is thought that these lumps were formed by little globules of poorly dispersed polymers onto which clay particles had

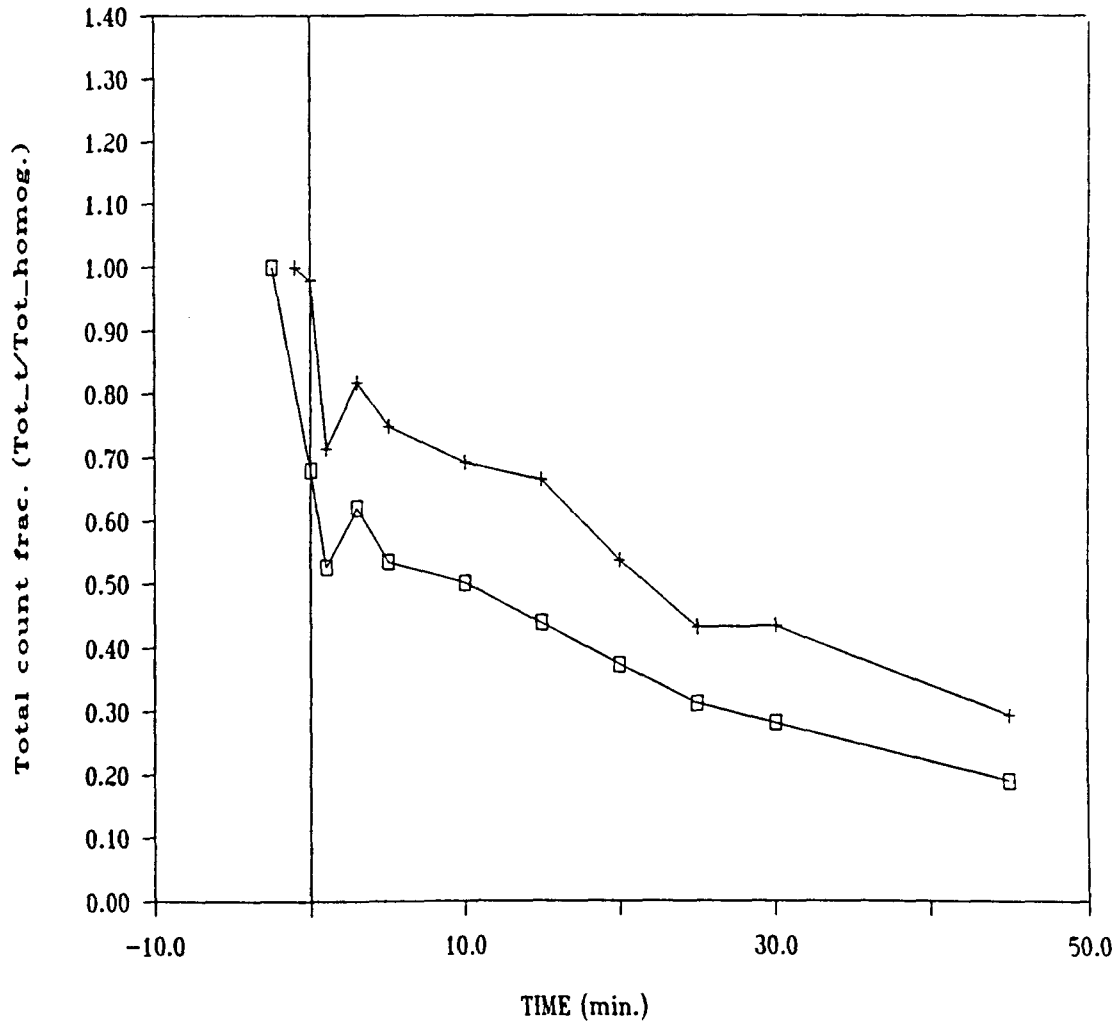


Figure 5.19: Comparison of experiments 'PD' and 'PE' to identify the influence of rapid mixing conditions on a clay suspension.  $\square$  represents mixing at 500 rpm for 2.25 min. while  $+$  represents mixing at 250 rpm for 1 min. Other conditions—temperature: 5°C, flocculation at 60 rpm

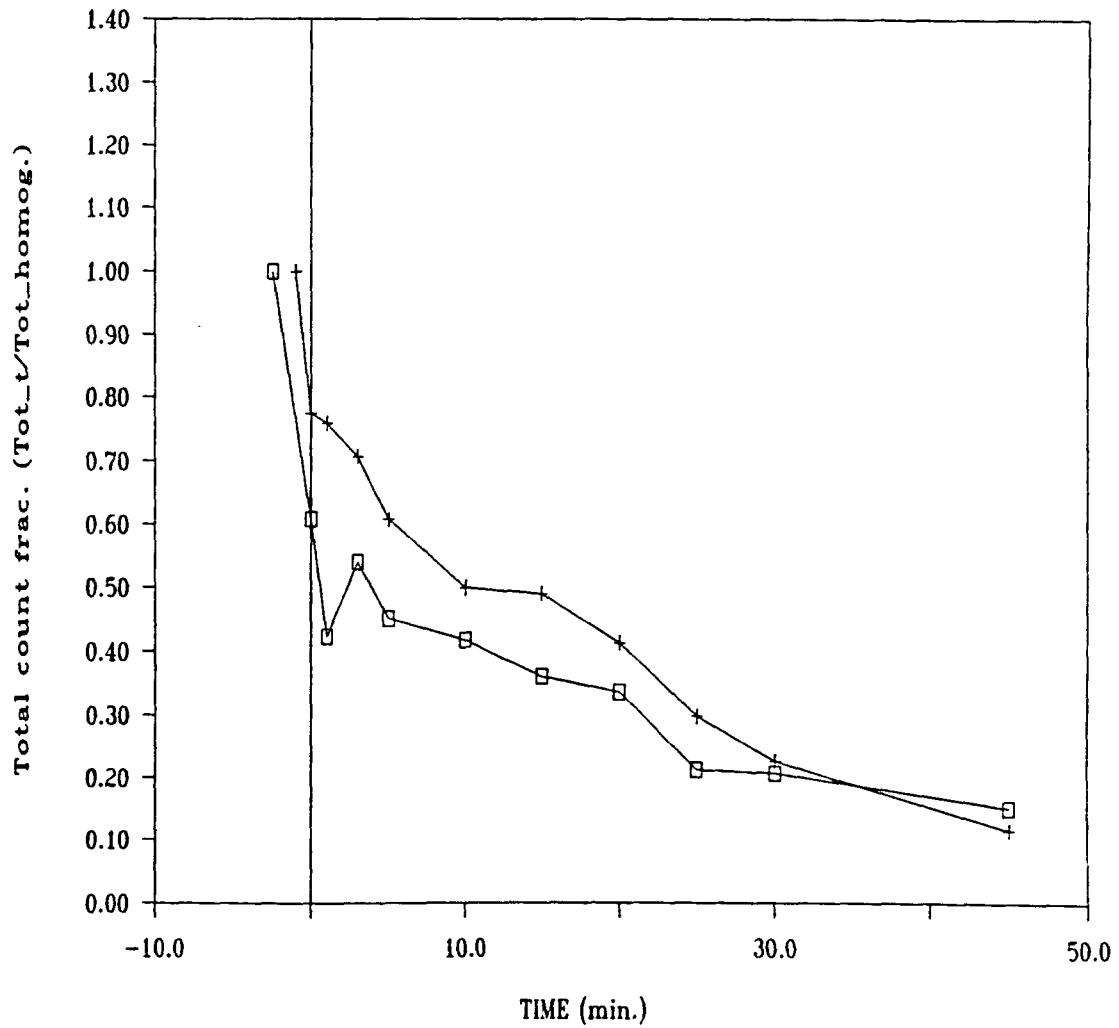


Figure 5.20: Comparison of experiments 'PA' and 'PB' to identify the influence of rapid mixing conditions on a clay suspension. □ represents mixing at 500 rpm for 2.25 min. while + represents mixing at 250 rpm for 1 min. Other conditions—temperature: 20°C, flocculation at 60 rpm

adhered. Intense rapid mixing was not only able to shear such polymer lumps into dispersed polymers, it also was able to reduce the scale of segregation (see Section 3.7.) much more rapidly to much smaller levels than mixing at 250 rpm, producing a much superior distribution of polymeric coagulants in the suspension. We must remember that the molecular weights of such polymeric species are extremely large and thus, their diffusion coefficients, would be extremely small. This implies that we would need to assist the polymers by using intense turbulence to disperse them to as fine a scale as possible so that we do not have to depend as much on their ability to diffuse and therefore form a uniform solution at the molecular level. These well dispersed polymer molecules are not only able to destabilize the colloids in an improved fashion, the higher turbulent intensity provides superior transport of these destabilized colloids, causing them to *flocculate* even during the rapid mixing period.

The question to ask would be why these flocs do not break up in the same manner as the alum flocs do, when subject to such intense mixing conditions? This is because the polymers form much stronger flocs than hydrolyzed metal coagulants.

It must be added that these explanations concerning the superior behavior of polymer rapid mixed at 500 rpm are conjectures which need to be verified with further experiments.

### **5.1.3. Comparing rapid mixing of alum and Magnifloc 573C polymer**

Having seen the impact of rapid mixing conditions on both, alum and Magnifloc 573C polymer, we now compare the response of these two coagulants. Shown in Figure 5.21 are the conditions at which the various experiments were conducted. It is actually a combination of Figures 5.1 and 5.15 to make comparisons easy. The

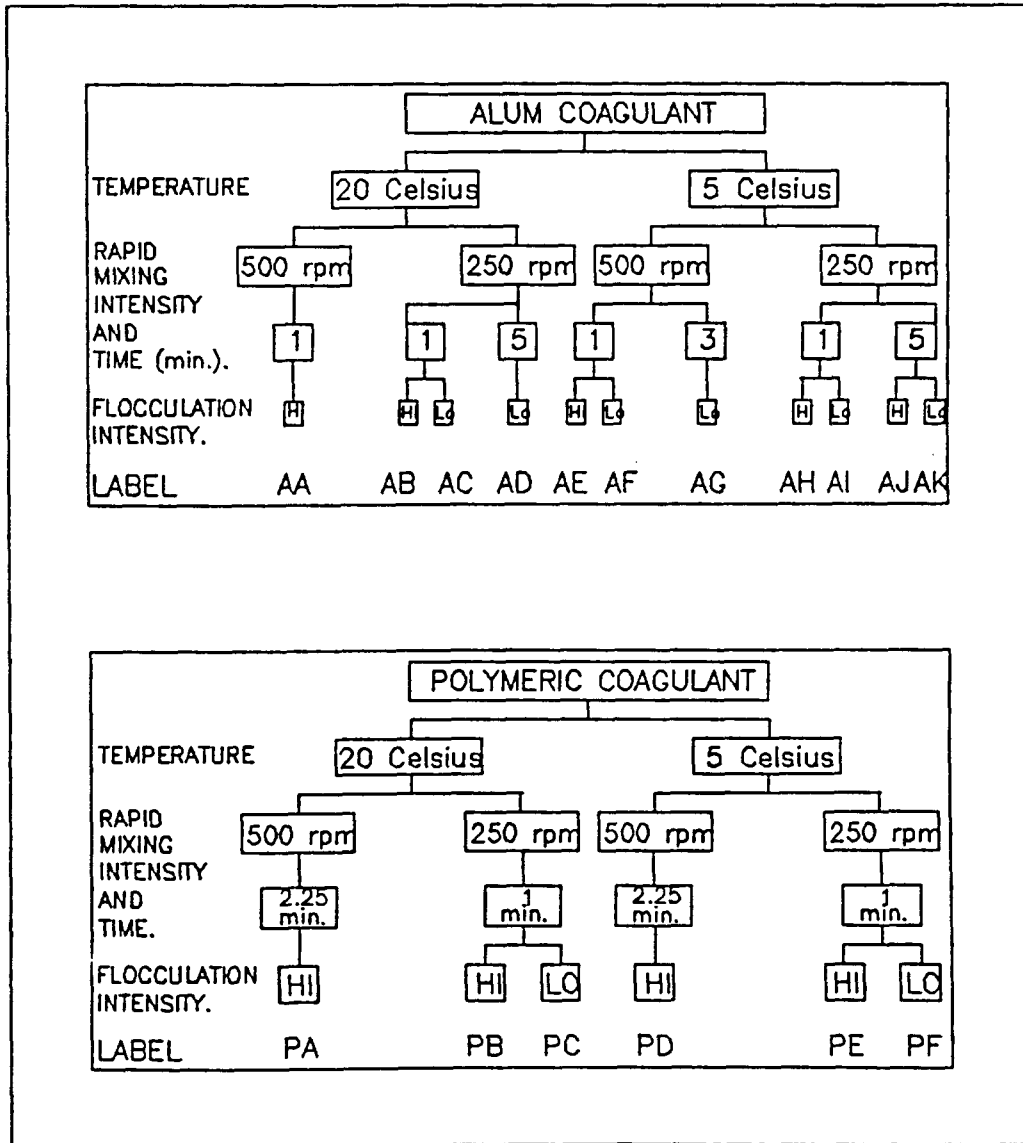


Figure 5.21: Experimental plan involving alum and Magnifloc 573C polymer. 'Hi' and 'Lo' flocculation intensities correspond to 60 and 30 rpm respectively. Samples in all of these experiments were collected and analyzed in the deep sample cells



Table 5.3: List of experiments to compare the response of alum and Magnifloc 573C under different rapid mixing conditions

Comparison
AI-PF
AH-PE
AC-PC
AB-PB
AG-PD

comparisons being made are listed in Table 5.3.

Figures 5.22, 5.23, 5.24, 5.25 and 5.26 show results of experiments conducted under similar rapid mixing conditions. Our objective here is to compare the manner in which the two coagulants are influenced by the rapid mixing conditions and the subsequent flocculation.

Figures 5.22 and 5.23 were conducted under the same set of rapid mixing conditions (250 rpm for 1 min., at 5°C—see Figure 5.21) the only difference being the flocculation intensity. We see that in Figure 5.22, corresponding to the low flocculation intensity, the initial stages of flocculation show alum as being inferior to the polymer, in terms of the total count fraction. However, as time is allowed to elapse, alum quickly surpasses the performance of the polymer and this superiority is maintained thereafter. In case of the experiment involving a higher flocculation intensity (Figure 5.23), exactly the same behavior is displayed except that the ‘overtaking’ by alum occurs at a much earlier stage.

In neither case do we see a remarkable change in the total count fraction at  $t = 0$ , meaning that, perhaps, not much flocculation of the clay particles occurs

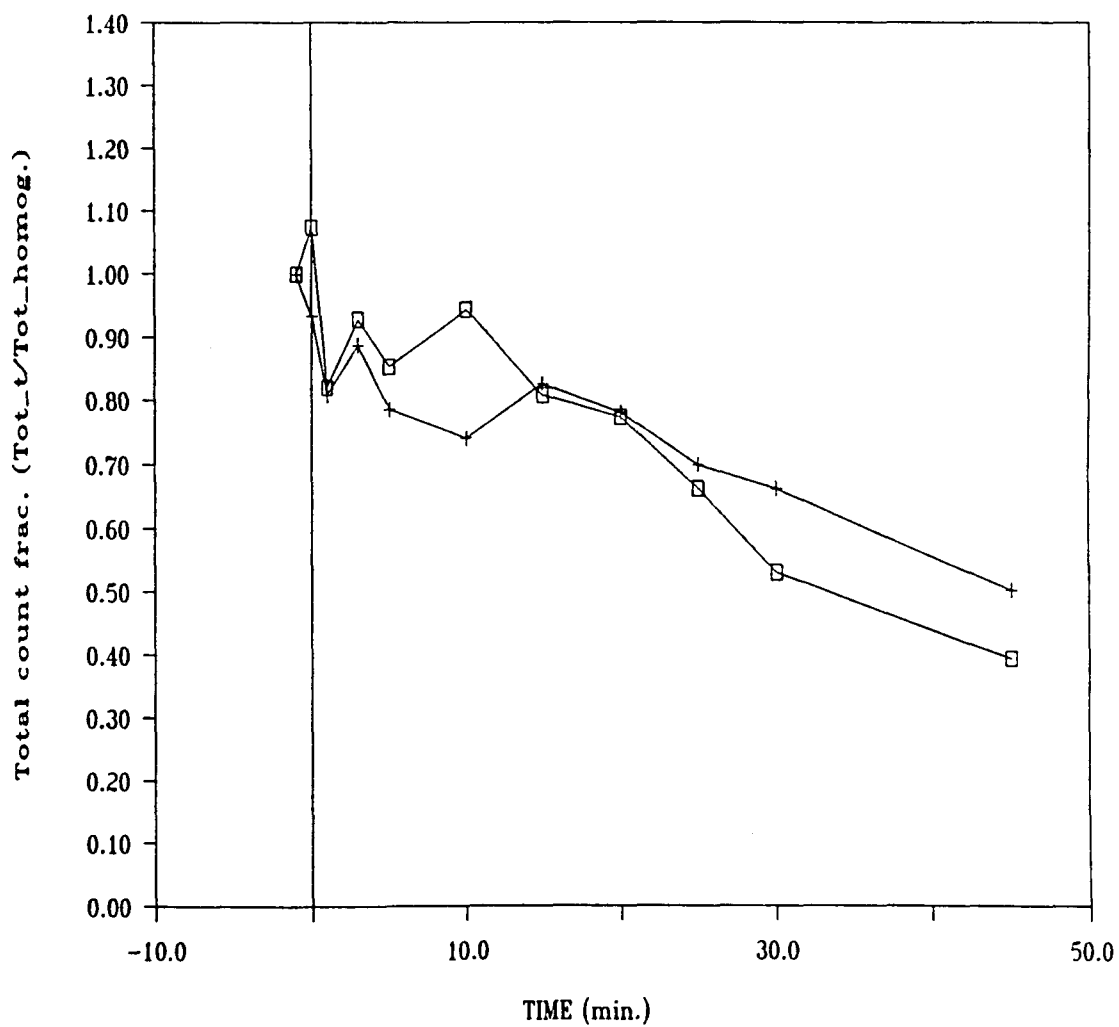


Figure 5.22: Comparing alum (experiment 'AI') and Magnifloc 573C (experiment 'PF'). □ represents alum and + represents Magnifloc 573C. Experimental conditions—mixing: 250 rpm for 1 min., temperature: 5°C, flocculation at 30 rpm

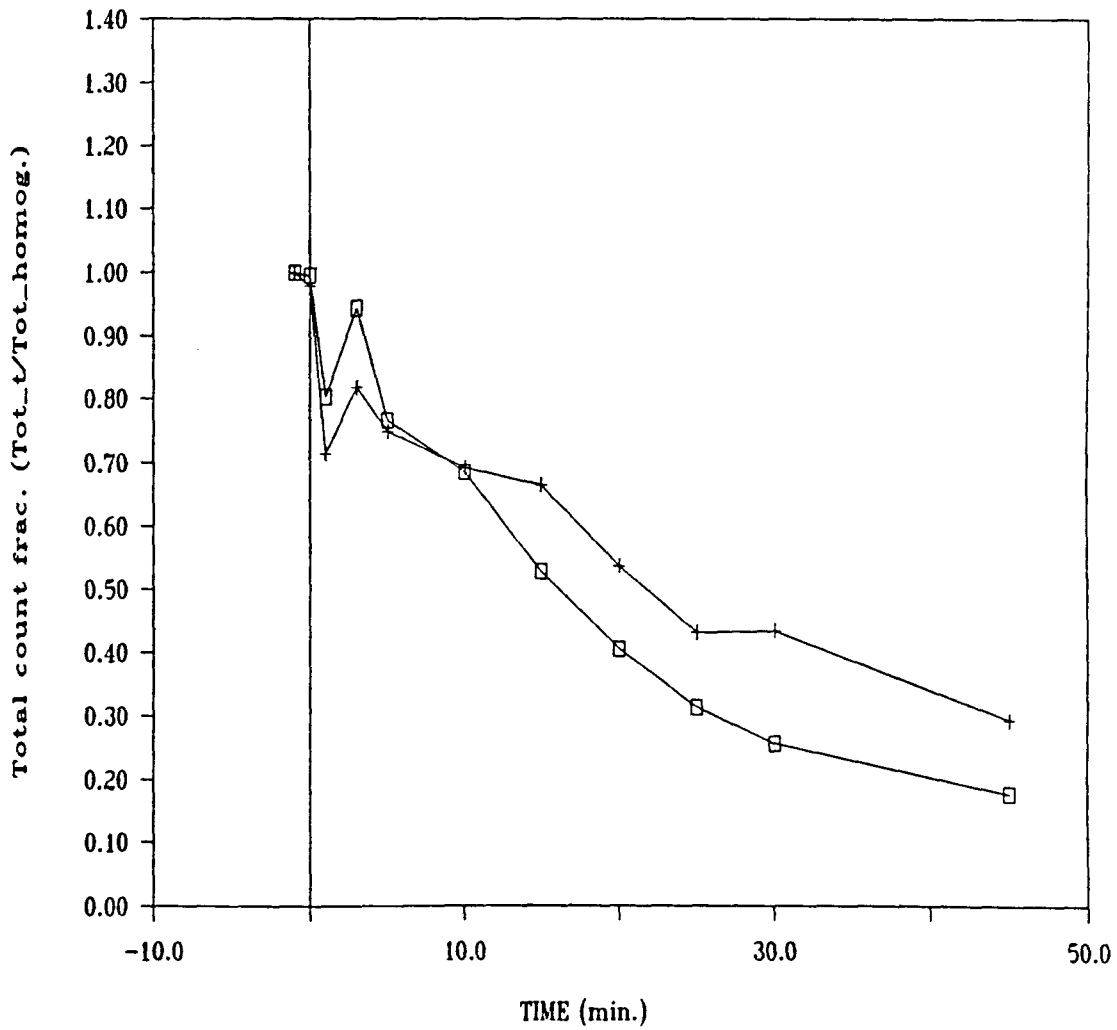


Figure 5.23: Comparing alum (experiment 'AH') and Magnifloc 573C (experiment 'PE'). □ represents alum and + represents Magnifloc 573C. Experimental conditions—mixing: 250 rpm for 1 min., temperature: 5°C, flocculation at 60 rpm

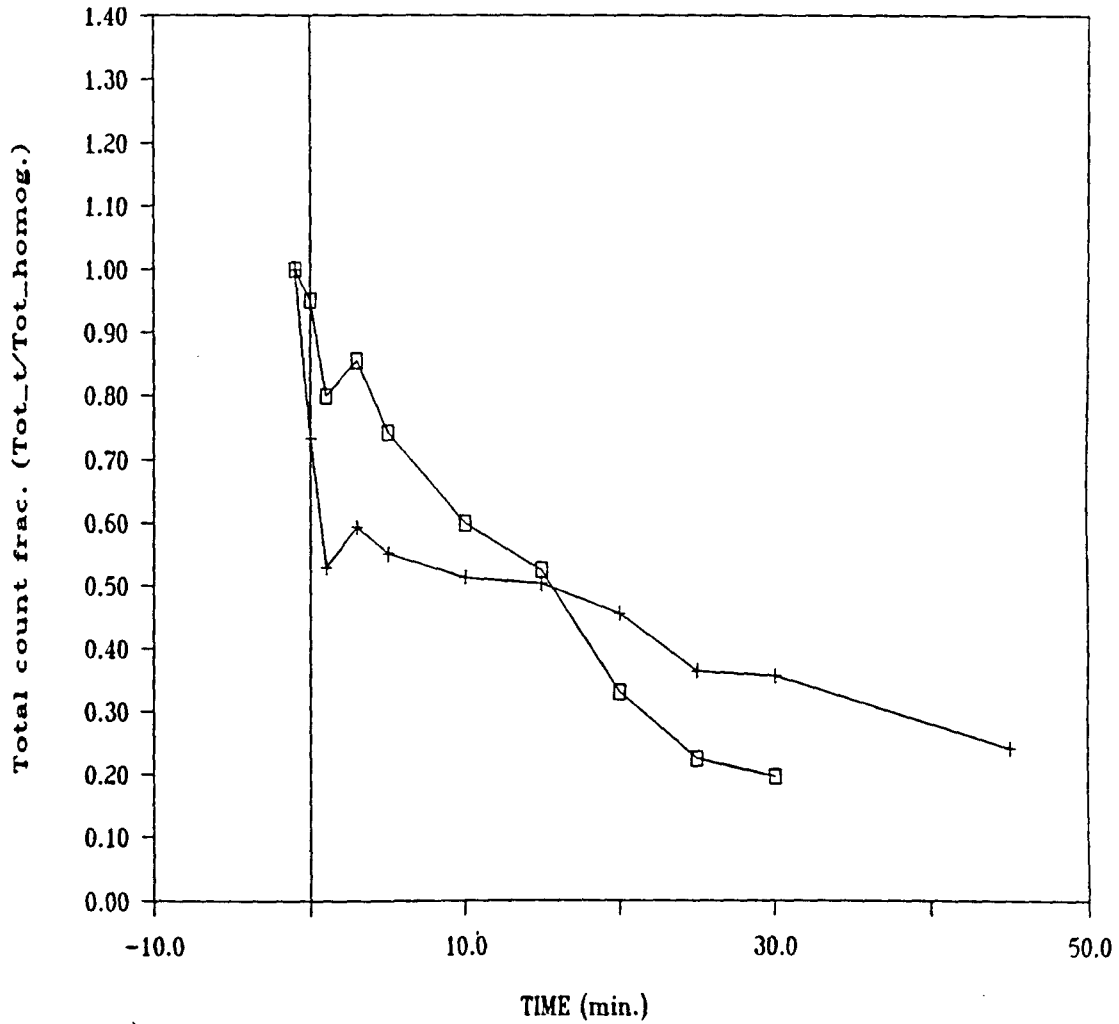


Figure 5.24: Comparing alum (experiment 'AC') and Magnifloc 573C (experiment 'PC'). □ represents alum and + represents Magnifloc 573C. Experimental conditions—mixing: 250 rpm for 1 min., temperature: 20°C, flocculation at 30 rpm

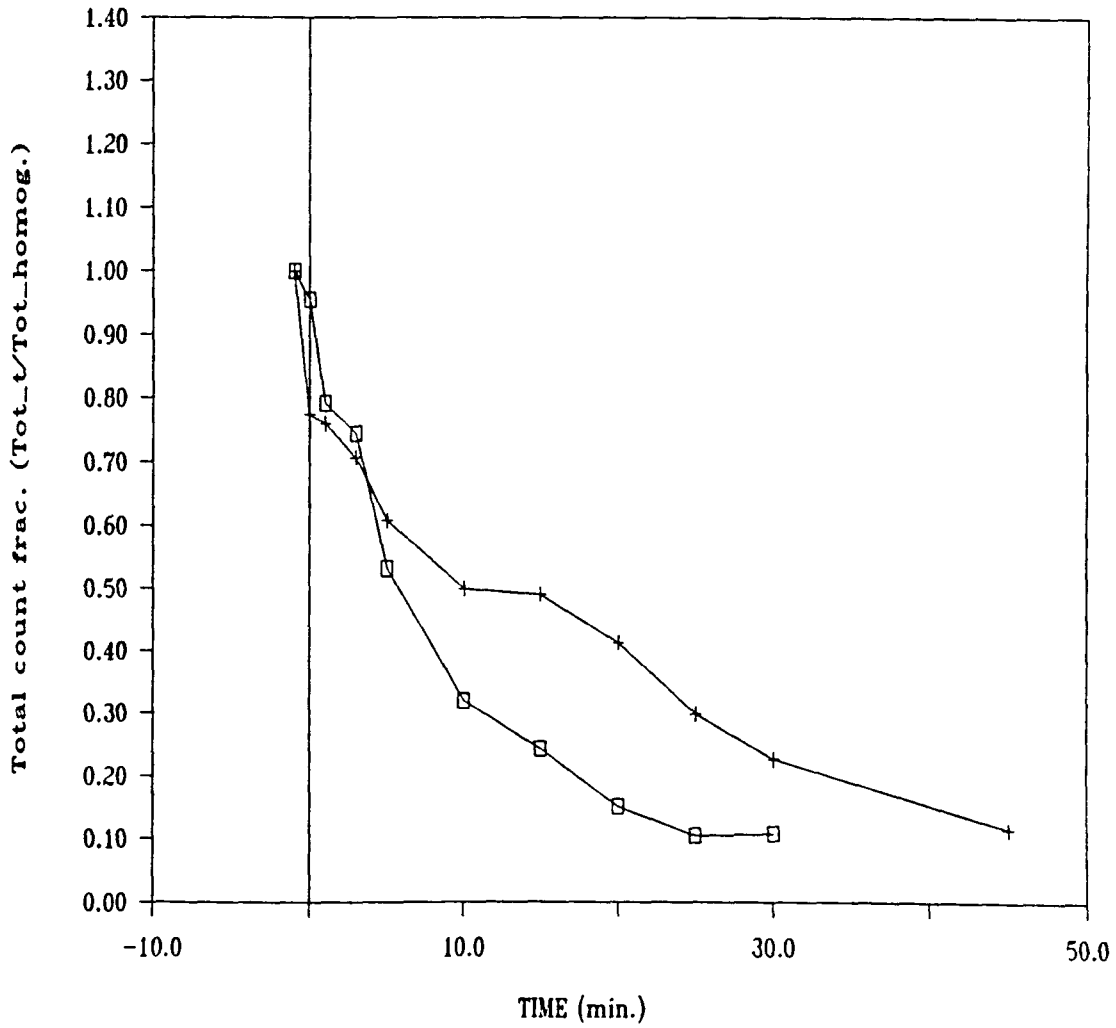


Figure 5.25: Comparing alum (experiment 'AB') and Magnifloc 573C (experiment 'PB'). □ represents alum and + represents Magnifloc 573C. Experimental conditions—mixing: 250 rpm for 1 min., temperature: 20°C, flocculation at 60 rpm

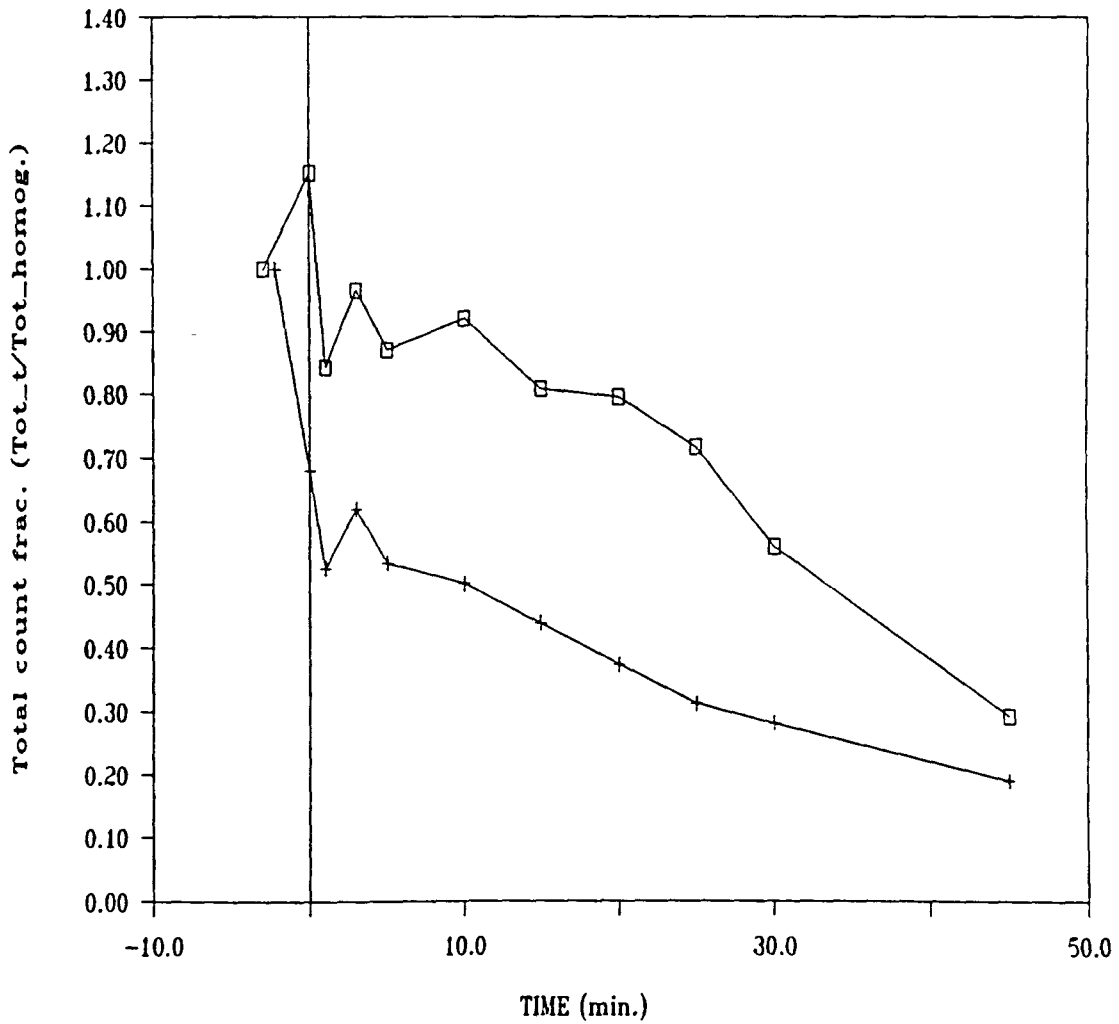


Figure 5.26: Comparing alum (experiment 'AG') and Magnifloc 573C (experiment 'PD'). □ represents alum—mixed for 3.0 min., + represents Magnifloc 573C—mixed for 2.25 min. Experimental conditions—mixing: 500 rpm, temperature: 5°C, flocculation at 60 rpm

during the rapid mixing period under the conditions of these experiments.

If, however, we go to Figures 5.24 and 5.25, all of which were conducted under the same set of rapid mixing conditions (250 rpm for 1 min., at 20°C—see Figure 5.21) with 30 and 60 rpm of flocculation, respectively; we see that by  $t = 0$ , there is a marked reduction—20%–30%—in the total count fraction for Magnifloc 573C. However, the alum samples show no such drastic changes. Surprisingly, this ‘lead’ which the polymers have over alum (in terms of reduction of the total count fraction) is quickly lost, as is evident in both these figures.

Why does this happen? As was apparent in these experiments, samples coagulated using Magnifloc 573C always seemed to have—even after 30 or 45 minutes of flocculation—a large number of small, unflocculated particles coexisting with much larger floc. This, however, was not true for samples coagulated using alum. This difference seems to be due to the fact that the destabilizing species formed when alum is hydrolyzed are much smaller in size than the polymer molecules. Their smaller size, and the correspondingly higher numbers and high diffusivities, would make alum much more efficient in rapidly destabilizing *all* clay particles, once turbulence has helped the process of diffusion by dispersing alum quickly throughout the reactor. This is not completely true of the polymeric coagulant Magnifloc 573C. As long as turbulent flow exists in the reactor, the polymers will be well dispersed throughout the reactor. However, given their comparatively smaller molecular diffusivities, it seems that the adsorption of the polymers onto clay particles occurs predominantly through the relative movement between the clay particles and the polymer molecules, as induced by turbulent flow. One can think of this process as occurring through *collisions between polymer molecules and clay particles*. Since

larger clay particles, because of their ability to sweep through larger regions of the fluid (larger particles present a larger frontal area—i.e., area of sweep—than smaller particles), the larger clay particles would gather most of the polymers and, therefore, be better ‘destabilized’ than smaller clay particles. Therefore, some small clay particles are not as well destabilized and remain in suspension even at the end of the flocculation period.

In the case of alum, all particles have been destabilized more or less uniformly and so, collisions between all these destabilized particles should result in flocculation. As this flocculation continues for much longer durations of time, the larger flocs sweep through the suspension, gathering the smaller destabilized particles and growing. This would result in the formation of still larger flocs and a corresponding reduction in the total count fraction. In the case of Magnifloc 573C, the clay particles which have been destabilized by the polymers also interact with each other and form larger particles or flocs. However, when these larger flocs ‘sweep’ through the suspension, the smaller clay particles they encounter are not destabilized properly and so, these smaller particles do not get attached to the larger flocs as easily as it would happen in suspensions destabilized using alum. This, perhaps, is why the suspensions coagulated using alum show a much smaller total count fraction towards the end of the flocculation period than evidenced by suspensions coagulated using Magnifloc 573C.

This would make us think that a suspension being coagulated using Magnifloc 573C, which has been rapid mixed at a much higher turbulence intensity, should show superior performance. With this in mind, we turn to Figure 5.26. If we check with Figure 5.21, we notice that while all other conditions of these experiments are



similar, there is a slight difference in the period of their rapid mixing: 'AG' was rapid mixed for 3.0 min. while 'PD' was rapid mixed for 2.25 min. If we ignore this little difference of 0.75 min., the two experiments can be thought of as being identical in all respects—except for the difference in the coagulants being used to coagulate the suspensions. We see that, surprisingly enough, the polymer performs *better* than alum! We see a marked reduction in the total count fraction in the suspension coagulated with polymer. Is this difference at 5°C because of an improvement in the behavior of Magnifloc 573C or a worsening of the performance of alum? We check Figures 5.18 and 5.19 and conclude that it is not an improvement in the behavior of the polymer that has caused this immense difference in the response visible in Figure 5.26. In fact, the performance of the polymer at 5°C is inferior to its performance at 20°C! It is a worsening of alum's performance at 500 rpm and 5°C that is responsible for the difference. The reasons for the deterioration of alum's behavior have already been identified earlier in the chapter and will not be repeated here.

In conclusion, we can say that at low rapid mixing intensities, alum performs much better than polymers at both, warm and cold water temperatures. However, in situations involving low water temperatures, the use of high rapid mixing intensities results in a decline in the performance of alum but an improvement in the behavior of Magnifloc 573C.

#### **5.1.4. Changes in particle size distribution with rapid mixing**

We have, thus far, discussed the influence of various rapid mixing conditions on the flocculation of clay suspensions by gaging, for each experiment, the variation

in the total count fraction as a function of time while the suspension is undergoing flocculation. In these experiments, we concluded that rapid mixing, in fact, begins to flocculate the destabilized colloids.

If such a phenomenon is actually occurring, we should also be able to detect remarkable changes in the particle size distribution of these suspensions during the rapid mixing process. This subsection presents evidence to this effect.

Figure 5.27 shows the experiments conducted in which samples were collected specifically for the identification of changes in the particle size distribution due to rapid mixing. This is the same set of experiments as identified in Figure 5.1 except that flocculation of the suspension does not enter the picture at all. In addition to that difference, we have two other differences: (1) In all the experiments, the samples were collected and analyzed in the shallow sampling cells so as to avoid the problems of the type mentioned on page 227 (where particles which were not counted in the homogenized samples grew into the range of detection of the image analysis system, after being rapid mixed), and also to make easier the detection of any differences in the particle size distribution following rapid mixing. (2) One experiment was conducted at 5°C in which rapid mixing was carried out at 340 rpm (with the attempt at keeping the Kolmogorov microscale the same as in experiments conducted at 20°C with mixing at 250 rpm) for a duration of 1 minute.

As usual, each experimental condition has been labelled for easy identification. And, the various comparisons to be made in order to distinguish the influence of different rapid mixing conditions on the particle size distribution of the clay suspension during the rapid mixing, have been identified in Table 5.4. Unfortunately, in the experiments involving polymers, such samples were never collected and so, all

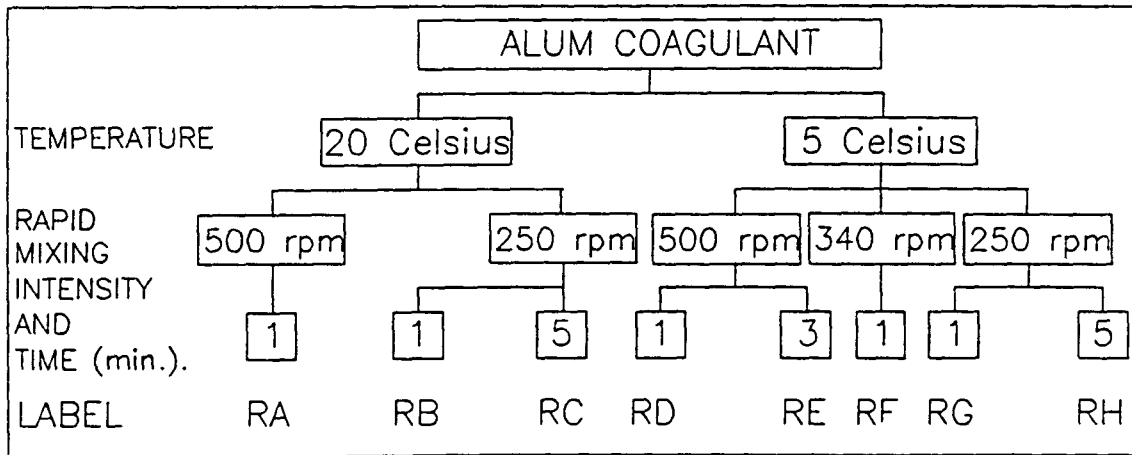


Figure 5.27: Experimental plan for detection of changes in the particle size distribution of clay suspensions during rapid mixing with alum. Samples were collected and analyzed in the shallow sampling cells

Table 5.4: List of experiments to be compared to identify the influence of various rapid mixing conditions on the particle size distribution of the clay suspensions using alum

Variable	Comparison
Temperature	RA-RD
	RB-RG
	RC-RH
Intensity	RA-RB
	RD-RF-RG
Time	RB-RC
	RD-RE
	RG-RH

the comparisons shown here will be based solely on the use of alum as a coagulant.

**5.1.4.1. Temperature Effects** Based on our experiments identified in Figures 5.2, 5.4 and 5.5, we know that rapid mixing has little impact on the total count fraction and therefore, there must not be a marked difference in the particle size distribution between the homogenized and rapid mixing clay suspensions. This is borne out by Figures 5.28 and 5.29. In these figures, the percentage of total particle count/ml is plotted as a function of the geometric mean diameter ( $\mu\text{m}$ ) of a circular disk equal in area to the projected area of the particles—which is what the AIA system detected. In Figure 5.28, if we look closely at the data points corresponding to 2.94 and 4.35  $\mu\text{m}$ , we can see a larger change at 20°C than at 5°C. However, it is doubtful if these differences could be considered significant. A similar trend is apparent in Figure 5.29.

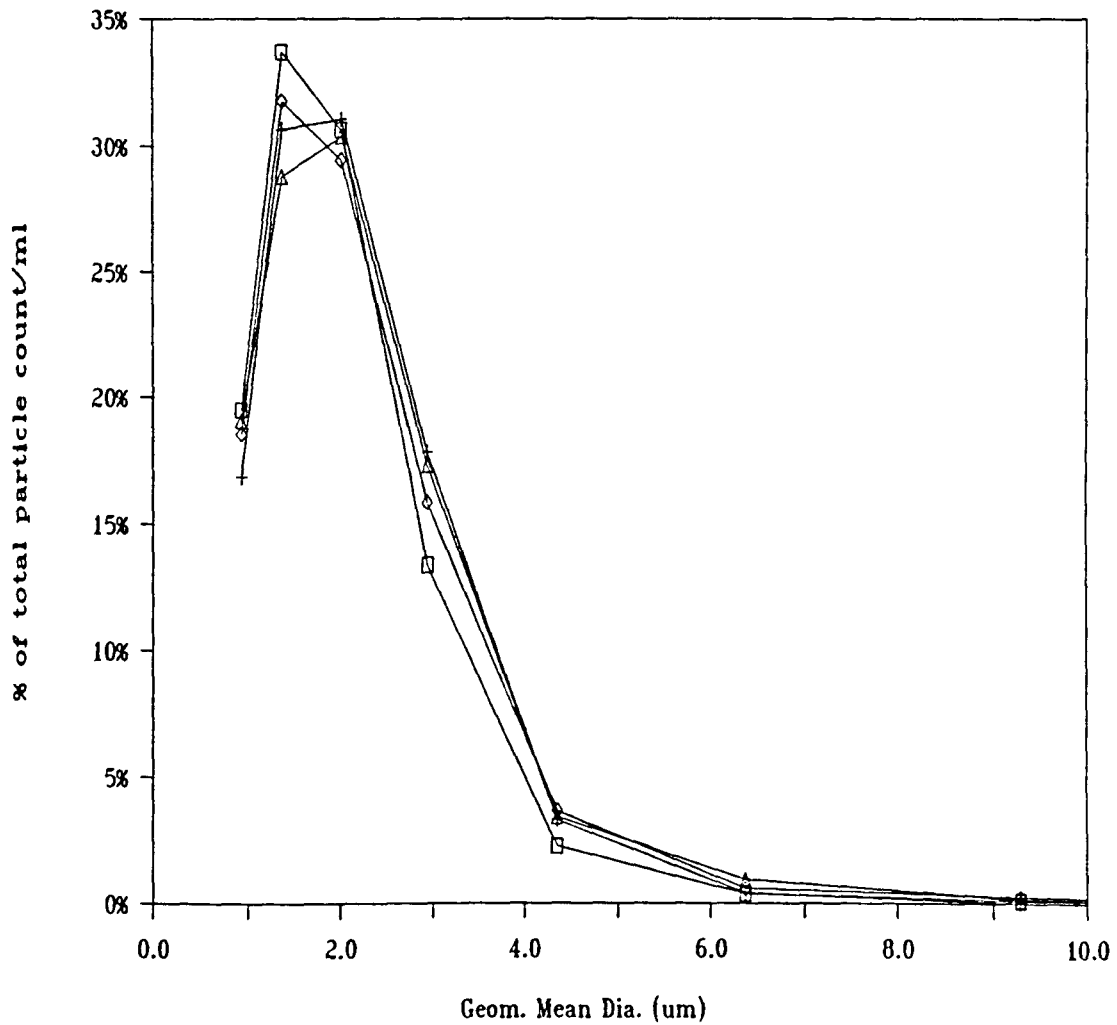


Figure 5.28: Influence of temperature on changes in particle size distribution due to rapid mixing. Experiments compared are 'RA' and 'RD'.  $\square$  homogenized samples at 20°C, + rapid mixed sample at 20°C,  $\diamond$  homogenized sample at 5°C,  $\triangle$  rapid mixed sample at 5°C. Rapid mixing conducted at 500 rpm for 1 minute

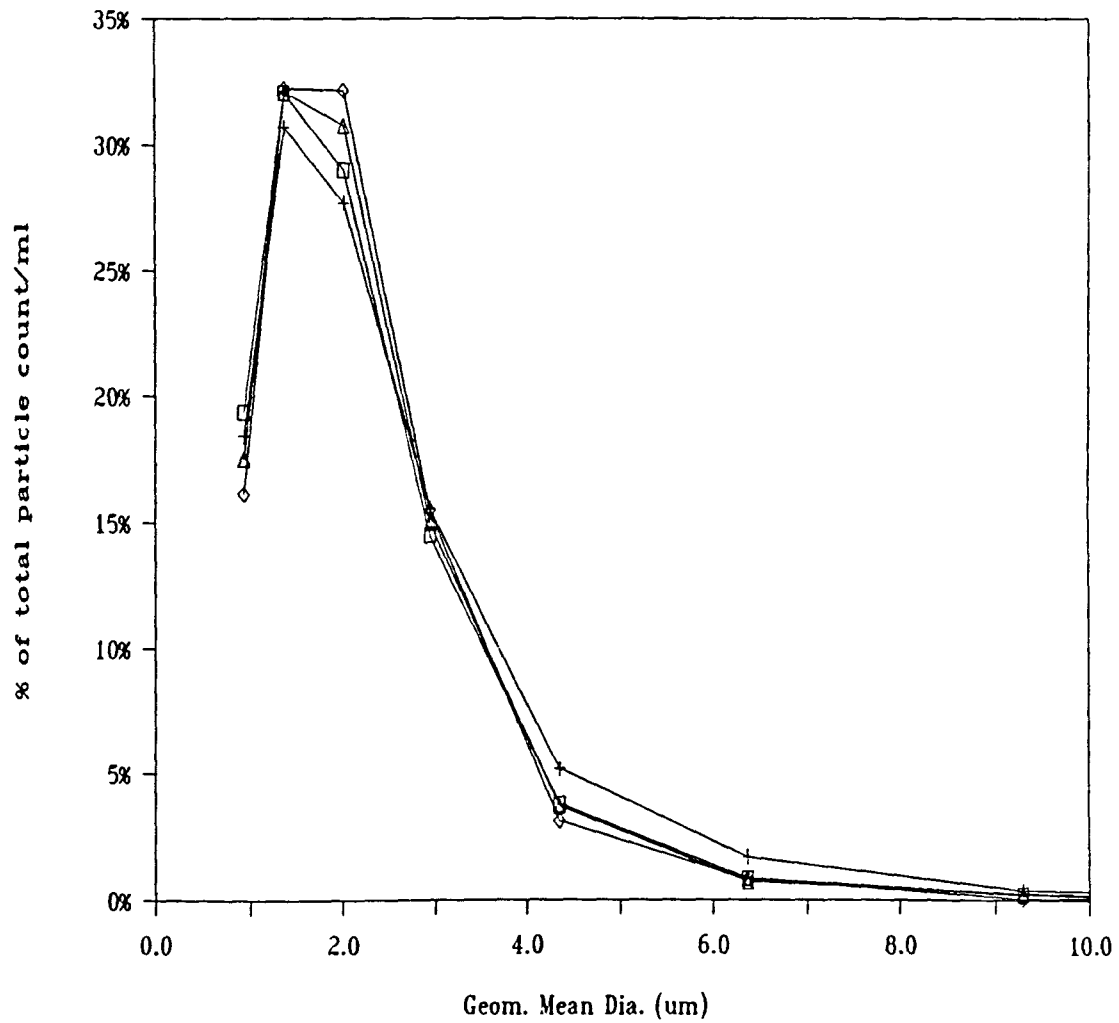


Figure 5.29: Influence of temperature on changes in particle size distribution due to rapid mixing. Experiments compared are 'RB' and 'RG'. □ homogenized samples at 20°C, + rapid mixed sample at 20°C, ◇ homogenized sample at 5°C, △ rapid mixed sample at 5°C. Rapid mixing conducted at 250 rpm for 1 minute

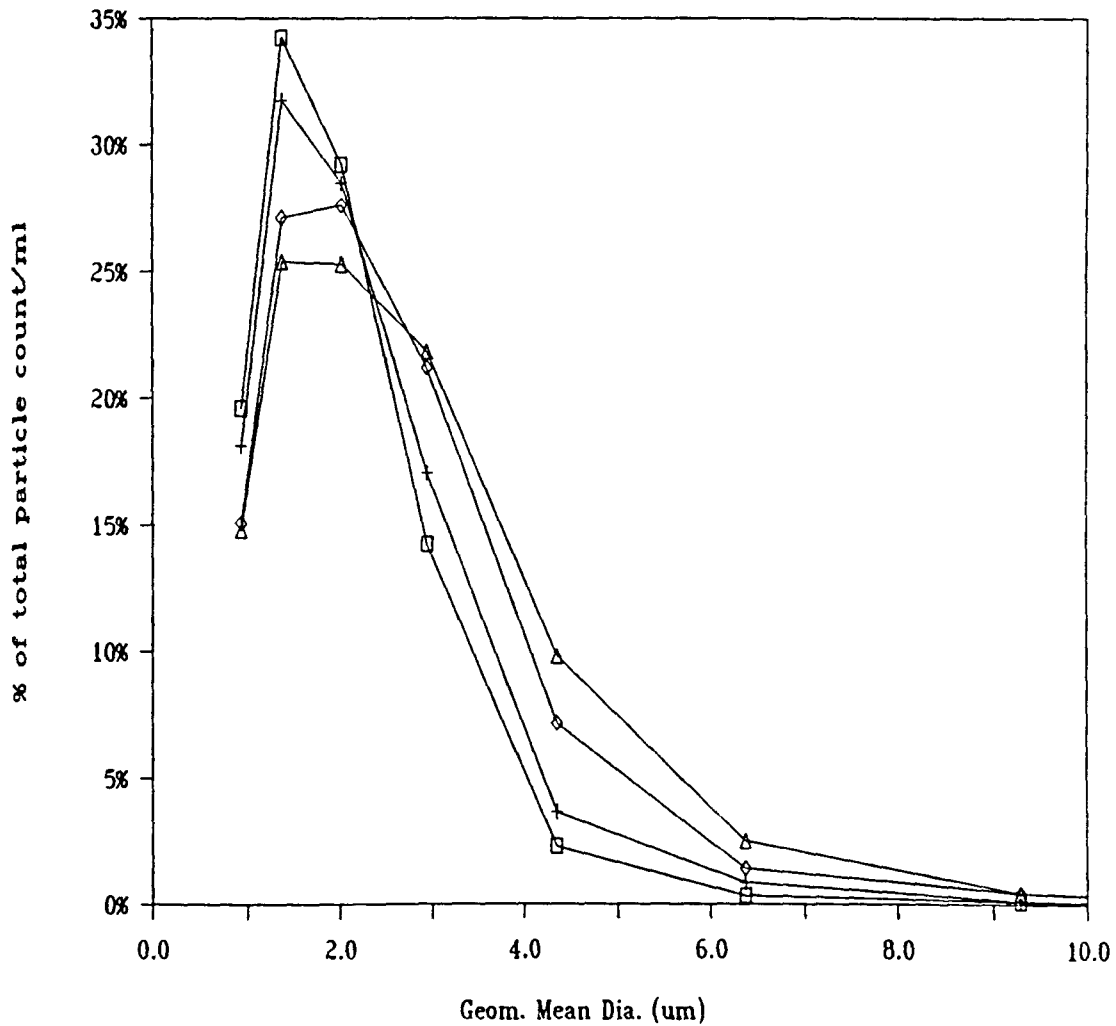


Figure 5.30: Influence of temperature on changes in particle size distribution due to rapid mixing. Experiment 'RC' with rapid mixing at 250 rpm for 5 min. at 20°C. □ homogenized, + 1 min., ◇ 3 min., and △ 5 minutes of rapid mixing

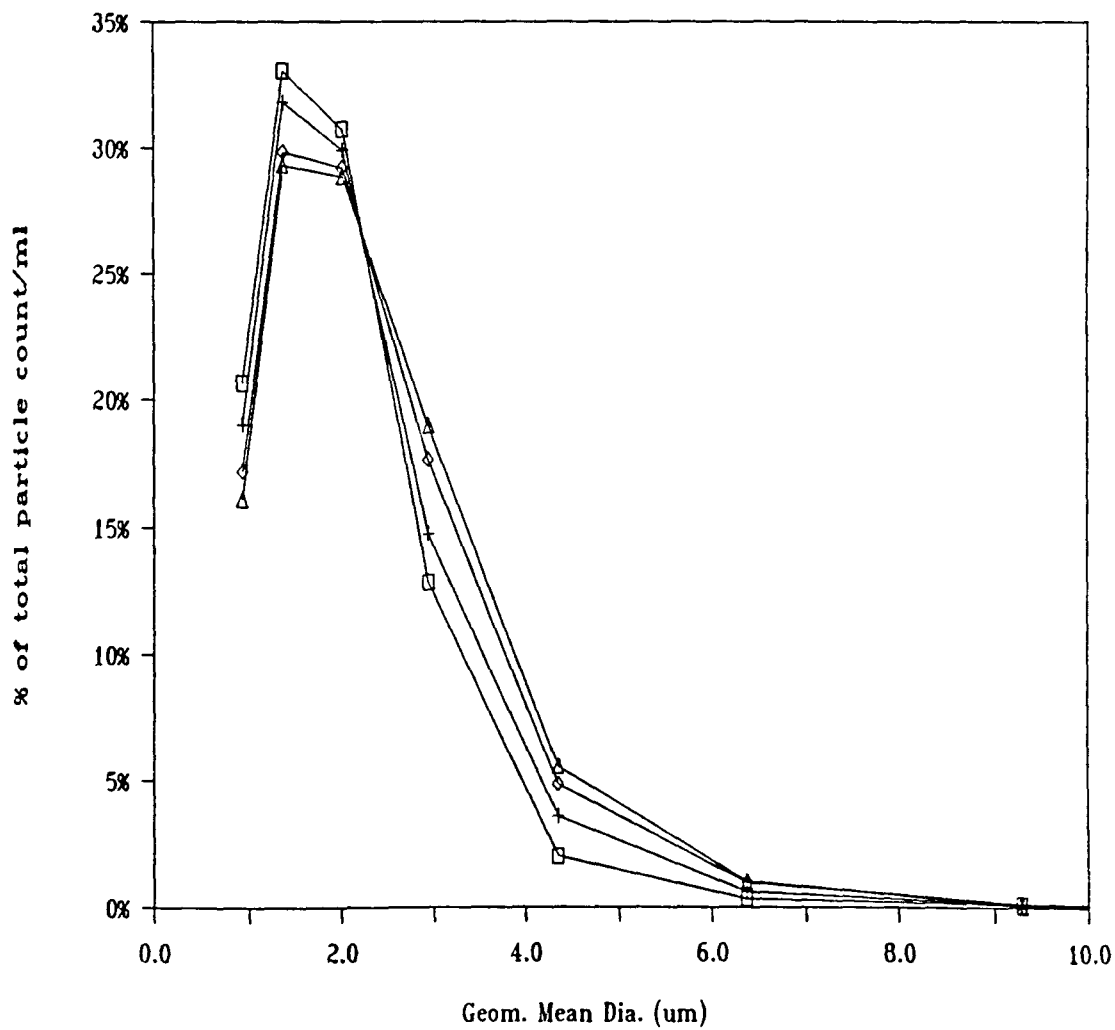


Figure 5.31: Influence of temperature on changes in particle size distribution due to rapid mixing. Experiment 'RH' with rapid mixing at 250 rpm for 5 min. at 5°C. □ homogenized, + 1 min., ◇ 3 min., and △ 5 minutes of rapid mixing



If we now turn to Figures 5.30 and 5.31 with extended rapid mixing—the former corresponds to 20°C and the latter to 5°C—we see a marked change in the particle size distribution as a function of time. Not only that, we can see that the changes are much more pronounced at 20°C than at 5°C. This is identical to our observations in Figure 5.3, at  $t = 0$ .

We can conclude, therefore, that rapid mixing, indeed, does flocculate particles and that a reduction in temperature causes a decline in the growth of particles.

**5.1.4.2. Intensity Effects** Figures 5.32 and 5.33 show results of experiments designed to detect the influence of rapid mixing intensity on the particle size distribution.

Figure 5.32 is the plot of the particle size distribution corresponding to  $t = 0$  of Figure 5.6, where we saw no marked changes in the total count fraction. Here, in Figure 5.32, we see precisely that—no marked changes in the particle size distributions. However, we can definitely note that the sample mixed at 250 rpm has a greater amount of the large sized particles than the one rapid mixed at 500 rpm. Whether these differences are significant is, however, is open to question.

Figure 5.33 compares rapid mixing at 3 different intensities at 5°C (... and it looks like a total mess!). We have already seen that alum does not perform well at 5°C. This figure does not show much—except the point that at 5°C, all of the 3 mixing conditions produce equally bad results, in terms of changes in the particle size distribution of the clay because of rapid mixing.

In conclusion, one can say that while a reduction in rapid mixing intensity at 20°C may help grow particles somewhat, at 5°C, rapid mixing seems to cause little

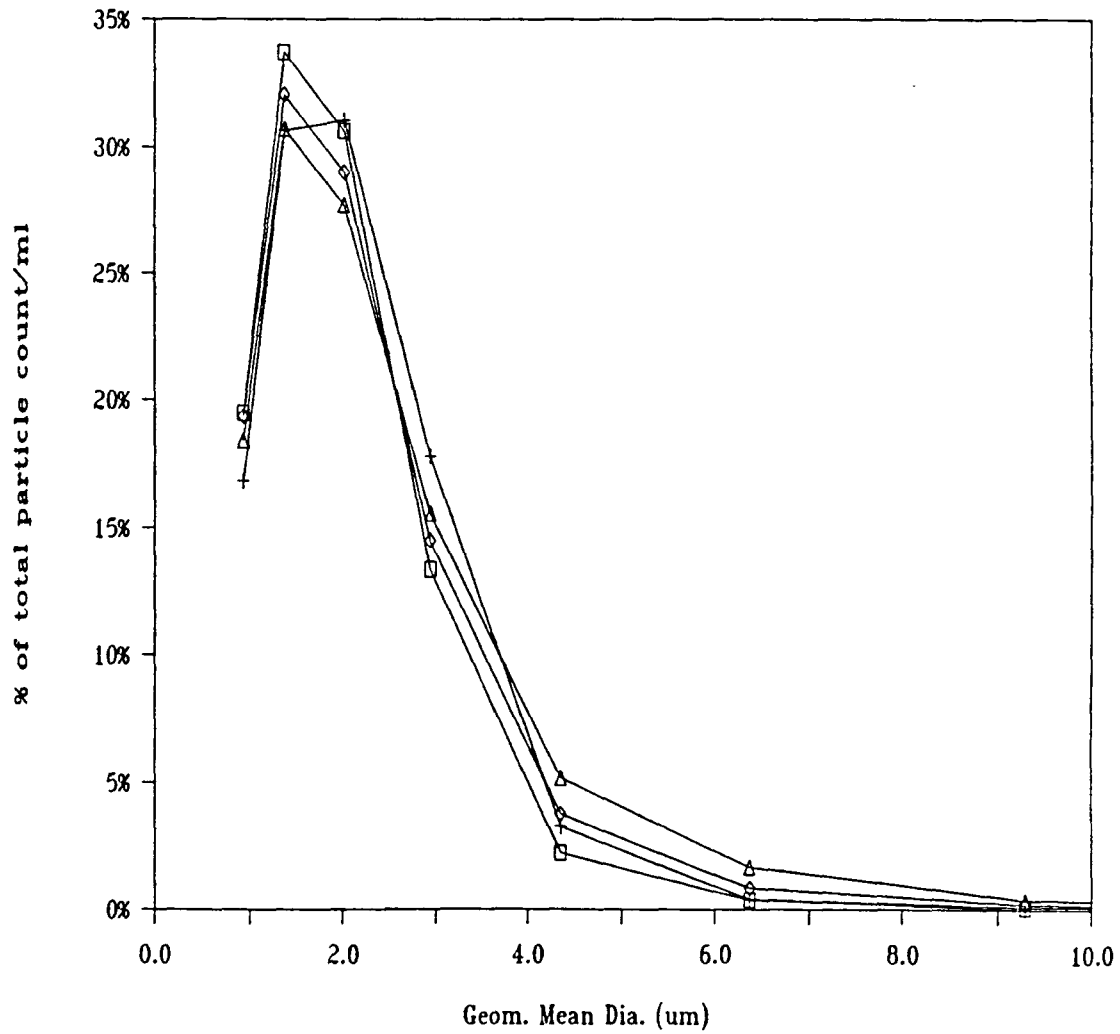


Figure 5.32: Influence of mixing intensity on changes in particle size distribution due to rapid mixing. Experiments compared are 'RA' and 'RB'. □ homogenized sample at 500 rpm, + rapid mixed sample at 500 rpm, ◇ homogenized sample at 250 rpm, △ rapid mixed sample at 250 rpm. Rapid mixing at 20°C for 1 minute

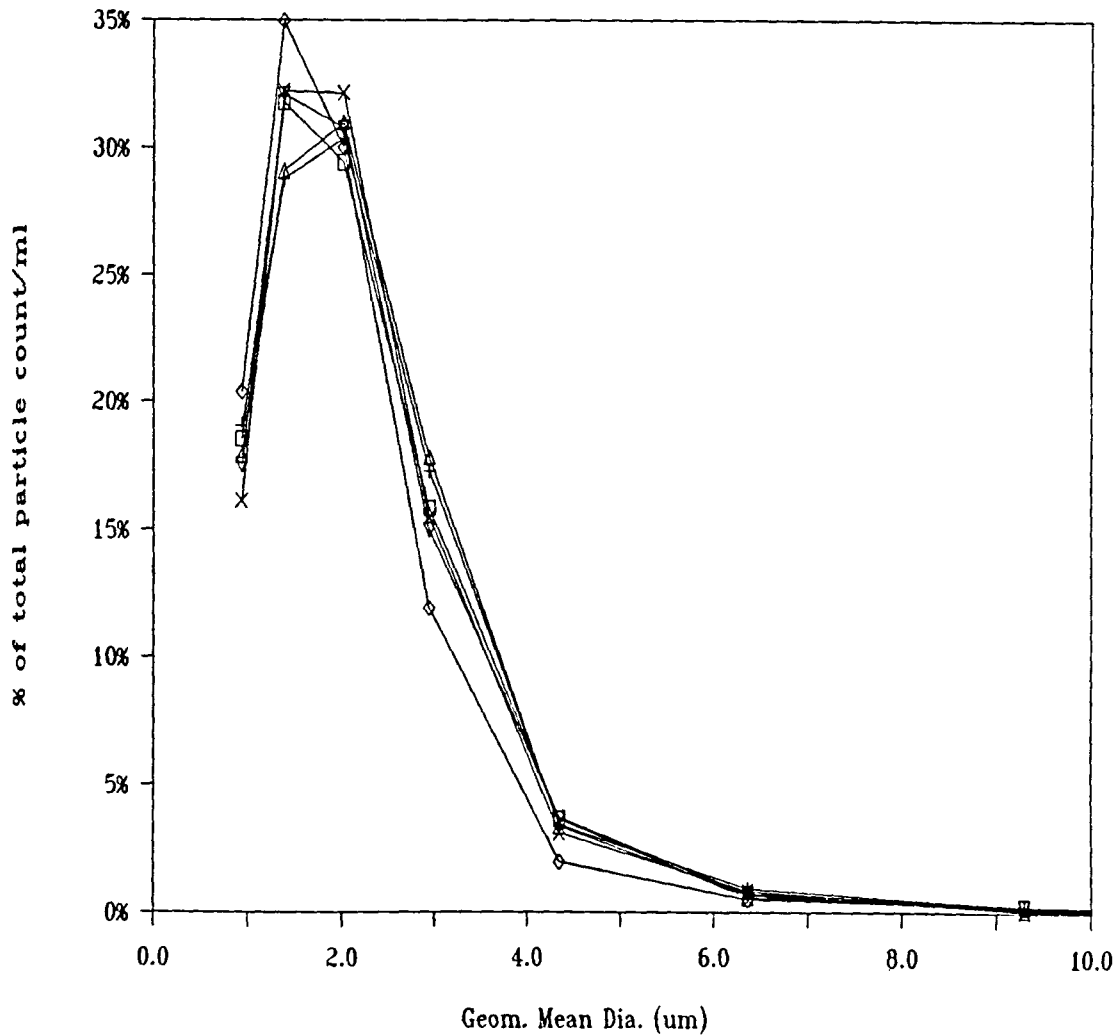


Figure 5.33: Influence of mixing intensity on changes in particle size distribution due to rapid mixing. Experiments compared are 'RD', 'RF', and 'RG'. □ homogenized sample at 500 rpm, + rapid mixed sample at 500 rpm, ◇ homogenized sample at 340 rpm, △ rapid mixed sample at 340 rpm, × homogenized sample at 250 rpm, ▽ rapid mixed sample at 250 rpm. Rapid mixing at 5°C for 1 minute

or no change in the particle size distribution.

**5.1.4.3. Time Effects** Figures 5.34, 5.35 and 5.36 identify the influence of duration of mixing on the changes in the particle size distribution of a clay suspension due to rapid mixing.

We have already seen, in Figure 5.12, that the duration of rapid mixing has very little impact on the total count fraction, at  $t = 0$ , mixed 500 rpm and  $5^{\circ}\text{C}$ . This is also evidenced in Figure 5.34, where there seems to be no discernible difference between the suspension mixed for 1 min. or 3 min.

If we now turn to Figure 5.35, which involves rapid mixing at 250 rpm at  $5^{\circ}\text{C}$ , we see that the use of an extended rapid mixing period makes a visible difference in the particle size distribution of the suspension. This same trend was seen, in terms of total count fraction at  $t = 0$ , in Figures 5.10 and 5.11.

Yet another proof of the impact of duration of rapid mixing is shown in Figure 5.36. We can see that the sample rapid mixed for 5 min. has a large shift in the particle size distribution at the end of the rapid mixing period as compared to the sample rapid mixed for just 1 min. The same trend, in terms of the total count fraction, was seen in Figure 5.9.

To sum up, we can, once again, conclude that rapid mixing, indeed, does flocculate the destabilized colloids and that at lower mixing intensities, extended periods of rapid mixing produce a marked growth of particles—particularly at higher temperatures.

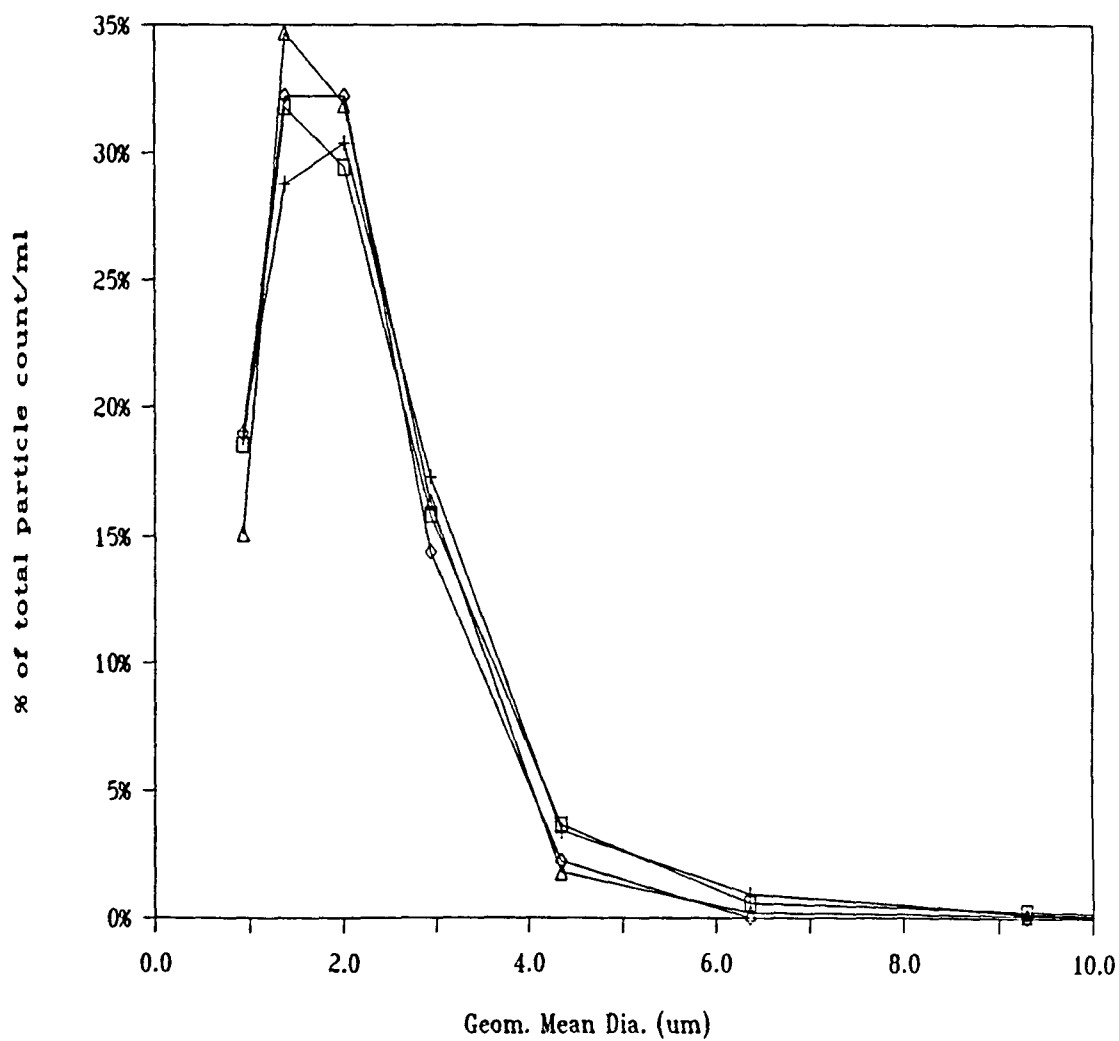


Figure 5.34: Influence of duration of mixing on changes in particle size distribution due to rapid mixing. Experiments compared are 'RD' and 'RE'. □ homogenized sample for 1 min. rapid mix duration, + sample after 1 min. of rapid mixing, ◇ homogenized sample for 3 min. rapid mixing duration, △ sample after 3 min. of rapid mixing. Rapid mixing conducted at 500 rpm and 5°C

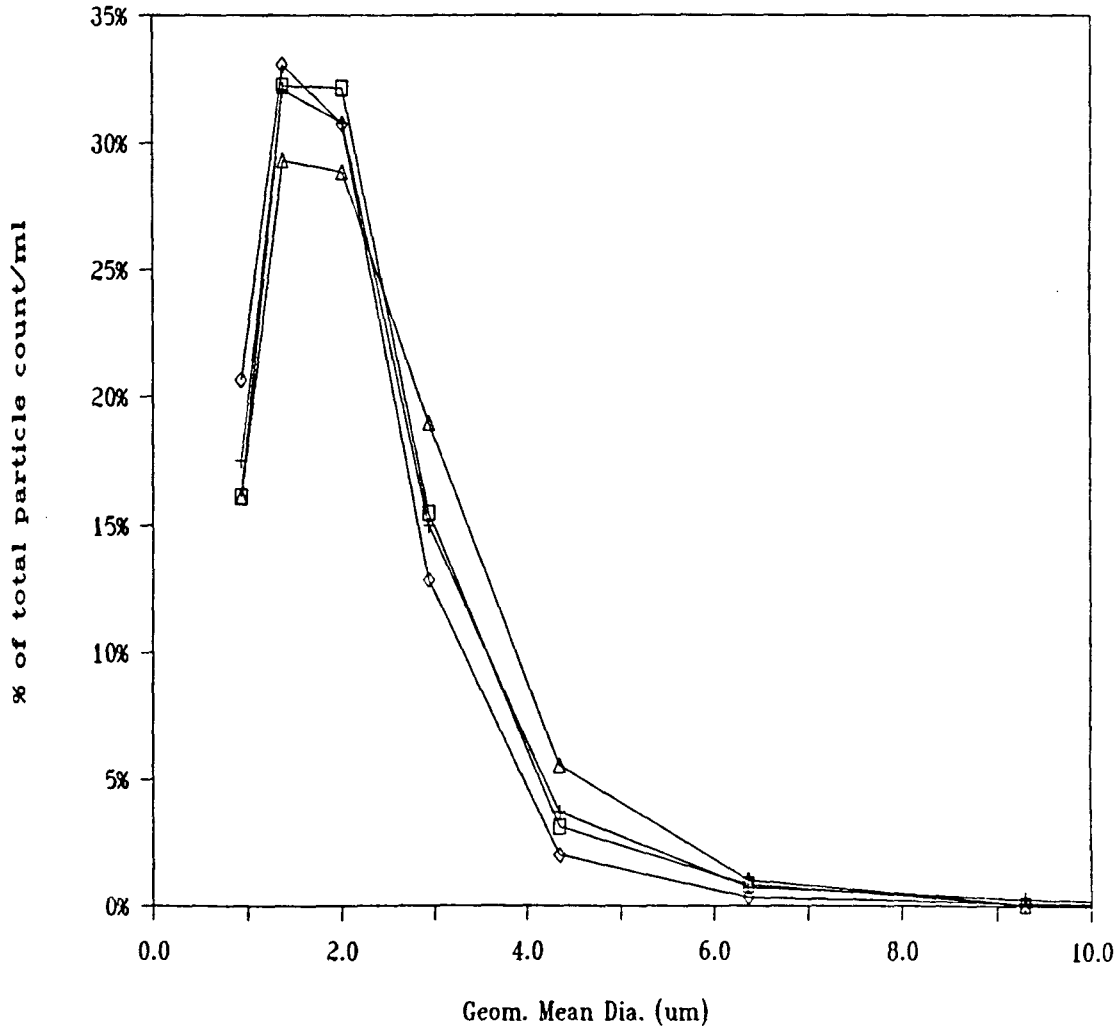


Figure 5.35: Influence of duration of mixing on changes in particle size distribution due to rapid mixing. Experiments compared are 'RG' and 'RH'. □ homogenized sample for 1 min. rapid mix duration, + sample after 1 min. of rapid mixing, ◇ homogenized sample for 5 min. rapid mixing duration, △ sample after 5 min. of rapid mixing. Rapid mixing conducted at 250 rpm and 5°C

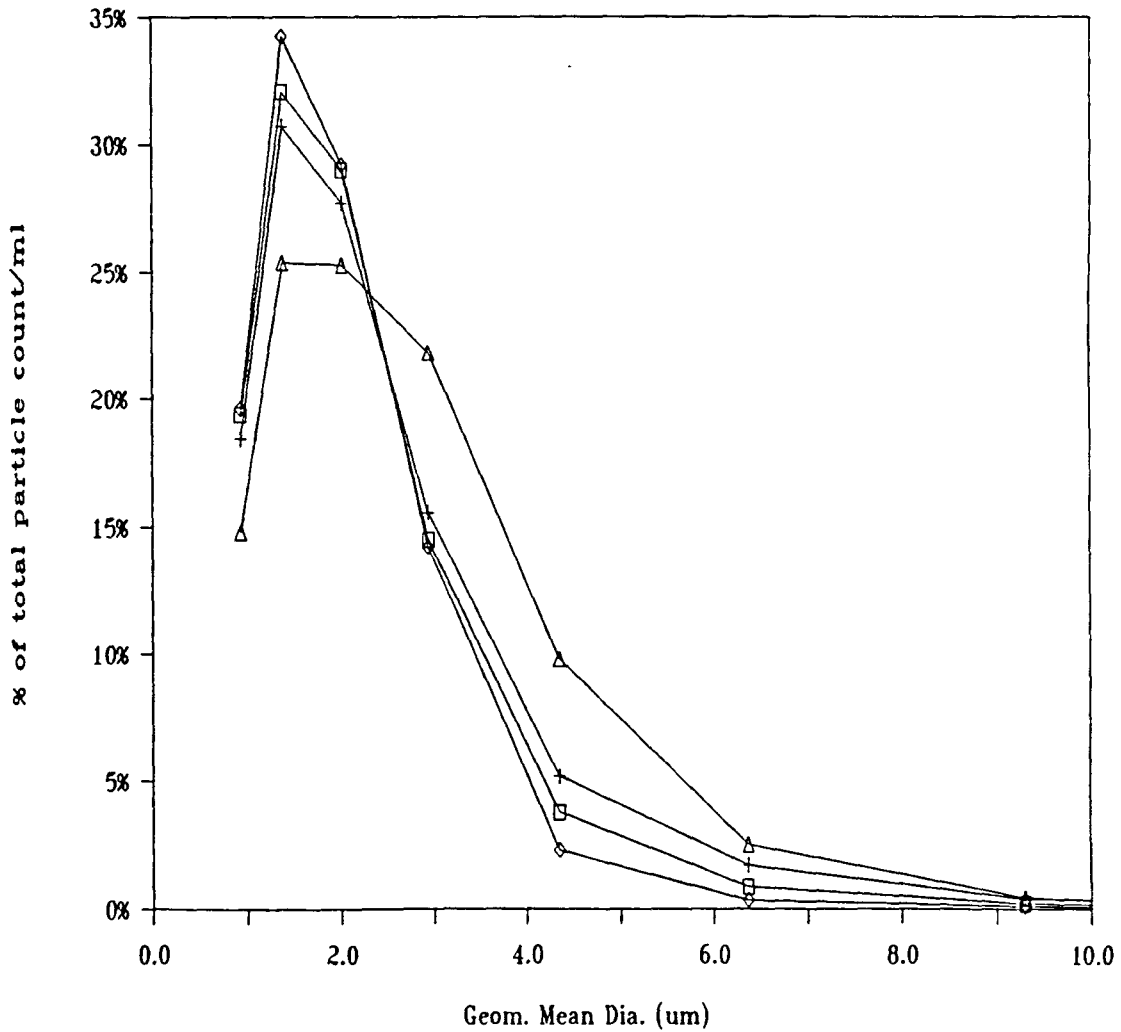


Figure 5.36: Influence of duration of mixing on changes in particle size distribution due to rapid mixing. Experiments compared are 'RB' and 'RC'. □ homogenized sample for 1 min. rapid mix duration, + sample after 1 min. of rapid mixing, ◇ homogenized sample for 5 min. rapid mixing duration, △ sample after 5 min. of rapid mixing. Rapid mixing conducted at 250 rpm and 20°C

## 5.2. Inferences

We have, thus far, traversed the entire domain of the experimental plan and, based on our observations in various sub-sets of the overall experimental plan, made a variety of conclusions.

We now integrate all our sundry inferences:

**What is the true role of rapid mixing?** Having seen

1. a significant reduction in the total count fraction during the rapid mixing period, and
2. a growth of particles, as evidenced by marked changes in the particle size distribution,

we can infer that turbulent rapid mixing serves more than just one purpose—that of uniformly distributing the coagulant throughout the reactor. In fact,

- it rapidly disperses the coagulant so as to assist molecular diffusion in producing a uniform mixture of the coagulant, throughout the solution, at a molecular level;
- it helps in a better destabilization of clay and similar colloidal particles—particularly in the case of polymeric coagulants like Magnifloc 573C—making them more amenable to flocculation;
- it helps in flocculating the destabilized colloids, causing a reduction in the total count of particles because of the growth of particles into larger units.



**What is the influence of temperature?** In all cases, temperature had a marked effect on the suspensions being rapid mixed. A reduction in temperature causes a decrease in the flocculation rate, as evidenced by lesser changes in the particle size distribution and in the total count fraction at the end of the rapid mixing period.

**What is the influence of rapid mixing intensity?** It can be concluded that at the higher level of turbulence intensity investigated in this study, intense rapid mixing actually harms the performance of alum, but improved the performance using cationic polymers. It is my conjecture that the improvement in the performance of polymer in experiments involving extended rapid mixing at higher turbulence intensities is predominantly due to the turbulence and not because of the time factor—even though this extended time period did help the overall flocculation process. More experiments need to be conducted to verify this.

**What is the effect of changes in the duration of rapid mixing?** Time has the most remarkable effect on the results of rapid mixing in experiments involving alum. When using alum, extended periods of rapid mixing at the lower rapid mixing intensity produced the best results, in terms of total particle count reduction. Again, as mentioned in the previous paragraph, an extended duration of rapid mixing (at the higher turbulent intensity) may have some role to play in the improved performance of the polymeric coagulant—but this needs to be verified in other experiments.

### 5.3. Comparison with results of previous studies

Having made the inferences outlined in Section 5.2., we try to look at the previous works with these thoughts in the back of our minds. Direct comparisons with previous work identified in Section 4.1., i.e., that by Vrale and Jorden [113], TeKippe and Ham [108], Letterman et al. [72], Stenquist and Kaufman [101], Amirtharajah and Mills [3] and Amirtharajah and Trusler [7] are extremely difficult because all of these studies—except for [7] have relied entirely on settled, supernatant turbidities in the measurement of the influence of rapid mixing parameters. The reason why such comparisons (i.e., comparing results of settled, supernatant turbidities with total particle counts, of the type monitored in these experiments) are difficult have already been specified in Chapter 4. and will not be repeated here. The problem of comparing results is severely compounded by the fact that in some experiments in the above studies, attempts were made to compare the influence of the reactor geometry so as to identify the superior mode of effecting rapid mixing. Given our observations in Chapter 3., we know that while the finer scales of turbulence are dependent solely on the absolute rate of energy dissipation in the reactor, the reactor geometry has a marked influence on the large scale turbulence parameters. And, since these large scale movements are necessary for the spatial distribution of the coagulant, it is easy to see why comparison of such experiments with our results would not be an easy task.

These difficulties notwithstanding, we can still make general comparisons between the arguments advanced by the earlier experimenters and our own thoughts—based on our experimental evidence.

We first discuss the work involving a backmix reactor, done by Vrale and Jorden

[113]. Among their other conclusions already mentioned in Chapter 4., Vrale and Jordan [113] say that “A backmix reactor is very inefficient for rapid mixing.” As mentioned in Chapter 4., this student does not agree with this conclusion. While their experiments did show this to be true, the reasons why their backmix reactor gave worse results as compared to the tubular reactor may be:

- the grid type reactor has multiple injection points for dosing coagulants into water. As we saw in Chapter 3., this has an immense impact on the kinetics of mixing. Multiple injection points helps in mixing because we do not need as high a turbulence intensity here as would be needed if we were trying to disperse, in the same time period, coagulant dispersed at just 1 point.
- the backmix reactor, which was 1 liter in capacity, had excessively high shear throughout this volume, causing any agglomerated particles to break up. In contrast to this, the tubular mixers had much more uniform shear throughout the pipe resulting in a greater aggregation rate and thus a superior performance.

In fact, the same set of arguments would apply to the results obtained by Stenquist and Kaufman [101].

The work by TeKippe and Ham [108] did involve a variation of the rapid mixing conditions. Unfortunately, their objective was to prove incorrect the idea that  $Gt$  should be kept constant for a rapid mixing/flocculation combination. Therefore, even though they had a variety of rapid mixing conditions in their experiments, they simultaneously varied the flocculation conditions in order to keep the  $Gt$  constant. This makes it very difficult to take their results and compare them. They, too, were

working with settled supernatant turbidity.

The work by Letterman et al. [72], involved a fairly complicated experimental design with a large number of parameters (coagulant dosage, colloid content, pH, rapid mixing intensity, etc.) being varied, again making any direct comparisons difficult. However, they did show that for a given rapid mixing intensity used in combination with a given set of flocculation, sedimentation conditions, there is an optimal duration of the rapid mixing period. This was based on supernatant turbidity of the settled, flocculated suspension. From our study, it is apparent that there must be an optimum rapid mixing period at which the growth and breakup become equally important, causing a reduction in the rate of total particle count reduction.

Amirtharajah and Mills [3] and Amirtharajah and Trusler [7] held  $Gt$  constant in the mixing period. In the first experiment, settled turbidity was monitored while in the second experiment, direct filtration was carried out and the response of the filter gauged using a Filtration number. Again, results of these experiments cannot be directly compared with our results. The difficulty of direct comparisons notwithstanding, the paper by Amirtharajah and Trusler [7] has some interesting aspects. Their approach tries to relate characteristics of the turbulent flow field during the rapid mixing step with the response of the filter column. In this venture, they have relied upon the work of Cutter [37] in determining their turbulence parameters. Some of Cutter's conclusions have since been proved incorrect [92,44,50,51,70,88,89,90]. This means correlations between the ratio (microscale size around impeller)/(particle diameter) and other parameters (like Filtration number) are somewhat incorrect. This argument does not entirely invalidate their overall

conclusion that "...particle destabilization seems to be controlled by the maximum turbulence in the zone around the impeller of a backmix rapid mixing device" [7]; it does show a possible reason why the correlations carried out by them did not match the experimental results. This aspect of their work deserves further exploration.

In the end, we can say that a direct comparison cannot be made between our experiments and those conducted by any of the previous investigators. This implies that further work needs to be done to corroborate these findings.

#### 5.4. Where do we go from here?

One could easily get carried away by purely academic concerns and suggest innumerable possible studies with little or no practical implications. Some of the possible questions to be answered in terms of their practical value would be as follows:

- Most of the recent research in rapid mixing has focussed on the adsorption-destabilization mode of colloid coagulation when using metal coagulants. Since a large fraction of the water treatment plants operates in the 'sweep-floc' mode, it would be appropriate to conduct studies in this region of coagulation/flocculation. This is a particularly challenging problem, I think, because of the difficulties associated with characterizing amorphous alum or iron hydroxide precipitate flocs. Even though Amirtharajah and Mills [3] did some experiments to detect the influence of rapid mixing in this region, it would be proper to corroborate their findings.

- Since direct filtration is a popular mode of water treatment, it would be particularly interesting—in the light of our results—to analyze the work done so far, involving variation of rapid mixing parameters and their influence on the response of the filtration unit.
- Experiments to identify the true cause in the observed improvement of polymer performance during high intensity and extended duration rapid mixing—is it because of the high mixing intensity or the extended period of mixing or both?
- If rapid mixing causes flocculation, shouldn't 'tapered' rapid mixing be used in water treatment? What about tapered rapid mixing for direct filtration units?
- How do organic contaminants (such as color) respond to initial mixing conditions? Is there reason to suspect any changes in their behavior?
- How can the detrimental effects of cold water temperature on rapid mixing/flocculation be ameliorated?
- If alum is more capable of 'cleaning up' small particles out of the system than organic polymer, whereas organic polymers can help make stronger flocs, could the positive aspects of these two coagulants be used simultaneously to our advantage? This is already a common practice in many plants today. However, the optimal design of rapid mixing/flocculation for such applications needs further study.

- Studies to investigate to the reasons why alum performed poorly at the high mixing intensity used in some of the experiments conducted in this study.

One could actually sit down and think up hundreds of possible questions to be answered. For example, this was a batch study. What would happen in a continuous flow system?

However, it is time to stop and end this thesis with the following statement:  
**Rapid mixing DOES flocculate a colloidal suspension.**

## 6. BIBLIOGRAPHY

- [1] Adamson, Arthur W. *A Textbook of Physical Chemistry*. Second Edition. New York, N.Y.: Academic Press, 1979.
- [2] Amirtharajah, A. "Initial Mixing." *Coagulation and Filtration: Back to the Basics*. Proceedings of an American Water Works Association Seminar, St. Louis, Missouri, June 7, 1981, 1-22.
- [3] Amirtharajah, A. and Kirk M. Mills. "Rapid-mix Design for Mechanisms of Alum Coagulation." *Journal American Water Works Association*, 74, 4 (1982): 210-216.
- [4] Amirtharajah, A. "Chapter 8: Design of Rapid Mix Units." In *Water Treatment Plant Design*. Edited by Robert L. Sanks. Ann Arbor, Michigan: Ann Arbor Science Publishers, 1982, 131-147.
- [5] Amirtharajah, A. "Chapter 11: Design of Flocculation Systems." In *Water Treatment Plant Design*. Edited by Robert L. Sanks. Ann Arbor, Michigan: Ann Arbor Science Publishers, 1982, 195-229.
- [6] Amirtharajah, Appiah and Susumu Kawamura. "System Design for Polymer Use." *Use of Organic Polyelectrolytes in Water Treatment*. Proceedings of an American Water Works Association Seminar, Las Vegas, Nevada, June 5-9, 1983, 51-71.
- [7] Amirtharajah, Appiah and Scott L. Trusler. "Destabilization of Particles by Turbulent Rapid Mixing." *Journal of the Environmental Engineering Division, Proceedings of the American Society of Civil Engineers*, 112, 6 (1986): 1085-1108.
- [8] Amirtharajah, Appiah. "Rapid Mixing and the Coagulation Process." Presented in a Preconference Seminar on Coagulation at the Annual Conference of the American Water Works Association, June 14-18, 1987, Kansas City, Missouri.



- [9] Angst, W., J. R. Bourne and F. Kozicki. "Some Measurements of Micromixing in Commercial-Scale Stirred Reactors." *Proceedings of the Third European Conference on Mixing*. Volume 1. BHRA, The Fluid Engineering Centre, Cranfield, Bedford, England, 1979, 61-72.
- [10] Angst, W., J. R. Bourne and R. N. Sharma. "Mixing and Fast Chemical Reaction—IV. The Dimensions of the Reaction Zone." *Chemical Engineering Science*, **37**, 4 (1982): 585-590.
- [11] Angst, W., J. R. Bourne and R. N. Sharma. "Mixing and Fast Chemical Reaction—V. Influence of Diffusion within the Reaction Zone on Selectivity." *Chemical Engineering Science*, **37**, 8 (1982): 1259-1264.
- [12] Angst, W., J. R. Bourne and P. Dell'ava. "Mixing and Fast Chemical Reaction—IX. Comparison Between Models and Experiments." *Chemical Engineering Science*, **39**, 2 (1984): 335-342.
- [13] Argaman, Yerachmiel and Warren J. Kaufman. *Turbulence in Orthokinetic Flocculation*. Sanitary Engineering Research Laboratory, College of Engineering and School of Public Health, University of California, Berkeley, California, SERL Report No. 68-5, July, 1968
- [14] Atkins, P. W. *Physical Chemistry*. Second Edition. San Francisco: W. H. Freeman and Company, 1982.
- [15] Baes, Charles F., Jr. and Robert E. Mesmer. *The Hydrolysis of Cations*. New York, N.Y.: John Wiley & Sons, 1976.
- [16] Baldyga, J. and J. R. Bourne. "Mixing and Fast Chemical Reaction—VIII. Initial Deformation of Material Elements in Isotropic, Homogeneous Turbulence." *Chemical Engineering Science*, **39**, 2 (1984): 329-334.
- [17] Belevi, H., J. R. Bourne and P. Rys. "Mixing and Fast Chemical Reaction—II. Diffusion-reaction model for the CSTR." *Chemical Engineering Science*, **36**, 10 (1981): 1649-1654.
- [18] Benefield, Larry D., Joseph F. Judkins and Barron L. Weand. *Process Chemistry for Water and Wastewater Treatment*. Englewood Cliffs, New Jersey: Prentice-Hall, Inc., 1982.
- [19] Bolzern, O. and J. R. Bourne. "Mixing and Fast Chemical Reaction—VI. Extension of the Reaction Zone." *Chemical Engineering Science*, **38**, 7 (1983): 999-1003.

- [20] Bourne, J. R., U. Moergeli and P. Rys. "Mixing and Fast Chemical Reaction: Influence of Viscosity on Product Distribution." *Proceedings of the Second European Conference on Mixing, Cambridge, U.K., March/April 1977*. BHRA, The Fluid Engineering Centre, Cranfield, U.K., 1978, B3-41-B3-54.
- [21] Bourne, J. R., F. Kozicki and P. Rys. "Mixing and Fast Chemical Reaction—I. Test Reactions to Determine Segregation." *Chemical Engineering Science*, **36**, 10 (1981): 1643-1648.
- [22] Bourne, J. R., F. Kozicki, U. Moergeli and P. Rys. "Mixing and Fast Chemical Reaction—III. Model-Experiment Comparisons." *Chemical Engineering Science*, **36**, 10 (1981): 1655-1663.
- [23] Bourne, J. R. "Mixing on the Molecular Scale (Micromixing)." *Chemical Engineering Science*, **38**, 1 (1983): 5-8.
- [24] Bourne, J. R. and S. Rohani. "Mixing and Fast Chemical Reaction—VII. Deforming Reaction Zone Model for the CSTR." *Chemical Engineering Science*, **38**, 6 (1983): 911-916.
- [25] Bourne, J. R. and J. Garcia-Rosas. "Fast Chemical Reaction in High Intensity Ystral Dynamic Mixer." *Proceedings of the Fifth European Conference on Mixing, Wurzburg, Germany*. BHRA, The Fluid Engineering Centre, Cranfield, Bedford, England, 1985, 81-87.
- [26] Bradshaw, Peter, Tuncer Cebeci and James H. Whitelaw. *Engineering Calculation Methods for Turbulent Flow*. London: Academic Press, 1981.
- [27] Brodkey, Robert S. *The Phenomena of Fluid Motions*. Reading, Massachusetts: Addison-Wesley Publishing Company, 1967.
- [28] Brodkey, Robert S. "Chapter II: Mixing in Turbulent Fields." In *Turbulence in Mixing Operations: Theory and Application to Mixing and Reaction*. Edited by Robert S. Brodkey. New York, N.Y.: Academic Press, Inc., 1975, 49-120.
- [29] Brodkey, Robert S. "Fundamentals of Turbulent Mixing and Kinetics." In *Mixing of Liquids by Mechanical Agitation*. Edited by Jaromir J. Ulbrecht and Gary K. Patterson. New York, N.Y.: Gordon and Breach, 1985, 29-58.
- [30] Clark, Mark M. "Critique of Camp and Stein's RMS Velocity Gradient." *Journal of the Environmental Engineering Division, Proceedings of the American Society of Civil Engineers*, **111**, 6 (1985): 741-754.

- [31] Clark, Mark M. "Scale-up of laboratory flocculation results." Presented at the Annual Conference of the American Water Works Association, Denver, Colorado, June 22-26, 1986.
- [32] Clark, Mark M., René David and Mark R. Wiesner. "Effect of Micromixing on Product Selectivity in Rapid Mix." *Proceedings of the Annual Conference of the American Water Works Association, June 14-18, 1987, Kansas City, Missouri.*
- [33] Cleasby, John L. "Is Velocity Gradient a Valid Turbulent Flocculation Parameter?" *Journal of the Environmental Engineering Division, Proceedings of the American Society of Civil Engineers*, 110, 5 (1984): 875-897.
- [34] Committee on Water Treatment Chemicals, Food and Nutrition Board, Assembly of Life Sciences, National Research Council. *Water Chemicals Codex.* Washington, D.C.: National Academy Press, 1982.
- [35] Corrsin, S. "Turbulent Flow." *American Scientist*, 49 (1961): 300-325.
- [36] *CRC Handbook of Chemistry and Physics.* 66th Edition, 1985-1986. Edited by Robert C. Weast. Boca Raton, Florida: CRC Press, Inc., 1985.
- [37] Cutter, Louis A. "Flow and Turbulence in a Stirred Tank." *A.I.Ch.E. Journal*, 12, 1 (1966): 35-45.
- [38] David, R., J. P. Barthole and J. Villiermaux. "Poster 3: Interpretation of Micromixing Experiments Involving Consecutive Competitive Reactions in a Stirred Tank by a Simple Interaction Model." *Proceedings of the Fifth European Conference on Mixing, Wurzburg, West Germany.* BHRA, The Fluid Engineering Centre, Cranfield, Bedford, England, 1985, 433-437.
- [39] Eagland, D. "Chapter 1: The Influence of Hydration on the Stability of Hydrophobic Colloidal Systems." In *Water: A Comprehensive Treatise. Volume 5.* Edited by Felix Franks. New York, New York.: Plenum Press, 1975.
- [40] Edwards, M. F., J. Bertrand, H. Bruxelmane. Discussions of "Some Measurements of Micromixing in Commercial-Scale Stirred Reactors," by W. Angst et al. *Proceedings of the Third European Conference on Mixing. Volume 2.* BHRA, The Fluid Engineering Centre, Cranfield, Bedford, England, 1979, 26-27.
- [41] Harnby, N., M. F. Edwards and A. W. Nienow (Editors). *Mixing in the Process Industries.* London: Butterworths, 1985.

list of sources

- [42] Edzwald, James K. "Coagulation." *Back to the Basics*. Proceedings of an American Water Works Association Seminar, St. Louis, Missouri, June 7, 1981, 23-44.
- [43] Feinberg, Ellen. "Zoning Patterns in a Molecular World." *Changing Scene*. Ames Laboratory, Iowa State University, Ames, Iowa 50011, 13, 3, 1987.
- [44] Fort, I., J. Ulbrecht, R. I. Fox, E. T. Sweeney, C. Koen, A. M. Shepherd, G. J. Bertrand, C. Ramshaw. Discussions of "Laser Doppler Measurements of Turbulence in a Standard Stirred Tank," by X. B. Reed, Jr. et al. *Proceedings of the Second European Conference on Mixing, Cambridge, U.K., March/April, 1977*. BHRA, The Fluid Engineering Centre, Cranfield, U.K., 1978, X13-X22.
- [45] Freundlich, H. *Colloid and Capillary Chemistry*. London, U.K.: Methuen, 1926.
- [46] Frost, W. and J. Bitte. "Chapter 3: Statistical Concepts of Turbulence." *Handbook of Turbulence. Volume 1. Fundamentals and Applications*. Edited by Walter Frost and Trevor H. Moulden. New York, N.Y.: Plenum Press, circa 1977, 53-84.
- [47] Frost, Walter. "Chapter 4: Spectral Theory of Turbulence." In *Handbook of Turbulence. Volume 1. Fundamentals and Applications*. Edited by Walter Frost and Trevor H. Moulden, New York, N.Y.: Plenum Press, circa 1977, 85-125.
- [48] Glaberson, W. I. and K. W. Schwarz. "Quantized Vortices in Superfluid Helium-4." *Physics Today*, 40, 2 (1987): 54-60.
- [49] Gleick, James. *Chaos: Making a New Science*. New York, N.Y.: Viking, 1987.
- [50] Günkel, Alfred A. and Martin E. Weber. "Flow Phenomena in Stirred Tanks. Part I. The Impeller Stream." *AIChE Journal*, 21, 5 (1975): 931-939.
- [51] Günkel, Alfred A. and Martin E. Weber. "Flow Phenomena in Stirred Tanks. Part II. The Bulk of the Tank." *AIChE Journal*, 21, 5 (1975): 939-949.
- [52] Haarhoff, Johannes. "Direct Filtration of *Chlorella* and *Scenedesmus* for Potable Water Treatment." Dissertation. Iowa State University, Ames, Iowa, 1987.
- [53] Hahn, Hermann H. and Werner Stumm. "Chapter 9: Coagulation by Al(III): The Role of Adsorption of Hydrolyzed Aluminum in the Kinetics of Coagulation." In *Adsorption from Aqueous Solution. Advances in Chemistry Series 79*.

Edited by Robert F. Gould. Washington, D.C.: American Chemical Society Publications, 1968, 91–111.

- [54] Hahn, Hermann and Werner Stumm. "Kinetics of Coagulation with Hydrolyzed Al(III). The Rate-Determining Step." *Journal of Colloid and Interface Science*, **28**,1 (1968), 134–144.
- [55] Haken, Hermann. *Synergetics: An Introduction*. Third Edition. Berlin, F. R. G.: Springer-Verlag, 1983.
- [56] Healy, T. W., R. O. James and R. Cooper. "The Adsorption of Aqueous Co(II) at the Silica Water Interface." In *Adsorption from Aqueous Solution. Advances in Chemistry Series 79*. Edited by Walter J. Weber, Jr. and Egon Matijević. Washington, D.C.: American Chemical Society, 1968, 62–73.
- [57] Hirtzel, C. S. and Raj Rajagopalan. *Advanced Topics in Colloidal Phenomena*. Monograph. Department of Chemical and Environmental Engineering, Rensselaer Polytechnic Institute, Troy, New York, 1985.
- [58] Holland, F. A. and F. S. Chapman. *Liquid Mixing and Processing in Stirred Tanks*. New York, N.Y.: Reinhold Publishing Company, 1966.
- [59] Hudson Jr., H. E. and J. P. Wolfner. "Design of Mixing and Flocculating Basins." *Journal American Water Works Association*, **59**, 10 (1967): 1257–1267.
- [60] Hunter, Robert J. *Foundations of Colloid Science. Volume I*. Oxford, U.K.: Oxford University Press, 1987.
- [61] Ives, Kenneth J. (Editor). *The Scientific Basis of Flocculation*. Alphen ann den Rijn, The Netherlands: Sijthoff & Noordhoff, 1978.
- [62] James M. Montgomery Consulting Engineers Inc. "Chapter 6: Precipitation, Coagulation, Flocculation." In *Water Treatment Principles and Design*. New York, N.Y.: John Wiley & Sons, Inc., 1985, 116–134.
- [63] Jenson, V. G. "A Model for Mixing With Fast Chemical Reactions." *Chemical Engineering Science*, **38**, 8 (1983) 1151–1157.
- [64] Jullien, R. and R. Botet. *Aggregation ad Fractal Aggregates*. Singapore: World Scientific, 1987.

- [65] Kavanaugh, Michael C. and James O. Leckie. Preface to *Particulates in Water. Characterization, Fate, Effects and Removal. Advances in Chemistry Series 189*. Edited by Michael C. Kavanaugh and James O. Leckie. Washington, D.C.: American Chemical Society, 1980, ix-xi.
- [66] Kawamura, Susumu. "Considerations on Improving Flocculation." *Journal American Water Works Association*, **68**, 6 (1976): 328-336.
- [67] Kimmels, H., J. Bridgwater, C. Ramshaw. Discussions of "Mixing and Fast Chemical Reaction: Influence of Viscosity on Product Distribution," by J. R. Bourne et al. *Proceedings of the Second European Conference on Mixing, Cambridge, U.K., March/April 1977*. BHRA, The Fluid Engineering Centre, Cranfield, U.K., 1978, X20, X23.
- [68] Koh, P. T. L., J. R. G. Andrews and P. H. T. Uhlherr. "Flocculation in Stirred Tanks." *Chemical Engineering Science*, **39**, 6 (1984): 975-985.
- [69] Koh, P. T. L. "Compartmental Modelling of Stirred Tank for Flocculation Requiring a Minimum Critical Shear Rate." *Chemical Engineering Science*, **39**, 12 (1984): 1759-1764.
- [70] Laüfhutte, H. D. and A. B. Mersmann. "Paper 33: Dissipation of Power in Stirred Vessels." *Proceedings of the Fifth European Conference on Mixing, Wurzburg, Germany*. BHRA, The Fluid Engineering Centre, Cranfield, Bedford, England, 1985, 331-341.
- [71] Lesieur, Marcel. *Turbulence in Fluids*. Dordrecht, The Netherlands: Martinus Nijhoff Publishers, 1987.
- [72] Letterman, Raymond D., J. E. Quon and Robert S. Gemmill. "Influence of Rapid-Mix Parameters on Flocculation." *Journal American Water Works Association*, **65**, 11 (1973): 716-722.
- [73] Letterman, Raymond D. "Flocculation." *Coagulation and Filtration: Back to the Basics*. Proceedings of an American Water Works Association Seminar, St. Louis, Missouri, June 7, 1981, 45-58.
- [74] Levine, Ira H. *Physical Chemistry*. Second Edition. New York, N.Y.: McGraw-Hill Book Company, 1983.
- [75] Lumley, J. L. *Deformation of Continuous Media* (Motion Picture Film). Cambridge, Massachusetts: Educational Services Inc., 1963.

- [76] Lyklema, J. In *Colloidal Dispersions*. Edited by J. W. Goodwin. London, U.K.: The Royal Soc. Chem., 1982.
- [77] Moffett, J. William. "The Chemistry of High-Rate Water Treatment." *Journal American Water Works Association*, 60, 11 (1968): 1255-1270.
- [78] Monin, A. S. and A. M. Yaglom. *Statistical Fluid Mechanics: Mechanisms of Turbulence. Volume 1*. Editor to the English edition, John L. Lumley. Cambridge, Massachusetts: MIT Press, 1971.
- [79] Morel, François M. M. *Principles of Aquatic Chemistry*. New York, N.Y.: John Wiley & Sons, 1983.
- [80] Moulden, Trevor H. "Chapter 2: An Introduction to Turbulence Phenomena." *Handbook of Turbulence. Volume 1. Fundamentals and Applications*. Edited by Walter Frost and Trevor H. Moulden. New York, N.Y.: Plenum Press, circa 1977, 23-52.
- [81] Nabholz, F., R. J. Ott and P. Rys. "Mixing-Disguised Chemical Selectivities." *Proceedings of the Second European Conference on Mixing, Cambridge, U.K., March/April 1977*. BHRA, The Fluid Engineering Centre, Cranfield, U.K., 1978, B2-27-B2-40.
- [82] Nebergall, William H., F. C. Schmidt and H. F. Holtzclaw, Jr. *College Chemistry With Quantitative Analysis*. Fourth Edition. Lexington, Massachusetts: D. C. Heath and Company, 1972.
- [83] O'Brien, Edward E. "Chapter I: Theoretical Aspects of Turbulent Mixing of Reactants." In *Turbulence in Mixing Operations: Theory and Application to Mixing and Reaction*. Edited by Robert S. Brodkey. New York, N.Y.: Academic Press, Inc., 1975, 19-46.
- [84] O'Melia, Charles R. "A Review of the Coagulation Process." *Public Works*, 100, 4 (1969): 87-98.
- [85] O'Melia, Charles R. "Chapter 2: Coagulation and Flocculation." In *Physicochemical Processes for Water Quality Control*. Edited by Walter J. Weber. New York, N.Y.: Wiley-Interscience, 1972, 61-109.
- [86] O'Melia, Charles R. "Chapter 4. Coagulation." In *Water Treatment Plant Design*. Edited by Robert L. Sanks. Ann Arbor, Michigan: Ann Arbor Science Publishers, 1982, 65-82.

- [87] Panton, Ronald L. *Incompressible Flow*. New York, N.Y.: John Wiley & Sons, 1984.
- [88] Patterson, G. K. and H. Wu. "Paper 35: Distribution of Turbulence Energy Dissipation Rates in Mixers." *Proceedings of the Fifth European Conference on Mixing, Wurzburg, West Germany*. BHRA, The Fluid Engineering Centre, Cranfield, Bedford, England, 1985, 355-364.
- [89] Placek, Jiří and L. L. Tavlarides. "Turbulent Flow in Stirred Tanks. Part I: Turbulent Flow in the Turbine Impeller Region." *AIChE Journal*, **31**, 7 (1985): 1113-1120.
- [90] Placek, Jiří, L. L. Tavlarides, G. W. Smith and Ivan Fořt. "Turbulent Flow in Stirred Tanks. Part II: A Two-Scale Model of Turbulence." *AIChE Journal*, **32**, 11 (1986): 1771-1786.
- [91] Pourhamadi, F. and J. A. C. Humphrey. "Modeling Solid-Fluid Turbulent Flows With Application to Predicting Erosive Wear." *PCH PhysicoChemical Hydrodynamics*, **4**, 3 (1983): 191-219.
- [92] Reed Jr., X. B., M. Princz and S. Hartland. "Laser Doppler Measurements of Turbulence in a Standard Stirred Tank." *Proceedings of the Second European Conference on Mixing, Cambridge, U.K., March/April, 1977*. BHRA, The Fluid Engineering Centre, Cranfield, U.K., 1978, B1-1-B1-26.
- [93] Reynolds, A. J. *Turbulent Flows in Engineering*. London: John Wiley & Sons, 1974, 17-21.
- [94] Russel, William B. *The Dynamics of Colloidal Systems*. Madison, Wisconsin: The University of Wisconsin Press, 1987.
- [95] Schindler, Paul W. and Werner Stumm. "The Surface Chemistry of Oxides, Hydroxides, and Oxide Minerals." In *Aquatic Surface Chemistry*. Edited by Werner Stumm. New York, N.Y.: John Wiley & Sons, 1987, 83-110.
- [96] Shapiro, Ascher H. *Vorticity*. Parts I & II. (Motion picture film). Cambridge, Massachusetts: Educational Services Inc., circa 1961.
- [97] Sillén, Lars Gunnar and Arthur E. Martell. *Stability Constants of Metal-Ion Complexes*. Second Edition. Special Publication No. 17. London: The Chemical Society, 1964.



- [98] Smith, J. M. "Chapter 2: Kinetics of Adsorption." *Adsorption from Aqueous Solution, Advances in Chemistry Series 79*. Edited by Robert F. Gould. Washington, D.C.: American Chemical Society Publications, 1968, 8-22.
- [99] Smith, J. M. Discussions of "Mixing-Disguised Chemical Selectivities," by F. Nabholz et al. *Proceedings of the Second European Conference on Mixing, Cambridge, U.K., March/April 1977*. BHRA, The Fluid Engineering Centre, Cranfield, U.K., 1978, X20, X22.
- [100] Snoeyink, Vernon J. and David Jenkins. *Water Chemistry*. New York, N.Y.: John Wiley & Sons, 1980.
- [101] Stenquist, Richard J. and Warren J. Kaufman. *Initial Mixing in Coagulation Processes*. Environmental Protection Technology Series, EPA-R2-72-053. Office of Research and Monitoring, U.S. Environmental Protection Agency, Washington, D.C., November 1972.
- [102] Stewart, Robert W. *Turbulence*. (Motion picture film). Cambridge, Massachusetts: Educational Services Inc., 1969.
- [103] Stryker, Lynden J. and Egon Matijević. "Adsorption of hydrolyze Hafnium ions on Glass." In *Adsorption from Aqueous Solution. Advances in Chemistry Series 79*. Edited by Walter J. Weber, Jr. and Egon Matijević. Washington, D.C.: American Chemical Society, 1968, 44-61.
- [104] Stumm, Werner and James J. Morgan. "Chemical Aspects of Coagulation." *Journal American Water Works Association*, 54, 8 (1962): 971-994.
- [105] Stumm, W. and Charles R. O'Melia. "Stoichiometry of Coagulation." *Journal American Water Works Association*, 60, 5 (1968): 514-539.
- [106] Stumm, Werner and James J. Morgan. *Aquatic Chemistry*. Second Edition. New York, N.Y.: John Wiley & Sons, Inc., 1981.
- [107] Tambo, Norihito and Yoshimasa Watanabe. "Physical Aspect of Flocculation Process—I. Fundamental Treatise." *Water Research*, 13 (1979): 429-439.
- [108] Tekippe, Rudy J. and R. K. Ham. "Velocity-gradient Paths in Coagulation." *Journal American Water Works Association*, 63, 7 (1971): 439-448.
- [109] Tennekes, H. and J. L. Lumley. *A First Course in Turbulence*. Cambridge, Massachusetts: The MIT Press, 1972.

- [110] Toor, H. L. "Chapter III: The Non-premixed Reaction:  $A+B \rightarrow$  Products." In *Turbulence in Mixing Operations, Theory and Application to Mixing and Reactions*. Edited by Robert S. Brodkey. New York, N.Y.: Academic Press, Inc., 1975, 121-166.
- [111] Van Dyke, Milton. *An Album of Fluid Motion*. Stanford, California: The Parabolic Press, 1982.
- [112] Voke, Peter E. and Michael W. Collins. "Large-Eddy Simulation: Retrospect and Prospect." *PCH PhysicoChemical Hydrodynamics*, 4, 2 (1983): 119-161.
- [113] Vrale, Lasse and Roger M. Jorden. "Rapid Mixing in Water Treatment." *Journal American Water Works Association*, 63, 1 (1971): 52-59.
- [114] Westall, John C. "Adsorption Mechanisms in Aquatic Surface Chemistry." In *Aquatic Surface Chemistry*. Edited by Werner Stumm. New York, N.Y.: John Wiley & Sons, 1987, 3-32.
- [115] Zabusky, N. J. "Grappling with Complexity." *Physics Today*. 40, 10 (1987): 25-27.

**7. APPENDIX**

The following pages contain the data which were used in generating the plots shown in Chapter 5. The experimental conditions corresponding to each experiment are identified using labels which correspond to those shown in Figure 5.1 (page 218) for alum and Figure 5.15 (page 244) for Magnifloc 573C.

The sample characteristics are as follows:

Sample identification	Nature of sample
1. Homog. sample	Homogenized sample, corresponding to the clay suspension in the reactor BEFORE the coagulant was added to the reactor.
2. Rap. mix. sample	Suspension in the reactor after the coagulant has been added and rapid mixed for the specific duration of time. The sample corresponds to the END of the rapid mixing period.
3. 1.0, 3.0, 5.0, etc.	Samples corresponding to the specified duration of the flocculation period. Therefore, the sample associated with a 3.0 minute period of flocculation (i.e., a 3.0 minute period following the end of the rapid mixing process) is placed in a column identified with a 3.0 at the top.

Each number is the total count fraction for that particular sample. This is explained on page 221 of the thesis.

ALUM <=====> Experiments involving alum as a coagulant <=====> ALUM

Duration of flocculation (min)----->

Label	Homog. Sample	Rep. Mix. Sample	1.0	3.0	5.0	10.0	15.0	20.0	25.0	30.0	45.0	Label
AA	1.0000	1.0450	0.8893	0.8393	0.6508	0.4664	0.3122	0.1716	0.1479	0.0902	0.0638	AA
AB	1.0000	0.9013	0.8853	0.8080	0.5313	0.2950	0.2543	0.1538	0.1020	0.1144		AB
AB	1.0000	0.8788	0.6645	0.6781	0.4687	0.2613	0.2031	0.1398	0.1044	0.1095		AB
AB	1.0000	1.0868	0.8274	0.7454	0.5923	0.3984	0.2685	0.1594	0.1106	0.1029		AB
AC	1.0000	1.0771	0.8394	0.9111	0.7747	0.6026	0.5188	0.2983	0.2198	0.1897		AC
AC	1.0000	1.0362	0.8709	0.9136	0.8474	0.7091	0.6584	0.4008	0.2465	0.2036		AC
AC	1.0000	0.7406	0.6903	0.7434	0.6039	0.4827	0.3940	0.2891	0.2067	0.1940		AC
AD	1.0000	0.6661	0.5327	0.5353	0.5000	0.4413	0.3383	0.2847	0.1751	0.1939	0.0964	AD
AD	1.0000	0.5130	0.4742	0.4315	0.3277	0.3002	0.2325	0.2039	0.1327	0.1034	0.0743	AD
AE	1.0000	1.3236	1.0261	1.2580	1.0447	0.8604	0.7411	0.5919	0.5228	0.3657	0.1851	AE
AF	1.0000	1.2156	1.0009	1.0576	0.9727	1.0839	1.0450	0.8929	0.8515	0.7595	0.4754	AF
AF	1.0000	1.0055	0.8110	0.8016	0.8478	0.8155	0.8186	0.6610	0.5929	0.5200	0.2813	AF
AG	1.0000	1.1519	0.8429	0.9661	0.8706	0.9203	0.8080	0.7948	0.7169	0.5596	0.2911	AG
AH	1.0000	1.0890	0.9534	1.0181	0.8943	0.7332	0.5979	0.4456	0.3926	0.2558	0.2258	AH
AH	1.0000	0.8951	0.7446	0.8823	0.6982	0.6836	0.3961	0.3081	0.2049	0.2109	0.1658	AH
AH	1.0000	1.0034	0.7106	0.9319	0.7050	0.6354	0.5886	0.4604	0.3406	0.3037	0.1372	AH
AI	1.0000	1.0735	0.8213	0.9279	0.8534	0.9429	0.8075	0.7732	0.6607	0.5303	0.3917	AI

-----  
 ALUM <-----> Experiments involving alum as a coagulant =====> ALUM  
 -----

Duration of flocculation (min)----->

Label	Homog. Sample	1.0	3.0	5.0	10.0	15.0	20.0	25.0	30.0	45.0	Label
AJ	1.0000	0.8124	0.6697	0.6606	0.5100	0.4633	0.2309	0.1350	0.1377	0.0884	AJ
AK	1.0000	0.7975	0.7443	0.7349	0.6611	0.7072	0.4848	0.3235	0.2805	0.1939	AK
AK	1.0000	0.9881	0.7858	0.8639	0.7245	0.8133	0.4847	0.3873	0.3100	0.2058	AK

-----

-----  
 POLYMER <=====> Experiments Involving Magnifloc 573C as a coagulant =====> POLYMER  
 -----

Duration of flocculation (min)----->

Label	Homog.	Rap. Mix.	1.0	3.0	5.0	10.0	15.0	20.0	25.0	30.0	45.0	Label
Sample	Sample	Sample	Sample	Sample	Sample	Sample	Sample	Sample	Sample	Sample	Sample	Sample
PA	1.0000	0.6073	0.4233	0.5396	0.4505	0.4168	0.3599	0.3355	0.2124	0.2072	0.1499	PA
PB	1.0000	0.7743	0.7596	0.7063	0.6062	0.4984	0.4900	0.4128	0.2982	0.2266	0.1152	PB
PC	1.0000	0.7341	0.5289	0.5924	0.5498	0.5123	0.5027	0.4558	0.3632	0.3552	0.2394	PC
PD	1.0000	0.6795	0.5253	0.6186	0.5332	0.4999	0.4384	0.3725	0.3122	0.2813	0.1887	PD
PE	1.0000	0.8539	0.6019	0.7023	0.6974	0.4940	0.5197	0.4506	0.3778	0.4039	0.2973	PE
PE	1.0000	1.1045	0.8251	0.9342	0.7999	0.8885	0.8084	0.6224	0.4862	0.4646	0.2864	PE
PF	1.0000	0.9888	0.8453	0.8888	0.7616	0.7556	0.8628	0.7994	0.7288	0.6889	0.5314	PF
PF	1.0000	0.8776	0.7734	0.8850	0.8093	0.7249	0.7878	0.7613	0.6675	0.6319	0.4698	PF

Experiment	Total particle count in homogenized sample (no./ml)	Date
AA	5.97E+06	04-May-88
AB	4.98E+06	05-Nov-87
AB	5.06E+06	10-Nov-87
AB	4.66E+06	12-Nov-87
AC	5.79E+06	22-Oct-87
AC	6.38E+06	24-Oct-87
AC	5.33E+06	03-Nov-87
AD	5.87E+06	19-Apr-88
AD	6.89E+06	21-Apr-88
AE	4.78E+06	12-Apr-88
AF	4.80E+06	17-Mar-88
AF	5.13E+06	29-Mar-88
AG	5.16E+06	07-Apr-88
AH	4.55E+06	02-Jan-88
AH	6.02E+06	05-Jan-88
AH	5.85E+06	21-Jan-88
AI	5.57E+06	08-Dec-87
AJ	5.63E+06	09-Feb-88
AK	5.84E+06	01-Feb-88
AK	4.91E+06	05-Feb-88
PA	6.01E+06	02-May-88
PB	6.78E+06	28-Apr-88
PC	7.33E+06	26-Apr-88
PD	5.25E+06	14-Apr-88
PE	6.05E+06	23-Feb-88
PE	5.29E+06	25-Feb-88
PF	5.24E+06	01-Mar-88
PF	6.34E+06	03-Mar-88